New Concept for Evaluating the Risk of Hydrate Formation during Processing and Transport of Hydrocarbons

Master of Science Thesis in Process Technology
(*Specialization in Separation Technology*)

By
Solomon Aforkoghene Aromada

Department of Physics and Technology
University of Bergen, Norway
October 2017

Abstract

Transport of hydrocarbons from reservoir to gas processing plants and for supply to delivery terminals is predominantly done using pipelines, particularly within reasonable distance. In the North Sea of Norway, there are about 8000 km network of pipelines transporting hydrocarbons. Transport and processing operations of hydrocarbons in the North Sea are typically at elevated pressures. The seafloor temperatures are normally low; because of the seawater salinity it could be as low as 272.15 K in the northern part, and seldom rise above 279.15 K in the south. If liquid water condenses out of hydrocarbon gas streams at these conditions of high pressures and low temperatures, with favourable mass and heat transport, nucleation and growth of natural gas hydrate is expected to occur.

The typical technique the industry currently apply to examine the risk of hydrate formation is based on estimation of water dew-point for the gas in question. And if any condition of temperature and pressure in the pipeline or processing equipment is above water dew-point so that water condenses out, then the amount of water that will drop out is evaluated. This is followed by hydrate formation evaluation, including maximum amount of hydrate that can be expected to form from the condensed water. Prevention of hydrate formation with this classical approach known as dew-point method therefore involves estimating the maximum amount of water that can be permitted in the hydrocarbon gas without the risk of liquid water dropping out and eventually leads to hydrate formation.

The shortcoming of the classical scheme is that it totally disregards another (a new) concept which involves water dropping out of the bulk through the mechanism of adsorption on rusty surfaces. Pipelines and some equipment are generally rusty even before they are mounted together and put in place. Rust is a mixture of iron oxide and in this study refers to Hematite (Fe_2O_3) which is one of the most thermodynamically stable forms of rust. These rusty surfaces provide water adsorption sites that can also lead to hydrate formation. However, hydrate formation cannot occur directly on the surfaces covered by Hematite. This is because the distribution of partial charges of hydrogen and oxygen in the lattice are incompatible with the atom charges in the rusty (Hematite) surfaces. But the rusty surfaces act as catalyst that help to take out the water from the gas stream via the process of adsorption, and hydrate formation can follow slightly outside of the first two or three water layers of about one nanometre.

In this project, real hydrocarbon mixtures are studied for the first time using a novel thermodynamic scheme, with composition data which is openly available for the Troll gas and Sleipner gas from the North Sea. The model has been comprehensively validated in this work for pure and mixtures of hydrocarbons, CO_2, H_2S, and hydrocarbon mixtures with these inorganic gases with experimental data from 35 established literature. Estimates of maximum concentration of water tolerable in hydrocarbon gas systems containing structure I and structure II guest molecules during processing and pipeline transport with the classical dew-point technique is in order of 18-21 times higher than the estimates with the new concept of evaluating the risk of hydrate formation based on water dropping out by the process of adsorption on Hematite. This alternative route to hydrate formation through adsorption of water on hematite absolutely dominates in evaluating the risk of water dropping out from the gas mixtures (and pure components investigated) to form a separate water phase and eventually lead to hydrate formation. This reason is because the average chemical potential of the water adsorbed on Hematite is approximately 3.4 kJ/mol less than the chemical potential of liquid water. And thermodynamics favours minimum free energy.

The typical trend exhibited by methane, methane-dominated gas mixtures like Troll gas and Sleipner gas, and carbon dioxide is decline in the upper limit of water with increasing pressure. The heavier hydrocarbon (ethane, propane, and isobutane) gases exhibits opposite trend to that of CH_4 and CH_4-dominated gas mixtures where the permitted maximum water content increases with increase in pressure. This manifestation is due to the high density non-polar phase at the high pressures of the C_{2+}. The non-polar heavier hydrocarbons (especially of structure II hydrate formers) will act to draw down the maximum concentration of water that can be permitted in the gas mixture to a point where they completely dominate or dictate the trends. This is why the safe-limit of water tolerable in Sleipner gas is lower than that of Troll gas which contains lesser amount of C_{2+}. The safe-limit of water to prevent the risk of hydrate formation during processing and pipeline transport of CO_2 is only very slightly less than that CH_4. Higher concentrations of H_2S up to 5% and above would have a significant impact of reducing the maximum concentration of water that can be permitted in hydrocarbon gas mixtures during processing and pipeline transport operations.

Acknowledgement

My profound gratitude goes to my supervisor, Professor Bjørn Kvamme. His inspiration, guidance and feedbacks were invaluable. I learnt a lot from him during his lectures and this project (thesis). Despite his busy schedule, he was always available to inspire, encourage and to provide support and feedbacks. I am sincerely glad that I studied under his research group.

I am also grateful to all my fellow classmates and the department's Study Consultant for their support and for making the study environment pleasant.

I want to sincerely thank my mother, Madam Josephine Hossana Edoghor Edeh who did everything within her power to ensure that my dream of being educated is realised. My heartfelt appreciation goes to my wife, Mrs. Blessing Ijeoma Aromada and our three sons, Favour Oghale Aromada, Victor Orezioghene Aromada and Emmanuel Uvieoghenena Aromada for their invaluable sacrifice, support, encouragement and understanding during my study period. I want to thank Mr. Stephen Neba-Fuh, Mr. Otobong Ezekiel Ubengama and Enobong Ezekiel Ubengama, Mr. Samuel Egbona and his family, Mr. Akeno Oriomah and Mrs. Oluyemi Oriomah for their support.

Table of Contents

List of Figures

List of Tables

1 Introduction

Water is always produced together with the hydrocarbons from the reservoir side before the first three phase separator offshore. The presence of this water is a great flow assurance concern for the oil and gas industry [1]. This is because the water can condense out from the bulk hydrocarbon gas stream to form a separate water phase. This depends on the local conditions of temperature and pressure, composition of the bulk and the concentration of water in the hydrocarbon stream. With the presence of free water, hydrate will form when hydrate formation conditions of low temperature and high pressure are met with favourable mass and heat transport. Gas hydrate formation during processing and transport of hydrocarbons is a crucial problem that could result in eventual plugging and destruction of pipelines and equipment [1, 2], thereby halting operations; and consequentially, economic losses and even loss of lives [3] can result. It costs the petroleum industry around one billion dollars (USD) [2] annually for prevention of hydrate formation in wells, gas processing equipment and transport pipelines. These explain the significance of evaluating the risk of hydrate formation.

Processing of hydrocarbons (natural gas) involves unit operations like turbines, compressors and separators. Expansion in turbines leads to cooling of gas and hydrate can form if end point is inside hydrate stability region and water drops out to provide free water. Compression during processing and transport can also lead to situation inside hydrate stability region since it involves raising the pressure of the system. Risk of hydrate formation is also possible at the final separator in gas processing because it is always at low temperature and high pressure. The Troll gas is processed at Kollsnes near Bergen in Norway, from where natural gas is delivered to the continent. Due to limited content, and corresponding limited value, of hydrocarbons heavier than ethane the minimum temperature in this plant is about 251 K at a pressure of 7000 kPa. Gas from Kvitebjørn is processed at a separate plant also at Kollsnes. This gas has higher content of heavier hydrocarbons and lowest temperature in this plant is around 203 K also at a pressure of 7000 kPa. Snøhvit gas, from an offshore field far north in Norway, has similar conditions as Kvitebjørn.

Transport of natural gas from the production reservoir to the gas processing plants, and from the gas treatment plants to delivery terminals (market) is chiefly implemented using pipelines. In 2010, pipeline length of 1,942,669 kilometres [4] was already established in the world for transporting natural gas, crude oil, or petroleum products. And in the North Sea,

offshore of Norway, approximately 96 billion standard cubic metres of gas is transported every year through about 8000 km length of pipelines; these pipelines are laid generally on the seafloor and thus, they are exposed to low temperatures of approximately 275 K to 279 K [5]. Large amount of these hydrocarbon gases is transported through these pipelines at these low temperatures and elevated pressures. And if free water is available, these conditions are favourable for the risk of formation and deposition of the ice-like substance referred to as clathrate hydrates or natural gas hydrates in the pipelines, which could lead to eventual plugging [6] of pipelines and process equipment.

The technique the industry currently uses to evaluate the risk of hydrate formation is typically based on a three step evaluation. The first step involves a calculation of water dew-point for the gas in question. If any condition of temperature and pressure in the pipeline is above water dew-point so that water drops out then a second step involves evaluation of how much water will drop out. And the third step is the hydrate formation evaluation, including maximum amount of hydrate that can be expected to form from the condensed water. Natural gas transport lines are typically at very high pressures – even up to maximum 300 bars. For transport in pipelines at seafloor a typical of maximum temperature is 6°C but can even be lower than 0°C offshore the northern parts of Norway due to salinity. the assumption that liquid water will drop out of the bulk hydrocarbon gas stream during processing and transport to form a separate water phase that can possibly lead to hydrate formation [5]. The shortcoming of this traditional scheme is that it totally disregards the impact of solid surfaces that create alternative routes to hydrate formation. In this study, the impact of the presence of hematite (rust) on the internal walls of processing equipment and on transport pipelines are considered. These rusty surfaces provide water adsorption sites that can also lead to hydrate formation. The chemical potentials of the hydrate guest molecules will be different across the phases due to the inability of industrial or real systems outside of laboratory to attain equilibrium. However, hydrate formation cannot occur directly on the surfaces covered by rust. This is because the distribution of partial charges of hydrogen and oxygen in the lattice are incompatible with the atom charges in the rusty surface. But the rusty surface works as a catalyst that helps to take out the water from the gas stream via the process of adsorption, and hydrate formation can follow slightly outside of the first two or three water layers of about one nanometre.

This project is the application of a new thermodynamic scheme for evaluation of risk of hydrate formation during transport and processing of hydrocarbons containing water; for the first time, applying it on data from real gas fields in offshore, taking into consideration the

impact of solid surfaces as an alternative route to hydrate nucleation and growth. Since in real industrial processes, natural gas which is predominately methane also contains some amounts of higher hydrocarbons like ethane, propane and isobutane, this work evaluate the risk of hydrate formation when significant amount of structure II hydrate formers (propane and isobutane) in the natural gas stream and the impact of impurities of carbon dioxide and hydrogen sulphide are also evaluated.

1.1 Objective of the project

The main objective of this work is to evaluate the risk of hydrate formation during processing and transport of hydrocarbons using data of real offshore natural gas field, which has significant amount of hydrate formers of both structure I and structure II, applying a novel thermodynamic scheme where the movement of the guest molecule in the water lattice is taken into account. Risk analysis here refers to the "maximum water content that should be permitted in hydrocarbons gas streams to prevent the risk of hydrate formation". Evaluation is to be based on two alternative routes to hydrate nucleation; the classical dew-point approach currently employed by the industry, and a new concept where hydrate nucleation could occur from adsorption of water onto rusty surfaces of internal walls of processing equipment and gas transport pipelines. Then compare results and make inferences on the different routes. The specific objectives of this project are to:

- Write on classical theory of hydrate formation, and alternative routes to hydrate formation.
- Comprehensively verify the thermodynamic scheme/model. The model is to be validated with experimental data for pure and binary mixtures of hydrocarbons, and if possible ternary mixtures of hydrocarbons also. Verification should include structure II guest molecules (propane and isobutane). If possible, verification should also be done for mixtures of hydrocarbons containing carbon dioxide (CO_2) and hydrogen sulphide (H_2S).
- Evaluate the maximum water content permitted in hydrocarbons to prevent the risk of hydrate formation during processing and pipeline transport of hydrocarbons using both the classical dew-point approach currently used in the industry and the new concept of adsorption of water on hematite (rust). Compare results and make inference in respect of the new concept.
- Real well data from offshore, preferably from the North Sea of Norway should be used for the investigations.
- Some sensitivity analysis based on composition, temperature and pressure conditions should be performed.

2 Hydrate

Natural gas hydrates also known as clathrate hydrates are non-stoichiometric crystalline inclusion compounds that are formed when hydrogen-bonded water molecules form three-dimensional solid cage-like structures with cavities which entrap suitably small sized molecules of certain gases and volatile liquids known as guest molecules. The hydrogen bonded molecules are referred to as “hosts” to the “guest molecules” entrapped in the cavities of the lattice. The empty clathrate, that is without guest molecule occupying the cavity is not stable thermodynamically [7]. Therefore, guest molecules with diameter smaller than that of the water cavities must occupy the cavities at specific temperature and pressure, characteristically low temperatures and high pressures conditions to obtain thermodynamically stable hydrates. The guest molecules stabilize the hydrate.

Guest molecules as mentioned above are components in hydrocarbon stream (including some inorganic components as impurities) that can be entrapped in the water cavities to form gas hydrates. The common guest molecules include methane (CH_4), ethane (C_2H_6), propane (C_3H_8), iso-butane (C_4H_{10}) and some non-hydrocarbons-especially carbon dioxide (CO_2), hydrogen sulphide (H_2S) and Nitrogen (N_2) [3]. At typical hydrate formation conditions in oil and gas processing and pipeline transport, some guest molecules like nitrogen are not able to form hydrate as pure components [8], and pure normal-butane also cannot form a stable hydrate [9-11]. It is the guest molecule that determines the type of hydrate structure that will be formed [12]. Hydrate formation rate can also be dictated by the size and interaction characteristics of guest molecule. For example, considering the behaviour of pure methane, pure propane and pure hydrogen sulphide hydrates; at a particular temperature, less pressure is required for the formation of hydrate of pure propane compared to the higher pressure required for hydrate of pure methane to form, however propane is relatively less soluble in water compared to methane [12]. The reason is the perfect fit of propane to the large cavity of structure II and a strong short range interaction between the atoms in propane and water in the cavity. Natural gas is mainly made up of methane component, meaning we have more methane molecules in hydrocarbon stream from gas reservoirs. The smaller size of methane molecule coupled with its higher activeness and random motion makes it more difficult to form hydrate compared to propane. On the other hand, hydrogen sulphide with similar size has higher solubility compared to methane, and the rate of formation of its hydrate takes approximately only 5 per cent [12] of the time required to form methane hydrate. Hydrogen sulphide molecule also gives greater or extra stabilization to the lattice, by reason of average

extra attraction due to columbic interactions. The average field from partial charges in water (due to the dipole moment) constituting the cavity walls is negative inwards in the cavity. The average partial charges of H_2S results in an average positive coulumbic field outward since the negative S in centre contains most of the mass and the positive hydrogen are pointing outwards when the molecule rotates in the cavity. Carbon dioxide shows the opposite coulumbic effect since the negative charges on oxygen points outwards during rotation. But the short range interactions between CO_2 and water are strong and makes CO_2 an efficient hydrate former.

Natural gas hydrate also occur in nature and it is principally found trapped under clay or shale-sealing formations- in sediments as in sub-seafloor system, or permafrost having more but varying sealing added to the frozen layers above the hydrate zones as in permafrost with and tundra systems. There are two sources of naturally existing natural gas hydrate. The first is from biogenic degradation of organic materials in the upper crust of the earth through biological processes. About 99 per cent of trapped hydrates are from biogenic sources. Biogenic hydrocarbons are very pure and almost pure methane. The second source of naturally occurring gas hydrates is from thermogenic degradation of old (dinosaurs) and newer organic materials by high temperature at greater depth in the earth crust to release hydrocarbons.

2.1 History of Hydrate

The discovery of hydrate is dated back to 1810 when Sir Humphrey Davy [12-14] discovered the first gas hydrate, chlorine hydrate formed from chlorine and water. After the work of Davy, many other scientists started investigating hydrate through laboratory experimentations. Notable of them are Faraday in 1823 [15] who confirmed the chlorine hydrate, Woehler [6] reported gas hydrate from hydrogen sulphide in 1840, Wroblewski [16-18] who investigated carbon dioxide hydrate in 1882, Ditte (1882) [19], Maumene (1883) [20], and Roozeboom (1884) [21] that reassessed the water-chlorine ratio proposed by Faraday (1823) [15], and Cailetet and Bordet (1882) [22] that first measured hydrates formed from two components mixture [Sloan book]. But hydrates of hydrocarbons were only discovered seventy-eight (78) years after Davy discovered chlorine hydrate by Villard [23]. He was the first to measure hydrates of hydrocarbon in 1888; hydrates of methane (CH_4), ethane (C_2H_6), ethene (C_2H_4), ethyne (C_2H_2), and nitrogen dioxide (N_2O). Before the 19th

ended forty hydrate formers had been known, and hydrate science was perceived as an evolving subject focused particularly on thermodynamic studies [24].

Then, hydrate as a cause of plugging of natural gas pipeline became acknowledged in the 1930's through the work of Hammerschmidt [1] in 1934. Consequently, extensive research activities covering several areas of hydrate with focus on preventing its formation began. These research efforts were focused on evaluation of the composition of hydrate together with the impacts of various hydrate inhibitors on hydrate formation process up to initial correlations applied for estimation of hydrate phase equilibrium [14]. However, the knowledge of hydrate structures was just a puzzle before the 1930s, during which a hydrogen-bonded water lattice with cavities for the hydrate forming guest was propounded with van der Waals type of interactions between guest (hydrate former) and host (water). These ideas were validated between 1951 and 1952 when two hydrate structures, hydrate structure I and hydrate structure II were discovered by use of modelling and X-ray crystallography [25-29]. The recognition of hydrates as "clathrates" is based on Powell's nomenclature for inclusion compounds having molecules of guests trapped in cavities of the lattice of a host [30]. The development of statistical mechanical model by van der Waals and Platteeuw [31], and Barrer and Stuart [32] followed, which took into consideration the stability of hydrate lattices and several unique hydrate properties, for example non-stoichiometry, thanks to the knowledge of hydrate structure and thermodynamic information already available. Macro-scale thermodynamic properties like temperature and pressure of gas hydrate, utilizing micro-scale properties like intermolecular potentials became possible to be evaluated. Measurement of different properties of hydrate became possible by the application of physical methods after 1970; this includes being able to measure guest distribution over the cages of hydrate and composition of hydrates [24]. Moreover, a new hydrate structure type having larger guest molecules was identified as structure H [33].

A new era of hydrate studies led to the discovery of naturally occurring natural gas hydrates. In 1963, the first well [34] that revealed the possible occurrence of natural gas hydrate was drilled in Siberia by Makogen and his group. It is called Markhinskaya well. This led to the hypothesis [2, 35] of the occurrence of accumulations of natural gas hydrate in cold layers by Yuri Makogan. But experts seriously doubted Makogan's hypothesis and that the idea required experimental validation. Makogan finally verified his idea by experimentation in 1965 [35] that gas hydrates could accumulate by way of large natural deposits in porous rock. Following that, the first major natural occurring gas hydrate deposit in permafrost was discovered by the Soviet Union [36]. Makogan's discovery was officially

acknowledged and recorded in the Soviet Union in 1969; thus, he is recognised as the first to discover in-situ hydrate. Masssayokha gas hydrate field in the Soviet Union is where the first significant hydrate deposits in permafrost was discovered. The hydrate layer was assessed to be about 900 metres [3] deep in this gas reservoir was projected to be around thirty-three per cent or more of the entire quantity of natural gas that is available in the Masssayokha field. Ginsburg and Soloviev [37] in 1995 gave estimates of the world's natural gas in natural occurring hydrate in agreement with the work of [38]. Though the estimates are controversial, they are 5.7×10^{13} m^3 of natural gas in hydrates in land and 3×10^{13} m^3 natural gas in hydrates in oceans.

Later, more evidences of the occurrence of natural gas hydrate reservoirs were discovered in some other places. In 1972, a core of hydrate was found in the western hemisphere both at Alaska in the United States [39] and in Canada (MacKenzie Delta) [40]. Weaver and Stewart [41] in 1982 together with [42] in 1983 have shown well log responses in the Artic Archipelago area. And the summary of naturally occurring hydrates has been done by [43] in 1982 and [44] in 1995.

As at 2008, a total of twenty-three hydrate cores [3] have been found in the ocean (including Gulf of Mexico and 3 Soviet Union water bodies). And the finding of naturally existing hydrates in the earth initiated several research activities in several countries like USA, Japan, China, Canada etc. with focus spanning estimation of different properties of hydrates required for geological study and recovery to assessment of the feasibility and the quantity of recoverable gas from permafrost. Up till now studies on gas hydrates have continued with the latest development of pilot test production at Alaska in the United States of America and at Japan, off the Coast of Honshu Island [14].

2.2 Hydrate structures

Water gets an entropy penalty for needing to relate to an "intruder". The intruder here is the guest molecule like methane. It therefore minimizes the entropy penalty by organizing into a rigid (relative) lattice around the intruder. This is because water wants to be as close to other water as possible in consideration of the intruder (the intruder has volume and shape). The type of lattice formed determines the type of intruder that can be entrapped, therefore the structure of clathrate hydrate that would be formed. Many different hydrate structures are known. But structure I (sI) and structure II (sII) proposed by Clausen [25-27] are the

commonest structure types of natural gas hydrates that we come across in the natural gas industry. Structure H (sH) is considered the third hydrate structure [33]. It is not as common as the previous two, and we could not find any reference with record of it being found in industrial hydrate plug during processing or transport of natural gas. But it is more common than all other unusual structures that are formed from other compounds which are not natural gas guest molecules (including Jeffrey's structures III to VII [45]). The composition of each of the three structures is different. The smallest symmetrical unit crystal which is repeated in all cubic dimensions into macro crystals is known as a unit cell [12]. Details of the three major or recognized hydrate structures are presented below.

Each unit cell of structure I hydrate comprises forty-six (46) water molecules, and has two small and six large cages. The sI hydrate is formed from two types of cages known as dodecahedron (small cages) and tetrakaidecahedron (large cages). The dodecahedron cavity with twelve-sided polyhedron having pentagonal faces is represented as 5^{12} as proposed by [45]. The "5" stands for pentagonal face and "12" is the number of faces. Likewise, the tetrakaidecahedron cavity with fourteen-sided polyhedron with twelve pentagonal faces and two hexagonal faces can be represented as $5^{12}6^2$ [45]. The dimension of a cubic unit cell also known as cell constant of sI hydrate is approximately 12.01 Å at a temperature of 273.15 K. Normally, small hydrate formers like methane and ethane can form hydrates of both sI and sII. Both pure components and mixtures of CH_4, C_2H_6, H_2S and CO_2 will mostly form hydrate of sI.

Structure II hydrate type was first analysed by piston cores in water depth of 530 to 560 metres on the Gulf slope offshore of Louisiana [46]. The relative abundance of both propane and isobutane in the hydrate was the basis for identifying it as hydrate structure II [46]. This was validated by the use of solid-state nuclear magnetic resonance (NMR) [47]. The hydrates of structure II, like structure I are also made from two types of cages: dodecahedron (small cage) and hexakaidecahedron (large cage), also represented as 5^{12} and $5^{12}6^4$ respectively. The unit cell of sII hydrate structure comprises 136 water molecules, with 8 large and 16 small cages and a cell constant of 17.36 Å at a temperature of 273.15 K. The available space in the cages compared to the dimension of the guest molecules entering them determines the type of hydrate structure that will be formed. The actual stabilization of the hydrate depends on short range interactions referred to as van der Waal type interactions, but it is coulombic interactions between partial charges in guest molecules and host molecules in the lattice with no chemical bonding in some other cases [48]. Hydrogen sulphide is a good example. It has a dipole moment which is sufficiently strong to have substantial coulombic attractions towards

water in the lattice, yet weak as much as necessary to make certain that the water lattice does not collapse [8]. Due to the size of propane and isobutane molecules, being too large to fit into the large cavity of structure I, they can only forms hydrate of sII by occupying the large cavity. The small cage of sII is very similar to the small cage of sI, and therefore it can be occupied by smaller guest molecules like methane to stabilize the structure II hydrate. However, in a mixture of methane and propane, structure II hydrate will form first till the propane is used up in the formation process before the methane will start to form hydrate of sI. It is appropriate to state here that without the presence of propane and larger hydrocarbons molecules in the gas, only hydrates of sI would be formed.

Even though structure H hydrate type is not commonly encountered in industrial operations, naturally occurring Structure H hydrates have been reported in Gulf of Mexico [49]. And Mehta and Sloan [50] proposed that structure H hydrate may possibly occur in nature considering the common occurrence of petroleum. In addition, the phase equilibria data of [50] also give the indication that sH hydrate might coexist with sII hydrate. Structure H hydrates produced in the laboratory can entrap molecules larger than the guest molecules of both sI and sII hydrates. Common petroleum molecules like isopentane and others with diameters as large as 7.5-8.6 Å [50, 51] can be hosted by sH hydrate; it can host up to C_7. Structure H hydrate comprise of three cavity sizes. In sH, we have three pentagonal dodecahedrals in the small cavity represented as 5^{12}, the medium cavity has two irregular dodecahedron denoted as $4^3 5^6 6^3$, and the large cavity has one icosahedron that is signified by $5^{12}6^8$. The smallest cage of sH is similar to the small cavities in sI and sII, on the other hand the largest cavity is bigger than the large cavity in both sI and sII. In the presence of a smaller "help" molecule like methane, larger guest molecules like cyclopentane, cyclohexane and benzene can occupy the largest cavity.

The classic gas hydrate structure with molecules of water linked together to form cages and showing entrapped gas guest molecules is illustrated in Figure 2.1. And Figure 2.2 presents three commonest hydrate unit crystal lattices. While the summary of the structural properties of the three hydrate structure types, sI, sII and sH are given in Table 2.1. However, in this work only sI and sII are investigated since they are the hydrate structures encountered in industrial applications during processing and pipeline transport of hydrocarbons. To our knowledge (at the University of Bergen) structure H has not been reported even for hydrocarbon systems containing molecules that could fit into structure H. One reason could be that structure H is more complex, with three different types of cavities organized in a systematic fashion. Yet another reason might be the need for simultaneous access to hydrate

forming molecules that stabilizes the wide (relative) variety in cavity sizes of the structure. Typical mixtures that forms this structure is combinations of methane and volumetrically compact hydrocarbons of C_6 and C_7 like for instance neohexane and cycloheptane, which is not normally very abundant in typical hydrocarbon mixtures. This can also been seen from Table 2.1. The small and medium cavities fit methane very well. Medium cavity is slightly small for ethane and propane, while the large cavity is not large enough for normal alkanes of C_6 and C_7. Thus, in subsequent sections, only the first two hydrate structure will be mentioned and investigated since they are the hydrate structure type that are relevant to this study.

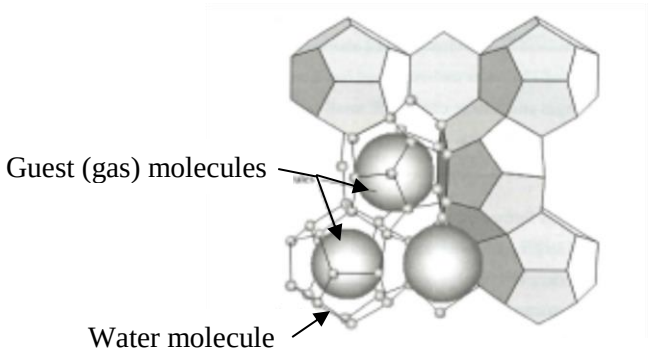

Figure2.1: Typical illustration of gas hydrate structure with water molecules linked together to form cages and trap gas molecules (like methane, propane and so on) [52]

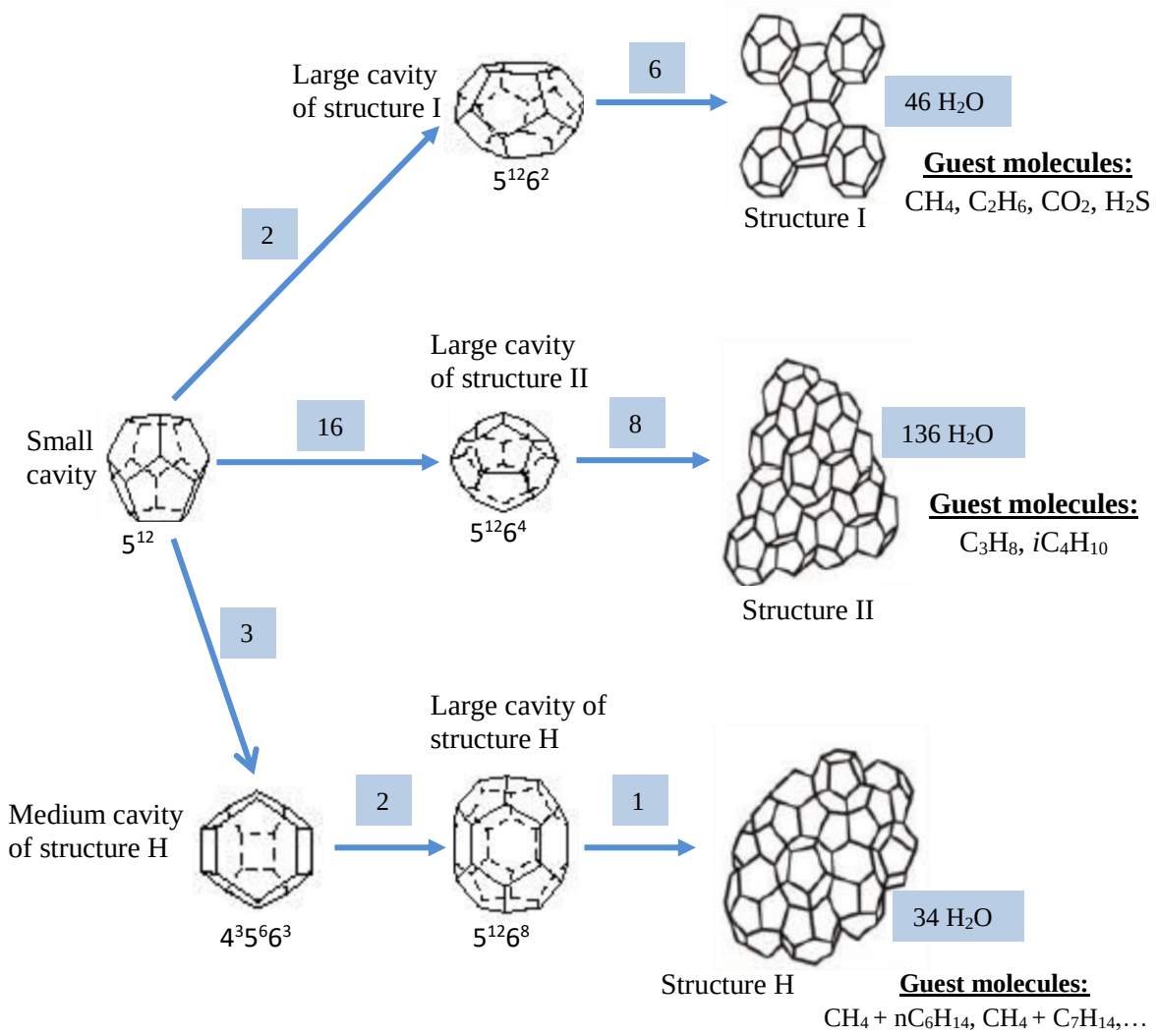

Figure2.2: Schematic illustration of structure of gas hydrate (modified from [53, 54])

Table 2.1: Summary of hydrate crystal structures [54]

Hydrate crystal structure	I		II		H		
Cavity type	Small	Large	Small	Large	Small	Medium	Large
Description	5^{12}	$5^{12}6^2$	5^{12}	$5^{12}6^4$	5^{12}	$4^35^66^3$	$5^{12}6^8$
Number of cavities per unit cell	2	6	16	8	3	2	1
Number of water molecule per unit cell	46		136		34		
Average cavity radius (Å)	3.95	4.33	3.91	4.73	3.91*	4.06*	5.71*
Coordination number^	20	24	20	28	20	20	36

**Estimates of structure H cavities from geometric models*
^Number of oxygen at the periphery of each cavity

2.3 Filling and stabilization of cavities

The relationship between hydrate forming guest molecules size and the hydrate structure type that would be formed is illustrated in Figure 2.4. Guest molecules with diameter between 4.2 Å and 6.0 Å generally form sI hydrate. To reiterate, the guest molecules that form sI hydrate type are methane, ethane, carbon dioxide, and hydrogen sulphide. While guest molecules with diameter between 6.0 Å and 7.0 Å (like propane or isobutane) would form sII hydrate type. Molecule with sizes below 4.2 Å and above 7.0 Å diameters will form no hydrate. From this illustration, we can say that the hydrate structure type formed chiefly depends on guest molecule's size; that is the hydrate structure formed is dependent on the space available in the cages relative to size of the guest molecules to be entrapped. But actual stabilization depends on short range interactions known as van der Waal type interactions, and in some circumstances like the case of hydrogen sulphide (H_2S) which is a slightly polar molecule, coulombic interactions between partial charges on the hydrogen and oxygen atoms in the water (the host) molecule in the cages and the hydrate forming guest molecules without chemical bonding. This is a result of the average inward negative field inside the water cavity (from the oxygen atom) facing the average positive charges on the hydrogen atom/ion in the H_2S molecule Figure 2.3. Detail discussion on this can be found in [55, 56]. Hydrogen sulphide (H_2S) has a dipole moment which is sufficiently strong to have substantial coulombic attractions towards water in the cages but weak enough to make sure that the water cages do not collapse [8]. Hydrogen sulphide is a better hydrate former than expected due to the impact of its polarity [55]. So also, the quadrupole moment of carbon dioxide causes average net stabilization effect from columbic interactions between the outer negative oxygen molecules of the CO_2 and the inward negative field from H_2O [57].

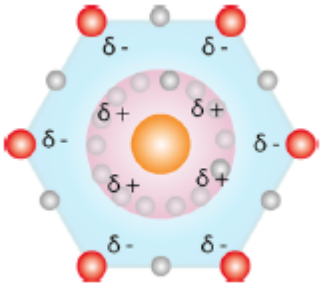

Figure 2.3: Schematic 2-dimensional illustration of H_2S behaviour in a hydrate cage or cavity [55, 58]. The red circles represent water oxygens in the walls of the cavity, and the gray circles show water hydrogens that would like to line along the water connection. The other hydrogens will have variable tipping (in and out of cavity);and on the average the sampled net balance [55, 58] is a -ve electrostatic field inward in the hydrate cavity. The H_2S has a +ve centre on the central "S"

(represented in orange colour), thus, the rotational modes of H_2S in the hydrate cavity result in an average +ve electrostatic field facing outward toward the walls of the hydrate cavity.

Other factors that could also determine the hydrate structure type are the conditions and the particular guest molecule. When another guest molecule is brought in as a second hydrate former, the issue becomes complex. For example, in Figure 2.4, it is sII hydrate type that Nitrogen (N_2) would form. But when methane or carbon dioxide is introduced, it is sI hydrate type that would be formed. But when a methane-nitrogen hydrate is subjected to high pressure condition, the hydrate changes back to sII. In contrast, a carbon dioxide-nitrogen hydrate does not undergo such change back to sII under high pressure [59]. Thus, it can be stated here that guest molecules give stabilization to the water cavity through both cavity filling and attraction to the water molecule. A summary of what stabilizes cavities is tabulated in Table 2.2.

Table 2.2: What stabilizes water cavities.

What stabilizes cavities	Reasons
Size and shape	Water lattice cannot collapse because the size and shape prevent it from collapsing.
Water-guest attraction	Assist in holding the water molecule together.
Coulombic interactions	Average extra attraction due to some coulombic interactions: In some cases like H_2S gives extra stabilizations in addition to hydrogen bonds as empty hydrate.

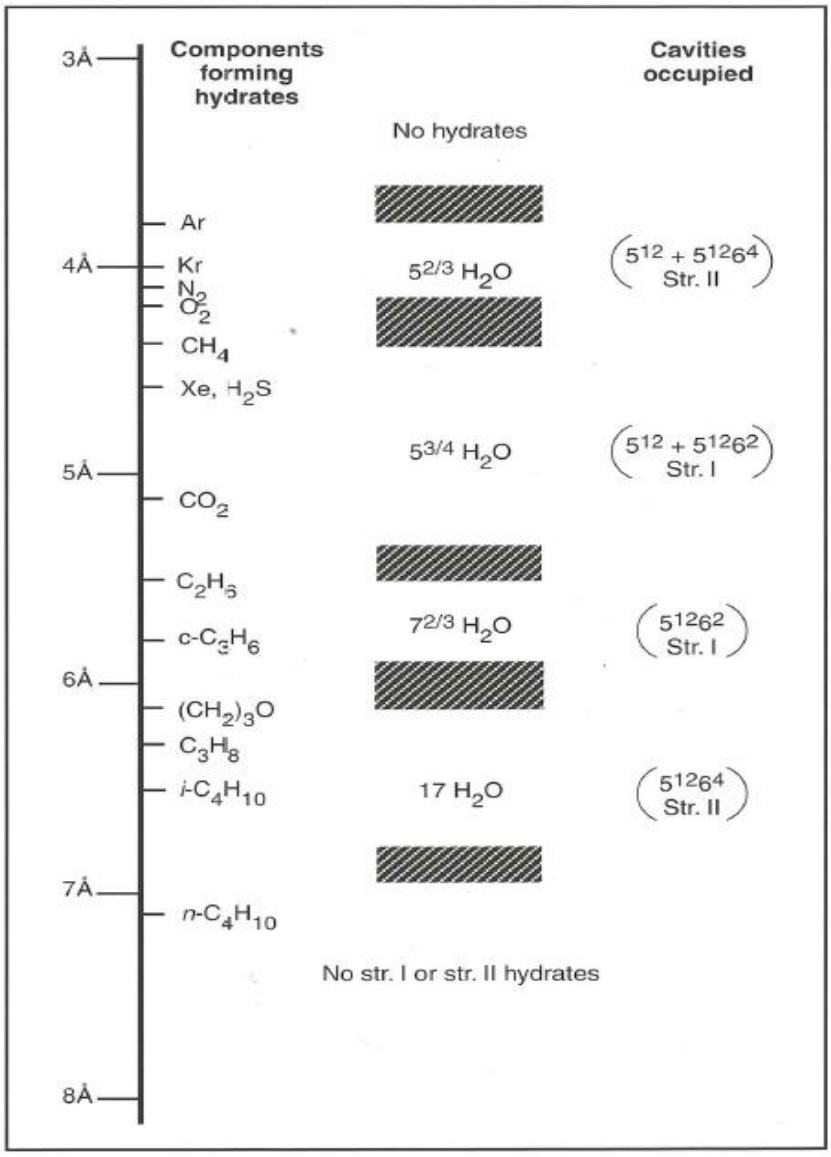

Figure2.4: Illustration of the relationship between hydrate forming guest molecules size and the hydrate structure type that would be formed [60].

3 Kinetics of hydrate formation

Gas hydrate formation occurs under the conditions of high pressure and low temperature, with sufficient amount of water and presence of hydrate former(s) like methane, ethane, propane, isobutane, carbon dioxide and hydrogen sulphide. However, hydrate formation is dictated by Gibbs free energy despite the fact that other factors like transport of heat of formation from the system and mass transport (supply) of constituents also play very significant roles. Hydrate formation occurs when the free energy of the hydrate phase (the new phase) is lower (that is having a higher negative value) than the free energies of the separate guest molecules phase and the separate water phase, because thermodynamics favours the lowest or minimum free energy. Systems will always move towards the lowest Gibb's free energy possible because not all systems can attain equilibrium, as it is for hydrate formation in industrial processes and in nature; it is a non-equilibrium process. For example a system involving one hydrate former, like methane and separate water phase, the free energy of the methane hydrate phase must be less than the free energies of both the methane in its separate gas phase and the separate water phase.

Hydrate formation process can be described using the classical theory of crystal formation and growth. The classical theory was introduced in the 1930s and it is chiefly credited to the works of Volmer and Weber [61] and Becker and Döring [62]. Other noteworthy works in this field are that of [63] and [64]. Figure 3.1 summarizes how to model hydrate formation based on the classical theory.

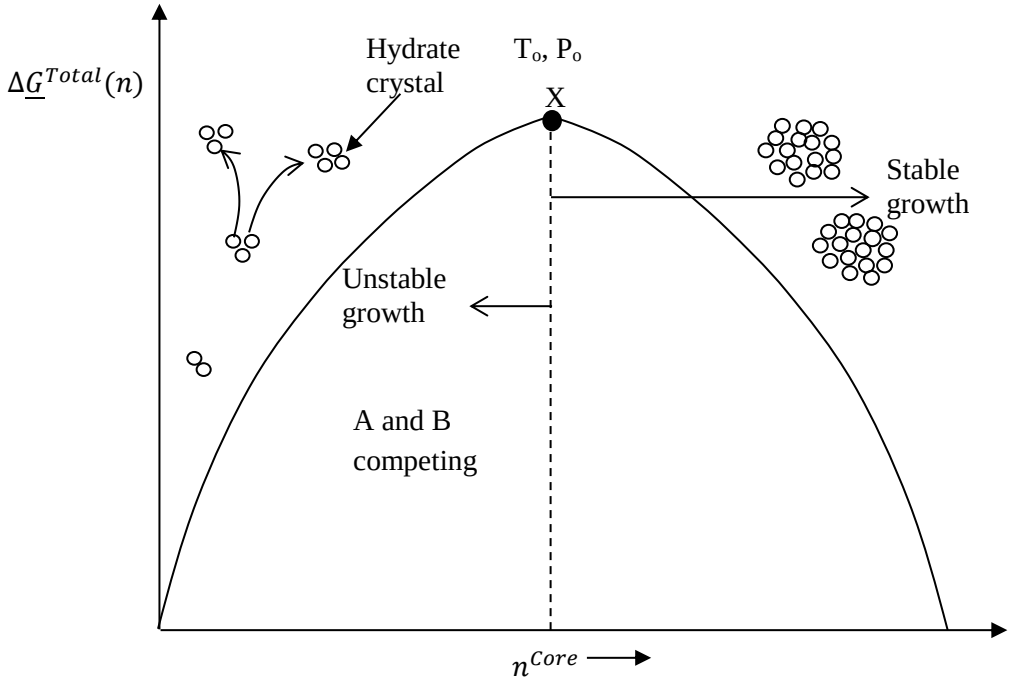

Figure3.1: Description of hydrate formation using classical theory of crystal formation and growth [8]

In Figure 3.1, "*n*" signifies the number of water molecules in hydrate core, while "$\Delta \underline{G}^{Total}(n)$" is the free energy change for a hydrate core. The free energy change of a growing hydrate core depends on two contrary contributions represented by "A" and "B", competing for dominance. Where "A" is the *benefit* of going into new (hydrate) crystalline phase as a result of phase transition to a hydrate crystal being favourable, that is having the most negative free energy. It is represented as $\Delta G^{Phase\ transition}$, which is free energy per unit volume. And "B" is the *work penalty* needed to push away the surroundings (the old phase) to give space for the hydrate core (the new phase). The penalty is given as "$\gamma . Area$," where "γ" is the interface free energy per unit area in Joules/m^2, and "$Area$" is the contact area between hydrate core and surroundings. The net free energy for these two competing processes, at a given temperature (T_o) and pressure (P_o), that is "A" and "B" is given as:

$$\Delta \underline{G}^{Total} = \Delta G^{Phase\ transition} . n^{Core} - \gamma . Area\ (n^{Core}) \qquad (3.1)$$

$\Delta \underline{G}^{Total}$ can be re-written to per water molecule through filling fractions, that is ΔG in Joule/mole H_2O instead of $\Delta \underline{G}^{Total}$ in Joule. Point X in Figure 3.1 represents an extreme point, a transition point (turning point) from unstable growth to stable growth of the hydrate

core due to the competition between the benefit and work penalty. And the radius of the hydrate critical core, R^H at this point which is the smallest core that can grow steadily is known as critical core radius. If we have a spherical core which is typically used crystal growth analysis as illustrated in Figure 3.2, then:

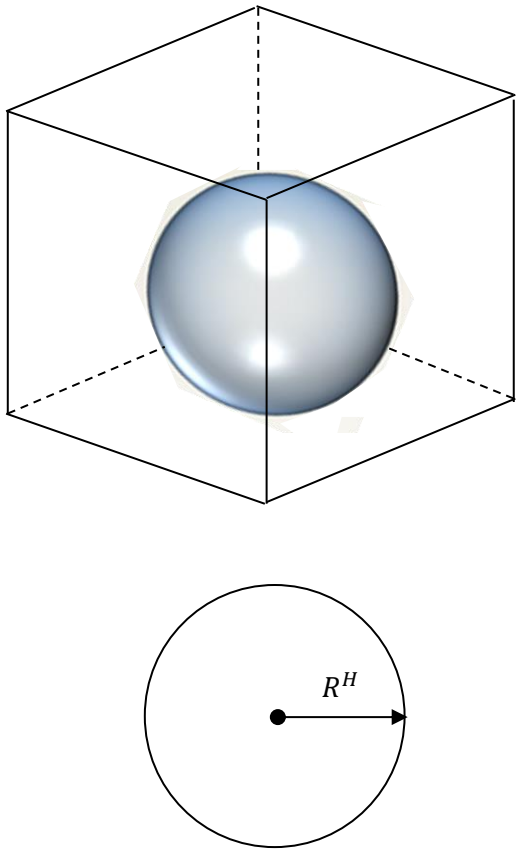

Figure3.2: Spherical core which is typically used crystal growth analysis as illustrated

$$n^{Core} = \rho_N^H . X_{H_2O}^H . \frac{4}{3}\pi (R^H)^3 \quad (3.2)$$

Where:

ρ_N^H is molar or molecular density of the hydrate core

$X_{H_2O}^H$ is mole-fraction of water in the hydrate core

and,

$$\text{Area} = 4\pi (R^H)^2 \quad (3.3)$$

Using equations (3.3) and (3.3) in (3.1), it can be re-written as:

$$\Delta \underline{G}^{Total} = \Delta G^{Phase\ transition}.\rho_N^H.X_{H_2O}^H.\frac{4}{3}\pi(R^H)^3 - \gamma.4\pi(R^H)^2 \qquad (3.4)$$

To obtain the R^H, we can find the first partial derivative of $\Delta \underline{G}^{Total}$ with respect to R^H at point X (derivatives at turning point is equal to zero):

$$\frac{\partial \Delta \underline{G}^{Total}(n^{core})}{\partial n^{core}} = 0 \qquad (3.5)$$

or

$$\frac{\partial \Delta \underline{G}^{Total}(n^{core})}{\partial R^H} = 0 \qquad (3.6)$$

$$\frac{\partial}{\partial R^H}\left[\Delta G^{Phase\ transition}.\rho_N^H.X_{H_2O}^H.\frac{4}{3}\pi(R^H)^3 - \gamma.4\pi(R^H)^2\right]$$

$$\pi(R^H)^2\left[\Delta G^{Phase\ transition}.\rho_N^H.X_{H_2O}^H\right] - 2\pi(R^H).\gamma = 0$$

$$\boldsymbol{R^H = \frac{2.\gamma}{\Delta G^{Phase\ transition}.\rho_N^H.X_{H_2O}^H}} \qquad (3.7)$$

Based on this oldest theory, we can divide the hydrate formation process into two separate physical stages or processes:

i. Nucleation of hydrate core
ii. The hydrate core stable growth stage

A third stage is a result of many different effects and often called the induction stage, or "onset of massive growth": The induction stage. Comprehensive discussion of this is found in Subsection 3.1.3.

3.1 Hydrate formation stages and theories

In this subsection, the two hydrate formation processes (or stages) and induction stage mentioned in above are discussed.

3.1.1 Nucleation of hydrate core and theories of hydrate nucleation

Hydrate nucleation process is a microscopic occurrence that involves the formation of small (micro-scale) clusters or nuclei of the new phase (hydrate phase) which are capable of growing irreversibly to macro-scale large sizes. This process, as the first stage of hydrate formation, comprises the two competing processes mentioned above, the benefit of going into or of stability of the new (hydrate) crystalline phase and the work penalty required for pushing the surrounding out of the way to make space for the formation of the hydrate core. Natural physical randomness related to mass transport and heat transport is involved in the progress towards stable growth. During nucleation, the growth and spreading of clusters of hydrate core from water and gas (as the guest molecules) is towards the attainment of the hydrate critical core radius (R^H) after which stable continuous growth can occur. And to attain this critical radius or size, the benefit, which is the overall gain in growth of hydrate dominates the work penalty associated with pushing away the surrounding to create space for the hydrate core to continue to form and grow. The nucleation process is hard to observe because it is a nano scale process that involves tens to hundreds of molecules aggregating and spreading (see Figure 3.1) to attain the critical size [3]. The critical size could be around 1-5 nanometres; consequently it is likely immeasurable [8]. The randomness is about the directions and momentum of movement of the building molecules. In the course of the nucleation, the exchange of energy as well contains random elements although heat will be primarily transported in directions of fastest heat transport. The rate of the system's local heat transport determines the amount of heat that can be transported out of the system during the process of hydrate formation. This rate is not fast in areas with high concentrations of hydrate guest molecules, but it is fast through hydrate and water [57].

From the works of Mullen, [65] and Kashchiev and Firoozabadi [66] on the theory of nucleation in crystallization, there are two types of nucleation, homogenous and heterogeneous nucleation. Homogenous nucleation of hydrate core takes place in a single phase. Outside the laboratory it is not a usual occurrence to observe. It does not mean that it does not happen but the solubility of hydrocarbons in water is very small. When hydrate is formed it is the lowest free energy phase of water and will control the possible remaining hydrocarbons of each type in the presence of hydrate. Typical examples can be found in [67-71]. Carbon dioxide is more soluble in water and although it does not adsorb well directly on Hematite (xx, yy) it can upconcentrate in structured, adsorbed water on Hematite. It will also have a higher solubility in a water film outside the water layer adsorbed on Hematite. Hydrate

formation from carbon dioxide phase outside the water film can be followed by homogeneous hydrate formation in the water film as well as heterogeneous hydrate formation for carbon dioxide that adsorbs on the initial hydrate film from below. So it is difficult to come by in practice. However, there is a possibility of hydrate to form in a homogenous system having a hydrate former's molecule dissolved in water [72]. THF (Tetrahydrofuran) is one example of a hydrate former which is soluble in water and which have been used in many laboratory and pilot studies related to fluid flow containing hydrate particles. THF and other water soluble hydrate formers are also used as assisting components to promote carbon dioxide hydrate formation in concepts for the use of hydrate for separation of carbon dioxide from flue gas or methane [73-76].

A case where formation of hydrate right in the aqueous phase from hydrate former dissolved in water is an example of homogeneous nucleation. There are more molecules than can possibly collide at the same time, therefore a successive biomolecular collisions of an autocatalytic characteristic is rather more feasible [3]. One type of heterogeneous nucleation of hydrate core happens in the presence of a foreign body (e.g. dust microparticles) or surface (e.g., container, or pipe wall). If the solid surface has some influence on water and/or hydrate former this heterogeneous nucleation can happen at smaller supercoolings than that required by homogeneous nucleation [3]. Typical examples of surface that are active in water adsorption are Hematite (a form of rust), Kaolinite (a clay mineral) and Calcite. These minerals structure water to extremes in density. For some of these minerals hydrate formers can be trapped in adsorbed water structures or even in some cases adsorbed directly on mineral surface, like for instance adsorption of carbon dioxide on Calcite. Stainless steel and other atomistic metals without charge distributions will typically be neutral. Plastic materials, on the other hand, will be hydrocarbon wetting and can lead to accumulation of hydrate formers on plastic surface and promote hydrate induction as has been observed experimentally [77]. In porous media nucleation towards mineral surfaces compete with another heterogeneous nucleation happening on the interface between liquid water and hydrate former phase. During transport of hydrate former phase (natural gas or carbon dioxide) rusty pipelines [78] promote water drop out from hydrate former phase due to very low chemical potential of water in the first water layers adsorbed on Hematite (one of the most stable forms of iron oxides under the composite name of rust).This is the type of nucleation that is commonly encountered in industrial applications and nature.

Modelling of nucleation is fundamentally approached in two different perspectives as can be found in literature [67]. The dissimilarity in these approaches is based on where the

occurrence of nucleation originates from: whether it is in the liquid water interface or towards the guest molecule side of the interface [67].

Based on the two approaches mentioned above, there are two major theories of hydrates nucleation that exist: they are propounded in [3] and the second by Kvamme [67] and Long [79]. According to the first one, nucleation commences with dissolved gas in liquid water. Clusters are formed from water molecules around the gas (guest molecule) and subsequently, transformation of the clusters to unit cells occurs; thereby resulting in the formation of either hydrate structure I (sI) or structure II (sII) hydrates. The type of hydrate structure formed is a function of the type of guest molecule(s) (i.e., hydrate former or formers) present. The clusters eventually amalgamate to attain the hydrate critical core radius for stable growth to continue. The second theory states that nucleation occurs from the vapour (hydrate former or guest molecule) side of the interface between the water and gas. This is as a result of the huge number of the gas (guest) molecules that are required inside the hydrate, with a maximum of 15% [57]. It is hardly ever to see this kind of gas concentration dissolved in the liquid phase. The hypothesis of this second theory was originally put forward by Kvamme in his works [80-82]. His proposal agrees with recent results in Nuclear Magnetic Resonance (NMR) spectroscopy [83, 84]. According to [67] the results obtained from his works reveal that methane hydrate starts from the vapour or hydrate former side of the interface and may be most influential in the formation of hydrate from methane gas and water with the same conditions investigated by [85]. This theory is a work in progress, because it will be revise whenever new results are obtained from on-going simulation works associated with hydrate nucleation origination process [67]. At the time of this publication [67], it stated that this is the only theory that is connected with the initiation of hydrate nucleation as a surface adsorption process, in agreement with the latest investigation works at Rice University in Houston [84] from NMR measurements. The required input parameters of the model at the time of the publication are temperature, pressure, hydrate former composition, and active interface surface area [67].

However, there are some other approaches: one of them is by Sloan and Fleyfel [86] in 1991, they recommended a models for hydrate nucleation designated as the Labile Cluster Hypothesis, where the process of hydrate nucleation is stated to happen in three steps: firstly, a spontaneous occurrence of formation of clusters from a hydrophobic solute dissolved in water in thermodynamically beneficial conditions of pressure, temperature and chemical potential for hydrate formation; secondly, a number of the clusters aggregate to form a nucleus, each cluster contains one gas molecule and 20-24 molecules; and finally, several

varied configurations of nuclei is formed, however, just one stable hydrate structure will be achieved which will undergo continuous growth. But the Labile Cluster Hypothesis has been severely faulted or criticized [87] due to the much availability of both molecular dynamics and Monte Carlo simulations. Moreover, experimental data from Neutron Diffraction and Differential Scanning Calorimetry [88] revealed that the hydrated shell encapsulating methane molecule is about 1 Å larger in the hydrate phase than in solution. The data also revealed that during hydrate formation, the shell is more disordered compared to when in both solution and the hydrate phase, thereby representing noteworthy changes to the hydration shell. Labile clusters are therefore agreed to merely form simply in dilute solutions and that the energy barrier required by the clusters to amass to a critical nucleus size is enormous [89]. Another approach is that of Christiansen and Sloan [90] where no assumption is made about where the nucleation process is initiated in their model. They proposed the application of thermodynamic cycle to model hydrate formation as a standard chemical reaction, and classical thermodynamic relations is applied to model the changes in free energies in the cycle leaving from liquid water and guest molecules [67]. Other macroscopic models have been suggested by Skovborg [91] with the concepts of Natarajan [92] and Yousif **[93]** founded on different formulations of the driving forces.

3.1.2 The hydrate core stable growth stage

This is represented by the right-hand-side of point X in Figure 3.1. It is the second stage of hydrate formation which occurs after the attainment of the hydrate critical core size (and shape). The growth rate is governed by availability of water and guest molecules (guest molecules need to be supplied) and a coupling of both mass transport and heat transfer [8]. This is where the significance of mass and heat transport is chiefly crucial. Within the simple classical theory the mass transport flux in front of the thermodynamic term (the exponent of the free energy change divided by RT) is either 3 D for homogneous flux in homogeneous formation or 2 D for heterogeneous hydrate growth.

The consistent heat release (heat of formation) is given by delta ((G/T)/dt) = - delta H/(RT)^2. There is a likelihood of the mass transfer of gas to the hydrate surface to dominate in the stable growth process. And the growth of the hydrate can also be influenced by the exothermic heat of hydrate formation. If the heat is not transported away, dissociation can occur instead.

This second main process, the growth phase or stage has been modelled as a crystal growth process by [94, 95]. It is fundamentally presumed that the gas moves from the vapour phase to the bulk liquid phase, and subsequently conveyed by diffusion to a reaction site at the surface of developed nuclei, at which the gas undergoes conversion at a given rate by a constant clearly and precisely stated. Like in a 2-film theory, the rate of guest molecule transport is depended on the rate of gas-transport and transport of the dissolved gas in the liquid phase. With the assumption that the crystals are covered by liquid water in this model, there exists a theoretical ambiguity [67]. This approach has however been simplified by Skovborg and Rasmussen [96] and they proposed the application of only one rate constant connected with the liquid water/hydrate interface area, together with the differences in mole fraction of the hydrate guest molecule both at bulk and at the interface. A different modelling approach, applying classical nucleation theory to stable growth of the crystal has been proposed in [80-82, 97, 98]. Here, the chemical potentials for water in the various phases were evaluated from the TIP4P [99] model, knowing that simulations of liquid water together with hydrate [100] show that this model has the ability to rightly recreate relevant dynamic features and also chemical potentials.

3.1.3 Induction time

A third stage of hydrate formation is frequently discussed in literature as induction time [8]. This can be seen as the time for the onset of massive growth. Other words used for induction time are hydrate nucleation time or lag time in some literature [3]. From a physical point of view, as discussed above nucleation time is something different. It is the time needed to establish a stable hydrate core which will then grow unconditionally provided access of mass and that heat of formation can efficiently be transported away from the core. A hydrate film formed on the interface between liquid water and a hydrate former phase will act as a sealing membrane with very slow transport of water and hydrate former through the membrane. Without stirring that break this film several processes will occur. Hydrate will grow from dissolved hydrate formers in water. Even small amounts of hydrate can form on the hydrate former side of the initial hydrate due to dissolved water in the hydrate former phase. And the hydrate film will not be uniform in terms of free energy. The most stable hydrate regions of the film will consume less stable regions. Solid surfaces and adsorption effects also play a role in this induction period. As such induction time is not a single physical process but a multitude of processes governed by thermodynamics as well as mass transport and heat

transport. Induction time can be considered as the time for "onset of massive growth". Critical size of a hydrate is in the order of 2.5 – 3.5 nm [101], so in the order of 100 to 200 water molecules, depending on thermodynamic driving forces and access to mass. Heat transport is fast for interface hydrate in which heat is more than two orders of magnitudes faster than mass transport through liquid water. Detection of induction can be based on measurement of gas consumption for an experiment at controlled temperature and pressure, or pressure reduction in an experimental cell with constant volume. But there is a variety of possible methods for detecting solid hydrate particles and as such also a variety in the accuracy of detecting this induction time. Practically the induction time has some value if the impact of hydrodynamic effects can mimic realistic forming conditions. This is an experimental challenge which has no universal solution.

It is a qualitative issue. In contrast to nucleation that is a micro-scale occurrence, induction time is a macro-scale phenomenon that can be visually observed. Induction time is the time passed until an observable volume of hydrate phase is detected. The resolution of monitoring is proportionally to accuracy of detection, using MRI, laser, pressure change etc. The work of [102] showed stochastically varying induction time for very similar freezing water. Based on that, it should be expected that predicting more complex systems such as gas hydrate involving two or more components and two or more phases would be more complicated. However, by increasing the driving force (higher degree of subcooling) the system begins to be more predictable [103].

Normally this stage is a result of limited access to mass for further growth. As an example hydrate from methane and water is very feasible on the interface between these two phases due to access of both water and methane. And formation heat is rapidly transported away through liquid but then the film of hydrate acts as a mass transport barrier since the diffusivity coefficients for water and methane through the solid hydrate film is several orders of magnitudes smaller than that of liquid water or gas. Stirring, or other hydrodynamic disturbances, can break the film reduce or eliminate induction time. But for a system of water and methane without stirring the induction time can be long. In one example as much as 100 hours at 83 bars and 176.15 K as can be found in Trygve Buanes' PhD Thesis [77] (and the attached papers).

Also note that the classical theory approximates the boundary between two phases as sharp (no interface thickness of varying structure and properties. This is obviously an approximation and consequences vary. The impact of interface thickness between water and air at atmospheric pressure may not be of very substantial importance while liquid/solid

interface like liquid water/hydrate interfaces can be in the range of 1 to 1.5 nm (refer to the theses of Svandal and Bunanes and papers in these) and properties change very much through the interface. As such MDIT theory [67-69] avoids this approximation. Yet another limitation of the classical theory is complexity when mass for further growth becomes a limitation. A typical example of this is a continuation of the hydrate film example above. Hydrate formation on a methane/water interface is not unform because of natural physics randomness caused by mass transport from gas, capillary wave dynamics and other factors. When all access to mass is used (growth from dissolved methane in water and condensed water on initial hydrate) the free energy differences between regions of the surface will lead to dissociation of some hydrate regions so as to facilitate further growth of more stable regions. This is a result of first and second laws of thermodynamics.

3.2 Gibbs phase rule

A phase is an ensembly of molecules with unique composition and unique density at a given thermodynamic state in temperature and volume. Through the canonical ensemble in statistical mechanics this will also define a unique free energy and other thermodynamic properties as mathematical functions of that by couplings to macroscopical thermodynamics. Single phases are uniform while phases controlled/generated by fluids in contact with solids are non-uniform. Water adsorbing on mineral surfaces will have structures directed by interactions with the mineral surfaces in one direction (z) and a desire to retain as strong hydrogen bondings as possible in the plane paralell to the mineral surface. Similar for water adsorbing on a hydrate crystal with fairly rigid (relative) locations of partial charges on hydrate water molecules. Hydrate formers adsorbing on liquid water is yet another example. The selective adsorption of hydrate formers depends on the individual molecules (in a gas mixture) interaction with the water molecules and the “desire” for the molecules to condense out from gas. The latter is expressed in a more popular fashion but can be visualized more clearly in terms of thermodynamics in the “D adsorption model utilized by Kvamme to illustrate selective adsorption of CO_2 on water from a CO_2/N_2 gas mixture [104, 105].

Hydrate formation from natural gas in industrial systems such as inside gas processing equipment and pipeline transport considered in this work cannot successfully attain equilibrium consequent on the limitation imposed by Gibbs phase rule. For a system to reach thermodynamic equilibrium, the temperatures, pressures and chemical potentials of all components must be equal in all co-existing phases. Thermodynamic equilibrium

determination for heterogeneous systems with non-reactive multicomponent is achieved by the use of Gibbs phase rule. This thermodynamic equilibrium analysis technique or rule was proposed by Josiah Willard Gibbs in his revolutionary work [106, 107]. This rule is used to obtain the number of independent thermodynamic properties that is required or that has to be specified for a system to reach equilibrium. The Gibbs phase rule is given by the following expression (equation (3.8)):

$$\tau = n - \pi + 2 \tag{3.8}$$

Here, "τ" refers to the degrees of freedom, which is the defined or specified independent thermodynamic variables in the system, and "π" represents the number of actively coexisting phases, while "n" is the number of active components in terms of hydrate phase transitions. A system is under-determined if τ is more than what is thermodynamically specified, and it is over-determined if τ is less than what is specified [108].

To illustrate how the Gibbs phase rule is used, let us consider a simple situation where there is merely one hydrate guest molecule in the system having bulk gas and water, say methane and water for illustration, with the presence of a hydrate nucleus, there will be three actively coexisting phases ($\pi = 3$) and two active components ($n = 2$). Base on Gibbs phase rule, the degrees of freedom have to be just one (τ = 1) for the system to reach equilibrium. However, the system will never reach equilibrium as for a real system such as the industrial case under consideration involving flowing stream, hydrodynamics and hydrostatics including phase transitions which involves heat exchange, the local pressure and temperature are specified; which indicates that even for the simplest system with one hydrate former (methane), the system will not attain equilibrium.

And with a system that comprises methane, ethane, propane, isobutane and water, before any nucleation in the system, n is 5. If probable adsorbed phase is disregarded, then π will be 2. Then, the independent thermodynamic variables necessary to be specified for the system to attain equilibrium will be 5, that is τ = 5 - 2+2 = 5. The system is over-determined. In the same way, it will be 4 when a hydrate phase is present ($\pi = 3$) and number of active components remains constant. This system is also over-determined and cannot reach equilibrium due to the fact that maximum independent variables we can define in this case are the local temperature and pressure. Therefore, hydrate formation systems in real industrial situations especially during natural gas processing and pipeline transport cannot attain

equilibrium. From the discussion thus far, the issue becomes more complex when we have a multicomponent gas stream; that is when the system comprises multiple guest molecules. But it is important to know that the combined first and second laws of thermodynamics will always control the system towards the minimum or lowest free energy possible. From the understanding of the first and second law of thermodynamics, hydrate formation will commence with the most stable hydrate from the best guest molecules. When these best guest molecules are used up in forming hydrate, the inferior hydrate guest molecules will subsequently form less stable hydrate. What we would end up with is a range of different hydrates with gradually increasing free energies, hence, would be less stable [8]. These different hydrates are regarded as different or separate phases [8] due to the fact that each of them has distinct composition, density and free energy. Moreover, surface effects like that of water absorbed onto the rusty surfaces of gas processing equipment and pipelines used for gas transport are also considered as a separate phase. Therefore, hydrate formation in practical world will never reach equilibrium because equilibrium is only possible when the number of thermodynamic variables that are defined equals τ.

The Gibbs phase rule is only used to know the maximum possible number of phases when the number of independent degrees of freedom is specified. It does not state anything about the likelihood of these phases occurring under specific thermodynamic conditions. This rule is just the conservation of mass under the constraints of thermodynamic equilibrium [8].

3.3 The impacts of mass transport in hydrate formation

The hydrate phase transition is a nano-scale process, whether formation or dissociation process, and it is governed kinetically by what happens on a thin interface of approximately three to five layers of water, that is approximately 1 to 1.5 nanometres. Mass transport is implicitly coupled and it is a molecular scale diffusion transport [48] across the interface. The diffusivity coefficients for water and hydrate formers across this boundary layer are different from liquid water diffusion due to the more (close to hydrate core) or less (close to surrounding phase) structured water. If the surroundings are not supplied with replacements of hydrate building molecules corresponding to the consumption growth will slow down and might enter a local limit of hydrate metastability where the hydrate is in a thermodynamic balance with surroundings. This situation can easily change into dissociation if surroundings get diluted to concentration below stability limits or they can grow if diffusion of hydrodynamics supply additional mass from a larger surrounding volume. The nano scale

process of hydrate nucleation and growth is therefore implicitly linked to larger scale dynamics. Mass transport limitation and low concentration of water in the hydrocarbon gas, especially methane which is the main component in natural gas could impede hydrate core (hydrate crystal nucleus) from ever reaching the critical core radius or size. Therefore, stable growth of the hydrate core may never be possible. In consideration of mass transport, the classical nucleation rate is thus given as follows [8]:

$$J = \underbrace{J_o}_{(i)} \underbrace{e^{-\beta\left[\Delta G^{Total}.\rho_N^H.\frac{4\pi}{3}.\left(R^H\right)^3\right]}}_{(ii)} \tag{3.9}$$

$$\beta = \frac{1}{R.T} \tag{3.10}$$

If ΔG^{Total} is based on Joule/mole-hydrate.

$$\Delta G^{Total} = \frac{\Delta G^{Total}}{n^{core}} \tag{3.11}$$

Where:

(i) Is the associated mass transport across a thin interface in order to supply mass for phase transition.

(ii) Represents the thermodynamic contribution to the phase transition kinetics.

"J" is the classical nucleation rate due to mass transport, and "J_o" is mass transport across a thin interface (around 1-2 nanometres) and it is diffusion (Fick's law) by nature. "n^{core}" is number of moles in hydrate core, and ρ is density. When the critical core size of the hydrate is very small, say 20 to 50 molecules, or a scenario where the molecules are polar, the classical nucleation approach does not apply [87]. In such situations, the sharp curvature of the surface will have a substantial influence on the interfacial energy, and the structure and corresponding energy of the hydrate core may be notably different from the bulk of the hydrate crystal (new phase) [89].

3.4 The impacts of heat transport in hydrate formation

Hydrate formation is exothermic, which means heat is released during the formation process. Another possible hindrance to nucleation and growth of the hydrate core would be caused by

heat transport in the system. Hydrocarbons (for example methane) have poor thermal conductivity relative to liquid water clusters and hydrate before hydrate formation occurs [8, 109]. Carbon dioxide (CO_2) also with very small amount of water is heat insulating. These implies there would be the problem of getting rid of the exothermic heat of hydrate formation (heat of crystallization) from the system and this as well could critically restrict the rate at which hydrate would be formed.

The heat released is uniquely related to $\Delta G^{Phase\ transition}$ and the thermodynamic relationship that gives the absolute value of the heat required to be transported away is given the following expressions:

$$\frac{\partial\left(\frac{\Delta G^{Phase\ transition}}{R.T}\right)}{\partial T}\Big|_{P,\vec{N}} = \frac{-\Delta H^{Phase\ transition}}{RT^2} \tag{3.12}$$

Similarly,

$$\frac{\partial\left(\frac{\Delta \underline{G}^{Total}}{R.T}\right)}{\partial T} = \frac{-\Delta \underline{H}^{Total}}{RT^2} \tag{3.13}$$

Where:

$\Delta \underline{H}^{Total}$ = Total enthalpy change associated with a certain route to hydrate formation in Joules.

$\vec{N}$ = The vector of mole numbers in the system

T = Temperature in Kelvin

R = The universal gas constant, which is 8.3143 Joules/mole·K

The "Total" includes "benefit" plus "penalty" and both $\Delta \underline{G}$ and $\Delta \underline{H}$ are extensive; their unit is Joules. This released enthalpy must be transported away from the system if not the hydrate being formed will eventually dissociate consequently. Transport of the heat released is accomplished by conduction, convection and/or radiation. This can be evaluated numerically and analytically based on the incorporated chemical potentials models. The real heat transport dynamics, which is implicitly coupled to the phase change thermodynamics is distinct for every single phase change and given by the possible directions to transport the hydrate formation (crystallization) heat from the system. Considering the case of hydrate formation slightly outside of the first water molecules on the internal walls of hydrocarbon gas processing equipment or transport pipeline, the enthalpy of formation is transported away

rapidly in the direction of the adsorbed water layer, then it is transported out through the pipeline walls. The formation of hydrate on the interface of water adsorbed on surfaces covered by rust would hence have fast heat transport. It is also the same way in situations when hydrate is formed from dissolved or adsorbed guest molecules. And the heat transport in the system would most likely be more rapid in two to three orders of magnitudes than mass transport.

3.5 Hydrate phase diagram

Phase diagrams of water, hydrate, and hydrate formers (hydrocarbon or inorganic gases) shows hydrate stability region in terms of temperature and pressure. This is illustrated in Figure 3.3. The straight line phase boundaries here are only for illustration to help to clearly show phase transition behaviours from ice to liquid water and from gas (or vapour) to liquid hydrocarbon guest molecules. Real phase boundaries do not necessary follow straight line as shown here, but are usually curved. Almost straight boundary lines are obtained from semi-logarithm plots **[3]**. Here, "I" stands for water in ice (solid) phase, "L_w" is liquid water, "H" represents hydrate, "V" is hydrate former in the vapour phase, and "L_{HC}" is liquid hydrocarbon. Quadruple points (found in literatures) **[3]** are points where four phases coexist and are usually represented as Q_n, where "*n"* merely stands for numbers (e.g. 1 or 2, for Q_1 or Q_2) to differentiate the one quadruple point from another. Since natural gas is predominantly methane, the L_w-H-V phase boundary line is the most important pressure-temperature conditions in natural gas systems **[3]**. L_w-H_L_{HC} line is vertical indicating phase transition from vapour hydrocarbon to liquid hydrocarbon. The I-H-V phase boundary line's (pressure-temperature) slope is less than that of the L_w-H-V line.

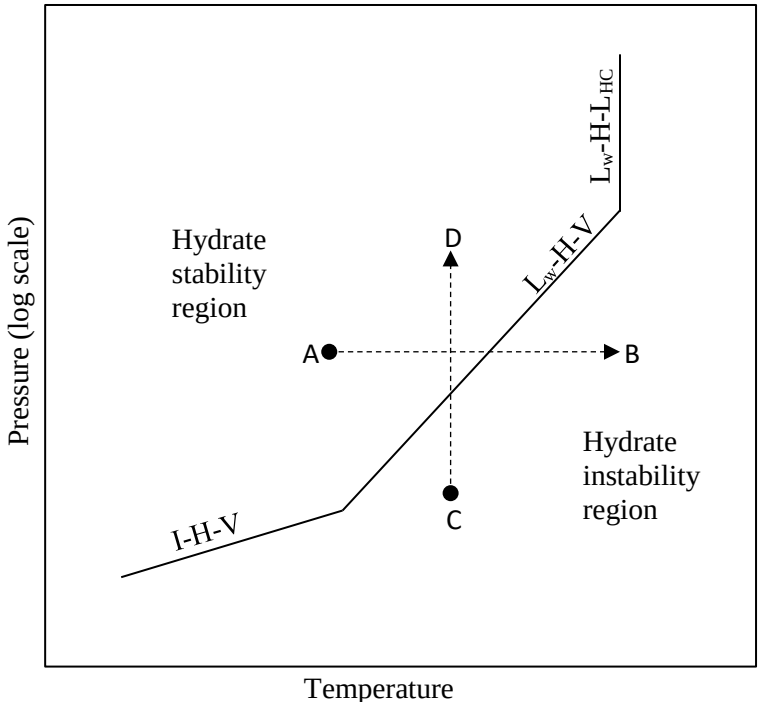

Figure3.3: Phase diagram for ice, water, hydrocarbon and hydrate

3.6 Hydrate formation driving forces

The hydrate formation driving forces are not merely temperature and pressure; kinetics of the situation also pose a limitation in hydrate formation [8, 57]. Sufficient constituents required to form hydrate must be present and need to be conveyed from other phases into the hydrate. Some hydrate formation driving forces can be found in published literature [96, 110-115]. But not much works give sufficient justifications [3] for these hydrate formation driving forces on the basis of equilibrium or non-equilibrium thermodynamics. But the work of [5] provides a lists of driving forces for alternative pathways to hydrate formation and dissociation applicable to pipeline transport of natural gas (which is relevant to this work) based on their related free energy changes as presented in Table 3.1:

Table 3.1: List of driving forces for formation and dissociation of hydrate [5].

i	δ	Initial phase(s)	Driving force	Final phase(s)
1	-1	Hydrate	Outside stability in terms of local P and/or T	Gas, Liquid water
2	-1	Hydrate	Sublimation (gas under saturated with water)	Gas
3	-1	Hydrate	Outside liquid water under saturated with respect to Methane and/or other enclathrated impurities originating from the methane phase	Liquid water, (Gas)
4	-1	Hydrate	Hydrate gets in contact with solid walls at which adsorbed water have lower chemical potential than hydrate water	Liquid water, Gas
5	1	Gas/fluid	Hydrate more stable than water and hydrate formers in the fluid phase	Hydrate
6	1	Gas + Liquid water	Hydrate more stable than condensed water and hydrate formers from gas/fluid	Hydrate
7	1	Surface reformation	Non-uniform hydrate rearranges due to mass limitations (lower free energy hydrate particles consumes mass from hydrates of higher free energy)	Hydrate
8	1	Aqueous Phase	Liquid water super saturated with methane and/or other hydrate formers, with reference to hydrate free energy	Hydrate
9	1	Adsorbed	Adsorbed water on rust forms hydrate with adsorbed hydrate formers.	Hydrate
10	1	Adsorbed +fluid	Water and hydrate formers from gas/fluid forms hydrate	Hydrate

3.7 Analysis related to hydrate

Hydrate analysis therefore follows these steps [8]:

(i) Evaluation to determine the possible phases that are active and significant with respect to hydrate phase transitions.

(ii) Perform Gibbs phase rule analysis. That is to determine if the system can reach equilibrium or not. It the system can reach equilibrium, solve equilibrium equations and conservation of mas and energy. But if the system cannot attain equilibrium like the systems investigated in this work and most real situations, then go to the next step.

(iii) Then, minimize free energy under the constraints of conservation of mass and heat. This is the technique of free energy analysis applied in this work since the reality is that hydrate formed from different phases would have different free energies due to the different chemical potential of the hydrate formers. Considering an equilibrium situation, the classical scheme applied for estimation of equilibrium is to simultaneously calculate the conditions for equilibrium, conservation of mass, and conservation of energy. But for a non-equilibrium situation, the combined first and second laws of thermodynamics are utilized in place of the equilibrium conditions by means of certain schemes for minimizing free energy locally under constraints of conservation of mass and energy. Modelling of every phase change for either hydrate formation or dissociation is implemented as pseudo reactions in consistent with changes in free energies as driving force for phase transition and coupled dynamically to mass and heat transport [116]. The free energy changes related to all phase transition is calculated from equation (2) [5]:

$$\Delta G_i = \delta\left[x_w^{H,i}\left(\mu_w^{H,i} - \mu_w^{P}\right) + x_{gas}^{H,i}\left(\mu_{gas}^{H,i} - \mu_{gas}^{P}\right)\right] \quad (2)$$

Where:

ΔG_i = free energy changes associated to all phase transition

x = composition

H = hydrate phase

I = phase transition scenario

μ =chemical potential

P = liquid, gas, adsorbed phases

w = water

gas = gas (gas guest molecule).

And as can be seen in Table 3.1, δ is +1 for hydrate formation and -1 for hydrate dissociation [5]. The chemical potentials of guest molecules in different phases are not equal; they are different as already mentioned above in a non-equilibrium scenario. This shows that the chemical potentials for the hydrate formers in the hydrate will likewise be different, as it is observed from a Taylor expansion from an equilibrium point [72].

(iv) Can any of the phases be totally consumed? If so, do the analysis based on *(i)* and *(ii)* until the number of phases have changed and repeat from *(i).*

4 Hydrates in the industry

Processing and transport are vital aspect of hydrocarbon gas (natural gas) operations. This is because natural gas is mostly produced from places (e.g. offshore, swamps and hinterland forests) which are far from its market, and processing is important to meet both transport and market quality requirements. Transport of natural gas from reservoir to the gas processing plants and for supply delivery terminals is chiefly done by the use of pipelines, especially within reasonable distance. LNG ships are used for transport involving farther distances. This section comprises analysis of both processing and transport of hydrocarbons (especially natural gas).

4.1 Natural gas processing and Hydrate formation

Hydrocarbons from the reservoir must necessarily be processed to meet quality demand or market needs. Natural gas comprises primarily methane but it also consists of other heavier hydrocarbons, inorganic or acid gases and water. Natural gas from the Troll gas field in the North Sea of Norway consist of mainly C_1 to iC_4 and nC_4, but that from Sleipner gas field comprises also significant amount of carbon dioxide (an inorganic gas). Risk of hydrate formation in both gas fields are investigated in this study. Processing of hydrocarbon gases involves separating out some of the heavy hydrocarbons' components (C_{2+}), inorganic gases like H_2S and CO_2 (for instance, CO_2 in Sleipner gas), and other fluids like water (H_2O) to meet transport and/or market requirement [117]. It is vital to separate the following components out to certain required extent [117]:

- Carbon dioxide (CO_2) as it is corrosive, it does not have heating value, and could also crystalize during cryogenic gas processing.
- Hydrogen sulphide (H_2S) because it is corrosive and toxic. The standard market specification for processed gas is around 6mg/Sm3 or approximately 4 ppmv [118].
- Heavy hydrocarbon (C_{2+}) since they could drop out as liquid during transport.
- Water (H_2O) pose hydrate formation risk, which when occurs would plug gas processing equipment and transport pipeline, it also leads to the risk of corrosion of the processing equipment and transport pipelines.
- Nitrogen (N_2) like CO_2 does not have any heating value.

- Mercury (Hg) is also removed because it is toxic and corrosive, especially with aluminium-based alloys.

The key hydrocarbon gas processing operations are presented in Figure 4.1. The initial step involves separation of the liquid components (liquid hydrocarbons and liquid water) that may be present. The subsequent step depends on the means of transport or transport system required or chosen; mostly pipelines and LNG carriers or ships, and depending mainly on the distance and the available infrastructures. This project focuses on pipeline transport.

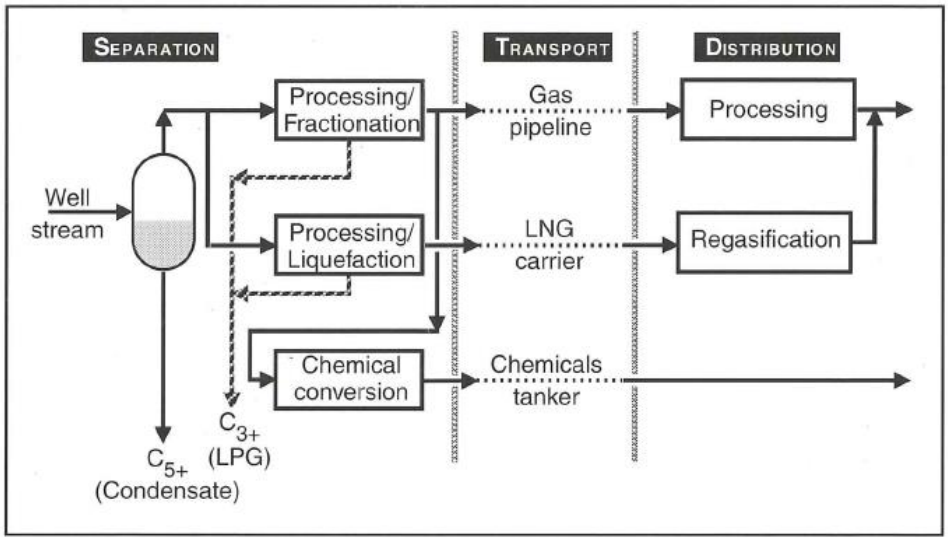

Figure 4.1: Typical natural gas processing operations [117]

In hydrocarbon gas processing in respect of pipeline transport, the goal is to avoid condensation of components into liquid phase, to prevent excessive corrosion, and most relevant to this study is to avoid the risk of hydrate formation which can eventually lead to plugging of pipeline. Consequently, the industry determines the maximum water content tolerable based on dew-point approach. However, in this study, another alternative route to hydrate formation is also investigated where a separate water phase is made available via the mechanism of adsorption of water on rusty surfaces of internal walls of hydrocarbons processing equipment and transport pipelines.

Water is always produced along with hydrocarbons, and the water is removed from the gas stream at the processing plant. Nevertheless, the gas will always contain some amount of water inherently and it is this water that can condense out from the gas and eventually form

hydrates. The first separator offshore will be 3-phase. A simplified model for illustration purpose is presented in Figure 4.2.

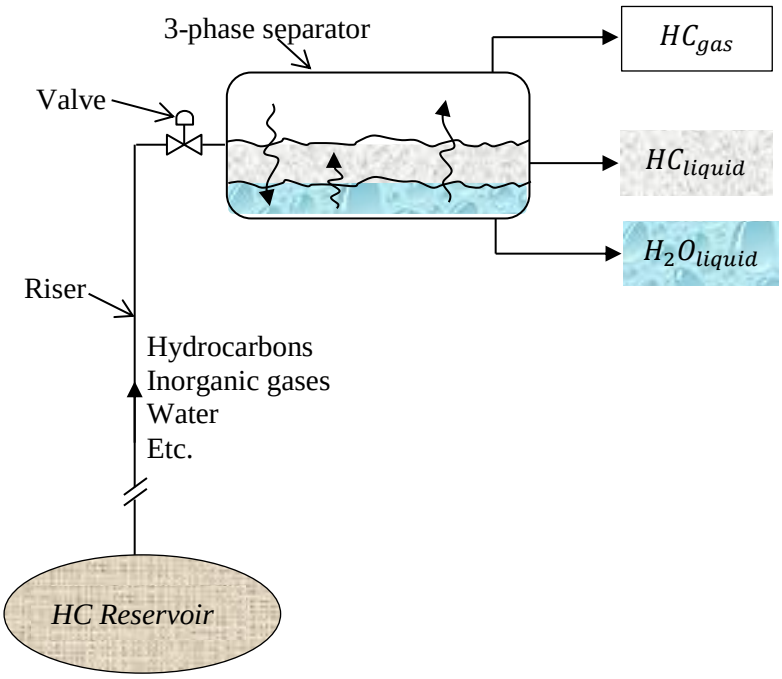

Figure 4.2: Simplified illustration of hydrocarbon production and processing with the first separator offshore

And the minimum concentrations of water is equilibrium saturation of water (H_2O) in hydrocarbon gas (HC_{gas}) and in liquid hydrocarbon (HC_{liquid}) respectively, turbulently distributed water droplets in addition. After separating out the gas, the resulting liquid phase will be a unique stream. A unique stream is created every time something is removed from that stream as shown in Figure 4.3. ($L_{1,unique}$) and ($L_{1,unique}$) represents unique HC_{liquid} streams after separating out the gas.

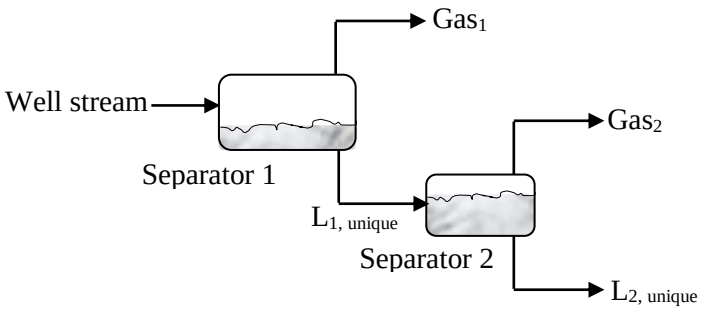

Figure 4.3: Two-stages (two-phase) separation system illustrating creation of unique streams

The thermodynamic model for evaluation in the case of the HC_{gas} is:

$$y_{H_2O}^{HC_{gas}} . \emptyset_{H_2O}^{HC_{gas}}(T, P, \vec{y}). P \approx x_{H_2O}^{(aq)} . \gamma_{H_2O}^{(aq)} . P_{H_2O}^{SAT}(T) \quad (4.1)$$

Where:

$x_{H_2O}^{(aq)}$ = mole-fraction of water in aqueous phase

$\gamma_{H_2O}^{(aq)}$ = activity coefficient of water in aqueous phase

$P_{H_2O}^{SAT}$ = saturation pressure of water at temperature T

$y_{H_2O}^{HC_{gas}}$ = mole-fraction of water in hydrocarbon gas phase

$\emptyset_{H_2O}^{HC_{gas}}$ = fugacity coefficient of water in hydrocarbon gas phase

P = pressure

$T =$ Temperature

(aq) = aqueous phase

HC_{gas} = hydrocarbon gas phase

And,

$$y_{H_2O}^{HC_{gas}} \approx \frac{x_{H_2O}^{(aq)} . \gamma_{H_2O}^{(aq)} . P_{H_2O}^{SAT}(T)}{\emptyset_{H_2O}^{HC_{gas}}(T,P,\vec{y}).P} \quad (4.2)$$

If methanol or other additives are continuously added to the system, then a model for activity coefficient of water in water phase $\left(\gamma_{H_2O}^{(aq)}\right)$ must be used and take full account of $\left[x_{H_2O}^{(aq)} . \gamma_{H_2O}^{(aq)}\right]$. However, this is not the case in this study, thus:

$\lim x_{H_2O} \rightarrow 1.0$ and $\lim \gamma_{H_2O} \rightarrow 1.0$

as a result of the low content of water in the fluid phase, equation (4.2) becomes:

$$y_{H_2O}^{HC_{gas}} \approx \left(\frac{1}{\emptyset_{H_2O}^{HC_{gas}}(T,P,\vec{y})}\right).\frac{P_{H_2O}^{SAT}(T)}{P} \quad (4.3)$$

Equation (4.3) is Raoult's law [109]. And since water is hydrodynamically distributed, then even Raoult's law can give a good enough first estimate. And $\emptyset_{H_2O}^{HC_{gas}}$ is conveniently calculated from Virial equation with B or B+C (second or second+third) Virial coefficient. Evaluation in the case of HC_{liquid} is done as follows, applying excess dilution in thermodynamics because water (H_2O) dissolves very little (low solubility of water) thus:

$$x_{H_2O}^{(HC_{liquid})}.\gamma_{H_2O}^{\infty\,(HC_{liquid})}\left(T,P,\vec{x}^{\,(HC_{liquid})}\right).f_{H_2O}^{\infty\,(HC_{liquid})}(T,P_o).poynting^{\infty} \approx$$

$$x_{H_2O}^{(aq)}.\gamma_{H_2O}^{(aq)}.P_{H_2O}^{SAT}(T).\emptyset_{H_2O}^{(H_2O,pure\ gas)}\left(T,P_{H_2O}^{SAT}(T)\right).poynting \quad (4.4)$$

Where:

$x_{H_2O}^{(HC_{liquid})}$ = mole-fraction of water in liquid hydrocarbon phase

$\gamma_{H_2O}^{\infty\,(HC_{liquid})}$ = activity coefficient of water in liquid hydrocarbon phase (infinite dilution)

f = fugacity

∞ = represents infinite dilution

(HC_{liquid})= liquid hydrocarbon phase

$poynting$ = 1.0

This is a Henry's law situation since we have very low solubility of water, and with the following approximations:

$poynting \approx 1.0$

$poynting^{\infty} \approx 1.0$

$\emptyset_{H_2O}^{(H_2O,pure\ gas)} \approx 1.0$

Equation (4.4) can be rewritten as:

$$x_{H_2O}^{(HC_{liquid})} . H_{H_2O}^{(HC_{liquid})}(T) = x_{H_2O}^{(aq)} . \gamma_{H_2O}^{(aq)} . P_{H_2O}^{SAT}(T) \quad (4.5)$$

$$x_{H_2O}^{(HC_{liquid})} = \left[x_{H_2O}^{(aq)} . \gamma_{H_2O}^{(aq)}\right] . \frac{P_{H_2O}^{SAT}(T)}{H_{H_2O}^{(HC_{liquid})}(T)} \quad (4.6)$$

Where $\left[x_{H_2O}^{(aq)} . \gamma_{H_2O}^{(aq)}\right]$ is close to 1.0 (pure water), therefore:

$$x_{H_2O}^{(HC_{liquid})} = \frac{P_{H_2O}^{SAT}(T)}{H_{H_2O}^{(HC_{liquid})}(T)} \quad (4.7)$$

Processing of hydrocarbon gas involves a number of unit operations that can bring about thermodynamic condition which is beneficial for the occurrence of hydrate formation. Typical examples are compressors that are used to increase pressure, application of turbines (expansion) that bring about gas cooling and low temperature flash tanks. The relevant processing equipment are analysed in the next subsections.

4.1.1 Turbine

Moving from point “A” to point “B” in the phase envelope illustrated in Figure 4.4 is an expansion process typical to turbines. Expansion can leads to cooling of gases and hydrate formation can occur if the end point “B” is inside hydrate stability region and liquid water drops out.

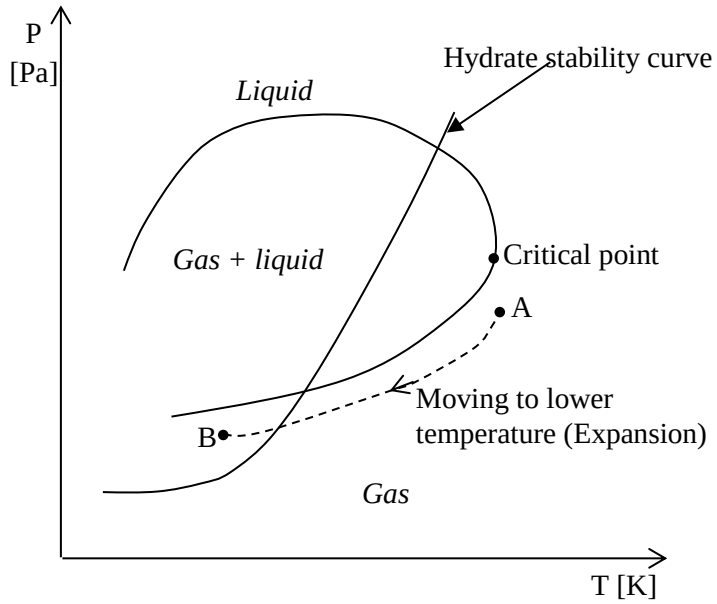

Figure 4.4: Phase envelope with hydrate stability illustrating turbine expansion process

The dew-point analysis thus follows:

At dew-point, the first liquid droplet appears from a uniform gas.

$$\vec{y} \approx \vec{z} \tag{4.8}$$

Original gas

Therefore:

$$x_i = \frac{y_i}{k_i} = \frac{z_i}{k_i} \tag{4.9}$$

$$\sum x_i = 1.0 = \sum \frac{z_i}{k_i} \tag{4.10}$$

Here, the concern is water dew-point. Therefore:

$$1.0 \approx \frac{z_{H_2O}}{k_i\left(T, P_{H_2O}^{Dew-point}\right)} \quad \rightarrow P_{H_2O}^{Dew-point} \text{ at a given T} \tag{4.11}$$

Then if P after turbine> $P_{H_2O}^{Dew-point}$(T), liquid water will drop out. And if (P, T) is inside hydrate stability region, then the hydrocarbon gas (remove parts of H_2O in the gas). To know the amount of water in the gas, a flash calculation at (P, T) is required.

4.1.2 Compressor

Compression likewise leads to situation inside the hydrate stability region as illustrated in Figure 4.5. Evaluation here is exactly as the case for expansion (turbine) based on compressor outlet (at point B) conditions of P and T.

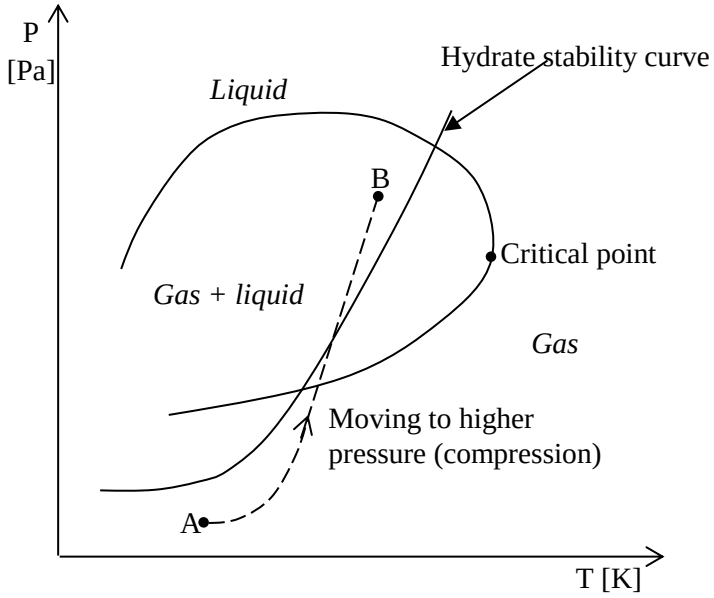

Figure 4.5: Phase envelope with hydrate stability illustrating turbine expansion process

4.1.3 Separators

The final separator in the gas processing is always at low temperatures and at high pressures. For lean gas (high in CH_4), the conditions are usually at around 251 K and 7000 kPa, while it is around 203 K and 7000 kPa for rich gas (containing significant amount of C_{2+}). The Troll gas processing plant operates at these conditions. These conditions are favourable for hydrate nucleation. During processing of the Troll gas, the final separator is a key critical point where it is likely to experience the risk of hydrate formation consequent on the low temperatures condition at which it operates. In the gas phase, a structure I hydrate dominated by methane is expected. The liquid outlet of the final separator will contain a high concentration of ethane. Therefore, at the liquid outlet (liquid phase) an ethane dominated structure I hydrate is expected. However, the presence of remarkable amount of propane (though limited compared to C_1 and C_2) could cause the formation of some structure II hydrate to occur, which would form first before the structure I hydrate. And if structure II hydrate eventually results in Troll

gas separation process, it could be small since the propane and iso-butane concentrations in the gas would be relatively small.

4.2 Hydrocarbons export and pipeline transport system and hydrate formation implications

The advancement in natural gas transmission lines initiated the development of a large natural gas pipelines network all over the world [117]. There has been immense growth in the development of hydrocarbon transport pipelines. The book published by [117] reported a total length of over one million kilometres of natural gas pipelines in the world, which was about twice of the length of pipelines for transporting crude petroleum; where Europe [119] accounted for 250 thousand kilometres. But In 2010, a total of about two million (precisely, 1,942,669) kilometres length of pipelines [4] was already established in the world, transporting natural gas, crude oil, or petroleum products. In the north sea specifically, about 96 billion standard cubic metres of gas is transported annually through about 8000 km long pipelines which are laid mainly on the seafloor and consequently exposing them to low temperatures of about 271 K to 279 K [5]. Back in 1994, the international natural gas pipeline trade was about 275 billion m^3 [120]. The work of [1] drew the world's attention to hydrate formation in pipelines being responsible for plugging of natural gas pipelines operating above 273.15 K at elevated pressures.

A typical pipeline system for transporting hydrocarbon gas is illustrated in Figure 4.6 and it comprises the following steps [117]:

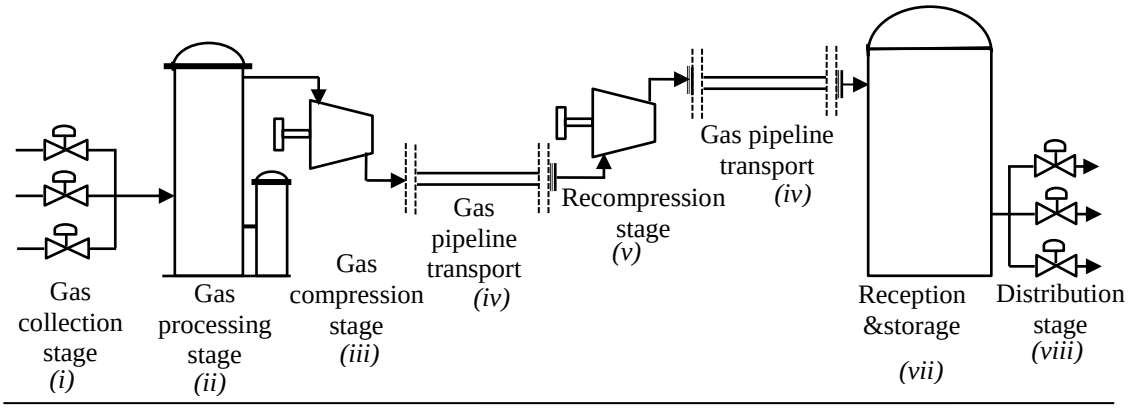

Figure 4.6: Schematic illustration of typical gas transport system; modified from Book. [117]

i. Collection of the hydrocarbon streams from the different wells.

ii. The hydrocarbon gas from the well is processed to meet the transport specifications; separating out C_{2+}, and dehydration of the gas to avoid condensation, formation of hydrate and corrosion.

iii. Compression of the gas in the case where the wellhead pressure comes to be lower than the pressure required for transporting the gas.

iv. Pipeline transport of the gas.

v. Recompression in the course of transport to offset the consequence of pressure drop for long distance pipeline transport.

vi. Additional processing, if required to adjust the gas to the specifications required for distribution to the receiving end (market).

vii. Storage and transmission to the distribution network.

viii. Gas distribution to the delivering ends.

These stages illustrate gas transport system from the well to the processing plant and from processing plant to distribution at delivery ends. The pressure and temperature conditions of this gas transport system at the North Sea are usually within the hydrate stability zone (seafloor temperature range of 272.15 K-279.15 K at elevated pressure of about 25000 kPa – 30000 kPa) [5]. And water is normally produced together with hydrocarbons from the well, and the presence of this water either in vapour or liquid phase means trouble for the transport pipeline systems [1]. The presence of water in these transport conditions will possibly lead to hydrate formation, thereby resulting deposition of masses of hydrates on the internal walls of the pipelines. As the hydrate deposition continues, the mass of hydrate deposits grow, thereby causing reduction or narrowing of the flow channel. A point will be reached where the hydrate wall deposits will not be able to withstand the stress of the combined impacts of the flowing fluid and the weight of the hydrate deposits, thus, they will detach from the wall and travel along with the stream. As the particles proceed downstream, they bridge across the pipeline (flow channel) resulting in formation of hydrate plug(s) with corresponding spikes [3]. If the hydrate plugs are allowed to grow unimpeded, the hydrate can severely obstruct the flow, resulting in total plugging of pipeline and could cause damage to processing and transport equipment [108]. A schematic illustration of hydrate plugs in gas dominated pipeline system is presented in Figure 4.7.

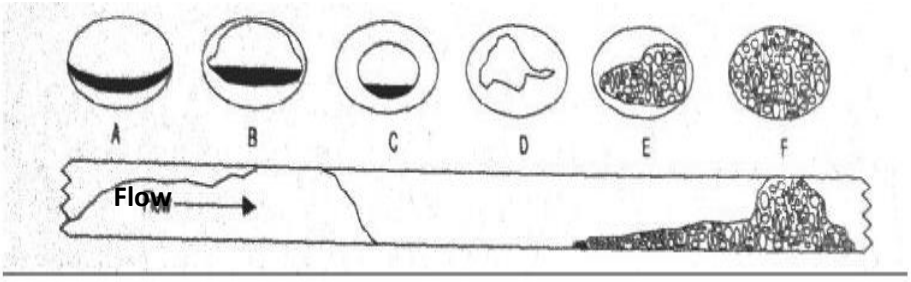

Figure 4.7: Schematic illustration of hydrate plugs being formed in a gas dominated pipeline system [3].

The final separator during processing of lean hydrocarbon gases at the North Sea operates at 7000 kPa and 251.15 K as shown in Figure 4.8. And the transport pipeline system with pressure and temperature conditions monitoring instruments is also schematically illustrated in Figure 4.9. This is a typical representation of the conditions of the pipeline systems at the North Sea. The important help equipment to analyse here are compressors and pumps. Compressors are vital help equipment in hydrocarbon (natural) gas transport systems applied for compression and recompression (required for long distance delivery) of gas. While pumps are required in pipeline transport of liquid hydrocarbons. Compressors have been discussed in Section 4.1.2. Therefore, only pumps are analysed here.

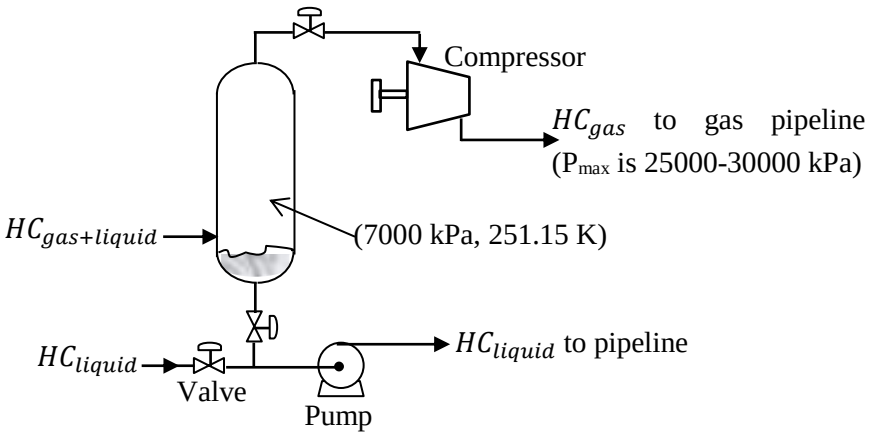

Figure 4.8: Schematic illustration of the typical final separator at the North Sea

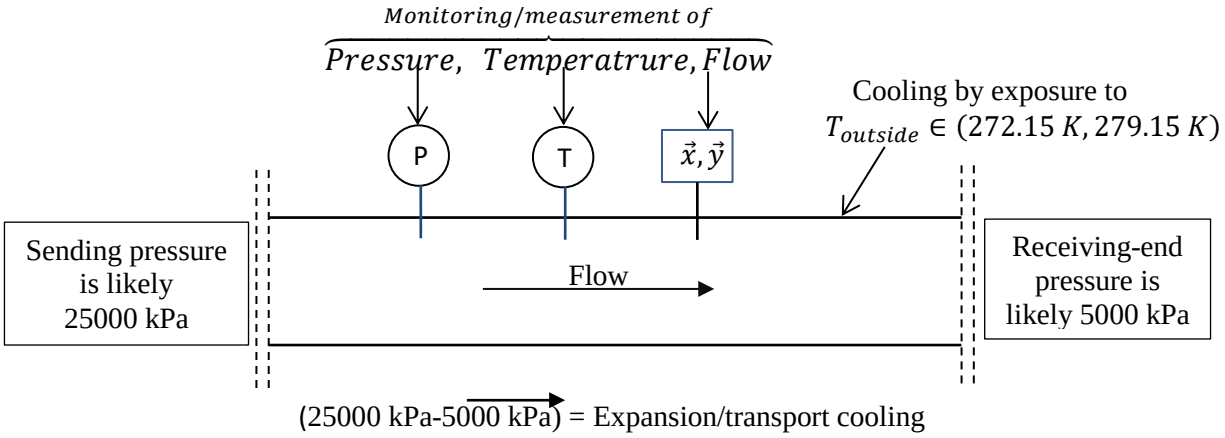

Figure 4.9: Schematic illustration of the typical pipeline system with pressure, temperature and flow monitoring system ($\boldsymbol{T_{outside}}$ is the outside temperature which the pipeline is exposed to)

4.2.1 Pumps

During processing of hydrocarbon gas, components in liquid phase, especially HC_{liquid} and water will be separated out. After the initial separation, some amount of water may still be dissolved or slightly dissolved in the new unique HC_{liquid} stream. The transport of the HC_{liquid} stream will be handled by pumps after processing, thus it is vital to look into pumps and hydrate formation implications during transport of HC_{liquid}. The question to ask is, will ΔP created by pump cause the stream to be in the hydrate stability region in terms of temperature and pressure? If so, we have to check water dew-point, but based on water model in HC_{liquid}. Basically, the water drop-out analysis is evaluated by using equation (4.12) for $x_{H_2O}^{(HC_{liquid})}$. That is:

$$\text{If } x_{H_2O}^{(HC_{liquid})} < x_{H_2O}^{(HC_{liquid}),real} \tag{4.12}$$

then water will drop-out and hydrate could form. $x_{H_2O}^{(HC_{liquid}),real}$ is measured or monitored as illustrated in Figure 4.9. The amount of water that will drop-out is evaluated from:

$$F.\left(x_{H_2O}^{(HC_{liquid}),real} - x_{H_2O}^{(HC_{liquid})}\right) \tag{4.13}$$

Where F is “flow” in moles/s. In this case methane hydrate is not likely to occur as it is mainly only C_{2+} components that would be in the liquid phase. Therefore, mixed hydrates of C_{2+} would possibly form.

5 Alternative routes to hydrate formation

It is pertinent to discuss the different routes to hydrate formation during processing and pipeline transport of hydrocarbon gases which are investigated in this work. This section presents analysis of the different thermodynamically feasible pathways for hydrate nucleation and growth.

5.1 Route of water drop-out at dew-point from the gas stream

The conventional technique currently apply in the industry to evaluate the risk of hydrate formation is based on the assumption that liquid water will condense out (drop-out) of the bulk hydrocarbon gas stream (with admixture of inorganic gases like CO_2 and H_2S) during processing and transport to form a separate water phase that can possibly and consequently lead to hydrate formation [5]. This approach is known as the dew-point route to hydrate formation, and it is executed by estimating the dew-point pressure of water in the hydrocarbon gas stream. Then check if the estimated dew-point pressure at the local temperature is within the temperature and pressure prediction of the hydrate stability region. If it is, then water will dropout as liquid droplets. Thus, the theoretical quantity of water that could condense out can be computed and the right measures are taken to dehydrate the gas. Otherwise, the required amount of a particular hydrate inhibitor that can adequately shift the hydrate stability curve's pressure and temperature projections beyond the risk region is estimated and implemented in the system to prevent hydrate formation.

The principle here once again is water dew-point calculation. The dew point is the (pressure-temperature) point at which first micro-scale droplets of water condenses out of the vapour phase of a component or mixture of components. For hydrate to form through this dew-point pathway, the chemical potential of water in hydrate phase must be less than that of the separate (liquid) water phase as given below:

$$\text{If } \mu_{H_2O}^{Hydrate} < \mu_{H_2O}^{Liquid\ H_2O} \tag{5.1}$$

This means water will prefer going into hydrate to remaining in the separate liquid water phase. So also, the chemical potential of the hydrocarbon gas (HC_{gas}) hydrate formers in hydrate phase must be less than its chemical potential in HC_{gas} phase as shown below:

$$\text{If } \mu_{HC_{gas}}^{Hydrate} < \mu_{HC_{gas}}^{HC_{gas}} \tag{5.2}$$

This also implies that the HC_{gas} hydrate forming components will also prefer going into hydrate phase to existing in the HC_{gas} phase.

The superscripts here represent the different phases, the subscript signifies the component, while "μ" denotes chemical potential. Similarly, the chemical potential of water (H_2O) in the separate (liquid) water phase must be less than the chemical potential of water in in the bulk hydrocarbon gas (HC_{gas}) phase for water to dropout through the dew-point route for hydrate formation to eventually occur. That is:

$$\text{If } \mu_{H_2O}^{Liquid\ H_2O} < \mu_{H_2O}^{HC_{gas}} \tag{5.3}$$

If so, liquid water will drop out of the gas stream to form a separate liquid water phase.

The superscripts here also denote the different phases, the subscript is the component, and "μ" is chemical potential. This means water will prefer to drop out to form a separated free (liquid) water phase at water dew-point conditions which can eventually lead to hydrate formation. Based on the above expression, the limit at which water drops out as a separate (liquid) phase in equilibrium with water dissolved and distributed hydrodynamically in the hydrocarbon gas phase is given by:

$$\mu_{H_2O}^{Liquid\ H_2O} = \mu_{H_2O}^{HC_{gas}} \tag{5.4}$$

Notations (superscripts, subscripts, signs etc.) here are same as above. Phase envelop showing the dew-point is illustrated in Figure 5.1.

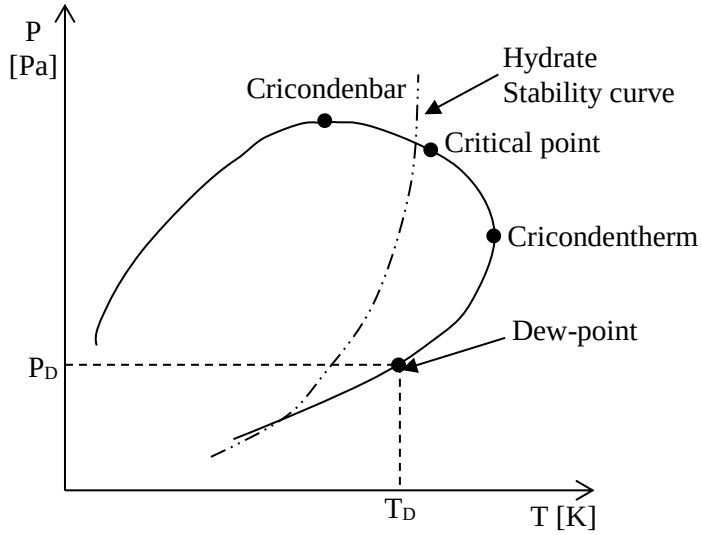

Figure 5.1: Phase envelope showing the dew-point.

From thermodynamics, we understand that to estimate $\mu_{H_2O}^{HC_{gas}}$ and $\mu_{H_2O}^{Liquid\ H_2O}$ a reference state is required for each of them. Residual thermodynamics is the reference state applied in the case of $\mu_{H_2O}^{HC_{gas}}$. While the estimation of $\mu_{H_2O}^{Liquid\ H_2O}$ requires symmetric excess thermodynamics. However, the chemical potential of pure liquid water is evaluated based on the molecular simulations work of [81].

To obtain the expression for the dew-point liquid water drop-out, which is the maximum water content ($y_{H_2O}^{Dew-point}$) before liquid water would drop out from the hydrocarbon gas stream, the fugacity formulation is applied; that is for water dissolved in HC_{gas} and that for water in liquid water phase ($\mu_{H_2O}^{Liquid\ H_2O}$). The expression for the dew-point liquid water drop-out is obtained as follows:

$$y_{H_2O}^{Dew-point}.\emptyset_{H_2O}^{HC_{gas}}(P,T,\vec{y}).P = x_{H_2O}.\gamma_{H_2O}(P,T,\vec{x}).\emptyset_{H_2O}^{pure\ HC_{gas}}\left(P_{H_2O}^{SAT},T\right).P_{H_2O}^{SAT}(T).e^{\int_{P_i^{SAT}}^{P}\left(\frac{v_i}{R.T}\right)dP} \quad (5.5)$$

$$y_{H_2O}^{Dew-point} = \frac{x_{H_2O}.\gamma_{H_2O}(P,T,\vec{x}).\emptyset_{H_2O}^{pure\ HC_{gas}}\left(P_{H_2O}^{SAT},T\right).P_{H_2O}^{SAT}(T).e^{\int_{P_i^{SAT}}^{P}\left(\frac{v_i}{R.T}\right)dP}}{\emptyset_{H_2O}^{HC_{gas}}(P,T,\vec{y}).P} \quad (5.6)$$

Where, $e^{\int_{P_i^{SAT}}^{P}\left(\frac{v_i}{R.T}\right)dP}$ is "poynting correction" and it is usually unity (1.0) for large regions of pressure as a result of low molar volume of water. γ_{H_2O} is approximated to 1.0 because of the

low content of water in the fluid phase. $P_{H_2O}^{SAT}$ is also sufficiently low which makes $\emptyset_{H_2O}^{pure\ HC_{gas}}$ to be very close 1.0. Therefore, the expression for dew-point liquid drop is reduced to:

$$y_{H_2O}^{Dew-point} = \frac{x_{H_2O}.P_{H_2O}^{SAT}(T)}{\emptyset_{H_2O}^{HC_{gas}}(P,T,\vec{y}).P} \tag{5.7}$$

There is little limit to mass transport for hyrate formation through the dew-point route. The above formulation is known as fugacity formulation but from chemical potential approach:

$$\mu_{H_2O}^{Ideal\ gas}(T,P) + R.T.\ln\left(y_{H_2O}.\emptyset_{H_2O}^{(gas)}\right) = \mu_{H_2O}^{(pure\ liquid)}(T,P) \tag{5.8}$$

With only y_{H_2O} unknown, water dew-point mole-fraction is calculated as follows:

$$\ln\left(y_{H_2O}.\emptyset_{H_2O}^{(gas)}\right) = \frac{\mu_{H_2O}^{(pure\ liquid)}(T,P) - \mu_{H_2O}^{Ideal\ gas}(T,P)}{R.T}$$

$$y_{H_2O} = \left[\frac{1}{\emptyset_{H_2O}^{(gas)}}\right].e^{-\left[\frac{\mu_{H_2O}^{(pure\ liquid)}(T,P) - \mu_{H_2O}^{Ideal\ gas}(T,P)}{R.T}\right]} \tag{5.9}$$

And y_{H_2O} here is the dew-point maximum mole-fraction of water $\left(y_{H_2O}^{Dew-point}\right)$ before liquid water drops out of the hydrocarbon gas stream. Thus, equation (5.9) can be written as:

$$y_{H_2O}^{Dew-point} = \left[\frac{1}{\emptyset_{H_2O}^{(gas)}}\right].e^{-\left[\frac{\mu_{H_2O}^{(pure\ liquid)}(T,P) - \mu_{H_2O}^{Ideal\ gas}(T,P)}{R.T}\right]} \tag{5.10}$$

This is the industrial classical approach of estimating maximum permitted water content for a given temperature and pressure. And if the real water content $\left(y_{H_2O}^{real}\right)$ in the hydrocarbon gas is higher than the estimated dew-point water content $y_{H_2O}^{Dew-point}$, then the risk of hydrate formation exist because water will drop out. The amount of water that will drop out, $W_{Drop-out}$ is:

$$W_{Drop-out} = F.\left(y_{H_2O}^{real} - y_{H_2O}^{Dew-point}\right) \quad (5.11)$$

Where "F" is the molar flow rate.

5.2 Route of water adsorbed on hematite from the gas stream

The second alternative route to hydrate formation reveals that there is a shortcoming with the traditional dew-point scheme; it absolutely disregards an alternative route to hydrate formation as a result of the presence of rust (known as hematite) on the internal walls of hydrocarbon gas processing equipment and on transport pipelines. These surfaces covered by hematite provide water adsorption sites that can also lead to hydrate formation. Nucleation and growth of hydrate could happen when water and hydrate guest molecules are adsorbed together on these rusty surfaces in the internal walls of gas processing equipment and gas transport pipelines or when only water is adsorbed on these hematite surfaces with molecules of hydrate formers being imported from the bulk hydrocarbon gas stream. The chemical potentials of the hydrate guest molecules will be different across the phases due to the inability of industrial or real systems outside of laboratory to attain equilibrium. However, the hematite will act as a catalyst for pulling out the water from the gas through adsorption mechanism; subsequently, the formation of hydrate can then occur slightly outside of the first two or three water layers of approximately one nanometre. Rust is formed from iron and oxygen under the influence of or exposure to water. It is a mixture of a number of different oxides of iron such as magnetite (Fe_3O_4), hematite (Fe_2O_3), and iron oxide (FeO). Even though magnetite usually forms very early, in the long run it is hematite that is most dominant, one of the most thermodynamically stable forms of ordinary rust. By ordinary rust we refer to different oxides of iron formed by the exposure of iron to water and oxygen. Impurities of components such as carbon dioxide and hydrogen sulphide can cause conversions over to iron carbonates and different iron and sulphur components [5].

For water to be adsorbed on hematite, the chemical potential of water in the adsorbed phase must be more negative than that of water in the gas phase:

$$\mu_{H_2O}^{Adsorbed} < \mu_{H_2O}^{HC_{gas}} \quad (5.12)$$

The superscripts here also denote the different phases, the subscript is the component, and "μ" is chemical potential. Therefore, hydrate can form from water molecules which are slightly more than 1nm outside the surface and either from adsorbed hydrate former or hydrate former from HC_{gas} phase as already mentioned [8]. Like the dew-point approach, the adsorption point can be evaluated as:

$$\mu_{H_2O}^{Adsorbed} = \mu_{H_2O}^{HC_{gas}} \tag{5.13}$$

Where superscript represents the phase, subscript is the component and μ stands for chemical potential. There is no mass transport limitation in a dynamic situation for hydrate formation through this route of adsorption of water onto solid surfaces covered by hematite (internal walls of hydrocarbon gas processing equipment and transport pipeline in this work). As explained above, the formation of hydrate occurs at about three to four molecules outside the rusty surface. To obtain the chemical potential of water in the adsorbed phase (water adsorbed onto hematite), equation (5.14) is useful:

$$\mu_{H_2O}^{Adsorbed}(P,T,\vec{x}_{Adsorbed}) = \mu_{H_2O,CH_4}^{ideal\ gas}(P,T,\vec{y}) + R.T.\ln[y_{H_2O.}\emptyset_{H_2O,CH_4}(P,T,\vec{y})] \tag{5.14}$$

Estimation of maximum water content $\left(y_{H_2O}^{Adsorbed}\right)$ in the hydrocarbon gas stream before water can be adsorbed on hematite surface is achieved in similar way to that of dew-point $\left(y_{H_2O}^{Dew-point}\right)$. Equation (5.16) and (5.17) are fugacity formulation and chemical potential formulation (from equation (5.14)) applied for estimating $y_{H_2O}^{Adsorbed}$.

$$y_{H_2O}^{Adsorbed} = \frac{x_{H_2O}.P_{H_2O}^{SAT}(T)}{\emptyset_{H_2O}^{HC_{gas}}(P,T,\vec{y}).P} \tag{5.16}$$

$$y_{H_2O}^{Adsorbed} = \left[\frac{1}{\emptyset_{H_2O}^{(gas)}}\right].\mathrm{e}^{-\left[\frac{\mu_{H_2O}^{(pure\ liquid)}(T,P)-\mu_{H_2O}^{Ideal\ gas}(T,P)}{R.T}\right]} \tag{5.17}$$

Similarly, the amount of water that will be absorbed can be estimated using equation (5.18):

$$W_{Adsorbed} = F.\left(y_{H_2O}^{real} - y_{H_2O}^{Adsorbed}\right) \quad (5.18)$$

And "*F*" is also the molar flow rate.

The estimation of $\mu_{H_2O}^{Adsorbed}$ in this work has been done from [121]. The short range interactions between water (H_2O) and hematite (rust) utilized Buckingham type potential with parameters obtained from de Leeuw and Cooper [122] and Tsuzuki et al. [123].

5.3 Direct route

Theoretically, a third route to hydrate formation exists which involves hydrate directly forming from water dissolved in hydrocarbon gas stream. Even though hydrate formation through this route is thermodynamically feasible, in practice, it is improbable because of low concentration of the water, and limitations in heat and mass transport also makes it doubtful. There would be a challenge of transporting the exothermic heat released through the non-polar hydrocarbon gas like methane which is relatively a heat insulator; this heat of formation necessarily needs to be transported away. Consequent on the above reasons, this route will not be investigated in this study.

However, if surface stress from flow does not have any influence on water/hydrocarbon system, then nucleation of hydrate would rapidly occur on the water/hydrocarbon interface and will very swiftly obstruct transport of more guest molecules and waters through the hydrate film (effect of very low coefficient of diffusivity). In this scenario, hydrate can nucleate from the guest molecules dissolved in water, and it can also form from water dissolved in gas, then this will benefit from nucleation on the surface of the hydrate. But considering a flowing case with turbulent shear forces, this is not a realistic occurrence. An additional difference between a flowing situation and a case where we have a stationary constant volume and constant mass experiment in laboratory is that new mass is continuously supplied. Consequently, the limiting situation where the water is completely consumed thereby causing hydrate formation to stop would not occur.

Considering this third theoretical case where water is dissolved in hydrocarbon gas, hydrate would directly form if:

$$\mu_{H_2O}^{Hydrate} < \mu_{H_2O}^{HC_{gas}} \quad (5.19)$$

The superscript represents the phase, the subscript stand for the component and "μ" is chemical potential. We need to remember that compared to the first two routes explained above, it is very questionable for hydrate to form through routes for hydrate formation under the same thermodynamic conditions [124].

6 Choice of Scientific method

Hydrate formation or dissociation (phase transition) studies as required in this project could be implemented from the following different scientific methods: molecular dynamic (MD) simulation, density function in classical regime or phase field theory (PFT), and free energy minimization technique in classical thermodynamics.

Molecular dynamic simulations [125-127] can be used for nano-scale studies of the kinetics of hydrate phase transition. However, there is a short-coming in this approach; the system will be too small in order to capture the important things. “Small” here refers to volume and time scales.

Hydrate formation or dissociation can also be studied using “density functional theory in classical regime method”, which is based on changes in structure for determination of kinetic rate; or “phase field theory” (PFT) [128, 129] that is based on both structure and free energy (canonical ensemble). This method is useful in studying systems in which movement through interface is significant, but the system will also be too small and will require intensive CPU (central processing unit) of computer. Though it is typically able to capture dynamic features and phase transitions of up to 2 order of magnitude of volumetric size and 1000 times the possible simulation times for MD.

Based on the limited scale of volume and time required in the approaches discussed above, they are inappropriate or inconvenient for this project. Therefore, free energy minimization technique in classical thermodynamics is the appropriate choice of scientific method for this work. Rigorous free energy minimization approach requires programming fairly comprehensive code, but a simplified approximation to such an approach is to compare a possible phase transition and analyse each in terms of free energy changes, and qualitatively there could be some mass and heat transfer challenges. Moreover, because the systems investigated in this work involves water phase, adsorbed phase, gas (or vapour) phase and hydrate phase, based on Gibbs rule, the systems cannot attain equilibrium. Thus, a principal tool for comparison has to be free energy minimization. It is also necessary to base the analysis on the same reference state, and this could be done by the use of chemical potential for liquid water and chemical potential for empty hydrate structures. This is however based on the MD simulations of Kvamme and Tanaka [81]. And the gas/fluid phase analysis is done on the basis of residual thermodynamics, using Soave-Redlich-Kwong (SRK) equation of state and ideal gas as a reference state. The programming codes for this study have been

developed using FORTRAN language by Professor Bjørn Kvamme and the compiler is Microsoft developer.

Yet another advantage of a discrete evaluation of possible hydrate formation routes based on free energy gain for hydrate formation, and consideration of associated heat- and mass-transport aspects is that these types of calculations will be straightforward to implement in industrial hydrate evaluation tools as extensions in the thermodynamic packages.

7 Case studies and data

The Troll gas and Sleipner gas from the North Sea of Norway are the case studies chosen for this project based on the components and composition of components present in the natural gas from both fields, the temperature [5] (272.15 K to 279.15 K) of the sea floor which pipelines are exposed to, and the operational pressure ranging from 5000 kPa to 30000 kPa. The natural gas from both gas fields have significant amount of both structure I and structure II hydrate formers which are pertinent in this study. The temperature and pressure conditions stated above are favourable for formation of both structure I and structure II hydrates during pipeline transport. The gas processing operations conditions as have been analysed in Section 4 could also lead to nucleation and growth of hydrate from both structure I and structure II guest molecules.

7.1 Troll gas field

The Troll gas field is located in the northern part of the North Sea covering an area of about 750 km^2 and it is approximately 65 km^2 west of Kollsnes, the landing site just outside of Bergen [130]. The largest gas field discovered in the North Sea is the Troll gas (the reservoir is 1,400 m below sea level), thus it is of very crucial importance to the Norwegian gas production. The Troll gas makes up forty per cent of all the gas reserves on the Norwegian continental shelf. The Troll A platform, the gas processing plant at Kollsnes together with the pipelines transporting hydrocarbons from the platform to the onshore processing plant all make up the Troll gas infrastructure. Norwegian Shell was in charge of the development of the first phase of Troll gas before Statoil became the operator as from 1996. The composition of the Troll gas used in this study has been obtained from [131]. The composition data contains components C_1 to C_{7+}, Toluene, Xylene, Nitrogen and carbon dioxide. But this work is focused only on the hydrocarbons that commonly form hydrate structure I and structure II. Therefore, only methane, ethane, propane and isobutane data are required and necessary normalisation of the composition of these four components has been done.

7.1.1 Composition of Troll gas

Four experimental tests were carried out by Statoil to determine the composition of the Troll gas, and the results of tests 3 and 4 are considered to be most reliable. Separator 2 was not considered because of its temperature and pressure conditions of 261.15 K and 4620 kPa respectively. This temperature is below the typical hydrate formation temperature. However, Separator 1 conditions are 274.15 K and 7000 kPa which is favourable for hydrate formation, the upper limit of water that could be permitted in the gas stream without the risk of hydrate formation together with that of the well-head fluid is thus investigated. For the well-head, pipeline transport conditions were applied. Temperature and pressure values of 273.15 K and 7000 kPa conditions exactly were particularly demanded by Statoil for the Thornton Research Centre analysis [131]. And we are aware that transport pressures range between 5000 kPa and 25000 kPa, thus the analysis in this work covers this pressure range.

Table 7.1: Molar composition of Troll gas [131]*

Components	Well-head fluid	Separator 1	**Separator 1	***Separator 1
	0°C and 70 bar	1°C and 70 bar	1°C and 70 bar	1°C and 70 bar
Methane, C_1	0.959213	0.959708	-	-
Ethane, C_2	0.034936	0.034704	0.8613	-
Propane, C_3	0.003115	0.003024	0.0751	0.541133
Iso-butane, iC_4	0.002736	0.002564	0.0636	0.458867

** Only hydrate forming hydrocarbon components have been considered*
***Molar composition of components after methane is separated out of the gas stream*
**** Molar composition of components after methane and ethane are separated out of the gas stream*

7.2 Sleipner gas from the North Sea

Natural gas from "Sleipner" gas field (precisely Sleipner Vest (West in English) gas field, from Sleipner B installation) is very appropriate for this study. Sleipner Vest gas field is located in the central part of the Norwegian North Sea with water depth of approximately 110 metres, but the reservoir depth is about 3,450 metres [132]. Natural gas mixture from Sleipner Vest contains substantial amount of propane and some isobutane which are structure II hydrate guest molecules, and the amount of CO_2 is also significant. Consequently, CO_2 is removed from the produced gas during processing and injected into the Utsira Formation in the North Sea (over 16 million tonnes of CO_2 have been stored in Utsira Formation since

1996) [133]. All these operations involve installations which include process equipment for gas processing and pipelines for transport. The wellstream from Sleipner B is routed through pipelines laid mostly on the seafloor of the North Sea to Sleipner A for processing. The processed gas is transported to the market through the Gassled pipeline system (which is the largest offshore gas transmission system in the world) [134] operated by the Norwegian Gassco. The daily gas export is put at 369,000,000 m^3 [134] and transported normally at high pressures ranging from 50 bar to about 300 bar. In addition, the temperatures these pipelines are exposure to on the seafloor at the North Sea are low, about 272 K to 279 K. These low temperatures and elevated pressures' conditions that the transported natural gas mixtures with CO_2 are exposed to are within hydrate formation conditions [109]. Under these conditions, there is a propensity for natural gas mixture to form hydrate [81] on the internal walls of pipelines and processing equipment during transport and processing respectively; gas processing operations are normally at low temperatures and high pressures too. Table 1 presents the normalized concentrations of only the structure I and structure II hydrate forming components in the Sleipner gas.

Table 7.2: Normalized concentration of components in Sleipner gas [135]

Guest molecules		Molar concentration	Molar concentration after CO_2 separation
Methane	(CH_4)	0.8448	0.8752
Ethane	(C_2H_6)	0.0876	0.0907
Propane	(C_3H_8)	0.0304	0.0314
Isobutane	(i-C_4H_{10})	0.0025	0.0026
Carbon dioxide	(CO_2)	0.0347	-

8 Thermodynamics

This section presents details of the thermodynamic models applied in the scheme used for the analysis of the different routes to hydrate formation during processing and transport of hydrocarbons. That is both the traditional approach currently employed by the industry and the new concept of absorption of water on internal walls of processing equipment and pipelines. Much of the information presented here are from [8].

It has been discussed in Section 3.5 that hydrate formation systems are not thermodynamically stable (Gibbs phase rule), they cannot attain equilibrium in real situations (outside of the laboratory) such as the ones investigated in this work. Thus, for any specific phase transition (be it formation or dissociation), the least criteria for hydrate formation to occur is that the free energy should be sufficiently negative to overcome the required work penalty, i.e. it overcomes the nucleation barrier for creating space for the new phase (the hydrate phase). The hydrate formed from different phases will possess different free energies since the chemical potential of each guest molecule will be different [8, 108] in non-equilibrium scenarios.

8.1 Free energy

The word affinity was initially employed by chemists so many years ago to explain the force that triggered chemical reactions [136] in physical chemistry. This out-of-date term (affinity) has been replaced by a more advanced and accurate one [136] known as Gibbs free energy. An American scientist called Josiah Willard Gibbs in the 1870s [137] developed the Gibbs free energy which was originally known as “available energy.” The term “free energy” is used in thermodynamics to describe ‘available energy’ that can be transformed to “do work”. Gibbs free energy is one of the most significant thermodynamic formulations employed in characterizing a system [136]. Furthermore, Gibbs free energy is the thermodynamic potential which is minimized once a system attains chemical equilibrium at constant temperature and constant pressure [136]. The derivative of Gibbs free energy with respect to the reaction coordinate of any system disappears at the point of equilibrium. Thus, a decrease in *Gibbs free energy* is a required condition for the spontaneity of processes at constant temperature and constant pressure [136].

Considering a constant temperature (isothermal) system, or a constant pressure (isobaric) system, the Gibbs free energy can be regarded as a "dynamic" quantity, because it is a representative measure of the competing impacts of the driving forces of enthalpy and

entropy associated with thermodynamic processes [136]. From the second law of thermodynamics, a common natural tendency to reach a minimum Gibbs free energy exists for systems reacting or phase transition at a given pressure-temperature condition, for example, standard-temperature-pressure (STP) condition.

The change in Gibbs free energy (usually represented as "ΔG*"* or "*dG*") resulting from a given reaction or phase transition gives a quantitative measure of the favourability (spontaneity) or driving force of the phase transition, be it hydrate formation or dissociation at constant temperature and constant pressure. At a thermodynamic condition of constant pressure and constant temperature, for phase transition to eventuate, the change in Gibbs free energy (ΔG) must necessarily be lesser than the non-expansion work, which is frequently equal to zero, therefore the change in Gibbs free energy must be less than zero ($dG \leq 0$); that is it must have a negative value. In a situation where we have a number processes or phase transitions as we have in the systems investigated in this study, the phase transition process with the most negative Gibbs free energy occurs first before the one with the next most negative Gibbs free energy will subsequently occur, and so on.

Gibbs free energy can be derived from the first and second laws of thermodynamics, which are based on the "conservation of energy" and "entropy (friction)" respectively. According to the first law of thermodynamics, energy cannot occur from nothing and it cannot disappear to nothing; energy can be distributed to other forms like heat, work and chemical work. And from the second law of thermodynamics we understand that an isolated system will always naturally strive towards maximum entropy. The second law places constraints on which conversion are possible (friction cannot be avoided). Considering an isolated system, the combination of the first and second law of thermodynamics gives an expression for the changes in the internal energy for a phase "i*"* as follows:

$$d\underline{U}^i \leq T^i d\underline{S}^i - p d\underline{V}^i + \sum_i^n \mu_j^i \, dN_j^i \qquad (8.1)$$

Where,

$\underline{U}$ = internal energy [J]

μ = chemical energy [J/mole]

T = temperature [K]

p = pressure [Pa]

$\underline{V}$ = volume [m^3]

$\underline{S}$ = entropy [J/K]

N_j = number of particles of a component [-]

$i = 1, 2, 3 \ldots n$ phases (gas, liquid, and/or solid) [-]

j = component

The term "$\sum_{i=1}^{n} \mu_i dN_1^i$" is chemical work which is the work required to take a molecule of a component from one phase and transfer it into the other phase. For all real and irreversible changes we have less than (<) sign. And by definition:

$$\underline{G}^i = \underline{H}^i - T^i \underline{S}^i \tag{8.2}$$

And since,

$$\underline{H}^i = \underline{U}^i + p^i \underline{V}^i \tag{8.3}$$

It can also be expressed as:

$$\underline{G}^i = \underline{U}^i + p^i \underline{V}^i - T^i \underline{S}^i \tag{8.4}$$

Where,

$\underline{G}$ = Gibbs free energy [J]

$\underline{H}$ = Enthalpy [J]

By means of Legendre transforms, applying total derivative natural variables for the Gibbs free energy; differentiating equation (d) we have:

$$d\underline{G}^i = d\underline{U}^i + d\left(p^i \underline{V}^i\right) - d\left(T^i \underline{S}^i\right)$$

$$d\underline{G}^i = d\underline{U}^i + \underline{V}^i dp + p d\underline{V}^i - \underline{S}^i dT^i - T^i d\underline{S}^i \tag{8.5}$$

Substituting equation (4.1) into (4.5) gives:

$$d\underline{G}^i \leq T^i d\underline{S}^i - p d\underline{V}^i + \sum_i^n \mu_j^i \, dN_j^i \; + \underline{V}^i dp + p d\underline{V}^i - \underline{S}^i dT^i - T^i d\underline{S}^i$$

$$d\underline{G}^i \leq \underline{V}^i dp - \underline{S}^i dT^i + \sum_i^n \mu_j^i \, dN_j^i \tag{8.6}$$

T, p and N_j are the natural variables of Gibbs free energy.

This expression in equation (g) shows that a system will always strive towards a minimum when subjected to changes in T, p or N_j. Free energy can be considered as the available energy considering friction losses. And equation (4.6) is reduced to the expression given in equation (4.7) at constant pressure and constant temperature situation ($i.e., when\ dp = 0\ and\ dT = 0$):

$$d\underline{G}^i \leq \sum_i^n \mu_j^i\, dN_j^i \qquad (8.7)$$

In this work, systems considered involve both reversible and irreversible processes. The process proceeds till the total free energy reaches a minimum. This imply that we can use the change in Gibbs free energy to state which reaction or phase transition will be favoured and ensue spontaneously as follows:

If $\Delta G \leq 0$, then phase transition is favoured and will ensue.

If ≥ 0 ; phase transition is not favoured and phase transition not will occur.

This expression shows that differences in free energy between two phases or among several phases in a systems is the driving force of the system; every system will always strive towards minimum free energy [8, 109].

By means of Gibbs phase rule analysis (Section 3.5) we understand that hydrates are not thermodynamically stable. For any specific phase change, be it formation or dissociation, the principal conditions required for a hydrate to form is that the free energy should be negative enough to overcome the work penalty, which is the nucleation barrier for pushing away the old phase and creating space for a new phase. In non-equilibrium scenario, the hydrate formed from different phases will possess different free energies as the chemical potential of all the guest molecules will be different [8, 108]. And in consideration of an equilibrium situation, the traditional scheme used to evaluate equilibrium is to simultaneously compute the conditions for equilibrium, conservation of mass, and conservation of energy. But non-equilibrium evaluation involves the use of the combined first and second laws of thermodynamics instead of equilibrium conditions through the use of some specific strategies for minimizing free energy locally under the constraints of conservation of both mass and energy [5]. The modelling of all phase transitions for hydrate formation or dissociation is executed as pseudo reactions corresponding to changes in free energies as driving force for phase transition and coupled dynamically to mass transport and heat transport [5]. The free energy changes corresponding to all phase changes can be estimated using equation (8.8):

$$\Delta G_i = \delta\left[x_w^{H,i}\left(\mu_w^{H,i} - \mu_w^P\right) + x_{gas}^{H,i}\left(\mu_{gas}^{H,i} - \mu_{gas}^P\right)\right] \quad (8.8)$$

Where

x = composition

H = hydrate phase

i = phase transition scenario

μ = chemical potential

p = parent phase; liquid, gas, adsorbed phases

δ = +1 for hydrate formation and -1 for hydrate dissociation

The chemical potentials (μ) of each hydrate former in different phases is not the same; the chemical potential of the same hydrate forming component in phase 1 is different from its chemical potential in phase 2, 3 and etc. in a non-equilibrium situation. This points out that the chemical potentials for the hydrate formers in the hydrate would also be different, as observed from a Taylor expansion from an equilibrium point [81].

8.2 Equilibrium thermodynamics

For a system to attain thermodynamic equilibrium, the pressures, temperatures, and chemical potentials of all components in the system must be equal in all co-existing phases [8]. The industrial and real systems considered in this study cannot achieve equilibrium. Nevertheless, by applying a quasi-equilibrium scheme the thermodynamic benefits of different paths to hydrate formation can be evaluated and that will require the classical equilibrium equations (8.9) to (8.11):

$$T^{(I)} = T^{(II)} = T^{(III)} \ldots = T \quad \text{Thermal equilibrium (no net heat transport)} \quad (8.9)$$

$$P^{(I)} = P^{(II)} = P^{(III)} \ldots = P \quad \text{Newton's law, mechanical equilibrium} \quad (8.10)$$

$$\mu^{(I)} = \mu^{(II)} = \mu^{(III)} \ldots = \mu \quad \text{Chemical equilibrium (no net chemical work)} \quad (8.11)$$

The superscript (I), (II), (III) and more signify phase index for each of the coexisting phases in consideration. Residual thermodynamics by application of Soave-Redlich-Kwong (SRK) equation of state [138] has been applied for all hydrate forming components in every phase;

that is hydrate, liquid water and ice inclusive. This was executed based on the molecular dynamics results for water in different phases (empty hydrates, liquid water, and ice) [81].

8.3 Fluid thermodynamics

Evaluation of phase distributions and compositions in equilibrium systems can be executed by minimizing free energy. And a free energy analysis can be employed to determine the most beneficial phase distributions locally in non-equilibrium systems, together with thermodynamic preference for each component to move across phase boundaries from the parent phase to other (new) phases. It is not crucial to choose a reference state for every component in different phases in equilibrium systems provided there are thermodynamic models. However, in non-equilibrium systems, applying the same reference state [58] for the free energy of all phases is convenient. Based on residual thermodynamics (applied for fluid), "ideal gas" is applied as the reference state for estimation of chemical potentials of every component in the different active phases as expressed in equation (8.12) [5].

$$\mu_i(T,P,\vec{y}) - \mu_i^{ideal\ gas}(T,P,\vec{y}) = RTln\emptyset_i(T,P,\vec{y}) \qquad (8.12)$$

$\lim(\emptyset_i) \rightarrow 1.0$ ...for ideal gas

Where $\emptyset_i$ refers to fugacity coefficient for component *I* in specific phase and $\vec{y}$ denotes mole fraction vector of the gas. The chemical potential of the ideal gas, $\mu_i^{ideal\ gas}$ comprises the trivial mixing term consequent on entropy of mixing ideal gases at constant pressure and constant temperature.

8.4 Aqueous thermodynamics

The evaluation of chemical potential of pure water is based on samplings from molecular dynamics (MD) simulations [81].

8.5 Symmetric excess

As an intermediate step, a different reference state (ideal liquid) is applied for modelling the chemical potential of component *i* in liquid (water) phase as expressed in equation (8.13) usually referred to as symmetric excess in thermodynamics:

$$\mu_i(T,P,\vec{x}) - \mu_i^{ideal\ liquid}(T,P,\vec{x}) = RTln\gamma_i(T,P,\vec{x}) \quad (8.13)$$

Where $\lim\gamma_i \rightarrow 1.0$ when $x_i \rightarrow 1.0$

And γ_i denotes the activity coefficient for component *i* in the liquid mixture. Here, the chemical potential of the ideal liquid also comprises the ideal mixing term. When this formulation (i.e. equation (8.13)) is used for water, ideal gas reference state can as be applied when the chemical potential of pure liquid water is estimated on the basis of molecular interaction models by the use of molecular dynamics simulations. And in this study data from [81] have been used.

8.6 Assymetric excess

It is very proper to apply infinite dilution of component(s) in water as a liquid reference state when the solubility of the gas component(s) is low. The solubility of methane and higher hydrocarbons in water is limited; consequently, equation (8.14) is appropriate:

$$\mu_i(T,P,\vec{x}) - \mu_i^{\infty}(T,P,\vec{x}) = RTln[x_i\gamma_i^{\infty}(T,P,\vec{x})] \quad (8.14)$$

$\lim\gamma_i^{\infty}$ when $x_i \rightarrow 0$

Where,

μ_i^{∞} = the chemical potential of component *i* in water at infinite dilution

γ_i^{∞} = the activity coefficient of component *i* in aqueous phase based on the same reference state

R = the universal gas constant [8.314 J/mol.K]

This given formulation is called the nonsymmetric or asymmetric excess convention since the limit of the activity coefficient for the component *i* will move to unity as the mole fraction goes to zero. A useful approach to calculate values on the basis of the ideal gas reference state for these infinite dilution chemical potentials is by means molecular dynamics simulations together with the use of the Gibbs−Duhem relation [72, 108]. As long as the thermodynamic properties of every phase is also defined and estimated outside of equilibrium, the first and second laws of thermodynamics necessitate that the available mass of every component, and the total mass, have to be distributed over every probable phase that can coexist under specific local pressure and temperature conditions [58]. This evaluation is

reasonably uncomplicated for most of the fluid phases considered in this study. The sole exception to this is the hydrate phase that needs special consideration; comprehensive discussion of this is presented in Kvamme et al. [72, 139]. When thermodynamic models for fluids in equations (8.12), (8.13) and (8.14) are combined with hydrate non-equilibrium models presented in [72, 139], it becomes reasonably uncomplicated to minimize the free energy and estimate values for local phase distributions complying with the first and the second law of thermodynamics. A number of algorithms that are able to execute this method are accessible in the open literature.

The cases considered in this study involve very low mutual solubilities and/or low concentrations; the solubility of hydrocarbon hydrate formers (i.e., C_1 to iC_4, each of them) is very low. Accordingly, equation (8.15) could be applied together with equation (8.14). This has proven acceptably accurate for most industrial applications having the risk of hydrate formation as a factor.

$$\mu_{i,j}(T,P,\vec{x}) \approx \mu_{i,j}^{\infty}(T,P,\vec{x}) + RTln\left[x_{i,j}\gamma_{i,j}^{\infty}(T,P,\vec{x})\right] \quad (8.15)$$

Where subscript *i* represents different phases and subscript *j* signifies different components.

8.7 Hydrate thermodynamics

Generally, the statistical mechanical model is used to evaluate the chemical potential of water in hydrate. It is a classic Langmuir type of adsorption model, but it is used in the form derived by Kvamme & Tanaka [81] as presented in equation (8.16). This formulation accounts for the lattice movements and corresponding effects of different hydrate formers; it accounts for collisions between guest molecules and water which are sufficiently strong to affect water motions. The model of van der Waal and Platteuw [31] presumes "rigid lattice"- it assumes that water movements in the lattice are not affected by guest (hydrate former) molecule *j*.

$$\mu_{H_2O}^{(H)} = \mu_{H_2O}^{(0,H)} - R.T\sum_{i=1}^{2} v_i ln\left(1 + \sum_{j=1}^{n_{guest}} h_{ij}\right) \quad (8.16)$$

Where,

H = hydrate phase

$\mu_{H_2O}^{(H)}$ = chemical potential of water in hydrate

$\mu_{H_2O}^{(0,H)}$ = chemical potential of water in empty hydrate structure

v_i = fraction of cavity type *i* per water molecule

h_{ij} = canonical cavity partition function of component *j* in cavity type *i*

n_{guest} = number of guest molecules in the system.

The unit cell of structure I hydrate comprises 46 water molecules. This structure I type of hydrate has 2 small and 6 large cavities, as a result, $v_{small} = 1/23$ and $v_{large} = 3/23$. The relation presented in equation (8.17) is used to evaluate the canonical partition function:

$$h_{ij} = e^{-\beta\left(\mu_i^H - \Delta g_{ij}^{inc}\right)} \tag{8.17}$$

Where $\beta = \frac{1}{R.T}$ = inverse of gas constant times temperature, and Δg_{ij}^{inc} is the effect on hydrate water from inclusion of the guest molecules *j* in the cavity *i* [54, 81].

8.8 Equilibrium thermodynamics of hydrate

The chemical potential of component "*j"* (that is the hydrate former) in hydrate phase "*H"* must be equal to its chemical potential in the (parent) phase it has been extracted from [8] at equilibrium. The presence of hydrogen sulphide (H_2S) and carbon dioxide (CO_2) affects the chemical potential of liquid water, with the concentration of hydrogen sulphide having a considerable effect on the value [5, 8]. In this study, water completely dominates the dew point. Equation (8.18) is applied for evaluation of hydrate formation for the route of liquid water dropped out. Nevertheless, the evaluation of the chemical potential of all gas components (hydrate former) of hydrate is implemented using equation (8.13) in the case of water dissolved in gaseous phase.

$$\mu_{H_2O}^{(0,H)} - R.T\sum_{i=1}^{2} v_i ln\left(1 + \sum_{j=1}^{n_{guest}} h_{ij}\right) = \mu_{i,H_2O}^{Pure\ water}(T,P) + RTln\left[x_{i,H_2O}\gamma_{i,H_2O}(T,P,\vec{x})\right] \tag{8.18}$$

The formulation of [81] is applied to evaluate the chemical potential of water in the empty hydrate structure. This model by [81] has been validated to have predictive capabilities [5]; consequently, it makes any empirical formulation for these chemical potentials to be meaningless and maybe unphysical based on the fact that chemical potential is a fundamental thermodynamic property. The right hand side of equation (8.18) was approximated by pure water because no ions are present in the water, but merely limited amounts of dissolved

gases. The impact would be just a slight shift in chemical potential of liquid water. For example, [48] at 15000 kPa and 274 K the correction is – 0.07 kJ/mole, though a little bit higher for 20000 kPa and 25000 kPa, even so it is still not dramatic for the purpose of this work.

Applying equation (8.18) for the specified local temperature will give the corresponding hydrate formation pressure. If this hydrate formation pressure is lesser than the local pressure given by flow's fluid dynamics, the mole fractions (concentrations) of condensed water, carbon dioxide, and hydrogen sulphide can be evaluated at the same time fulfilling the mass balance and equilibrium criteria. This method is like the flash calculations normally applied in chemical engineering, however in terms of fugacity model instead of a chemical potential one [5].

If the calculated hydrate formation pressure is lesser than the local pressure, hydrate formation will ensue through the classical dew-point route. And subsequently performing flash calculation using the local pressure and local temperature will yield the maximum content of liquid water mole fraction (or concentration) that can be permitted by the hydrocarbon gas-rich phase. Water will condense out (drop out) as a separate water (liquid) phase if water dew-point pressure is lower than the local pressure [5]. Consequently, it could be assumed that free water will be available for hydrate to form; hydrate of the lowest or most negative free energy commencing first. Knowing that hydrogen sulphide is a considerably more vigorous hydrate former compared to carbon dioxide, the initial hydrates formed would be significantly richer in hydrogen sulphide compared to subsequent hydrates that may be formed. Unlike the "standard" calculations, this method does not follow the usual hydrate formation from the "bulk" but instead, it seeks for the hydrate with the most negative or lowest absolute free energy capable of forming from the available hydrocarbon gas mixture under the kinetic limitations of mass and heat transport. In other words, one would aim to minimize the following equation in terms of hydrate formation pressure while considering the fact the systems investigated in this work cannot attain equilibrium; and equation (8.19) has been proven to be beneficial in estimation of free energy changes associated with a hydrate phase transition Δg^H [5].

$$\Delta g^H = \delta \sum_{j=1}^{n^H} x_j^H \left(\mu_j^H - \mu_j^P\right) \tag{8.19}$$

Where H is hydrate phase of molecule *j*, and *P* is parent phase of molecule *j*.

The summation includes every component in the hydrate phase, *H*. $\delta = +1$ and $\delta = -1$ for hydrate formation and hydrate dissociation respectively. For example, the free energy change in the case hydrate formation will at least be negative. Then again more rigorously, likewise, there will be a requirement that the implications of the gradients/slopes of free energy in all independent thermodynamic variables have to result in negative free energy changes [58]. For instance, formation of the hydrate of methane will occur provided that the conditions of temperature and pressure are within the hydrate stability region; nevertheless, the stability of this hydrate will as well be governed by the concentration of guest molecules (hydrate formers) in liquid water, likewise the water chemical potential in the hydrocarbon's (hydrate former's) phase(s)). During a pressure, volume, and temperature (P-V-T) experiment, the water phase as expected will get saturated in hydrate formers with regard to hydrate properties. Consequently, except an under-saturated water is used to replace the water this impact is not observed at all times. However, it can be very significant in an actual (real) flowing scenario where the water phase may not have enough time to saturate with hydrate formers consequent on the liquid and fluid transport flux dynamics [58]. The knowledge of "composition of hydrate" as well is required for the analysis of equation (8.19). The composition can be evaluated using the statistical thermodynamic theory to the adsorption model for hydrate **[58]**. The relation for the composition, filling fraction, and cavity partition function is expressed in equation (4.20):

$$\theta_{ij} = \frac{x_{ij}^{H}}{v_j(1-x_T)} = \frac{h_{ij}}{1+\sum_j h_{ij}} \tag{8.20}$$

Where:

θ_{ij} = filling fraction of component *j* in cavity type *i*

x_{ij}^{H} = mole fraction of component *j* in cavity type *i*

v_j = fraction of cavity type *i* per water molecule

x_T = total mole fraction of all guests in the hydrate

8.9 Free energy of inclusion

Estimated free energies of guest inclusion in the large cavity of structure I (sI) lattice have been fitted to a series in inverse reduced temperature [5, 58]; and the free energy of inclusion is given in equation (8.21):

$$\Delta g^{inclusion} = \sum_{i=0}^{5} k_i \left[\frac{T_c}{T}\right]^i \quad (8.21)$$

where T_c denotes the critical temperature of the guest molecule in consideration, and k = Ratio of gas mole-fraction versus liquid mole-fraction for the same component (gas/liquid K-values) . Methane, carbon dioxide, and hydrogen sulphide are sI hydrate guest molecules relevant to this study (See Table 8.1, 8.2, and 8.3). The critical temperatures, T_c for these three different types of guest molecule are specified in the tables' captions. There are certain different experimental evidences signifying that carbon dioxide (CO_2) can be entrapped in the small cavity of structure I lattice [140]. However, the molecular dynamics simulation study of [58] confirmed that CO_2 cannot give any stability to the small cavity of sI hydrate. The hydrate structure rather collapses with most of the CO_2 models they tested in their investigations. Despite the fact that these findings do not exclude CO_2 being "forced" into small cavities, they agreed that it would not have a substantial effect under dynamic flow situations, therefore, it can be safely disregarded in practical hydrate predictions **[5]**. And it has not been experimentally validated [5, 58] whether or not CO_2 will occupy the small cavities in a highly dynamic flow scenario. Besides, carbon dioxide's cavity partition function in a small cage (equation (8.17)) is approximately zero [58]. The free energy of inclusion was evaluated based on the work of [81]. In all the investigations in this study thermodynamic consistency is the main priority or concern; there was no aim of adjusting any parameter to fit experimental data. Table 8.1 and 8.2 [5, 104, 105] present free energy of inclusion parameters for methane (CH_4) and carbon dioxide (CO_2) respectively. While Table 8.3 presents updated free energy of inclusion parameters for hydrogen sulphide (H_2S) [58]. Empty hydrates and ice parameters were not remarkably affected and the parameters of [81] have been used.

Table 8.1: Coefficients for $\Delta g^{inclusion}$ (equation 7.21) series expansion in case of methane inclusion in both large and small cavities[a] [5].

k (kJ/mol)	Small Cavity	Large Cavity
0	−42.476832934435530	17.971499327861170
1	119.241243535365700	−23.440125959452020
2	−183.195646307320200	−161.815346774489700
3	128.392520963906600	45.205610253462990
4	−54.987841897868170	36.672606092509880
5	−78.556708653191480	138.002169135313400

[a]*Critical temperature (T_{cr}) of CH_4 is 190.56 K. And units for k is kJ/mol*

Table 8.2: Coefficients for $\Delta g^{inclusion}$ inverse-temperature expansion in case of CO_2 inclusion[a] [5]

k (kJ/mol)	Small Cavity	Large Cavity
0	0	14.852336735945610
1	0	2.707578918964229
2	0	−92.743171583430770
3	0	$-5.077678397461901 \times 10^{-001}$
4	0	9.402639104940899
5	0	21.652443372670030

[a]*T_{cr} of CO_2 is 304.13 K. It has been assumed that no CO_2 enters the small cavities.*

Table 8.3: Coefficient of $\Delta g^{inclusion}$ (eq 10) in the case of hydrogen sulphide inclusion in structure I. critical temperature for h_2s is 373.4 K [58]

k (kJ/mol)	Small Cavity	Large Cavity
0	−35.841596491485960	$-9.867851530796533 \times 10^{-001}$
1	75.644235713727100	$-5.091001628046955 \times 10^{-001}$
2	−49.924309029873280	−41.197126767481830
3	−31.868805469546190	−13.013675083152700
4	−1.638643733127986	5.462790477011296
5	12.738557911032440	8.535406376549272

[a]*Critical temperature (T_{cr}) of CH_4 is 190.56 K. And units for k is kJ/mol*

9 Analysis and Discussion of Results I: Validation of theoretical model

This model has previously been applied for investigation of structure I hydrate from mainly methane, ethane, carbon dioxide and hydrogen sulphide [5, 48]. In this project, investigation of limit of water content in hydrocarbons' stream is more comprehensive; it has been extended further to cover structure II hydrate formation from both pure and mixtures of sI and sII hydrocarbons hydrate formers. Impacts of inorganic gases of CO_2 and H_2S are also considered. This is because natural gas from several gas fields contains in addition to methane other components such as ethane, propane, isobutane, and sometimes significant amount of CO_2 as in the case of Sleipner gas field in the North Sea which is being investigated in this study. H_2S could also be present and thus it is also considered in this project. Free energy and water chemical potential for pure hydrocarbon components are also estimated in this work. There is no intention to tune empirical model parameters since the priority is to keep the statistical mechanical model [81] free of adjustable parameters in all terms, as well as chemical potentials of empty hydrate and chemical potentials for ice and liquid water. Thus, a reasonable qualitative agreement is quite acceptable for the purpose of this study. Nonetheless, all who intends to use the scheme and analysis presented in this study could make adjustment to their own models at their discretion.

The qualitative agreements between hydrate equilibrium estimates from this model [81] and established experimental data are presented in Figures 9.1 to 9.19; Section 9.1 presents figures for pure hydrocarbons, Section 9.2 for binary mixtures of hydrocarbons, Section 9.3 for ternary mixtures of hydrocarbons, Section 9.4 for pure CO_2 and mixtures of CO_2 and hydrocarbons, and Section 9.5 for H_2S and its mixtures.

It is vital to know that when comparing results from this model [81] and experimental data, the estimation of the free energy of inclusions has been implemented using molecular dynamics (MD) simulations and there was no tuning of the model as has been explained above. In addition, it is imperative to recall that formation of more than one hydrate having distinct properties (composition, densities and free energies) do result from multicomponent gas mixtures. From the first and second laws of thermodynamics, hydrate formation commences first with the most stable hydrate and formation of a variety of hydrate compositions will subsequently occur. For a multicomponent natural gas mixture like Sleipner gas, hydrate formation will commence with structure II hydrate guest molecules (isobutane and propane) first then the hydrate structure I guest molecules will finally form

hydrate. Therefore, it is more probable that the hydrate which would be formed at the end for the cases presented in Figures 9.5, 9.6, 9.7, 9.8, 9.9, 9.10, 9.14 should be a combination of hydrates from both structures I and II having varying compositions of the initial guest molecules from gas or liquid. And only structure I hydrate can result from the cases in Figures 9.1, 9.2, 9.11, 9.12, 9.13, 9.17, while the cases shown in Figures 9.3 and 9.4 it is merely structure II hydrate formation that would occur. For systems investigated, both propane and isobutane would occupy the large cavity of structure II. While due to the small size of methane molecule, it would fill mainly the small cavity of structure I and ethane and CO_2 would be entrapped into the large cavity of structure I. Considering the fact that in structure II the ratio of small to large cavities is high, various hydrate compositions of both structures I and II should result.

The molecular dynamics (MD) simulations for the free energy of inclusion have mainly been performed for up to 280 K so the highest temperatures are to be taken as extrapolations. In this context it is vital that the cavity partition functions for these molecules is derived from MD simulations of model systems instead of fitting empirical models to experimental data. Other schemes which utilize the difference between the chemical potentials of pure liquid water and empty hydrate will probably be flexible enough to fit these experimental data sufficiently well as the chemical potential difference at a reference state is often treated as an empirical fitting parameter together with fitting of temperature dependence using the enthalpy of the same difference. Fitting of these parameters and molecular interaction parameters in the Langmuir constants towards these experimental data (and potentially additional experimental data) is likely to reproduce experiments well. As such perfect match between experimental data and estimates from this model [81] is not expected. However, based on the main focus and scope of this project, the comparisons between the estimates and theoretical predictions in this work with established experimental data as are satisfactorily acceptable.

9.1 Pure hydrocarbon guest molecules

The comparison of hydrate equilibrium estimates from this model with established experimental data are presented in Figures 9.1 to 9.4 below.

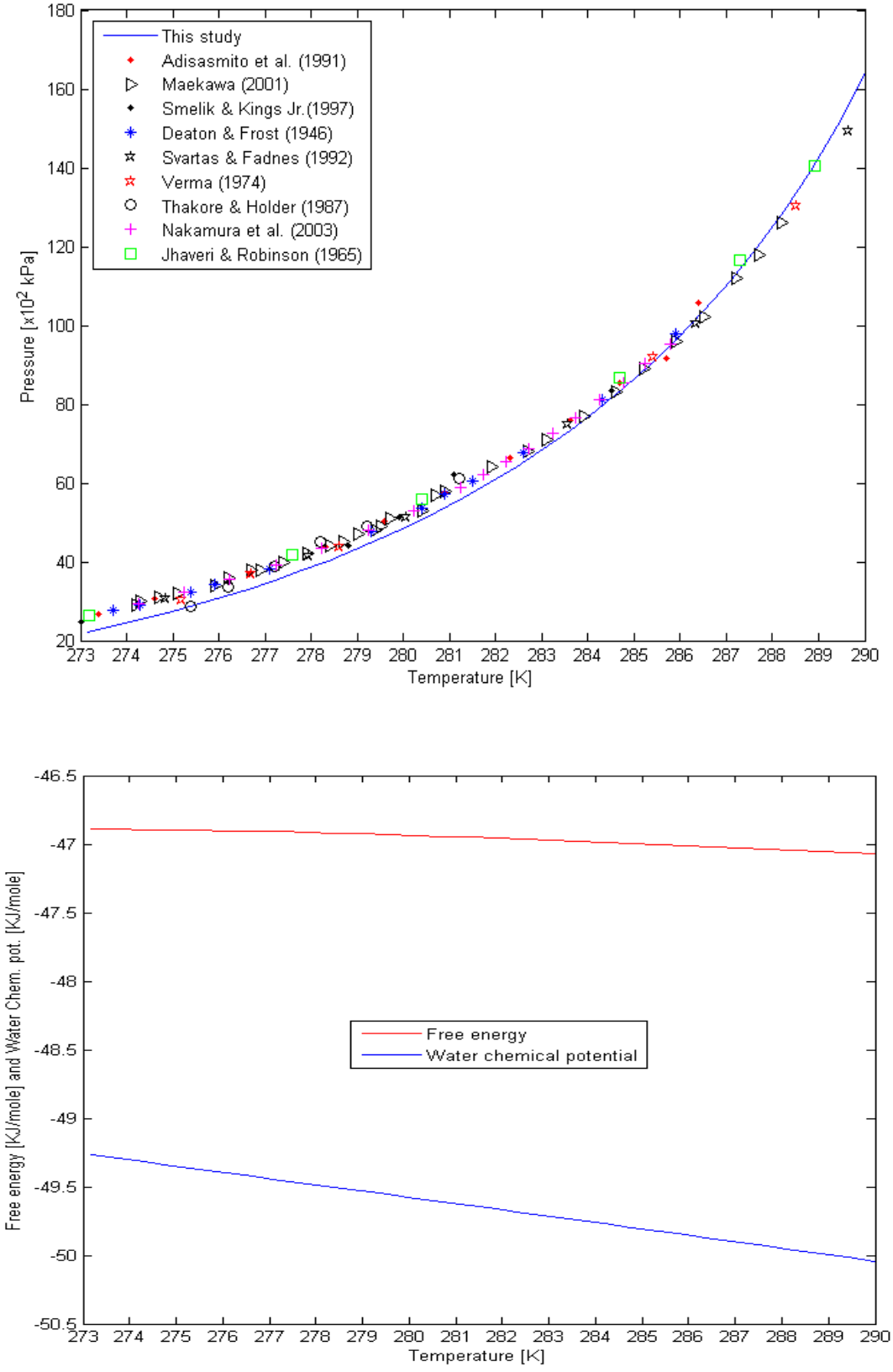

Figure9.1: Top curve is estimated equilibrium pressures for hydrate from pure methane as compared to experimental data from [141-149]. Bottom curve molar free energy for the hydrate and water chemical potential as function of temperature for the equilibrium pressures in the top curve

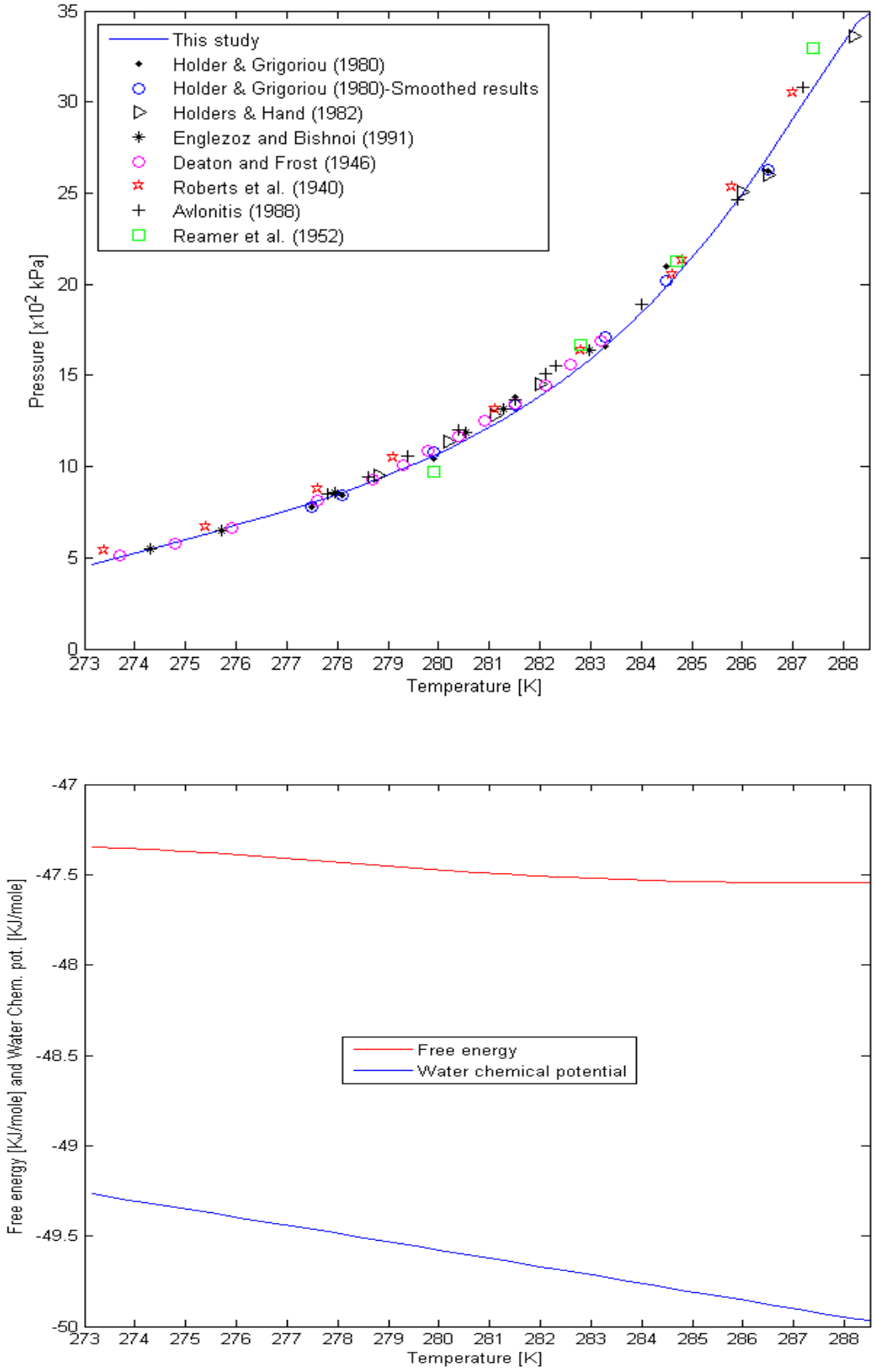

Figure9.2: Top curve is estimated equilibrium pressures for hydrate from pure ethane as compared to experimental data from [144, 150-155]. Bottom curve molar free energy for the hydrate and water chemical potential as function of temperature for the equilibrium pressures in the top curve

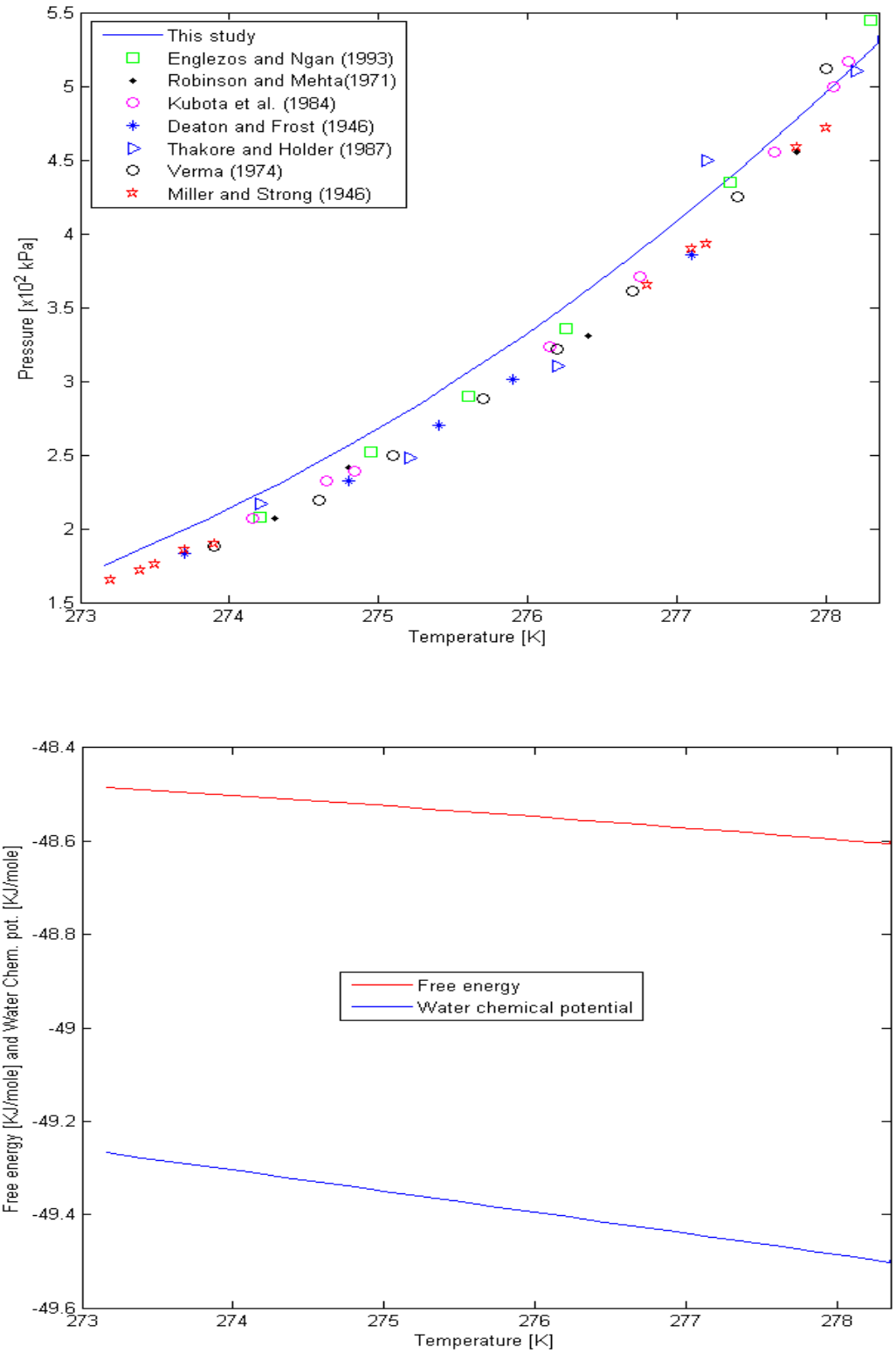

Figure9.3: Top curve is estimated equilibrium pressures for hydrate from pure propane as compared to experimental data from [7, 144, 146, 147, 156-158]. Bottom curve molar free energy for the hydrate and water chemical potential as function of temperature for the equilibrium pressures in the top curve

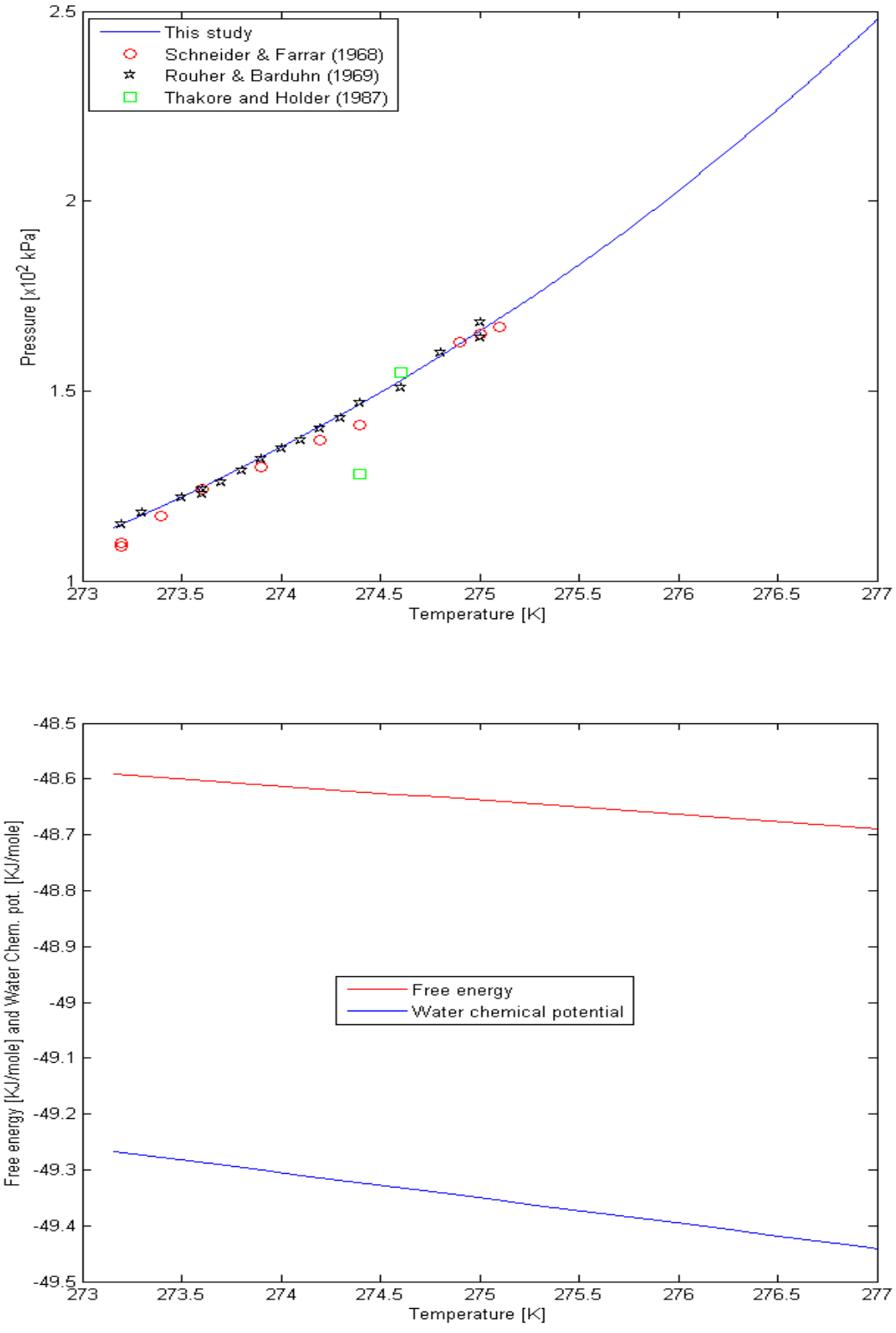

Figure9.4: Top curve is estimated equilibrium pressures for hydrate from pure isobutane as compared to experimental data from [147, 159, 160]. Bottom curve molar free energy for the hydrate and water chemical potential as function of temperature for the equilibrium pressures in the top curve

9.2 Binary mixtures of hydrocarbon guest molecules

Figures 8.5 to 8.7 present the validation of hydrate equilibrium estimates from this model with well-known experimental data.

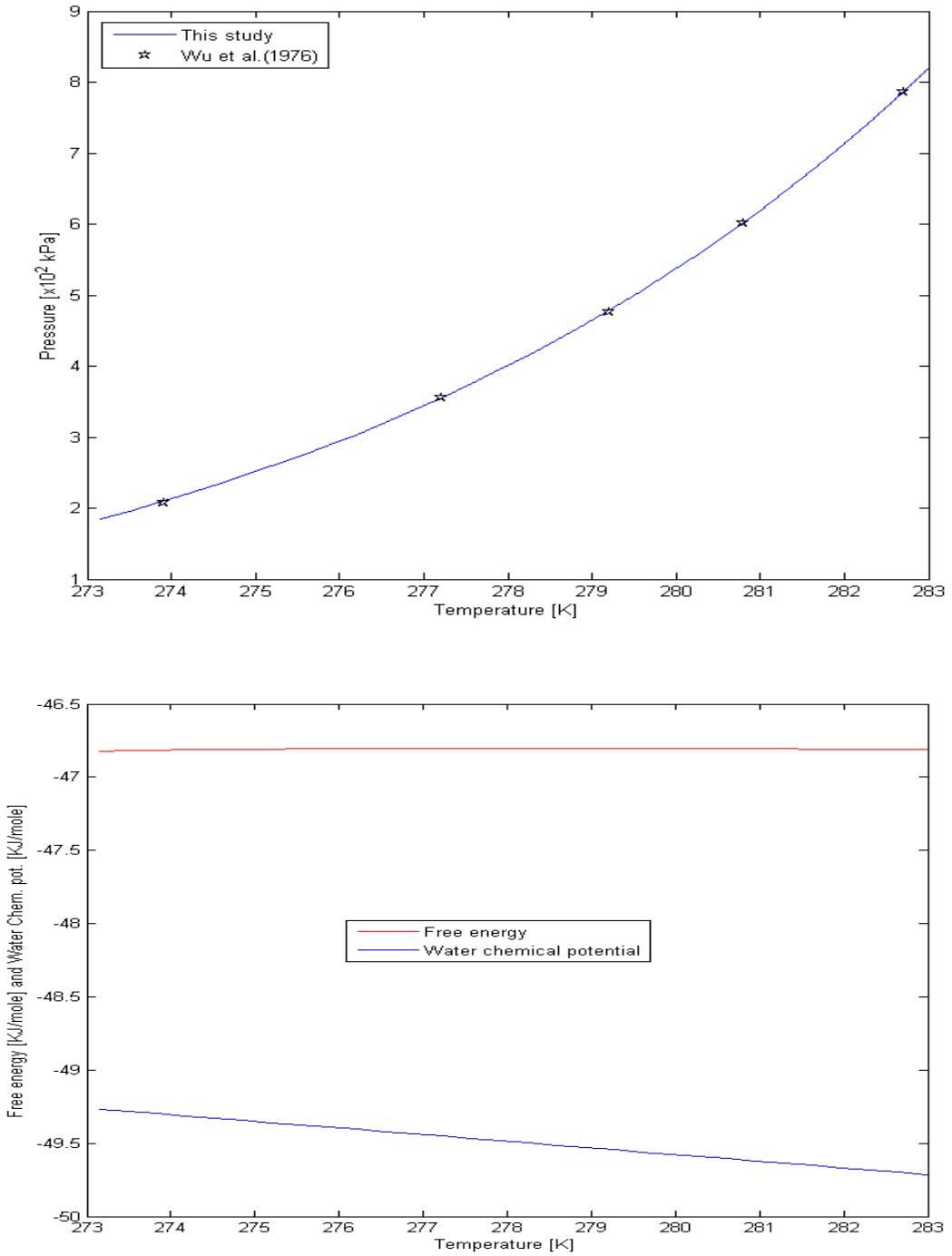

Figure 9.5: Top curve is estimated equilibrium pressures for hydrate from 0.714 mole of methane and 0.286 mole of isobutane as compared to experimental data from [161]. Bottom curve molar free energy for the hydrate and water chemical potential as function of temperature for the equilibrium pressures in the top curve

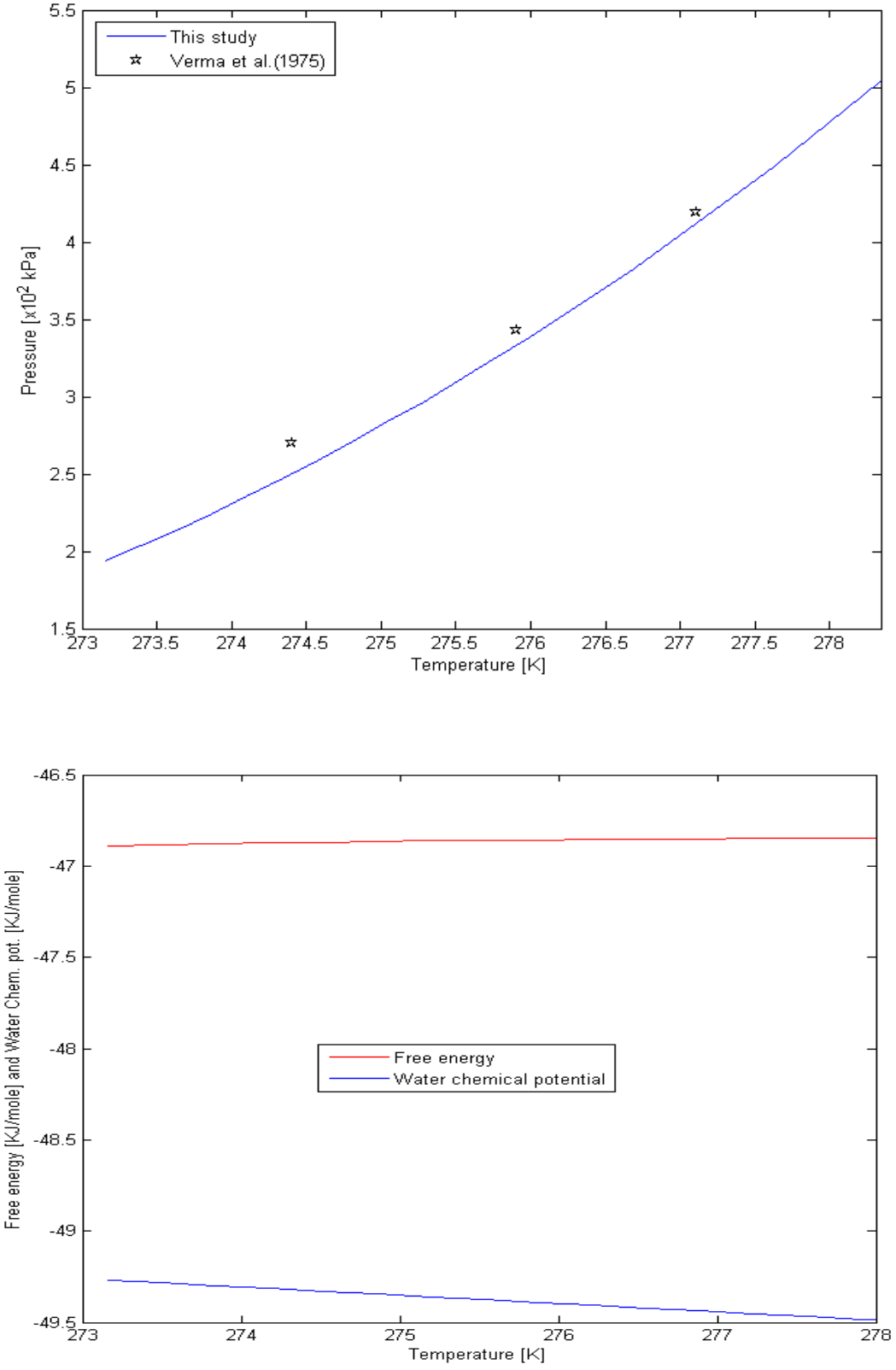

Figure 9.6: Top curve is estimated equilibrium pressures for hydrate from 0.371 mole of methane and 0.629 mole of propane as compared to experimental data from [162]. Bottom curve molar free energy for the hydrate and water chemical potential as function of temperature for the equilibrium pressures in the top curve.

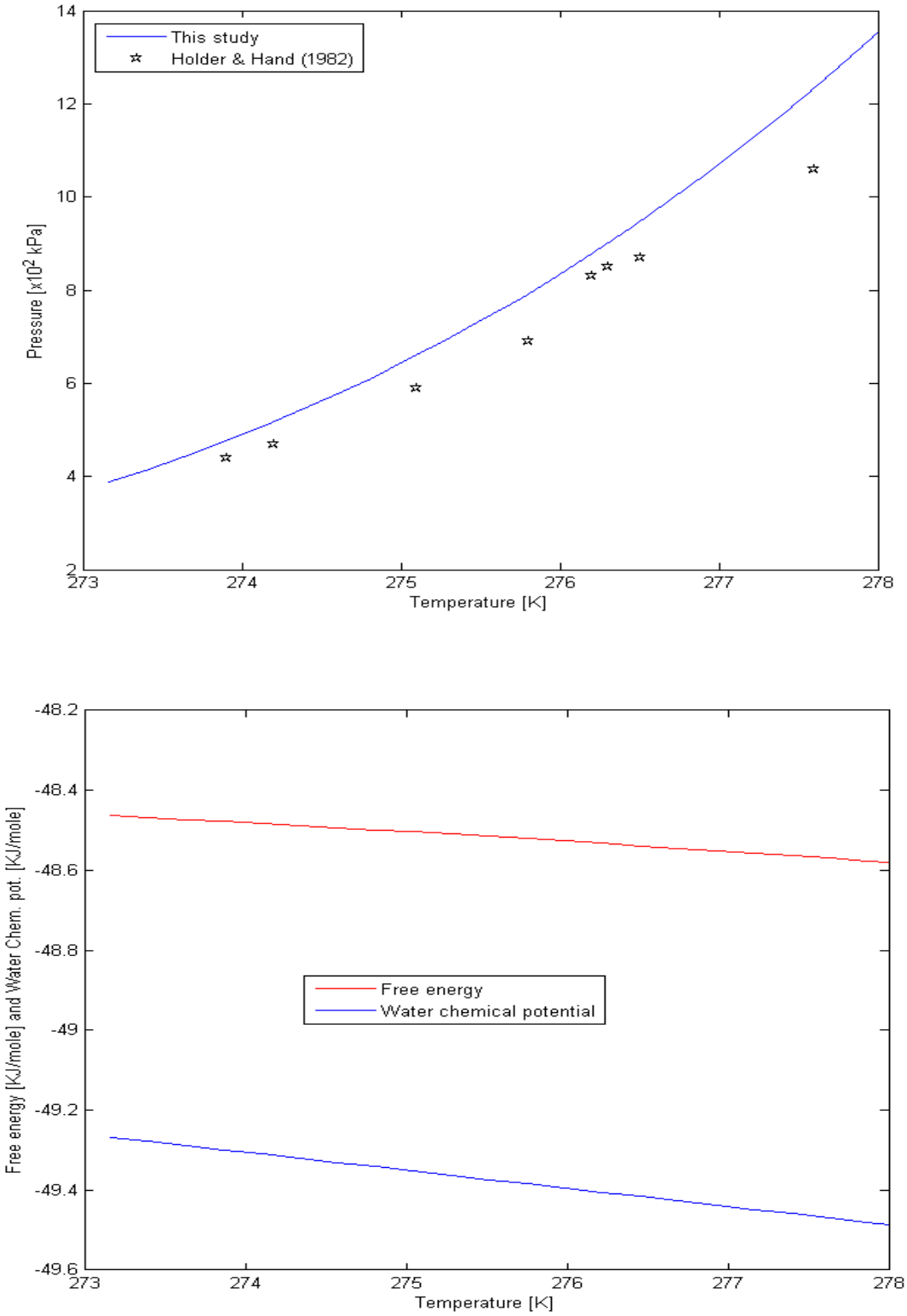

Figure 9.7: Top curve is estimated equilibrium pressures for hydrate from 0.658 mole of ethane and 0.342 mole of propane as compared to experimental data from [151]. Bottom curve molar free energy for the hydrate and water chemical potential as function of temperature for the equilibrium pressures in the top curve

9.3 Ternary mixtures of hydrocarbon guest molecules

Estimates of hydrate equilibrium of ternary hydrocarbon guest molecules from this model are compared with experimental as are presented in Figures 8.8 to 8.10 below.

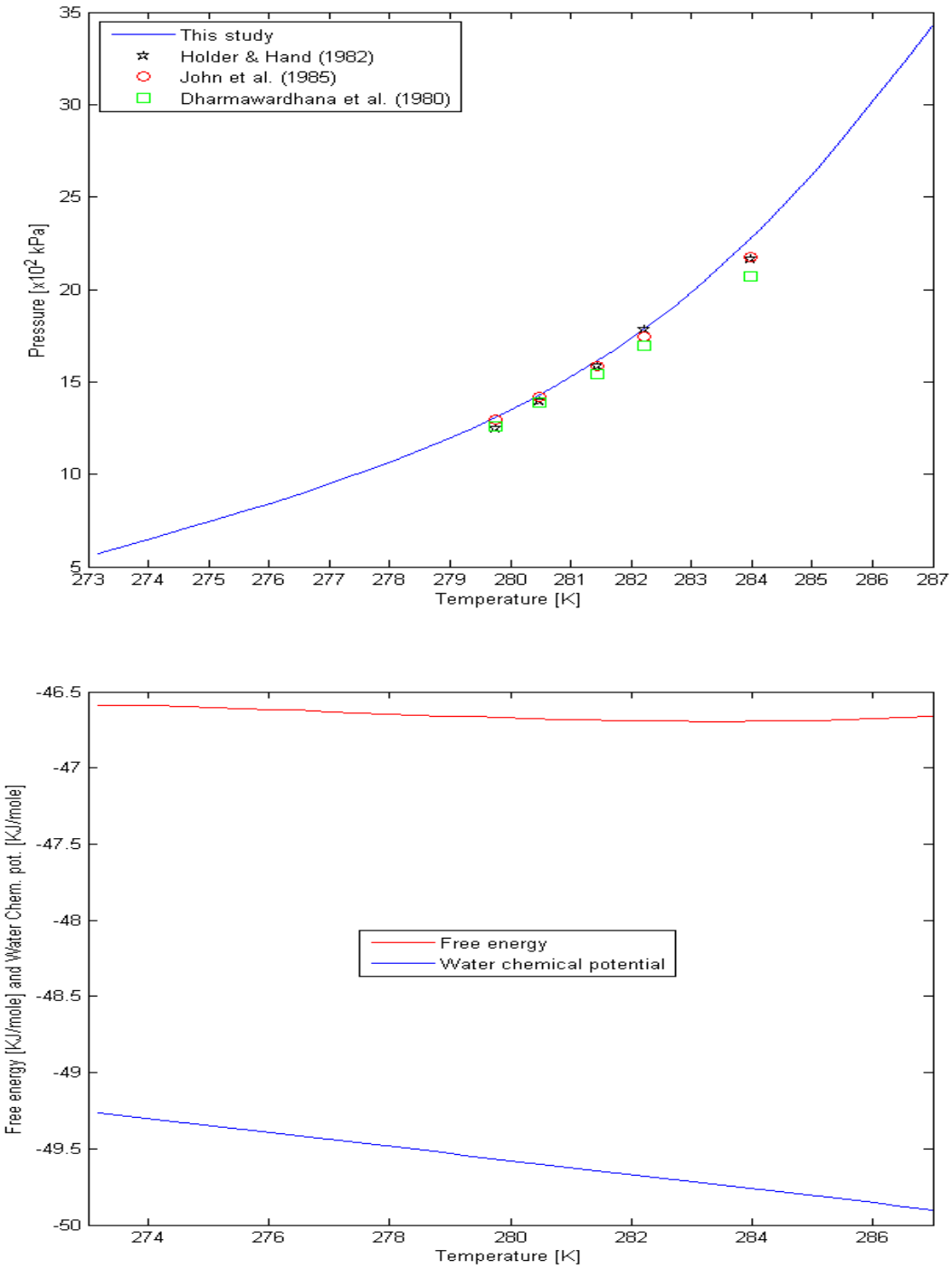

Figure9.8: Top curve is estimated equilibrium pressures for hydrate from 0.174 methane, 0.705 mole of ethane and 0.342 mole of propane as compared to experimental data from [151, 163, 164]. Bottom curve molar free energy for the hydrate and water chemical potential as function of temperature for the equilibrium pressures in the top curve

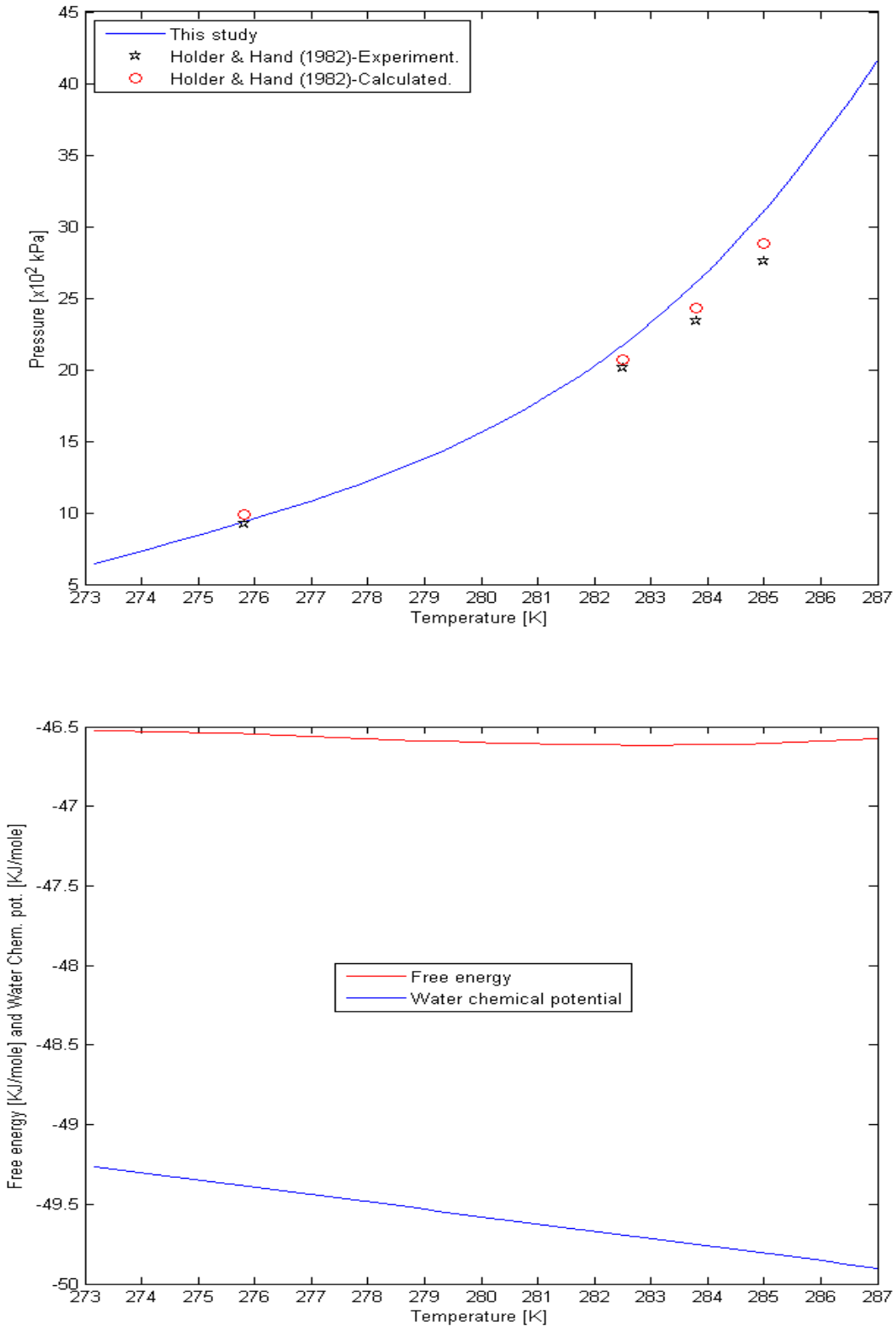

Figure 9.9: Top curve is estimated equilibrium pressures for hydrate from 0.364 methane, 0.541 mole of ethane and 0.095 mole of propane as compared to experimental data from [151]. Bottom curve molar free energy for the hydrate and water chemical potential as function of temperature for the equilibrium pressures in the top curve

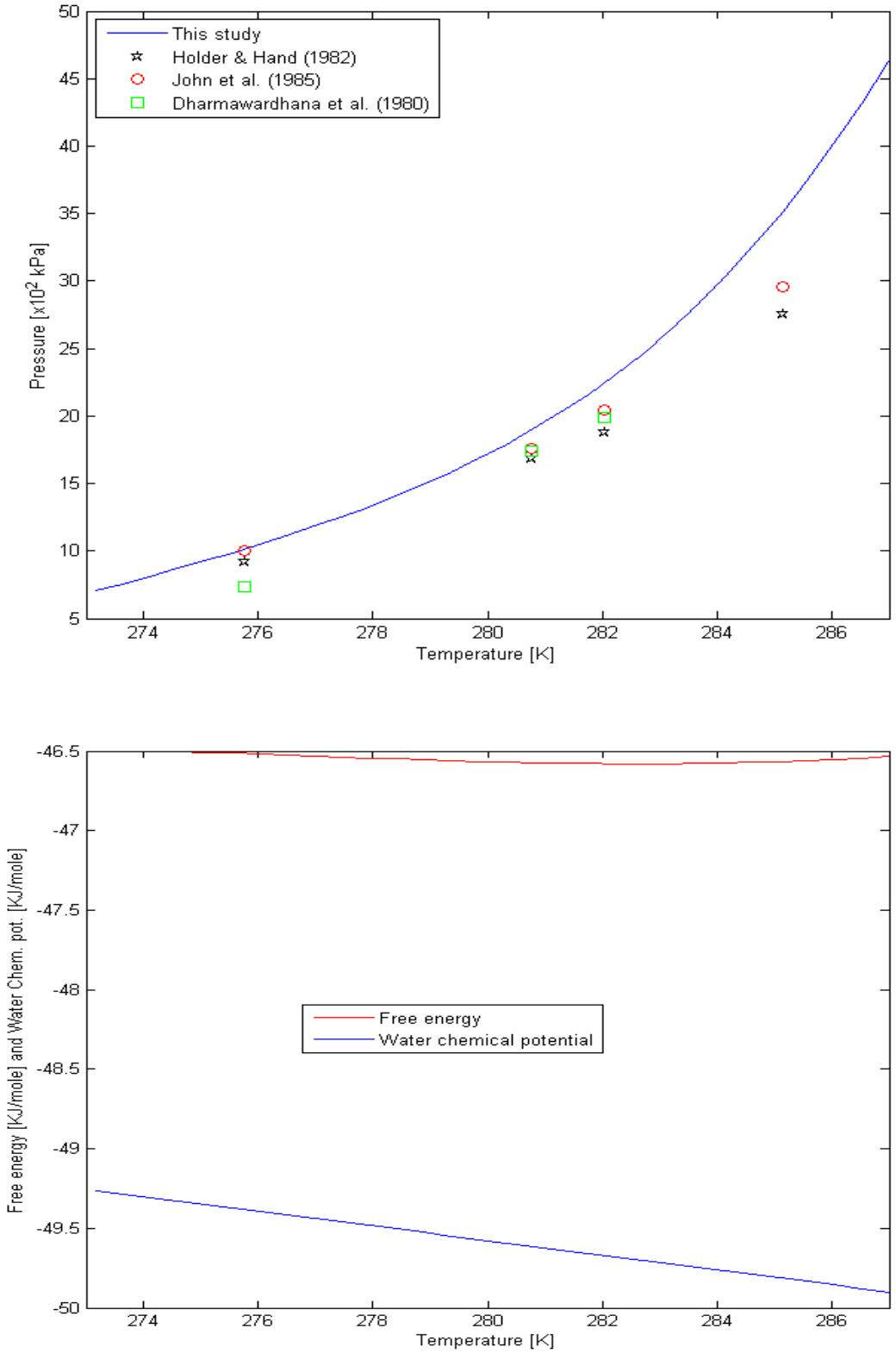

Figure9.10: Top curve is estimated equilibrium pressures for hydrate from 0.454 methane, 0.457 mole of ethane and 0.089 mole of propane as compared to experimental data from [151, 163, 164]. Bottom curve molar free energy for the hydrate and water chemical potential as function of temperature for the equilibrium pressures in the top curve

9.4 Pure CO_2 and mixtures with hydrocarbon guest molecules

Experimental data for hydrate equilibrium involving multicomponent hydrocarbon gas mixture with CO_2 as one of the components, especially for several temperature-pressure data points at constant concentration are not common in literature. Adisasmito and Sloan [165] as at 1992 stated that there were no data for binary mixtures containing carbon dioxide and either ethane or isobutane in literature. Thus, the estimates of hydrate equilibrium pressures for both multicomponent and binary mixtures from this theoretical model have been compared with experimental data from only Adisasmito and Sloan (1992) [165] and Adisasmito et al. (1991) [141] as presented in Figures 8.12 to 8.16. However, for pure CO_2, several experimental data are available in the literature as shown in Figure 8.11.

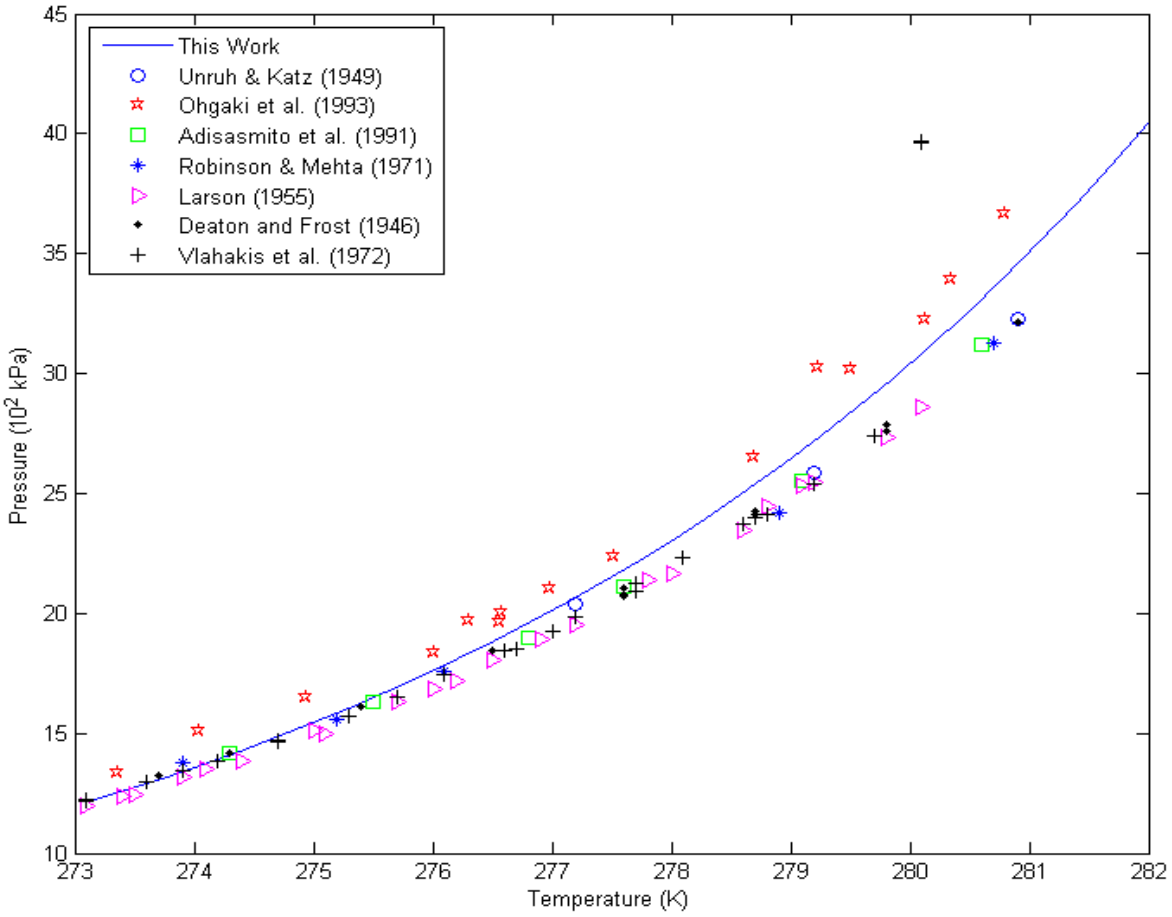

Figure 9.11: Estimated equilibrium pressures for hydrate from pure CO_2 as compared to experimental data from [141, 144, 156, 166-170].

In Figure 8.12 below experimental values and theoretical estimates for three structure II systems are compared [165].

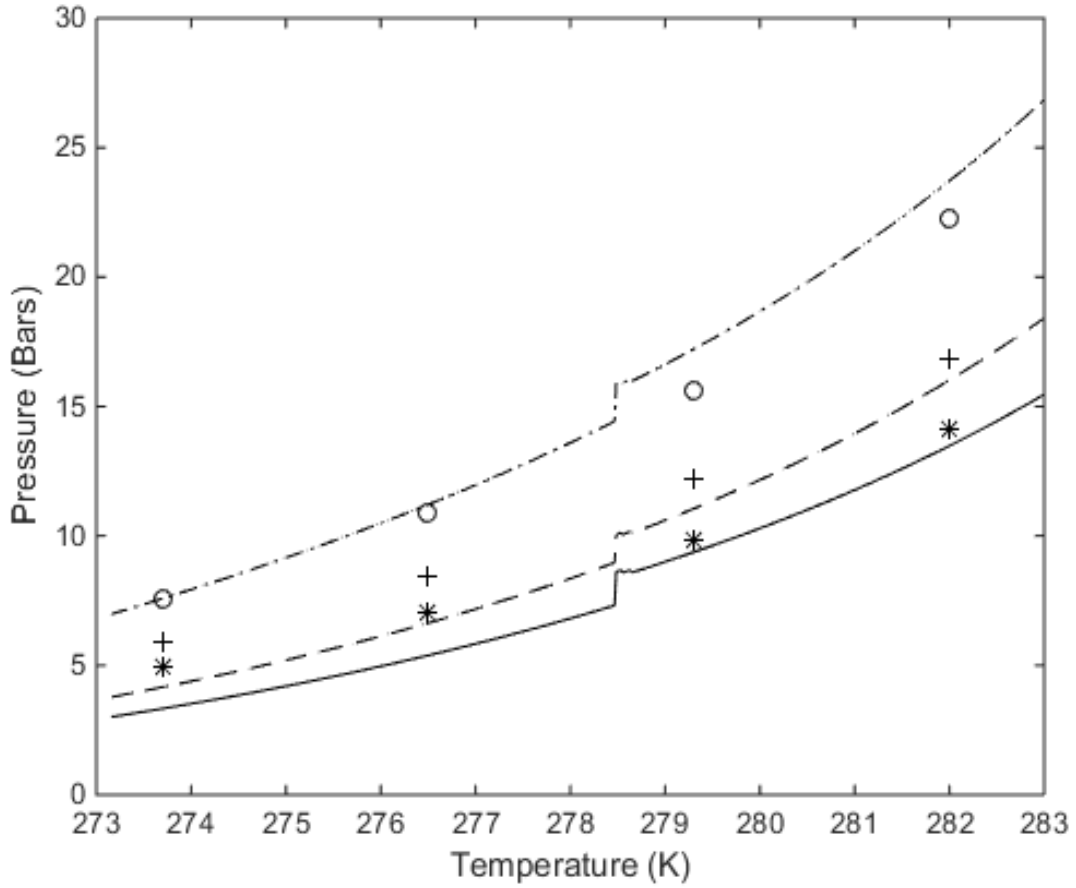

*Figure9.12: Experimental and predicted equilibrium curves for 3 different hydrocarbon systems, of which 2 systems contain CO_2. The order of mole-fractions is CH_4, C_2H_6, C_3H_8, iC_4, $n\text{-}C_4$, CO_2. In the first system * are experimental values [13] and solid curve is for a gas mixture with mole-fractions (0.7662, 0.1199, 0.0691, 0.0182, 0.0266 , 0). In the second system experimental values are plotted with + and predicted values are dashed. Composition of this system is (0.5255, 0.0812, 0.0474, 0.0319, 0.0188 , 0.314) . In the third system experiments are plotted with o and predicted values are plotted with dash-dot. Composition of this system is (0.2442, 0.0399, 0.0307, 0.0075, 0.0092, 0.6685).*

As mentioned above any perfect match is not expected as can be seen in Figure 9.12, there are deviations of significance for the lower temperature regions, except for the system without CO_2 which is in fairly good agreement. Nevertheless – the agreement is fair enough for qualitative analysis of various routes that can lead to hydrate formation. All three systems show a small jump in hydrate stability pressures between 278 K and 279 K. This jump has not been analyzed in detail since it is not very critical for the qualitative analysis in this work. It can be due to changes in partial molar densities of the various components of the gas mixtures (which enters ideal gas chemical potential calculations) or changes in the estimated fugacity coefficients for the components that enters residual chemical potential.

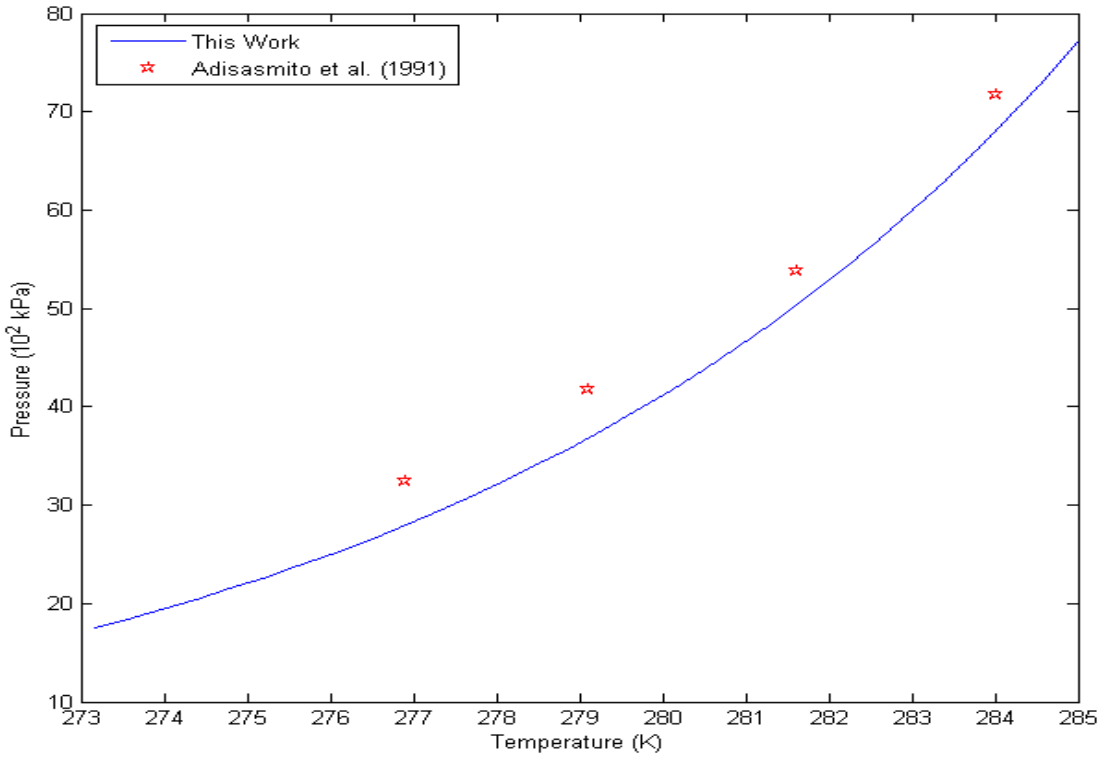

Figure 9.13: Estimated equilibrium pressures for hydrate from 0.86 mole of methane and 0.14 mole of CO_2 as compared to experimental data from [141].

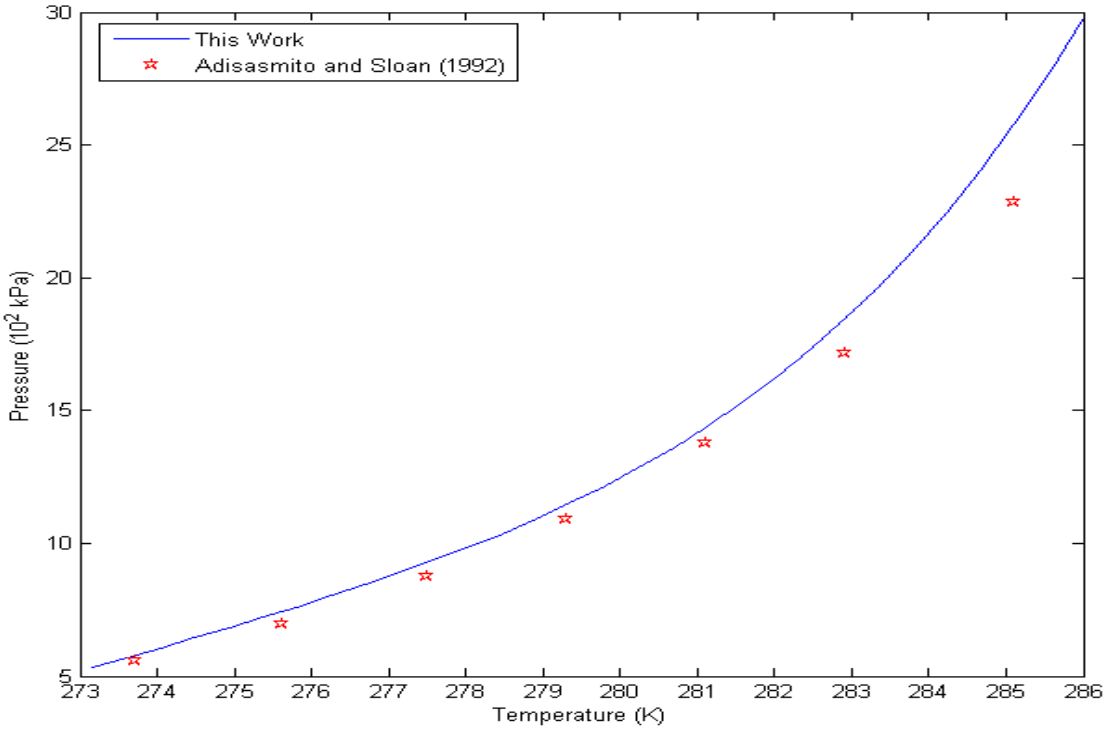

Figure 9.14: Estimated equilibrium pressures for hydrate from 0.80 mole of ethane and 0.20 mole of CO_2 as compared to experimental data from [165].

The system of propane and CO_2 as examined by Adisimoto and Sloan [165] (refers to Figure 9.15) appear to be more complex in terms of phase transitions. In this study this system has been examined using various equations of state and in-house software as well as commercial software. In all of these studies this systems undergo phase transitions for some of the higher temperatures. As such it might be worthwhile to experimentally re-examine this system. Interestingly enough the predicted equilibrium pressures is in perfect accordance with the gas phase for regions of conditions (pressure and temperature) before phase split and hydrate formed from the condensed liquid and water after the phase split. See also the captions to Figure 9.15 for more details.

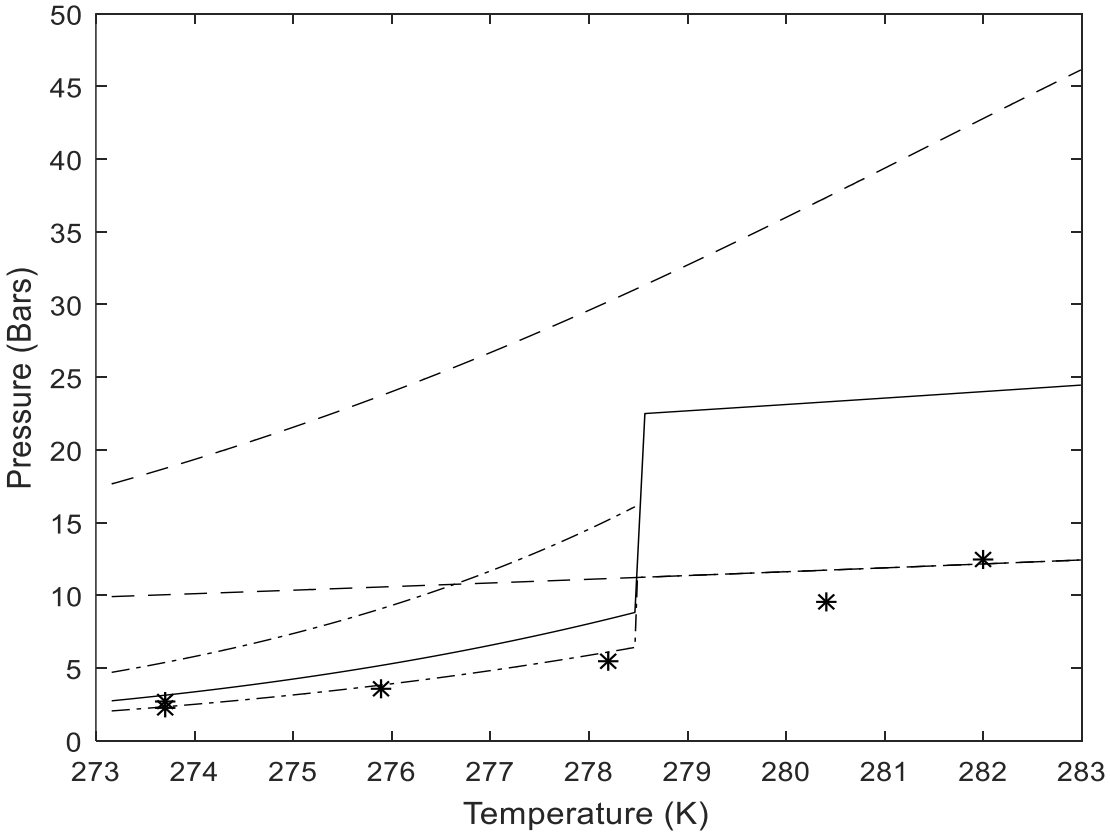

Figure9.15: Equilibrium curves for the initial 65% of propane and 35% of CO_2 system. Dashed dot curves are hydrates from the resulting gas and liquid mixtures after phase separation at a temperature 282.96 K. Upper dash dot curve is for a resulting phase consisting of 38.87% Propane and 61.13 % CO_2 while the lower dash dot curve is for 86.02% propane and 13.98% CO_2. Solid curve is the initial composition showing the change in pressure during crossing into the two phase region at 278.50 K. Note that the propane rich fraction also splits into a gas/liquid fraction at slightly higher temperature than the initial mixture. After the phase split the most stable hydrate phase almost coincides with the structure I estimates for the propane rich system (lower dashed curve). Structure I estimates are illustrated in dashed curve assuming no propane entering structure I. Upper dashed curve is for the 38.87% Propane and 61.13 % CO_2 while the lower dashed curve is for the 86.02% propane and 13.98% CO_2 mixture. Stars are experimental data [165].

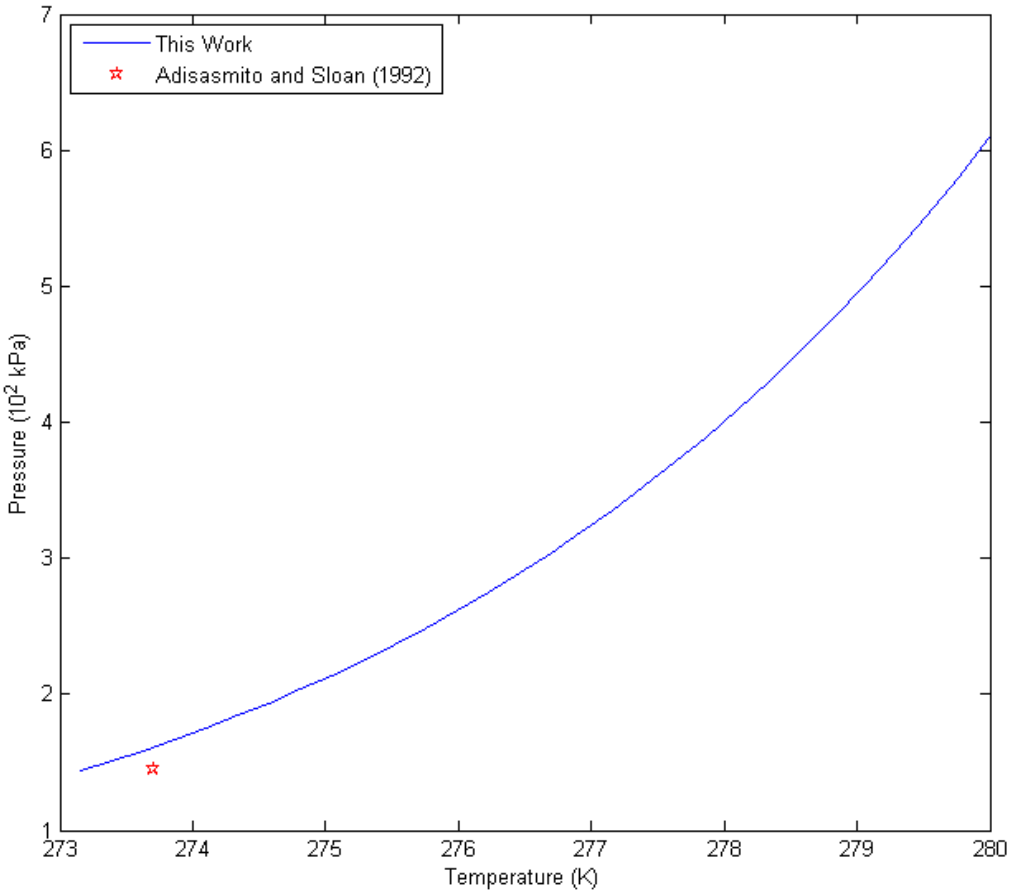

Figure9.16: Estimated equilibrium pressures for hydrate from 0.793 mole of isobutane and 0.207 mole of CO_2 as compared to experimental data from [165].

9.5 Pure H_2S and its mixtures

Figures 9.17 to 9.19 are the comparisons of hydrate equilibrium estimates from this model with established experimental data for pure H_2S together to that of its mixtures.

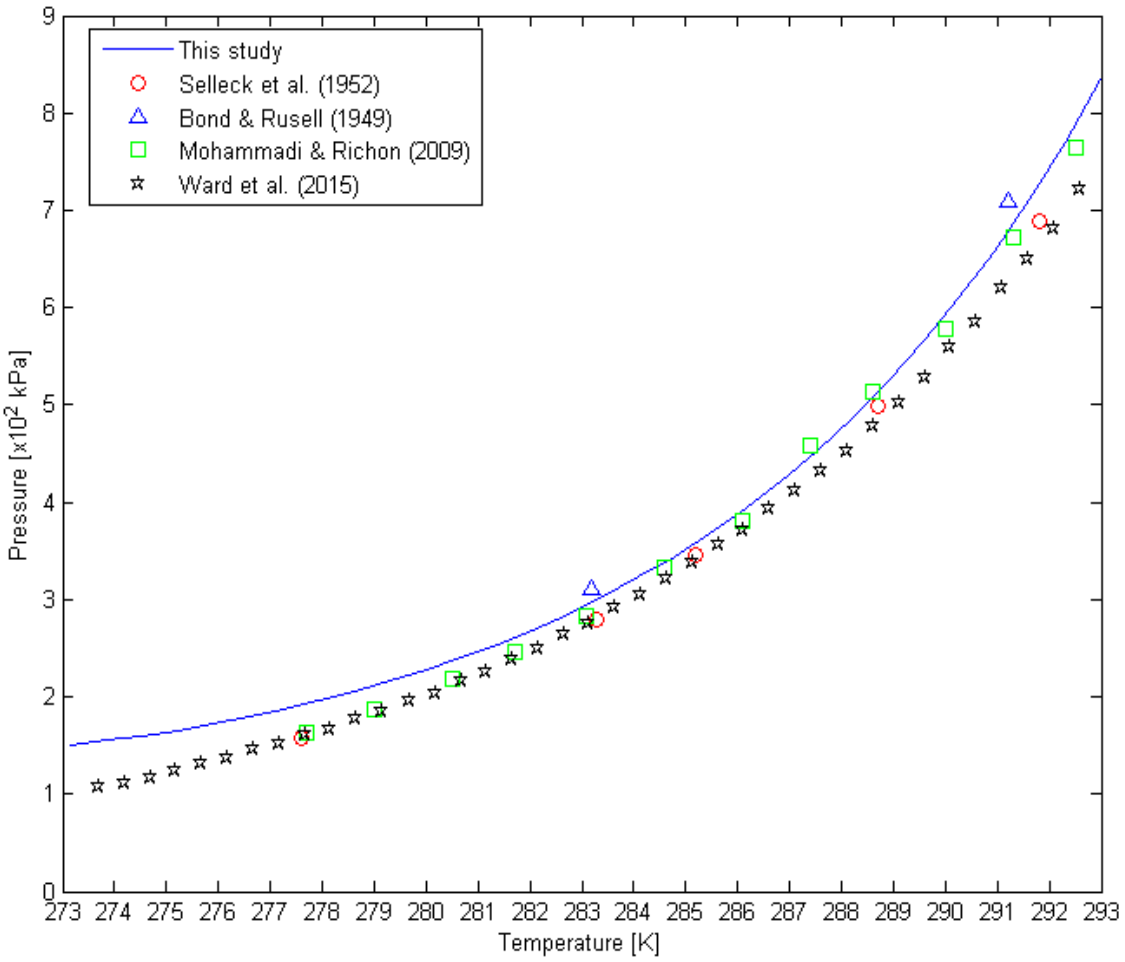

Figure9.17: Estimated equilibrium pressures for hydrate from H_2S as compared to experimental data from [171-174]

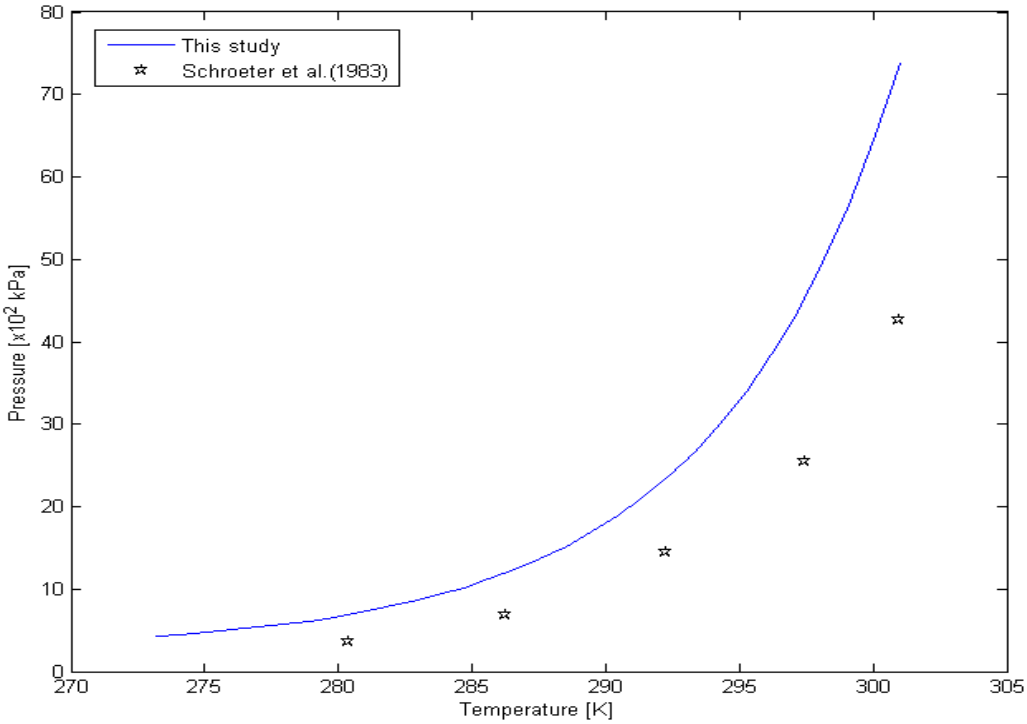

Figure9.18: Estimated equilibrium pressures for hydrate from 0.61 mole fraction of methane, 0.07 mole fraction of propane, 0.32 mole fraction of H_2S as compared to experimental data from [175].

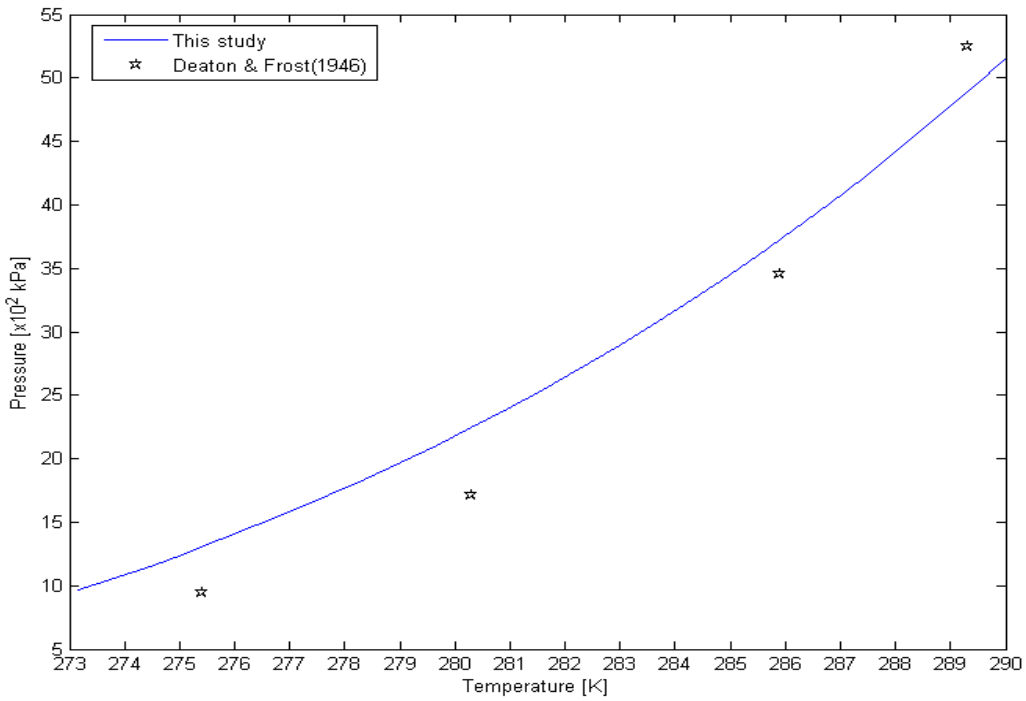

Figure9.19: Estimated equilibrium pressures for hydrate from 0.878 mole fraction of methane, mole 0.040 fraction of ethane, 0.021 mole fraction of propane, 0.015 mole fraction of isobutane, 0.0325 mole fraction of CO_2, 0.0025 mole fraction of H_2S, and 0.011 mole fraction of nitrogen as compared to experimental data from [144].

10 Analysis and Discussion of Results II: Troll gas from the North Sea

This section presents the results of investigation of a real industrial system involving hydrocarbon gas stream(s) during processing and transport, the Troll gas. This has been done using a novel thermodynamic scheme [81] for investigation of different routes to hydrate formation, applying ideal gas as reference state for all components in all phases including the hydrate phase. Results of both the new concept based on adsorption mechanism and the current approach based on dew-point calculation employed by the industry to evaluate the maximum water content that can be permitted to prevent the risk of hydrate formation are presented, analysed and discussed in this section.

10.1 Maximum water content that can be permitted during processing and transport of Troll gas.

For a specific hydrocarbon system in a process or pipeline transport system at a particular temperature and pressure, the upper limit of water in the hydrocarbon (gas or liquid) system before water condenses out is the initial step in a hydrate risk analysis. In typical hydrate risk analysis this is the concentration (mole fraction) of water in the hydrocarbon at water dew point. The final limits of water content in the gas need to be sufficiently low to stay in the gas without condensing out during transport from Kollsnes gas processing plant and all of the way to the receiving terminal at the continent.

Figures 10.1 to 10.8 and Table 10.1 illustrate the maximum amount of water that can be permitted in hydrocarbon gas streams without the risk of hydrate formation during processing and transport. As mentioned earlier, both routes have been considered: water dew-point approach, which is the conventional route currently used by the industry where free water condenses out from the gas stream, and the route where free water is adsorbed on the hematite that covers the internal surface of processing equipment and transport pipelines. All estimates show that it is more likely for free water to be made available by adsorption on hematite than the conventional dew-point route. These analyses show that the risk of hydrate formation still exists even below the upper limit of water content estimated by the usual approach (water dew-point). Considering the route of adsorption on hematite in the temperature range of 274 K to 280 K, only about 5 to 6 per cent of the dew-point approach

estimated maximum water contents should be permitted in hydrocarbon gas stream during processing and pipeline transport of hydrocarbon gas streams to avoid formation of hydrate. The gas mixtures with only the heavier hydrocarbons (without methane) exhibit opposite maximum water tolerance compared to the methane dominated Troll gas stream within the pressure range investigated. The higher the pressure, the higher the maximum amount of water that can be allowed without the risk of hydrate formation but it is opposite for the methane-rich Troll gas. As can be seen in Figures 10.1 to 10.4, the gap (i.e., the difference) between the pressure curves decreases from between 5000 kPa and 9000 kPa to between 21000 kPa and 25000 kPa. precisely, the curves of the last two higher pressures, that is 21000 kPa and 25000 kPa overlap. This is because the differences at the highest pressures are virtually insensitive to pressures due to the high density.

With assumption that all of the methane is separated out of the Troll gas stream in Separator 1, leaving the heavier hydrate forming hydrocarbon components, that is, ethane, propane, and isobutane, the compositions of the remaining components were normalized, and the maximum water concentration that could be allowed during processing and transport of the gas containing the remaining three components was estimated as presented in Figures 10.5 and 10.6. A further evaluation is performed with assumption that all the ethane is separated out leaving just the heavier components of propane and isobutane. The estimates of the latter are shown in Figures 10.7 and 10.8. Moreover, for the gas mixture containing only the C2+, the higher the number of carbon in each component's molecule, the higher the allowable amount of water without the risk of hydrate formation. Consequently, the maximum amount of water that can be permitted to avoid the formation of hydrate in the gas stream from separator 1 (containing just propane and isobutane) after methane and ethane are separated out is around 24−37% higher than that of the fluid at the liquid outlet of Separator 1, having ethane, propane, and isobutane within the pressure range of 5000−25 000 kPa and temperature range of 274−280 K. Consequently, the sensitivity of these C_{2+} on the Troll gas are further examined in Subsection 10.2.

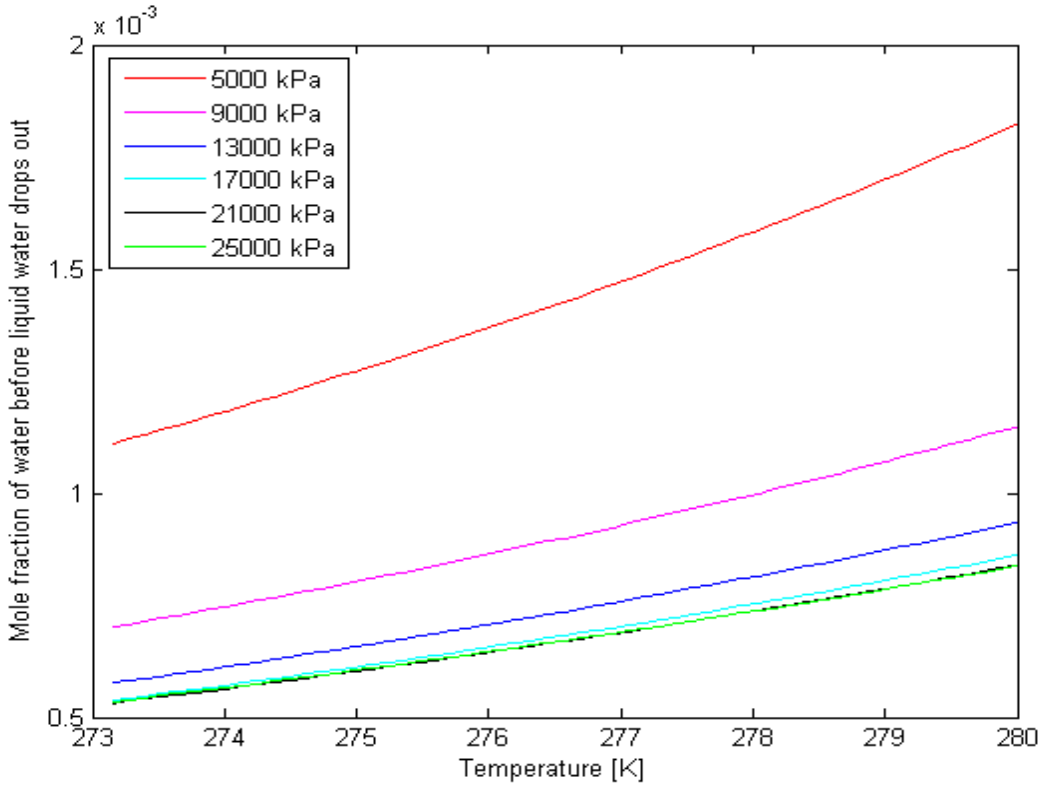

Figure10.1: Maximum water content before liquid water drops out from the well-head fluid (Troll gas).

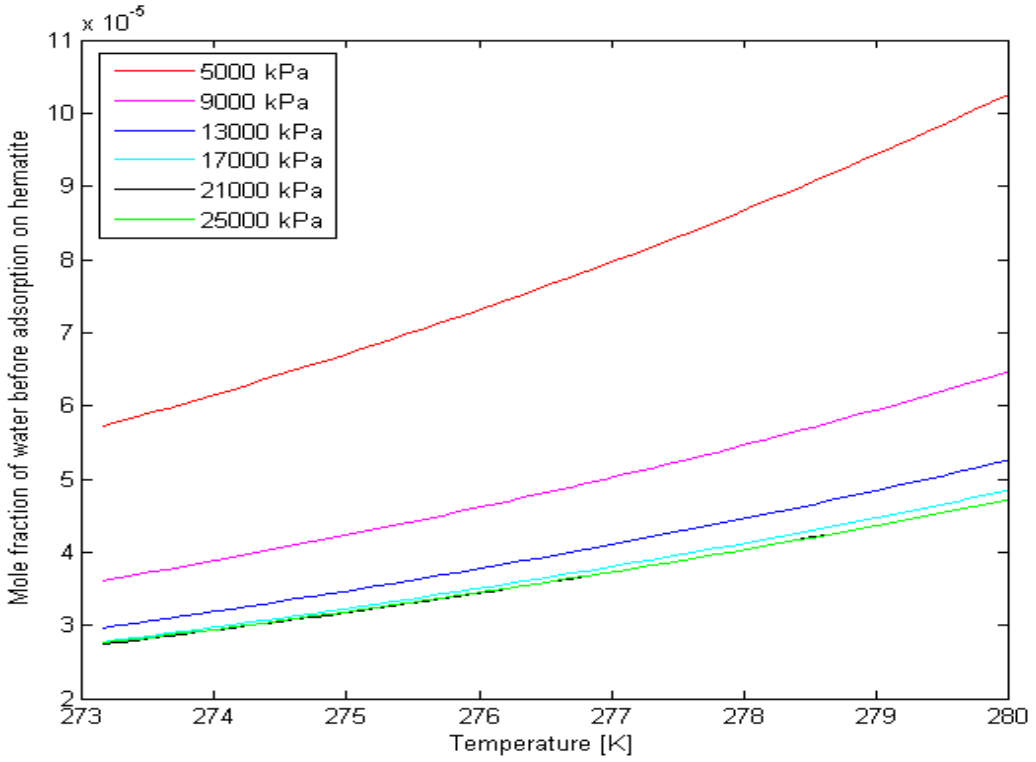

Figure10.2: Maximum water content before the adsorption of water on hematite occurs for the well-head fluid (Troll gas)

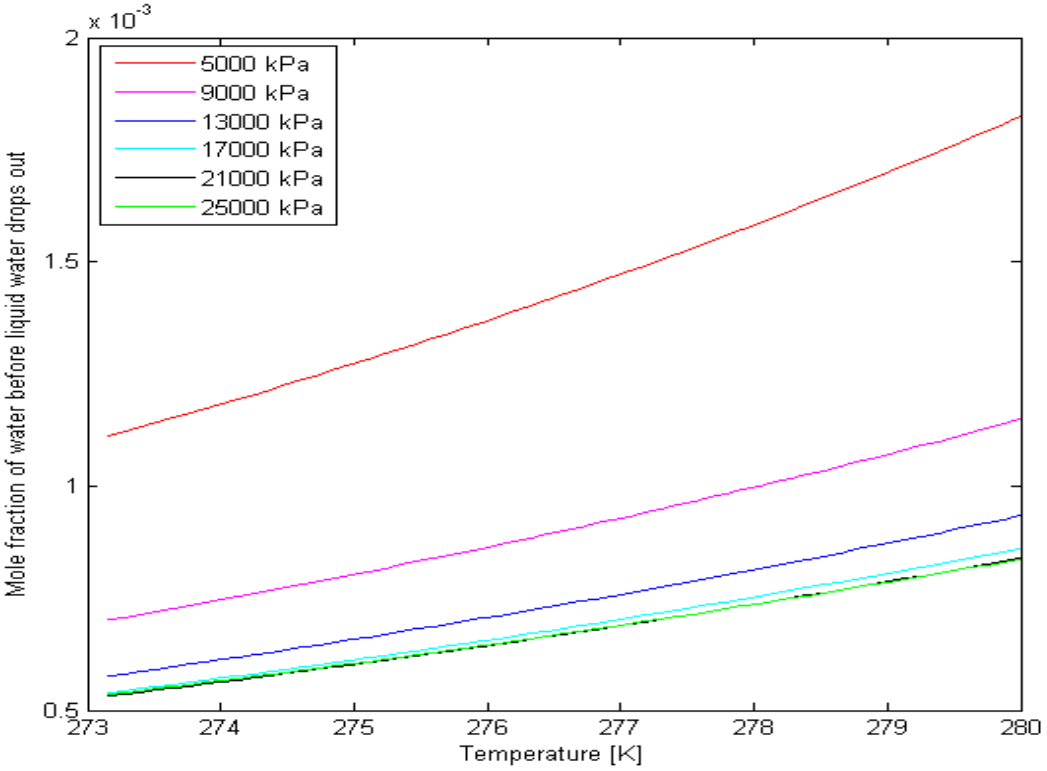

Figure10.3: Maximum water content before liquid water drops out from Troll gas at Separator 1.

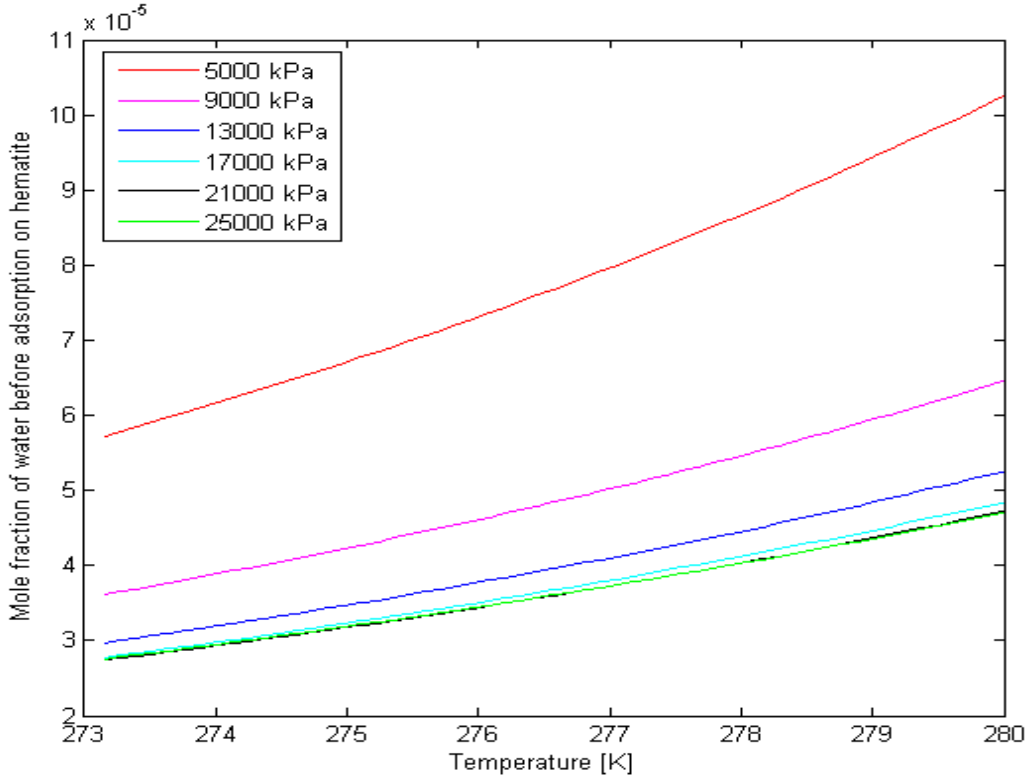

Figure10.4: Maximum water content before the adsorption of water on hematite occurs from Troll gas at Separator 1

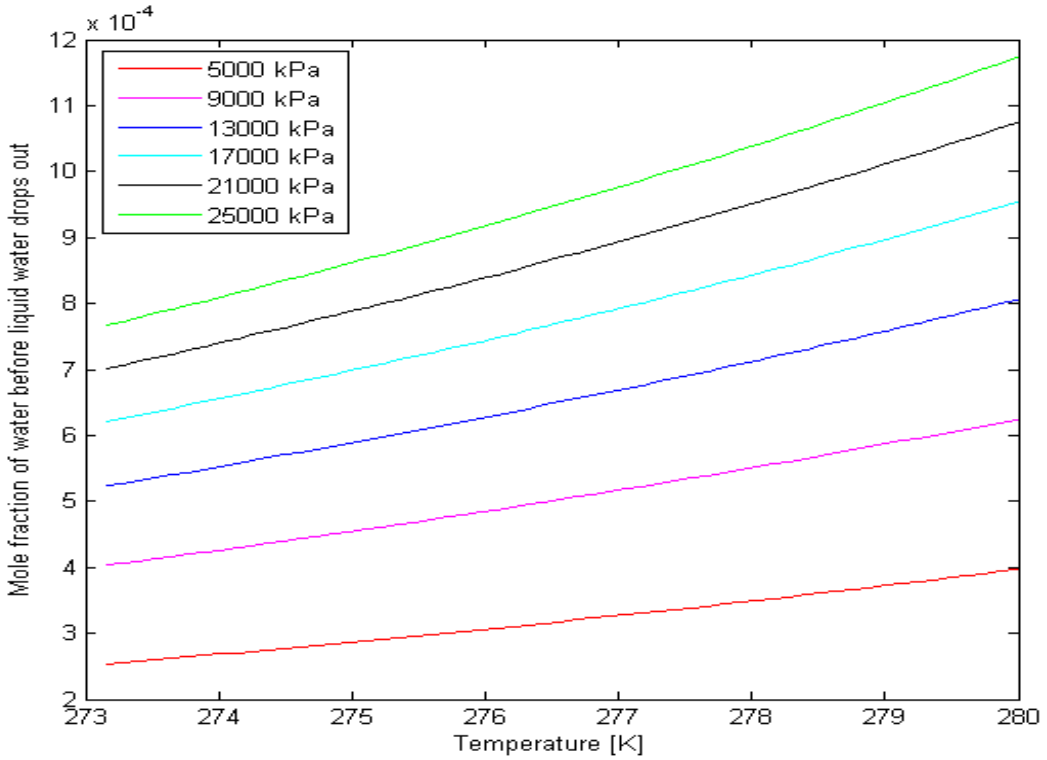

Figure10.5: Maximum water content before liquid water drops out from the gas stream after separator 1 containing 86.1% of ethane, 7.5% of propane, and 6.4% of isobutane (Troll gas).

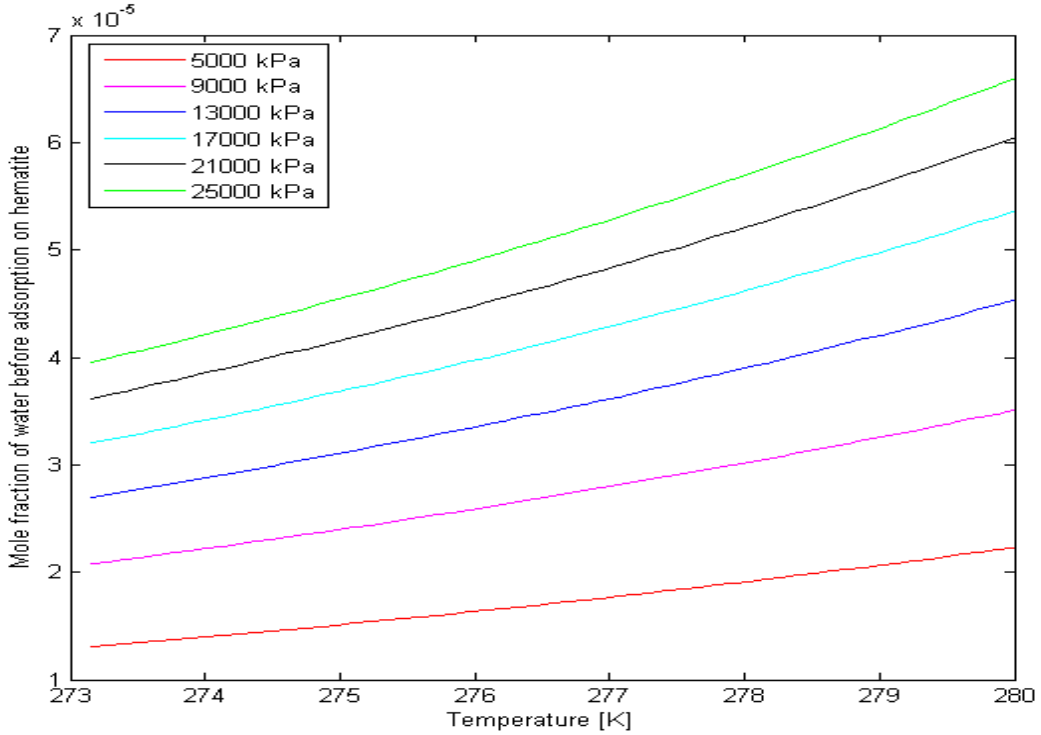

Figure10.6: Maximum water content before the adsorption of liquid water on hematite occurs from the gas stream after separator 1 containing 86.1% of ethane, 7.5% of propane, and 6.4% of isobutane (Troll gas)

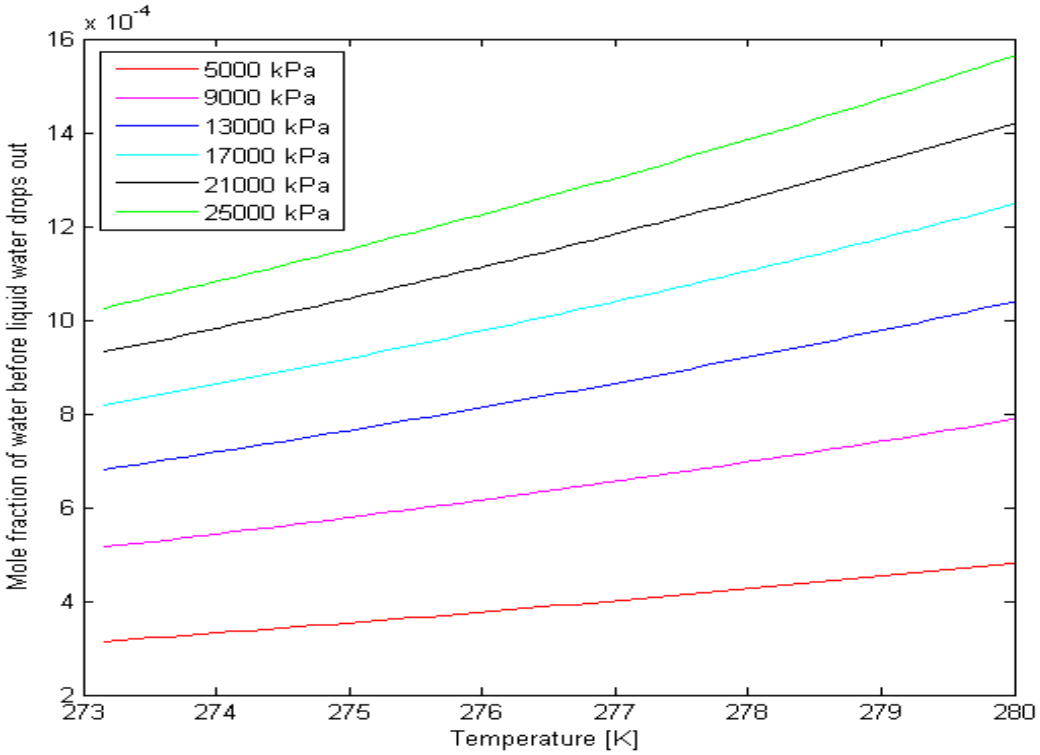

Figure10.7: Maximum water content before liquid water drops out from the gas stream after further separation, leaving only propane and isobutane with molar concentrations of 0.54 and 0.46, respectively (Troll gas)

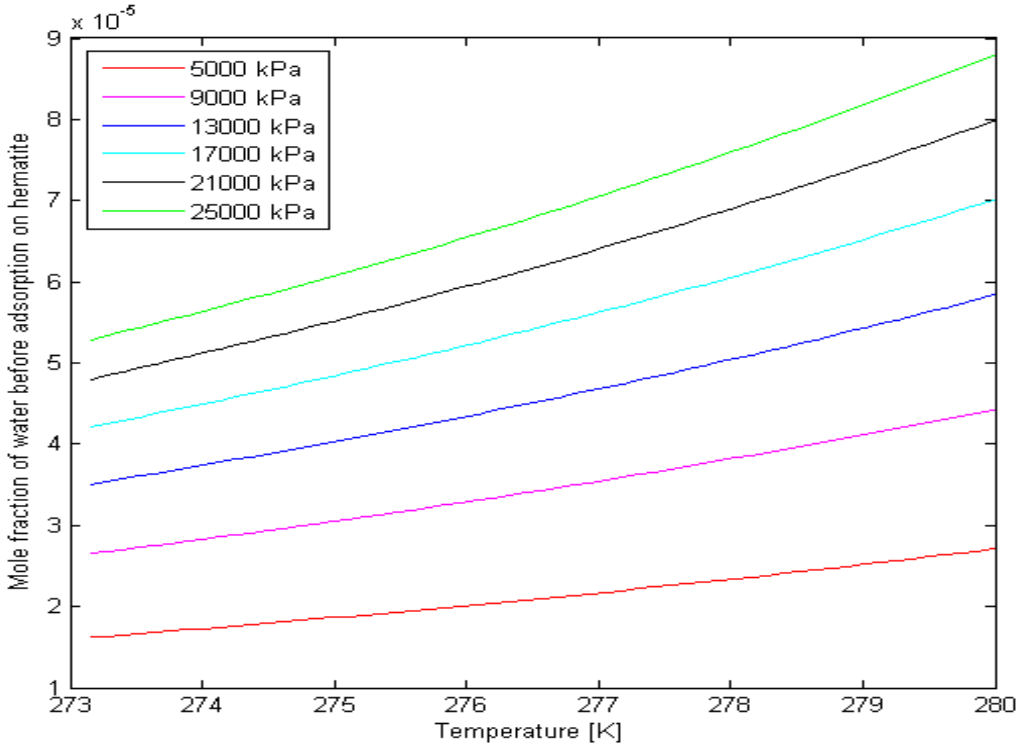

Figure 10.8: Maximum water content before the adsorption of liquid water on hematite occurs from the gas stream after further separation leaving only propane and isobutane with molar concentrations of 0.54 and 0.46, respectively (Troll gas)

Table 10.1: Maximum water content permitted without the risk of hydrate formation for Troll gas and pure components of hydrocarbons.

Gas Stream	Routes	Temperature [K]	Pressure [kPa]					
			5000	9000	13000	17000	21000	25000
Well-head fluid	Dew-point	274.14 K	0.001194	0.000753	0.000618	0.000577	0.000568	0.000571
	Hematite		0.000062	0.000039	0.000032	0.000030	0.000030	0.000030
	Dew-point	280 K	0.001822	0.001148	0.000934	0.000860	0.000839	0.000837
	Hematite		0.000102	0.000065	0.000052	0.000048	0.000047	0.000047
Separator 1 fluid	Dew-point	274.14 K	0.001194	0.000754	0.000618	0.000577	0.000568	0.000571
	Hematite		0.000062	0.000039	0.000032	0.000030	0.000030	0.000030
	Dew-point	280 K	0.001823	0.001148	0.000934	0.000860	0.000839	0.000837
	Hematite		0.000102	0.000065	0.000052	0.000048	0.000047	0.000047
Liquid outlet of Separator 1 fluid (i.e., C_2, C_3 and C_4)	Dew-point	274.14 K	0.000271	0.000430	0.000557	0.000661	0.000746	0.000816
	Hematite		0.000014	0.000022	0.000029	0.000034	0.000039	0.000043
	Dew-point	280 K	0.000397	0.000624	0.000806	0.000953	0.001074	0.001173
	Hematite		0.000022	0.000035	0.000045	0.000054	0.000060	0.000066
C_3 and iC_4 (with C_2 out)	Dew-point	274.14 K	0.000335	0.000548	0.000724	0.000870	0.000991	0.001091
	Hematite		0.000017	0.000029	0.000038	0.000045	0.000052	0.000057
	Dew-point	280 K	0.000482	0.000787	0.001038	0.001247	0.001419	0.001562
	Hematite		0.000027	0.000044	0.000058	0.000070	0.000080	0.000088

10.2 Sensitivity analysis of concentration of components on maximum water content that can be allowed in troll gas during processing and transport

The effect of higher molar concentration of each components of the C_{2+} (hydrate forming higher hydrocarbons) on the maximum permitted amount of water in Troll is investigated at 274K and 280K and within to pressure range of 5000 to 25000 kPa used in this work. The results are presented in Figures 10.9 to 10.14. The Troll gas is methane dominated gas, thus, the characteristic behaviour at these conditions show methane dominance, with permitted water content being higher at lower pressures and reducing with increasing pressures. Consequent on opposite characteristics exhibited by the C_{2+} as seen above, increasing the concentration of ethane to 10 per cent results in a slight change from the characteristics of a methane dominated gas to a C_{2+} dominated gas from around 17000 to 25000 kPa, thereby slightly raising the allowable water limit. Further increase of ethane concentration to 15 per cent and 20 per cent in the gas stream does not result in change in the pressure at which C_{2+}

dominance commences (i.e. about 17000 kPa). Both propane and isobutane at 10 per cent molar concentration show similar characteristic with ethane at approximately 17000 kPa. That is, C_{2+} dominance also commences as from around 17000 kPa with maximum permitted amount water slightly more than that of ethane; effect of isobutane being higher than propane. However, increase of propane further to 15 per cent and 20 per cent results in shifting the pressure at which the dominance of C_{2+} commences from around 17000 kPa to 13000 kPa. And for isobutane, the impact is more as the pressure at which the change from methane dominance to C_{2+} dominance occurs shifts backward with increasing molar concentration. At 10 per cent it is around 17000 kPa, 15 percent it is 13000 kPa while it is 9000 kPa at 20 per cent.

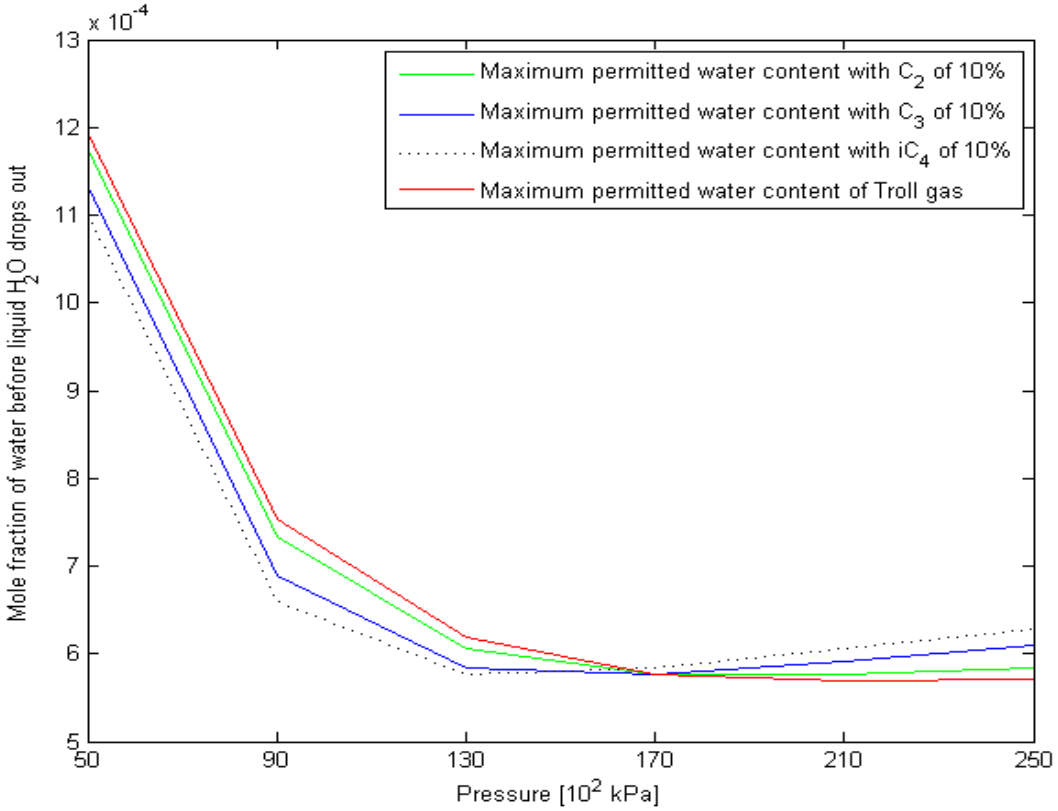

Figure10.9: Maximum water content before liquid water drops out of gas streams at a temperature of 274.14 K with 10% ethane, 0.31% propane, 0.27% isobutane, and the rest is methane; 10% propane, 3.5% ethane, 0.27% isobutane, and the rest is methane; 10% isobutane, 3.5% ethane, 0.31% propane, and the rest is methane; Troll gas well-head fluid

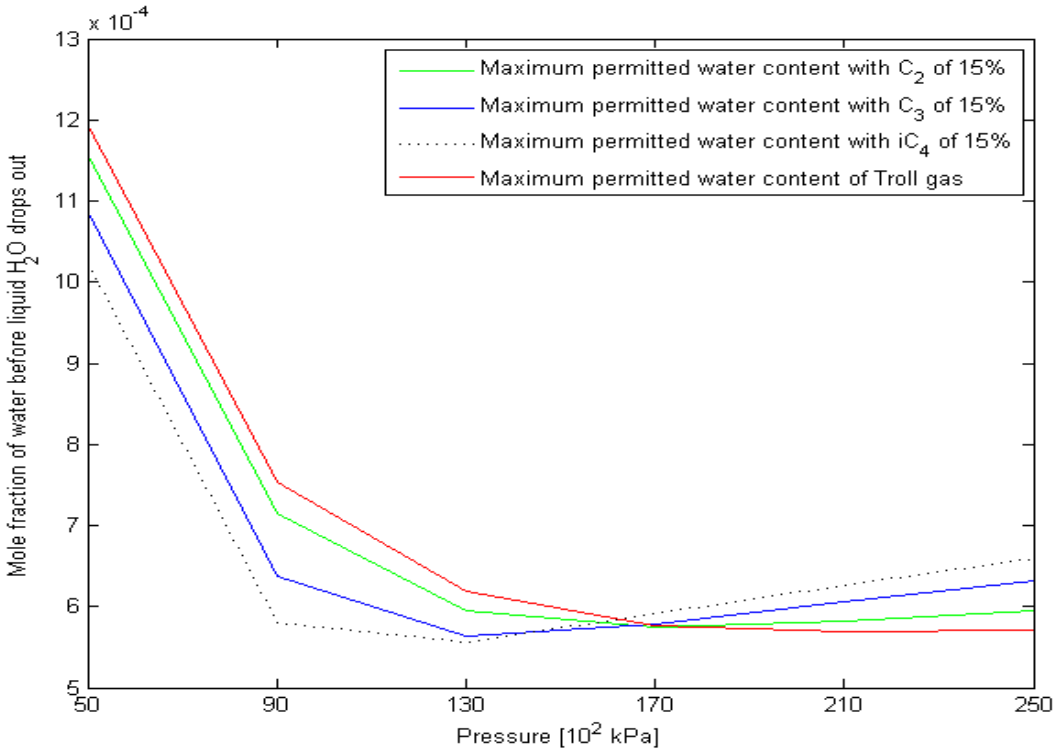

Figure10.10: Maximum water content before liquid water drops out of gas streams at a temperature of 274.14 K with 15% ethane, 0.31% propane, 0.27% isobutane, and the rest is methane; 15% propane, 3.5% ethane, 0.27% isobutane, and the rest is methane; 15% isobutane, 3.5% ethane, 0.31% propane, and the rest is methane; Troll gas well-head fluid

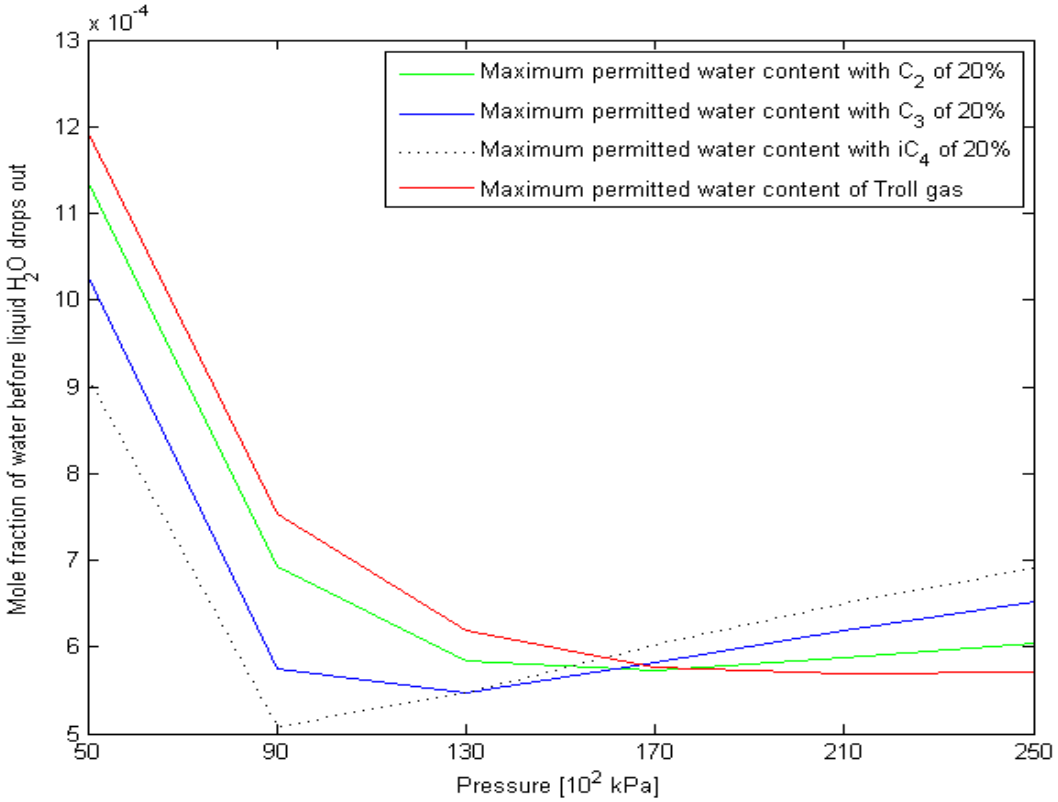

Figure 10.11: Maximum water content before liquid water drops out of gas streams at a temperature of 274.14 K with 20% ethane, 0.31% propane, 0.27% isobutane, and the rest is methane; 20% propane, 3.5% ethane, 0.27% isobutane, and the rest is methane; 20% isobutane, 3.5% ethane, 0.31% propane, and the rest is methane; Troll gas well-head fluid

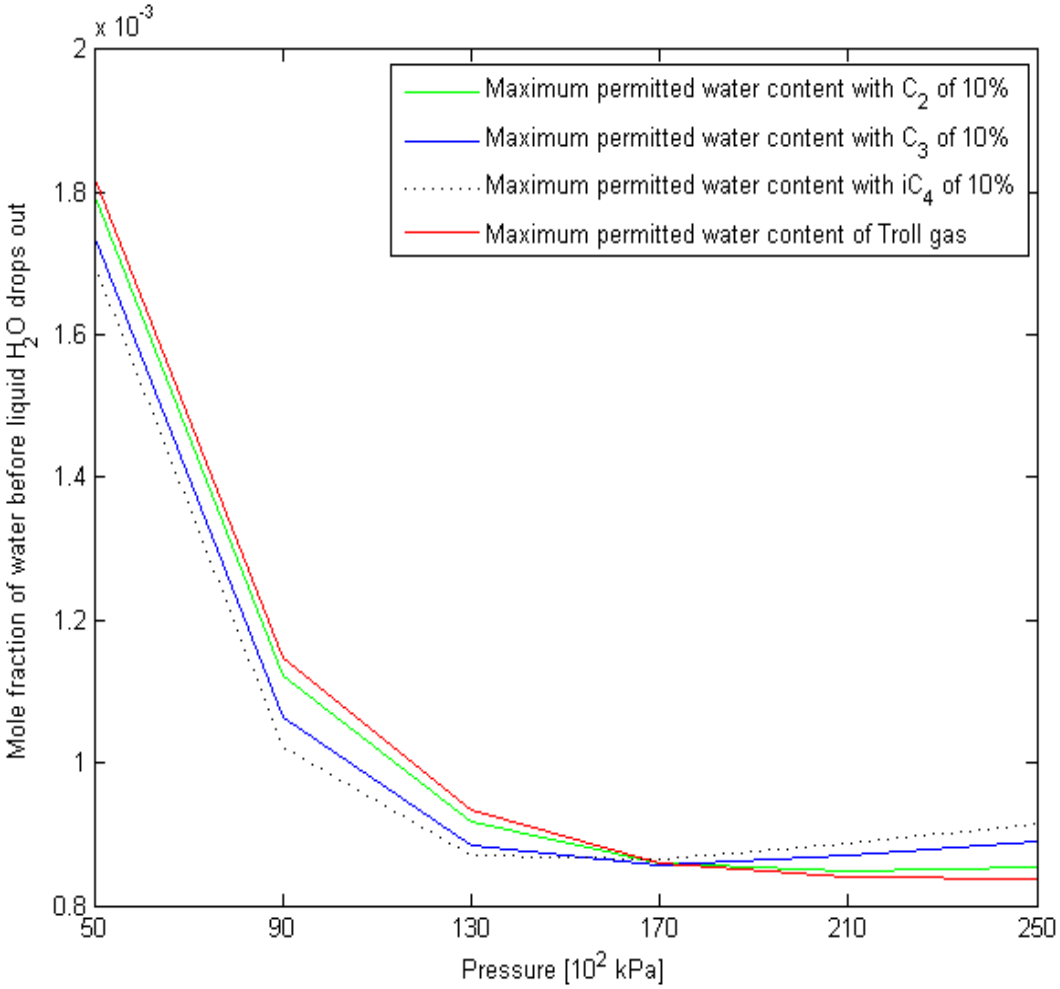

Figure10.12: Maximum water content before liquid water drops out of gas streams at temperature of 280 K 10% ethane, 0.31% propane, 0.27% iso-butane and the rest is methane; 10% propane, 3.5% ethane, 0.27% iso-butane and the rest is methane; 10% iso-butane, 3.5% ethane, 0.31% propane and he rest is methane; Troll gas well-head fluid.

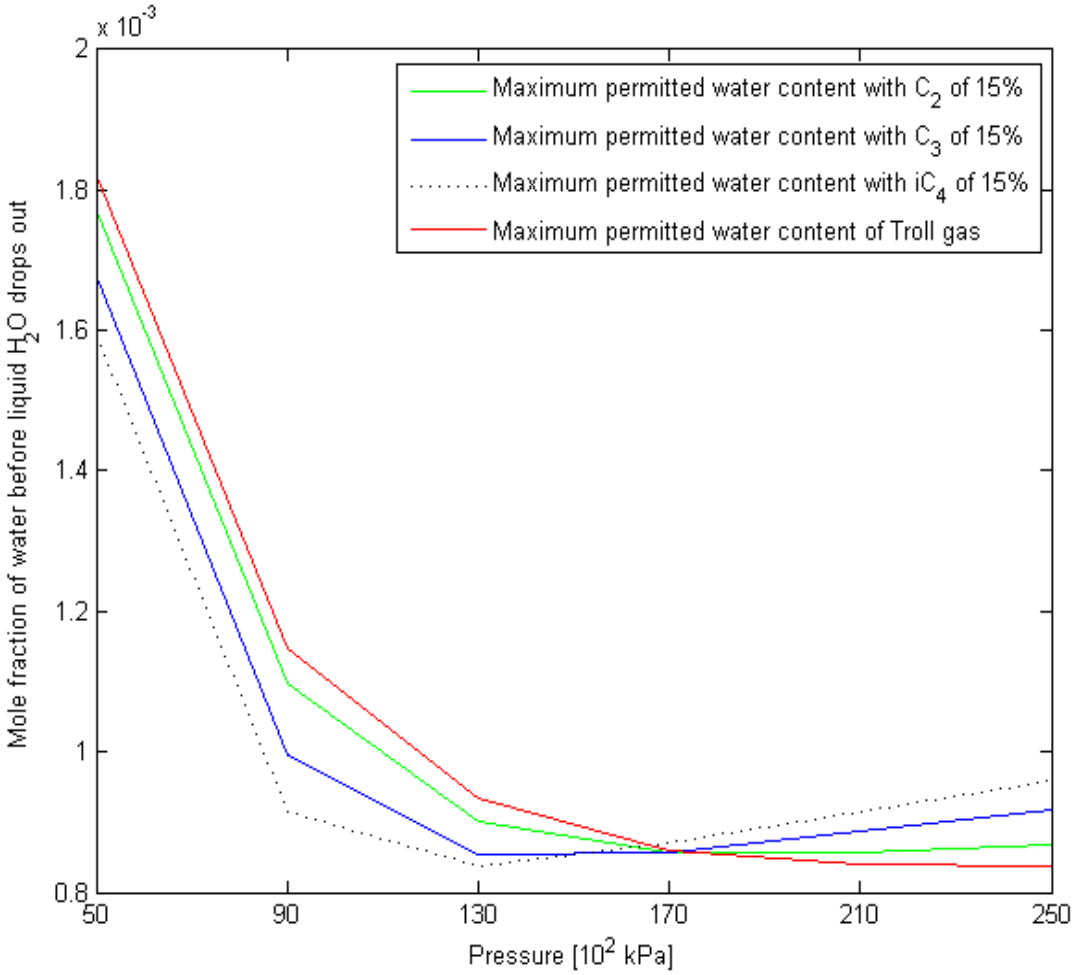

Figure10.13: Maximum water content before liquid water drops out of gas streams at temperature of 280 K 15% ethane, 0.31% propane, 0.27% isobutane and the rest is methane; 15% propane, 3.5% ethane, 0.27% isobutane and the rest is methane; 15% iso-butane, 3.5% ethane, 0.31% propane and the rest is methane; Troll gas well-head fluid

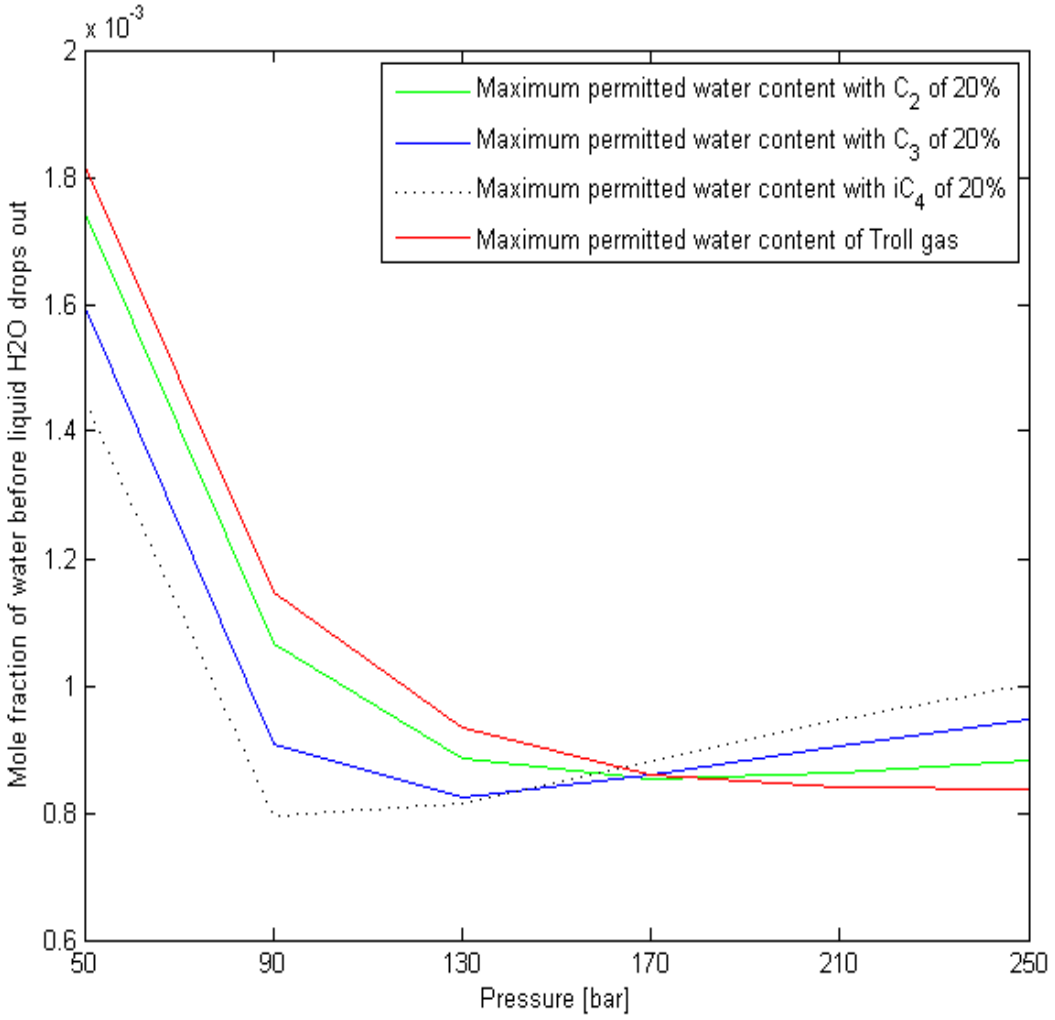

Figure10.14: Maximum water content before liquid water drops out of gas streams at temperature of 280 K 20% ethane, 0.31% propane, 0.27% isobutane and the rest is methane; 20% propane, 3.5% ethane, 0.27% isobutane and the rest is methane; 20% isobutane, 3.5% ethane, 0.31% propane and the rest is methane; Troll gas well-head fluid

11 Analysis and Discussion of Results III: Sleipner gas from the North Sea

A novel thermodynamic scheme [81] for investigation of different routes to hydrate formation, using ideal gas as reference state for all components in all phases including hydrate phase has been applied to investigate the maximum limit of water content that should be permitted in Sleipner gas from the North Sea without the risk of hydrate formation. And the new approach for evaluating the risk of hydrate formation based on adsorption on hematite has also been applied on Sleipner gas for the first time and the results are compared with the classical dew-point technique employed by the industry to investigate the maximum water content that can be permitted to prevent the risk of hydrate formation when both structure I and structure II hydrates hydrocarbon guest molecules with significant amount of carbon dioxide are present during processing and transport of hydrocarbons.

11.1 Maximum water content that can be permitted in Sleipner gas to prevent the risk of hydrate formation.

The initial step in hydrate risk analysis for a particular gas mixtures containing hydrate forming components of hydrocarbons (in this work, both structure I and II components) and also inorganics (CO_2 in this study) during processing or pipeline transport at a certain pressure and temperature is to evaluate the upper limit of water content that can be tolerated in the gas or liquid system before water can condense out as has been done in Section 10 for the Troll gas. The classical approach for hydrate risk analysis has been the mole-fraction of water in the gas or liquid at water dew-point. The final limits of water content have to be sufficiently low to stay in the transport natural gas from Sleipner A through the Gassled pipeline system to the receiving terminals at the continent. The final water content in the CO_2 transported from Sleipner T facility for storage at the Utsira formation in the North Sea also has to be necessarily low.

In the North Sea the sea floor temperature typically ranges from 272 K to 279 K and the operating pressure also range from around 5000 kPa to about 25000 kPa. Hence, investigation is within these temperature and pressure ranges. The composition of Sleipner gas has been presented in Table 7.1. Figures 11.1 to 11.4 and Table 11.1 qualitatively illustrate the safe limits of water content for Sleipner gas before and after CO_2 is separated

out of the bulk, with both the classical dew-point liquid water drop-out approach and the alternative route (the new concept) that involves adsorption of water on the surfaces of the internal walls of process equipment and transport pipelines covered with rust (hematite). There is almost no difference, in fact less than 0.1 per cent between the upper limit of water content for the Sleipner gas with CO_2 and that without CO_2. This is because in both cases, the system is methane dominated, CO_2 molar concentration is only approximately 0.035, and both methane and CO_2 exhibit similar trends at all pressures investigated as can be seen in Figures 11.5 to 11.8 and Table 11.1. There is only a very insignificant shift in absolute values of water drop-out mole-fractions with methane having the very slightly higher values compared to CO_2. In the case of the pure components of structure I hydrate guest molecules of methane and CO_2, the safe-limit of water content is lowered down as the pressure increases. This is same for the Sleipner gas investigated because it is methane (or structure I hydrate) dominated. However, the presence of the heavier structure II hydrate guest molecules of propane and isobutane makes the maximum mole fraction of water that can be tolerated in the Sleipner gas stream relatively insensitive to increase in pressure from 13000 kPa to 25000 kPa unlike the case of the pure components of methane and CO_2. The heavier hydrocarbons of pure ethane, propane and pure isobutane as presented in Figures 11.9 to 11.14 and Table 11.1 also exhibit opposite trends because of the high density non-polar phase at the high pressures.

Generally, for both routes to hydrate formation there is a significant reduction in the gap/difference between the pressure curves between 5000 kPa and 9000 kPa, and between 9000 kPa and 13000 kPa. But the curves for particularly the last two higher pressures, 21000 kPa and 25000 kPa (to be precise) for methane overlap and for CO_2 the last three higher pressure curves almost completely overlap, which indicates higher density impact with CO_2. In Figures 11.1 to 11.4, almost all the last four higher pressure curves (13000 kPa to 25000 kPa) overlap. The reason is that the differences at the higher pressures are almost insensitive to pressures consequent on the high density non-polar phase of especially the presence of higher hydrocarbons at the high pressures already mentioned above. Comparing Figures 11.1 to 11.4 with Figures 11.5 to 11.8 reveals the impact of the densities of the heavier hydrocarbons at higher pressures. The presence of the heavier hydrocarbon also result in slight shift in absolute values of the upper limit of allowable mole-fractions of water even at 5000 kPa and 9000 kPa. In the subsequent sections, sensitivity analysis of the mole-fractions of water that can be permitted at varying concentration of higher hydrocarbons (structure II guest molecules) of propane and isobutane are investigated.

For the two routes investigated with Sleipner gas system, the safe limit of water mole fraction with the route of water adsorbed on Hematite is over 18 times less than the values of water mole fraction with the classical dew-point approach that is currently applied by the industry. This explains why hydrate may still form in industrial processes if only the dew-point approach is used as a measure to operate safe from hydrate formation. Therefore, the alternative route to hydrate formation involving adsorption of water on rusty surfaces (making a free water phase available for hydrate nucleation) cannot be ignored if the risk of hydrate formation without addition of inhibitions or applying other costly measures during processing and pipeline transport of natural gas from the North Sea may be avoided. On the other hand, it is not possible for initial hydrate nuclei to attach directly to the surface of the rust (hematite) consequent on the low chemical potential of adsorbed water. The hydrate formed will be bridged (as a minimum) by three to four layers of structured water on the surface of the hematite. This alternative route to hydrate formation through adsorption on hematite absolutely dominates in examining the risk of water dropping out from the gas mixtures (and pure components investigated) to form a separate water phase and ultimately result in hydrate formation. This can be understood from the fact that the average chemical potential of the water adsorbed on Hematite (rusty surfaces) could be about 3.4 kJ/mol [8, 78] more negative than the chemical potential of liquid water. And thermodynamics favours minimum energy.

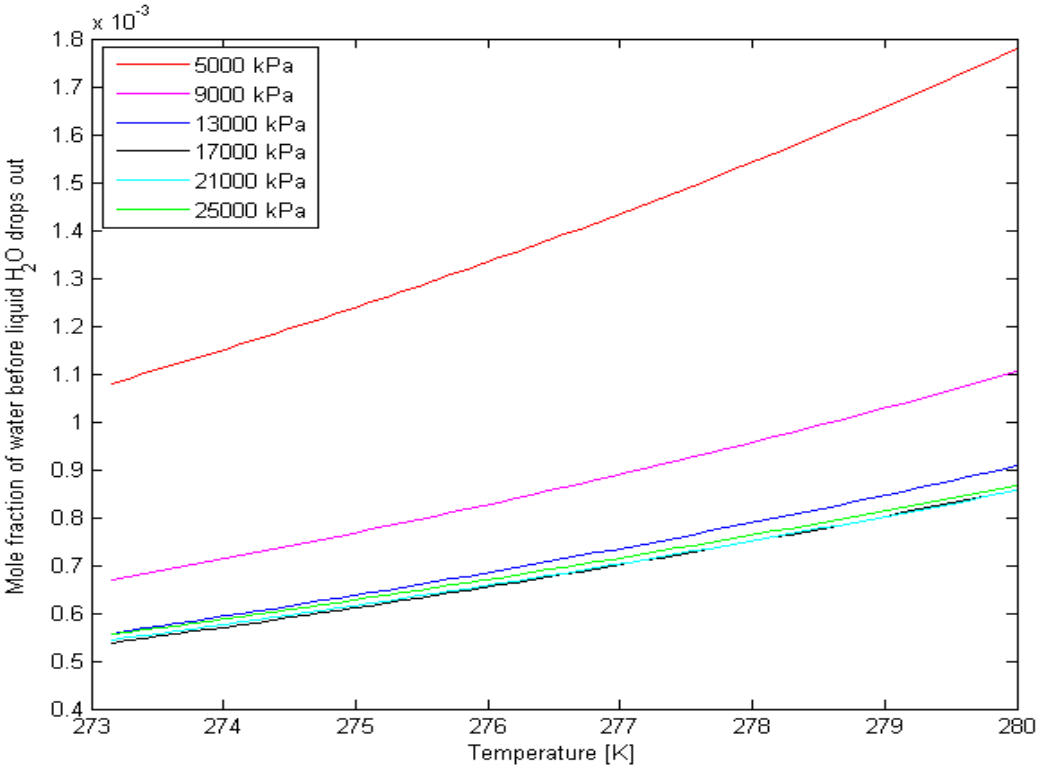

Figure 11.1: Maximum concentration of water that can be permitted in Sleipner gas (with CO_2) before liquid water drops out.

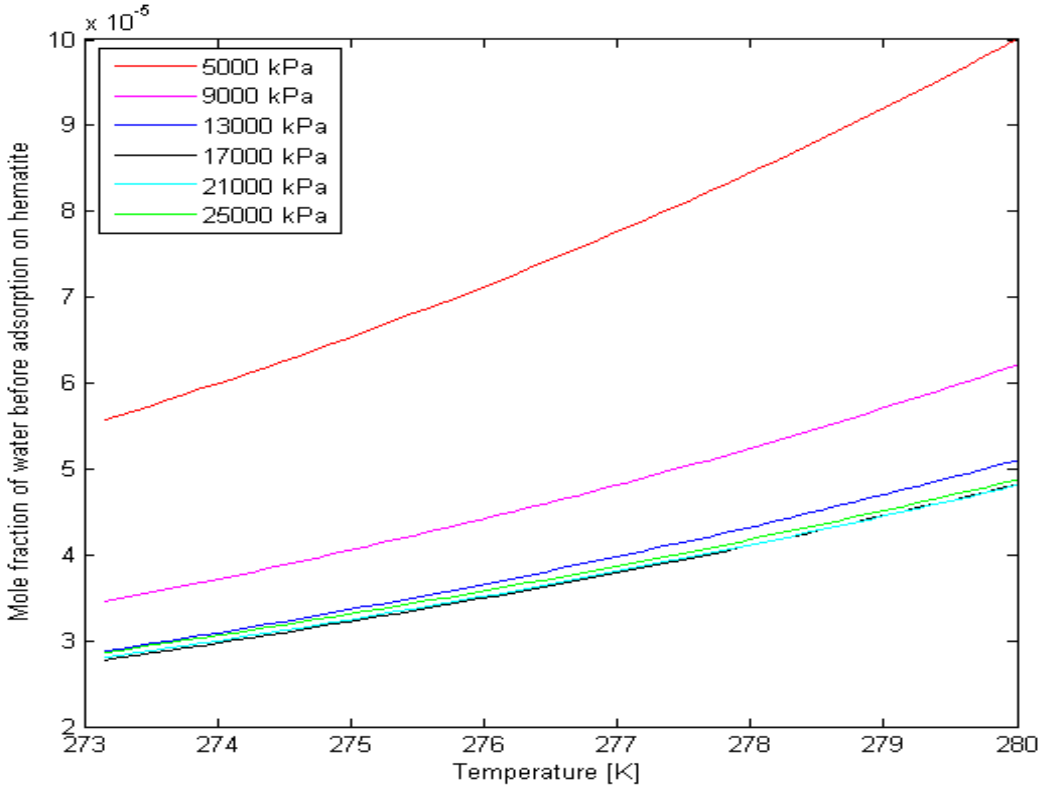

Figure 11.2: Maximum concentration of water that can be permitted in Sleipner gas (with CO_2) before water is adsorbed on hematite.

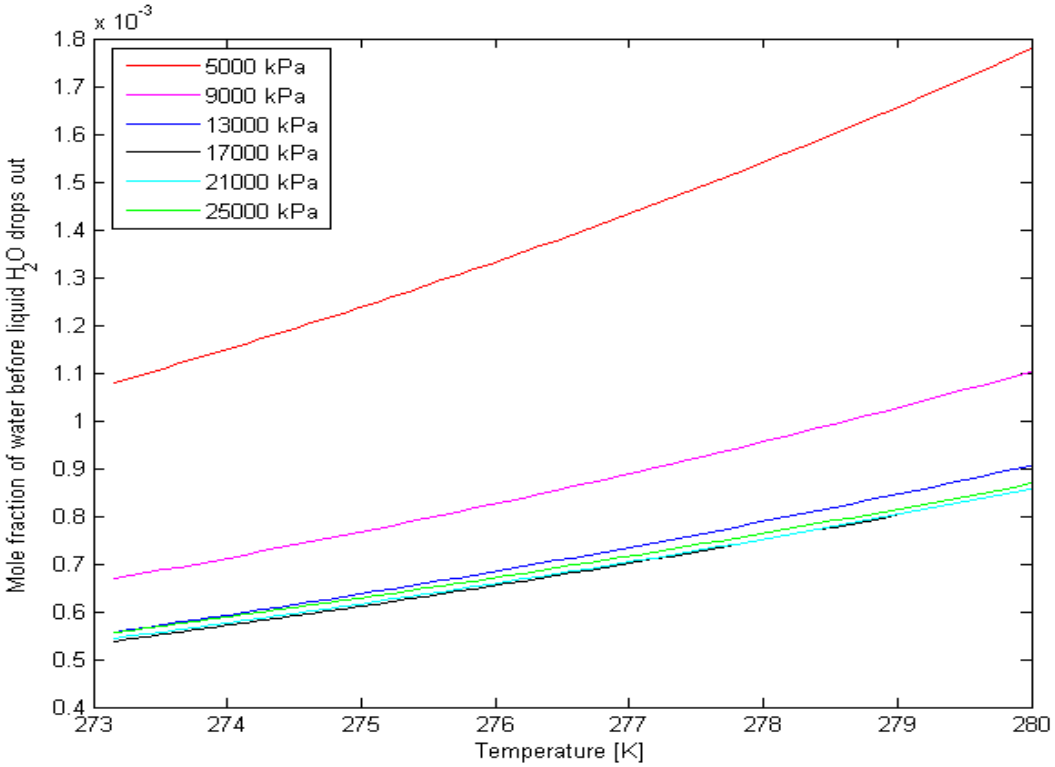

Figure 11.3: Maximum concentration of water that can be permitted in Sleipner gas (without CO_2) before liquid water drops out.

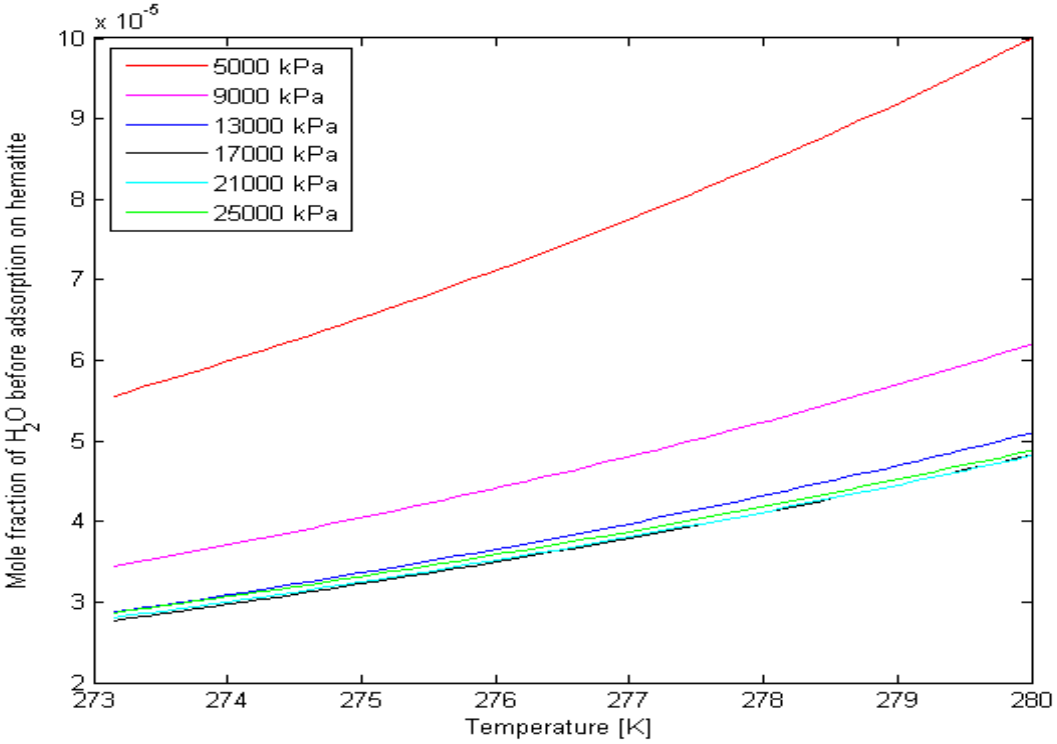

Figure 11.4: Maximum concentration of water that can be permitted in Sleipner gas (without CO_2) before water is adsorbed on hematite.

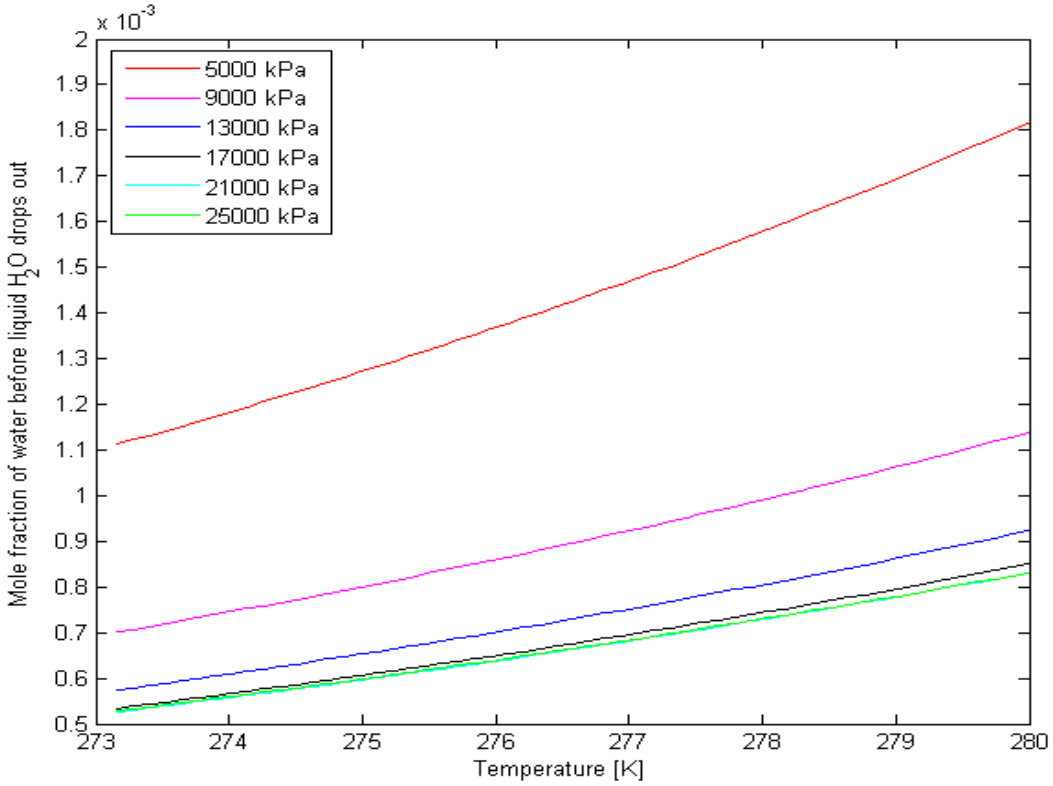

Figure 11.5: Maximum concentration of water that can be permitted in pure CO_2 before liquid water drops out

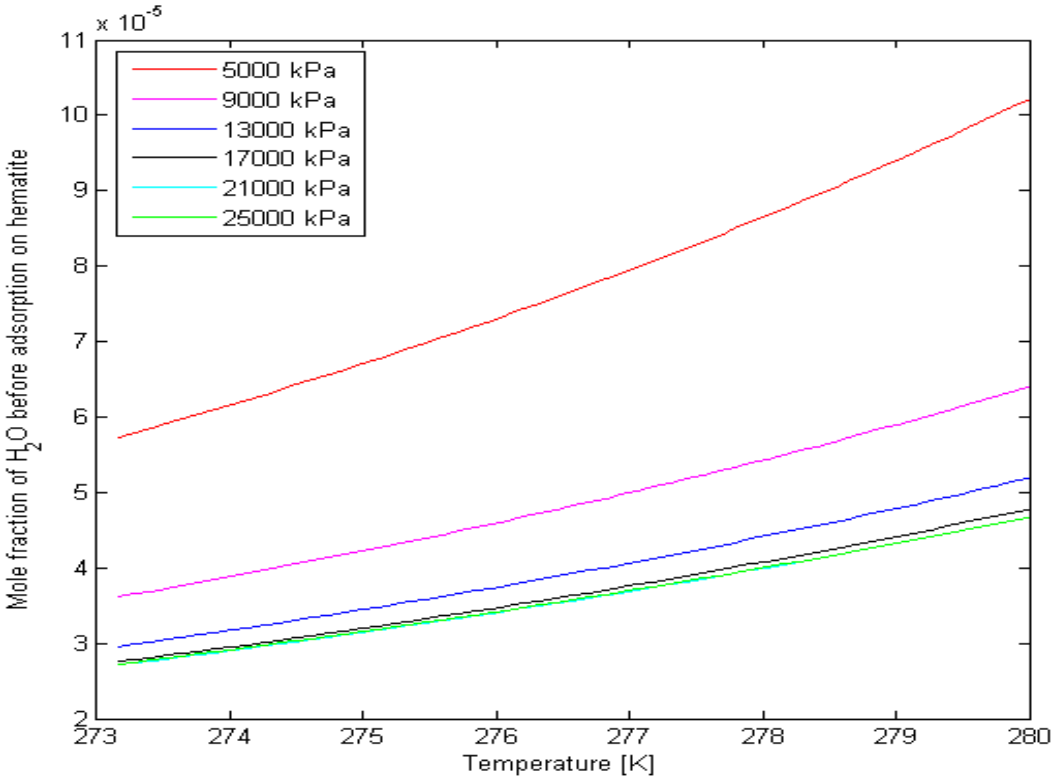

Figure 11.6: Maximum concentration of water that can be permitted in pure CO_2 before water can be absorbed on hematite

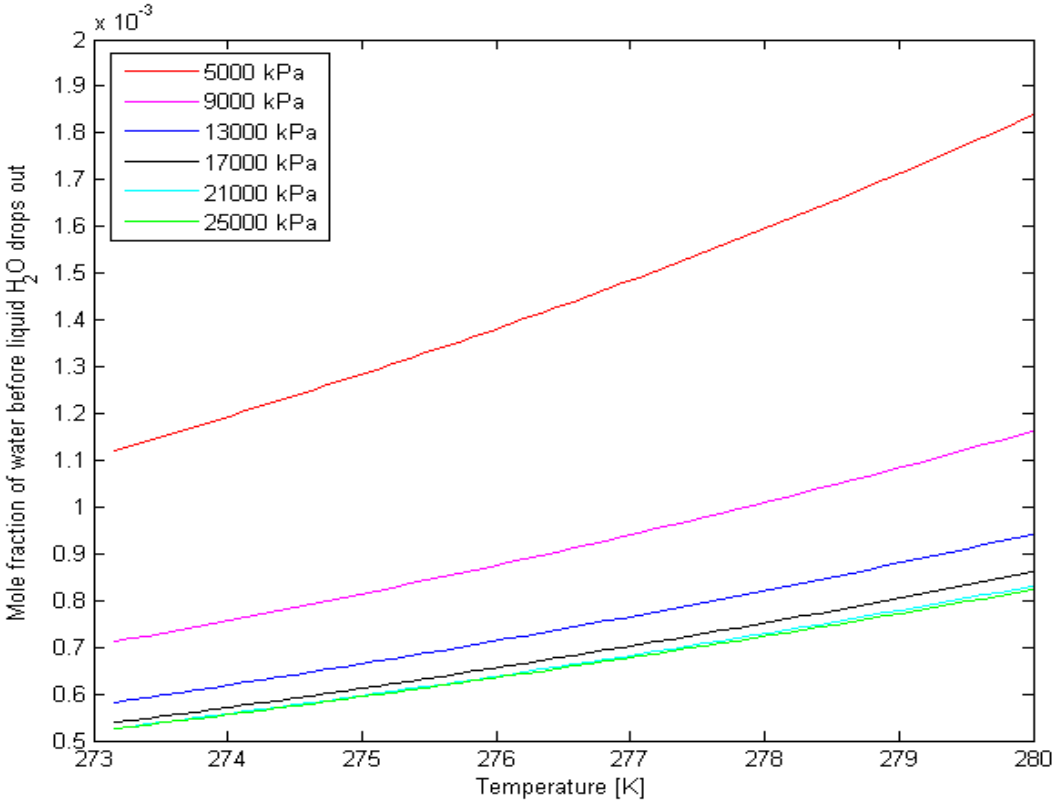

Figure 11.7: Maximum concentration of water that can be permitted in pure methane before liquid water drops out

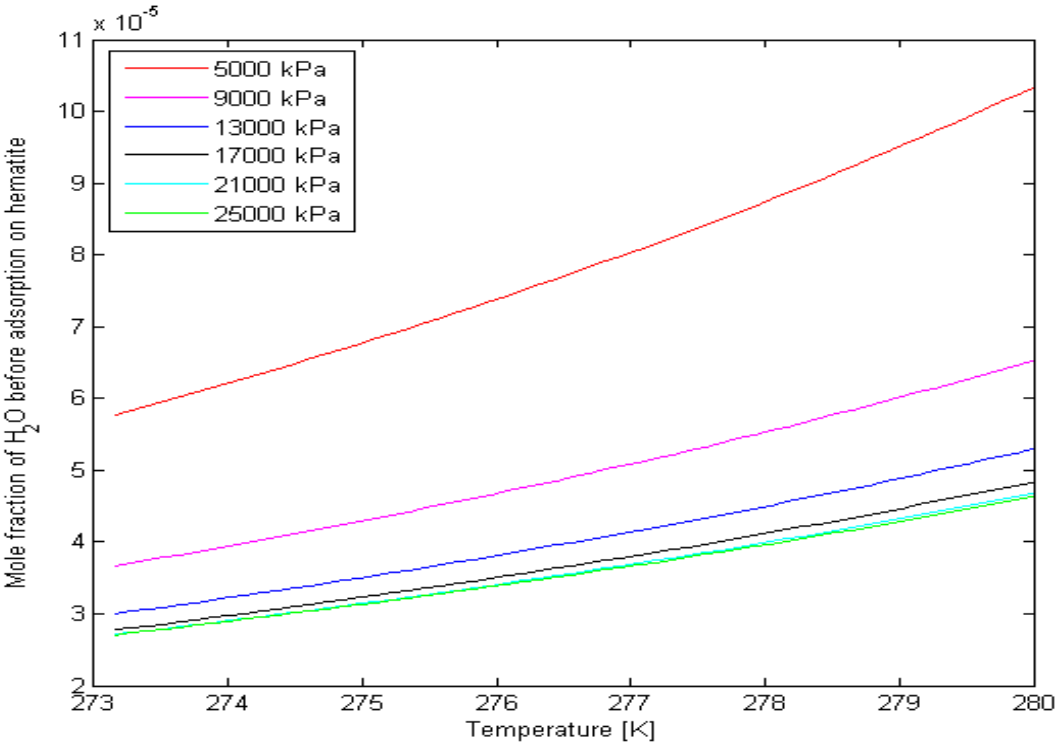

Figure11.8: Maximum concentration of water that can be permitted in pure methane be absorbed on hematite

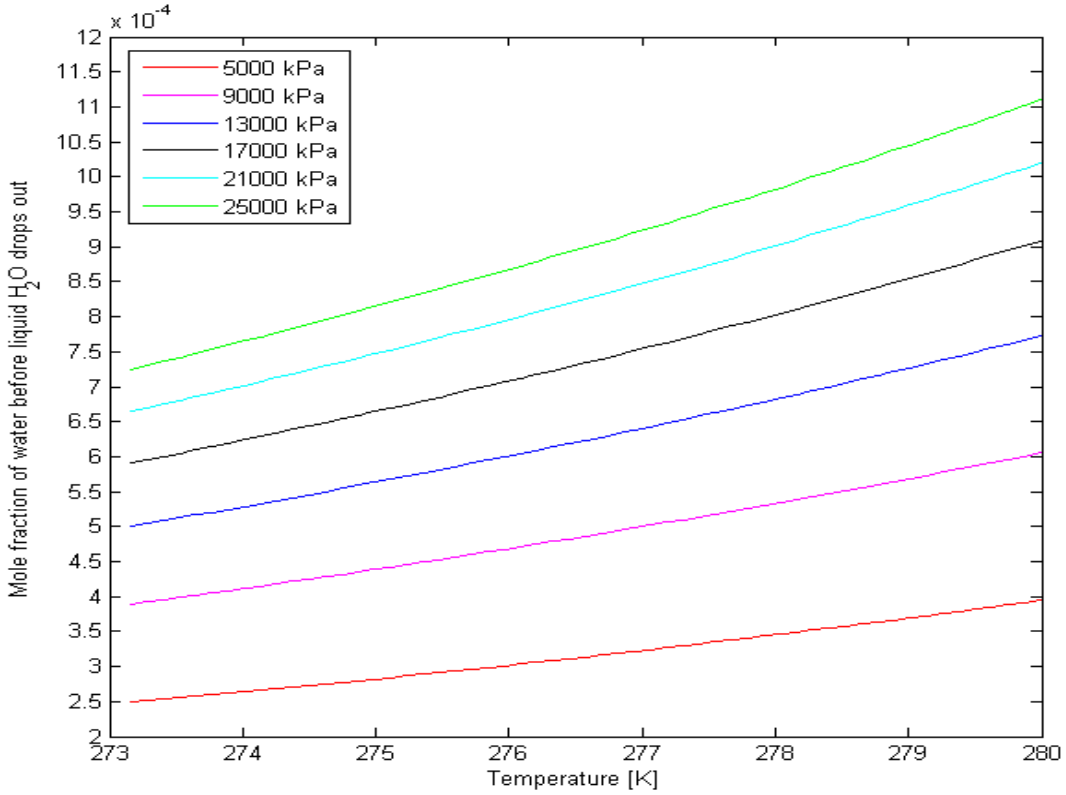

Figure11.9: Maximum concentration of water that can be permitted in pure ethane before liquid water drops out

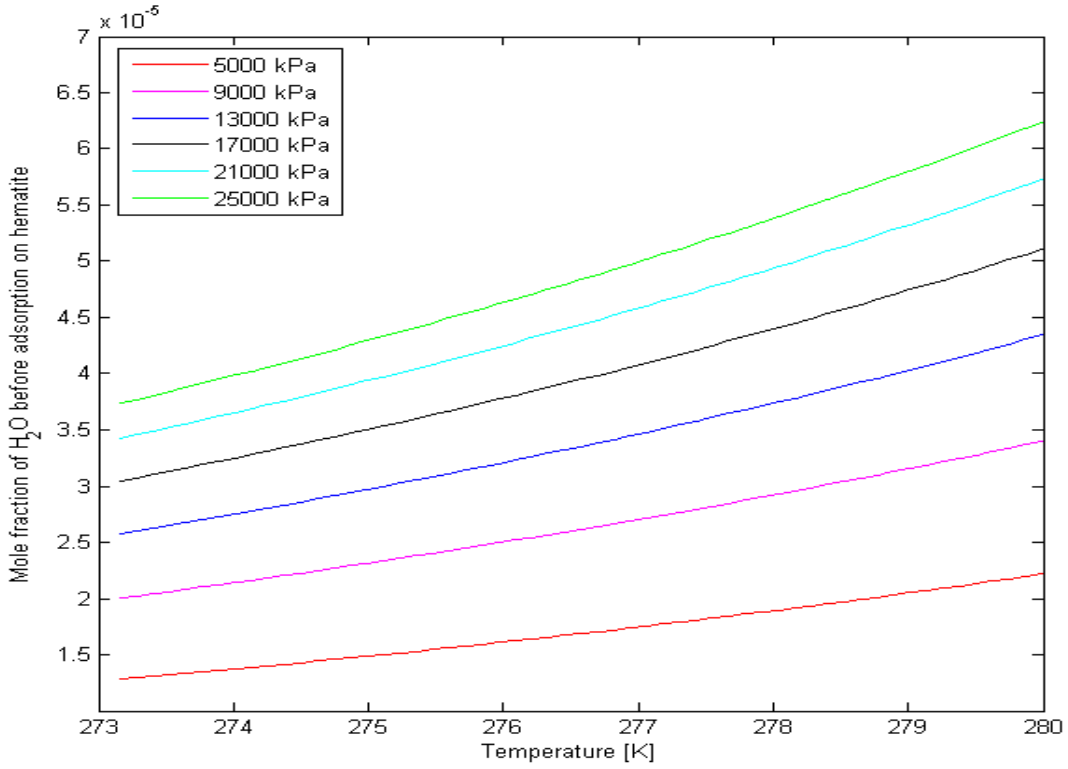

Figure 11.10: Maximum concentration of water that can be permitted in pure ethane before water can be absorbed on hematite

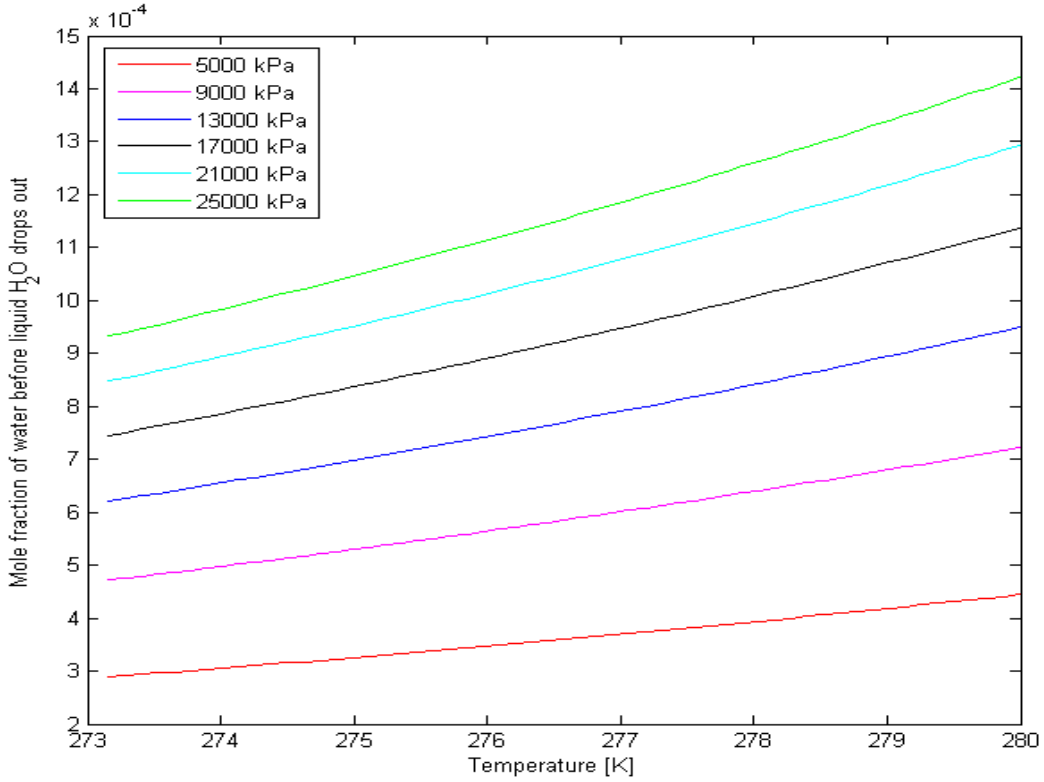

Figure11.11: Maximum concentration of water that can be permitted in pure propane before liquid water drops out

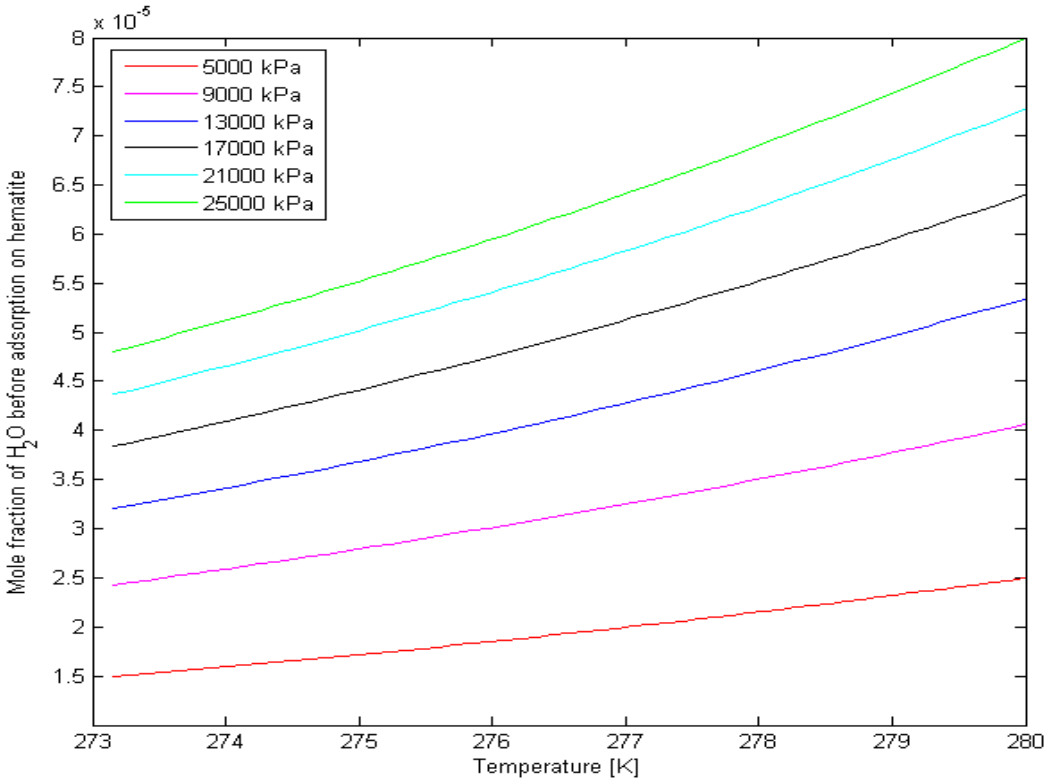

Figure11.12: Maximum concentration of water that can be permitted in pure propane before water can be absorbed on hematite

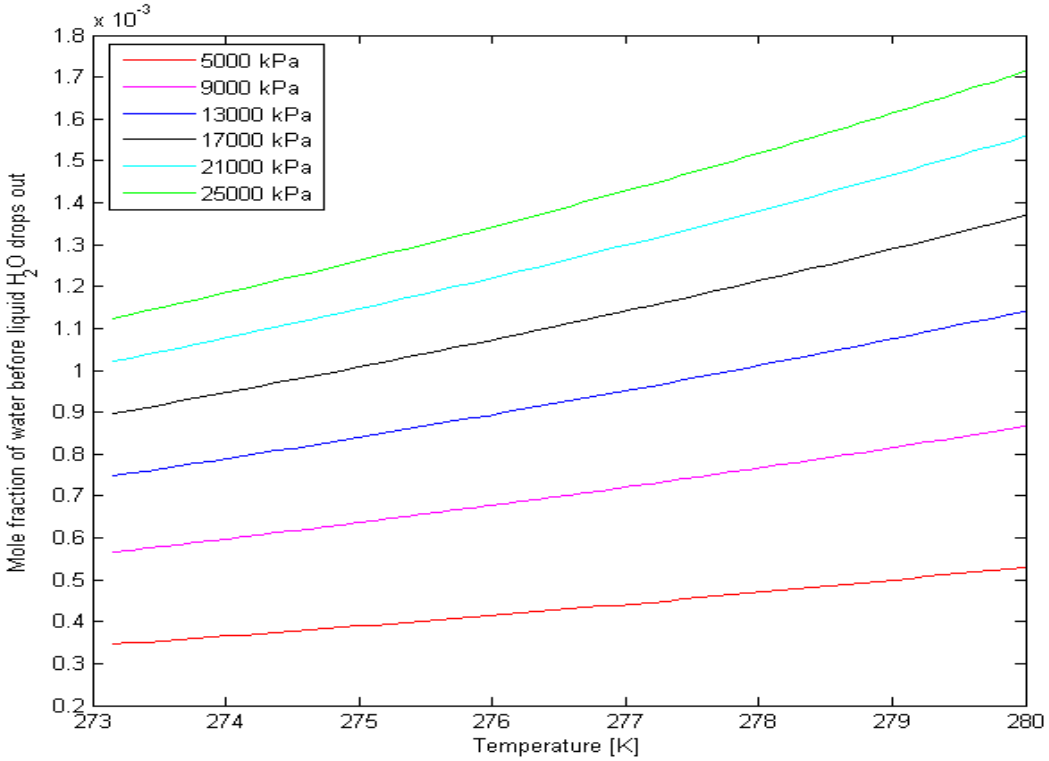

Figure11.13: Maximum concentration of water that can be permitted in pure isobutane before liquid water drops out

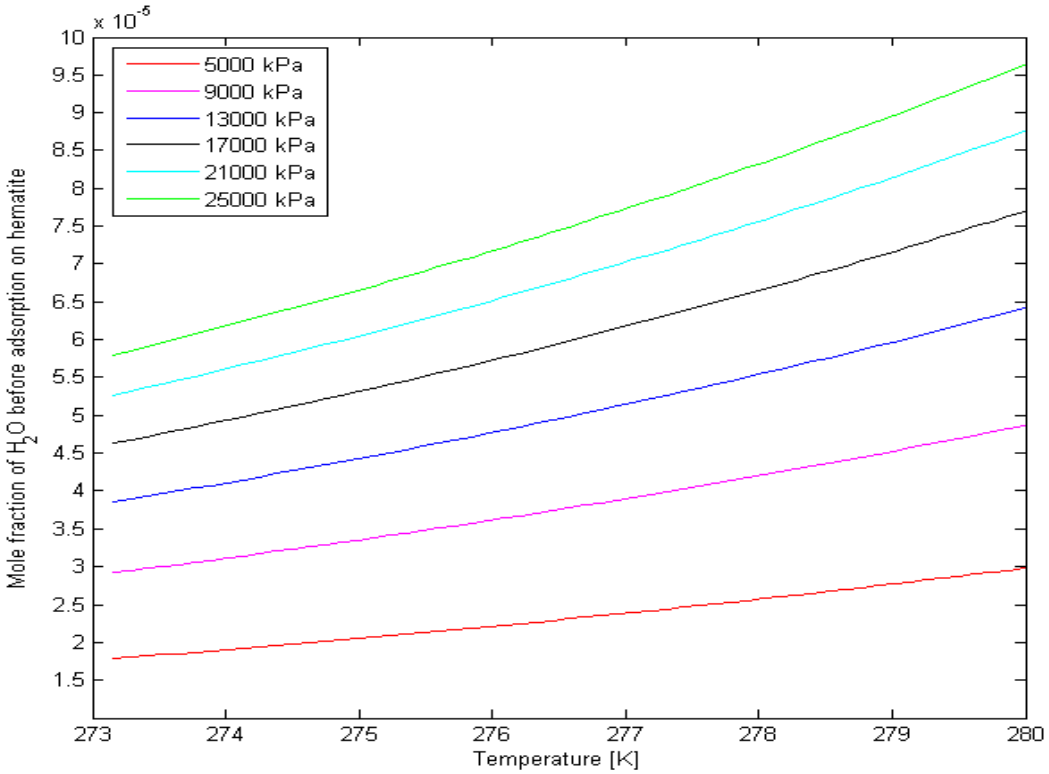

Figure 11.14: Maximum concentration of water that can be permitted in pure isobutane before water can be absorbed on hematite

Table 11.1: Maximum water content permitted without the risk of hydrate formation for Sleipner gas, pure CO_2 and pure methane.

Temperature [K]	Pressure [kPa]	Sleipner gas (with CO_2)		Sleipner gas (without CO_2)		Carbon dioxide (CO_2)		Methane (CH_4)	
		Maximum concentration of water [ ]							
		Dewpoint	Hematite	Dewpoint	Hematite	Dewpoint	Hematite	Dewpoint	Hematite
274	5000	0.001151	0.000060	0.001150	0.00006	0.001184	0.000062	0.001194	0.000062
	9000	0.000714	0.000037	0.000713	0.000037	0.000746	0.000039	0.000758	0.000039
	13000	0.000594	0.000031	0.000593	0.000031	0.00061	0.000032	0.000619	0.000032
	17000	0.000571	0.000030	0.000571	0.000030	0.000567	0.000030	0.000571	0.000030
	21000	0.000576	0.000030	0.000577	0.000030	0.000558	0.000029	0.000558	0.000029
	25000	0.000588	0.000031	0.000589	0.000031	0.00056	0.000029	0.000556	0.000029
280	5000	0.001779	0.00010	0.001778	0.00010	0.001816	0.000102	0.001838	0.000103
	9000	0.001104	0.000062	0.001102	0.000062	0.001138	0.000064	0.001162	0.000653
	13000	0.000907	0.000051	0.000906	0.000051	0.000922	0.000052	0.000942	0.000053
	17000	0.000857	0.000048	0.000858	0.000048	0.000850	0.000048	0.000860	0.000048
	21000	0.000855	0.000048	0.000856	0.000048	0.000831	0.000047	0.000831	0.000047
	25000	0.000867	0.000049	0.000868	0.000049	0.000831	0.000047	0.000823	0.000046

Table 11.2: Maximum water content permitted without the risk of hydrate formation for pure hydrocarbon hydrate formers

Temperature [K]	Pressure [kPa]	Structure I hydrate formers		Structure II hydrate formers					
		Methane		Ethane		Propane		Isobutane	
		Maximum concentration of water [ ]							
		Dewpoint	Hematite	Dewpoint	Hematite	Dewpoint	Hematite	Dewpoint	Hematite
274	5000	0.001194	0.000062	0.000264	0.000014	0.000306	0.000016	0.000366	0.000019
	9000	0.000758	0.000039	0.000412	0.000021	0.000498	0.000026	0.000598	0.000031
	13000	0.000619	0.000032	0.000529	0.000028	0.000656	0.000034	0.000789	0.000041
	17000	0.000571	0.000030	0.000624	0.000033	0.000787	0.000041	0.000948	0.000049
	21000	0.000558	0.000029	0.000702	0.000037	0.000895	0.000047	0.001078	0.000056
	25000	0.000556	0.000029	0.000765	0.000040	0.000984	0.000051	0.001186	0.000062
280	5000	0.001838	0.000103	0.000394	0.000022	0.000445	0.000025	0.000053	0.000030
	9000	0.001162	0.000653	0.000605	0.000034	0.000722	0.000041	0.000087	0.000049
	13000	0.000942	0.000053	0.000773	0.000043	0.000950	0.000053	0.001141	0.000064
	17000	0.000860	0.000048	0.000908	0.000051	0.001138	0.000064	0.001369	0.000077
	21000	0.000831	0.000047	0.001019	0.000057	0.001293	0.000073	0.001557	0.000088
	25000	0.000823	0.000046	0.001110	0.000062	0.001421	0.000080	0.001713	0.000096

11.2 The impact of varying concentration of propane on the maximum water content without the risk of hydrate formation for binary gas mixture of methane/propane and carbon dioxide/propane

The maximum mole-fractions of water that can be permitted at varying concentration of propane (structure II guest molecules) in binary mixtures of methane/propane and CO_2/propane have been investigated for pressures of 5000 kPa, 9000 kPa and 13000 kPa as presented in Figures 19 to 24. These pressures are chosen because of the high density non-polar phase at higher pressures and the presence of propane (heavier hydrocarbon) which makes the mole fraction of water to be insensitive to increase in pressure as discussed in the previous section. The analysis has been performed for temperatures of 274 K, 278 K and 280 K at each pressure and for both the classical dew-point approach and the route of adsorbed water on hematite surface. At 5000 kPa, the trends show decline in permitted maximum water content with increasing concentration of propane for both binary mixtures at all the temperatures investigated. This is a result of the high density non-polar phase at the high pressures which makes propane exhibits opposite trend to that of methane and CO_2 as discussed in the previous section and as can be seen by comparing Figures 11.11 and 11.12 with Figures 11.5 and 11.6 or with Figures 11.7 and 11.8. Thus, as the mole fraction of propane increases and having opposite trend with that of methane and CO_2, it is expected that the non-polar heavy hydrocarbon will act to draw down the upper limit of water content that can be tolerated in the gas mixture till it totally dominates or dictates the trend.

The difference between the trends of both binary mixtures in absolute values of permitted maximum mole fraction of water also widens with increasing concentration of propane and with increasing temperature. But higher pressures of 9000 kPa and 13000 kPa exhibit quite different trends even though there is a reduction in safe limits of water mole fraction with increase in concentration of propane. For 9000 kPa, the curves almost flatten from propane molar concentration of 0.35 where propane impact tends to dominate and the gap between the curves starts closing up. This starts from propane molar concentration of 0.25 for the 13000 kPa scenario (See Figures 11.15 to 11.20). The differences in maximum water content between the mixtures are higher with the classical dew-point route analysis compared with the alternative route of absorbed water on hematite (rust). The maximum water content that can be tolerated from the classical dew-point liquid water dropout

approach for these binary gas mixtures is over 17 times higher than that of the route of absorbed water on hematite.

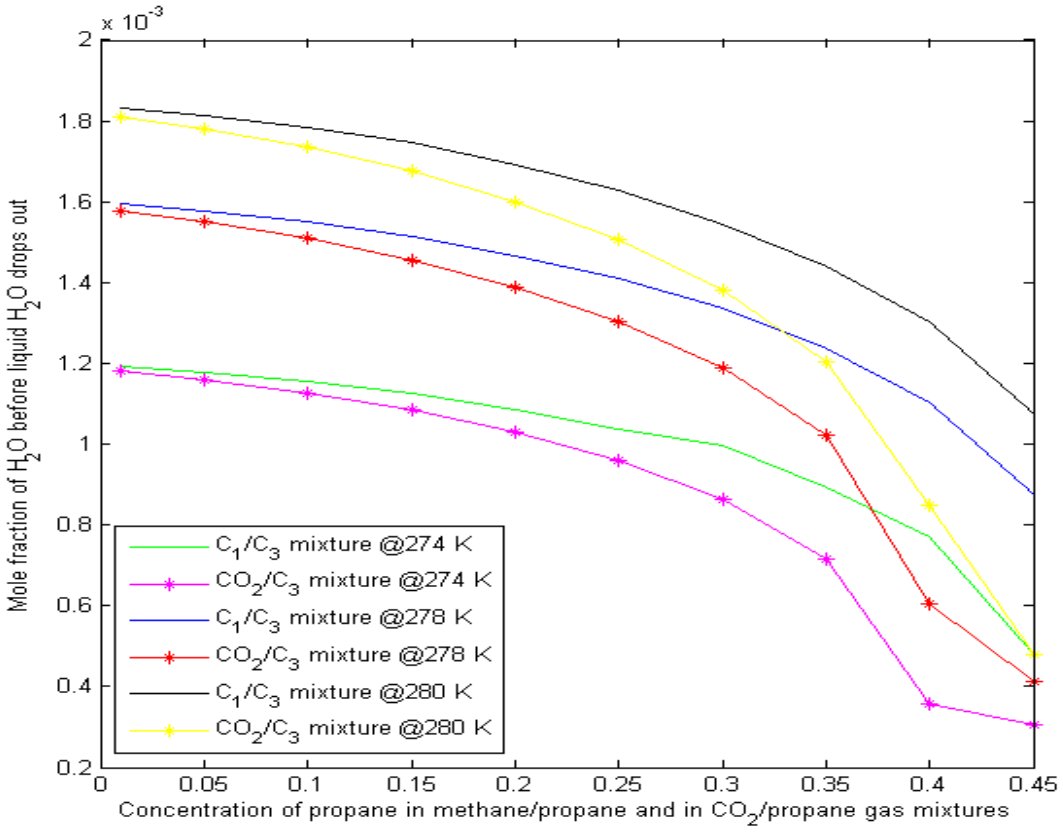

Figure 11.15: Maximum concentration of water that can be permitted in methane/propane and CO_2/propane gas binary mixtures before liquid water drops out at 5000 kPa

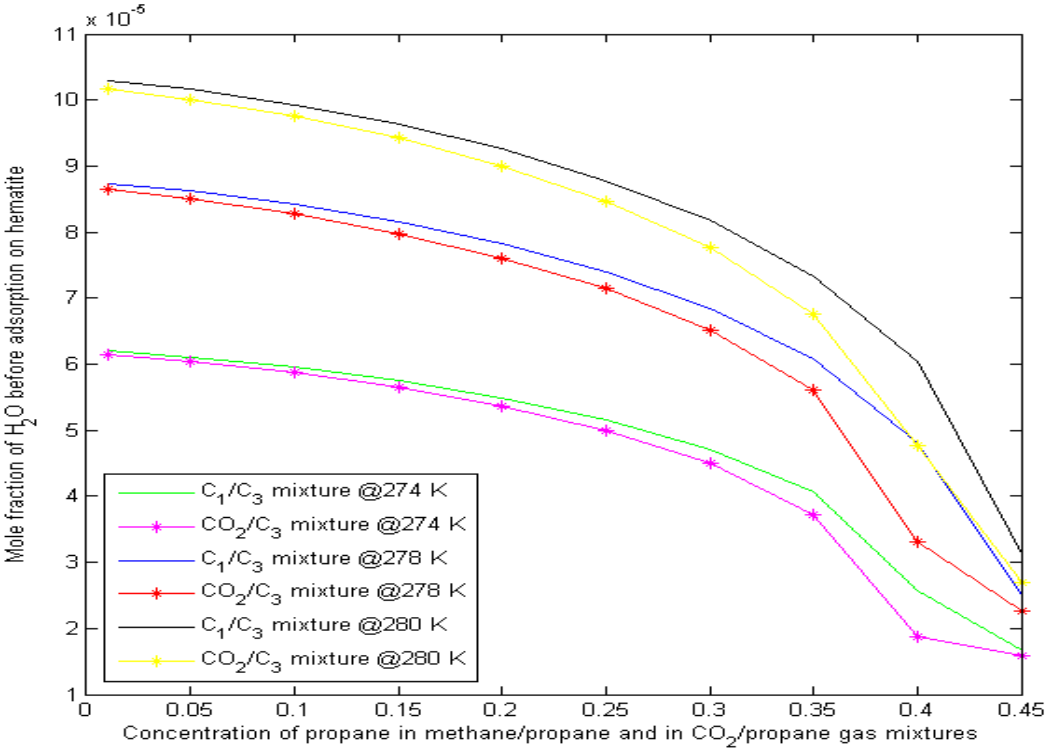

Figure 11.16: Maximum concentration of water that can be permitted in methane/propane and CO_2/propane gas binary mixtures before water is adsorbed on hematite at 5000 kPa

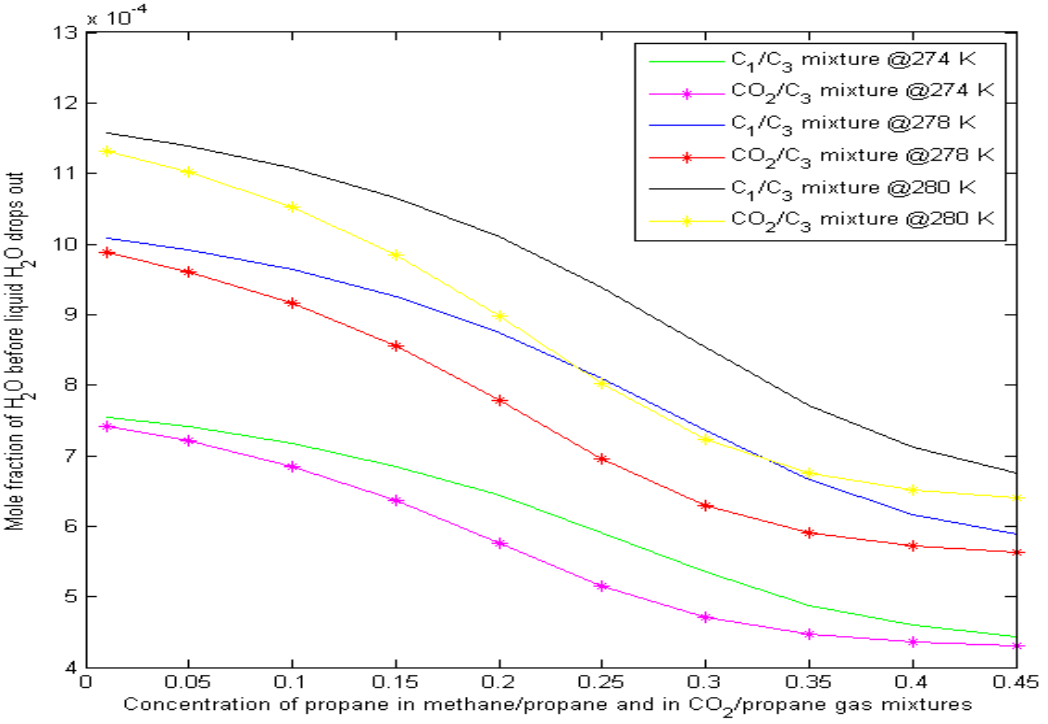

Figure 11.17: Maximum concentration of water that can be permitted in methane/propane and CO_2/propane gas binary mixtures before liquid water drops out at 9000 kPa

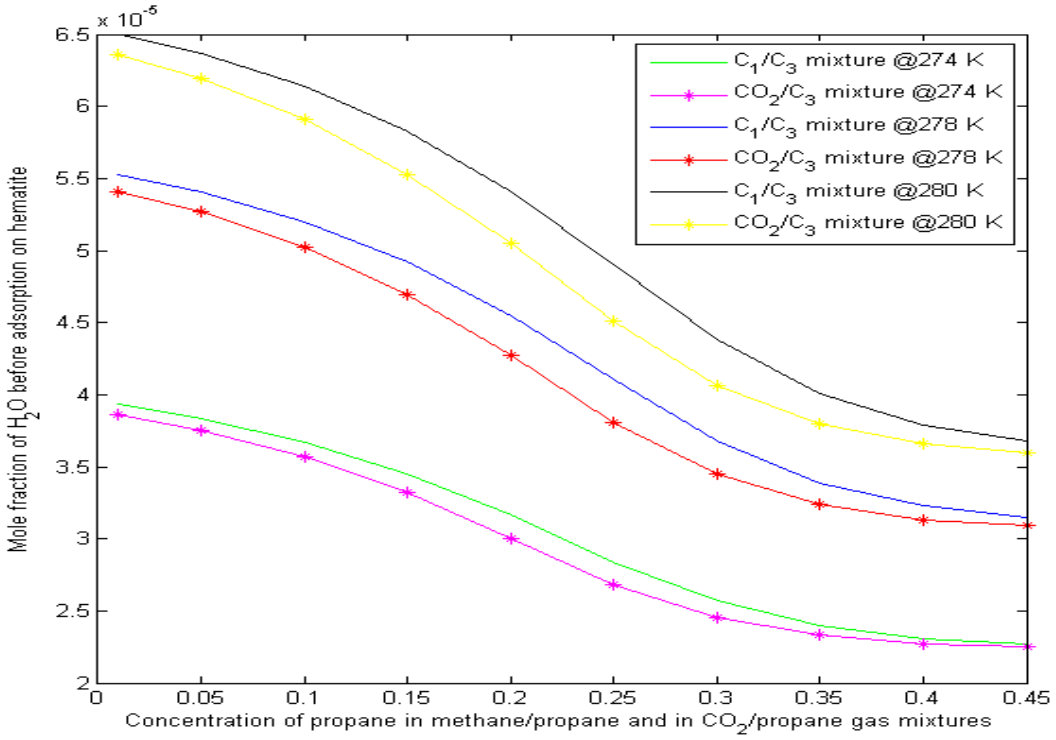

Figure11.18: Maximum concentration of water that can be permitted in methane/propane and CO_2/propane gas binary mixtures before water is adsorbed on hematite at 9000 kPa

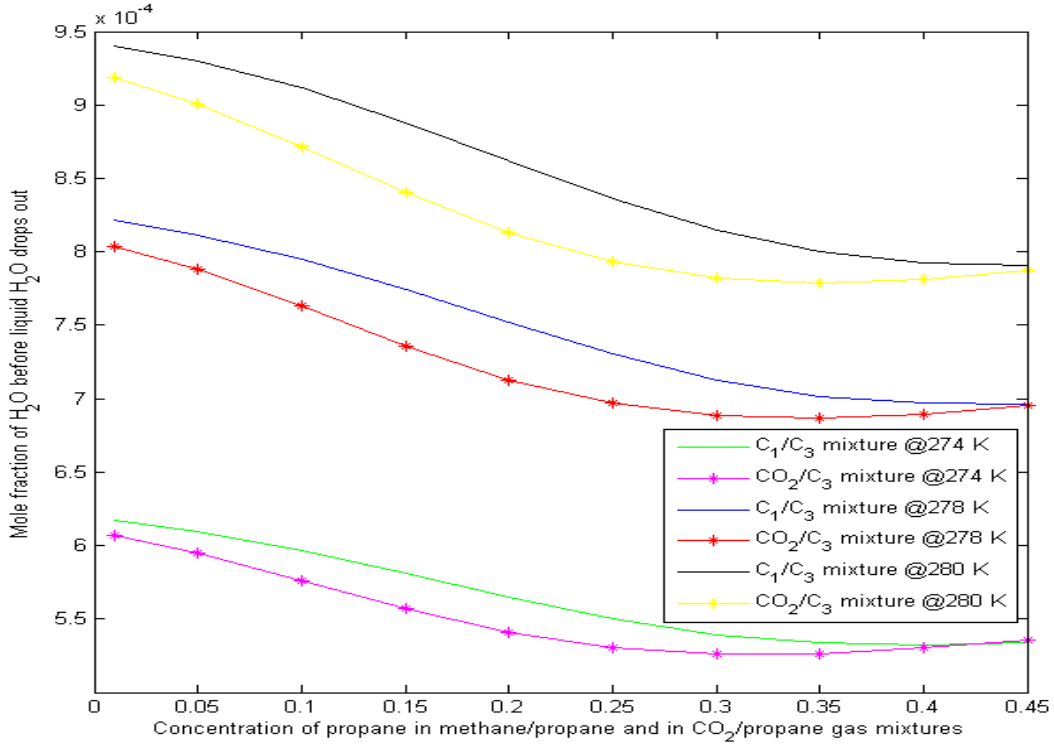

Figure11.19: Maximum concentration of water that can be permitted in methane/propane and CO_2/propane gas binary mixtures before liquid water drops out at 13000 kPa

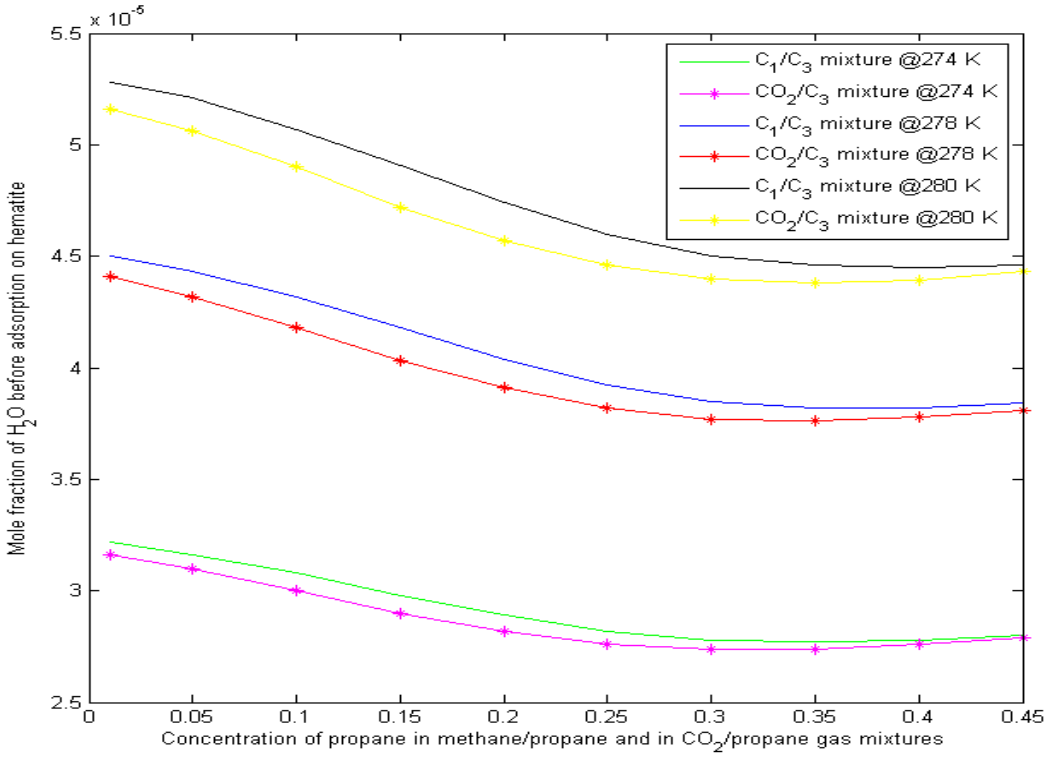

Figure11.20: Maximum concentration of water that can be permitted in methane/propane and CO_2/propane gas binary mixtures before water is adsorbed on hematite at 13000 kPa

11.3 Impact of varying the concentration of isobutane on the maximum water content without the risk of hydrate formation for binary gas mixture of methane/isobutane and carbon dioxide/isobutane

Similarly, the effect of isobutane on the safe limits of water content in the two binary mixtures (that is methane/isobutane and carbon dioxide/ isobutane mixtures) are shown in Figures 11.21 to 11.26. Comparing the results here with that of propane illustrated in Figures 11.15 to 11.20 above, shows the effect of the higher density isobutane to propane. The dominance of isobutane commences at 5000 kPa from molar concentration of 0.35 unlike the case of propane. The impacts are also higher with the classical dew-point method analysis compared with the alternative approach of absorbed water on hematite, and with a change in trends at 13000 kPa, where the curve of CO_2/isobutane becomes higher than that of methane/isobutane mixture at isobutane molar concentration of 0.30 at 274 K and 0.35 at 278K and 280 K.

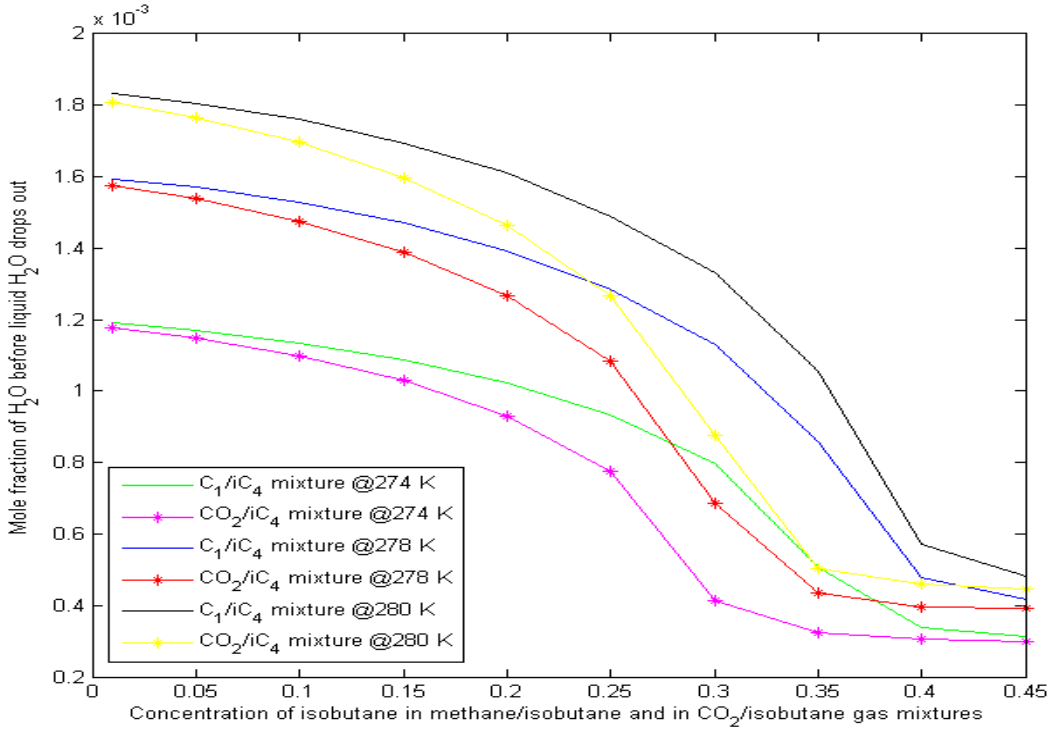

Figure 11.21: Maximum concentration of water that can be permitted in methane/isobutane and CO_2/isobutane gas binary mixtures before liquid water drops out at 5000 kPa

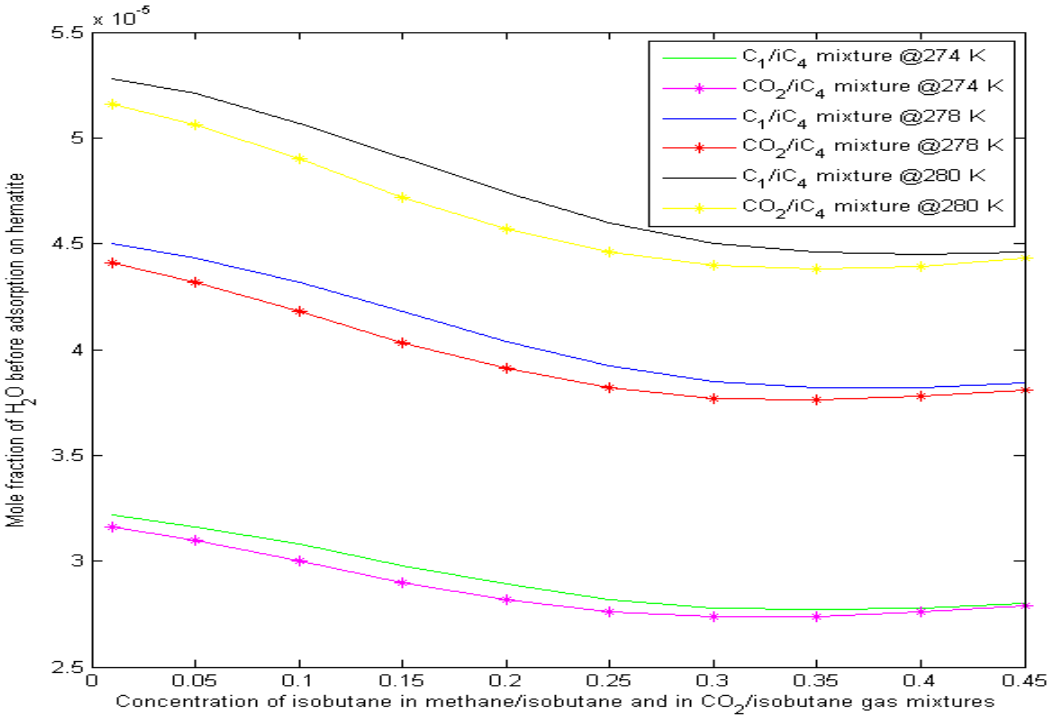

Figure 11.22: Maximum concentration of water that can be permitted in methane/isobutane and CO_2/isobutane gas binary mixtures before water is adsorbed on hematite at 5000 kPa

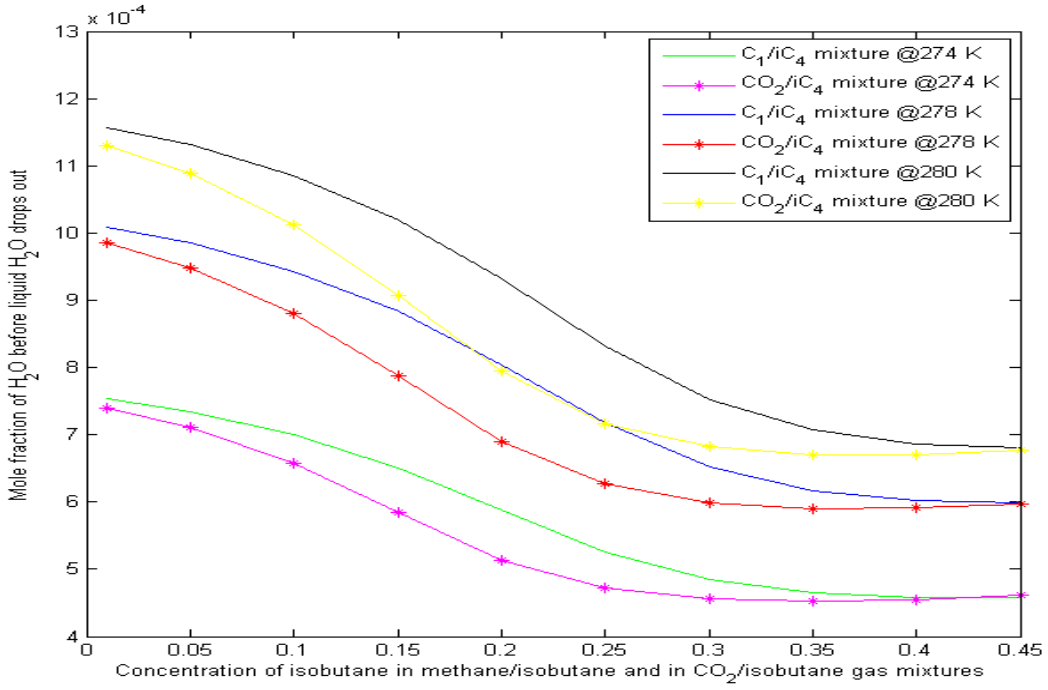

Figure 11.23: Maximum concentration of water that can be permitted in methane/isobutane and CO_2/isobutane gas binary mixtures before liquid water drops out at 9000 kPa

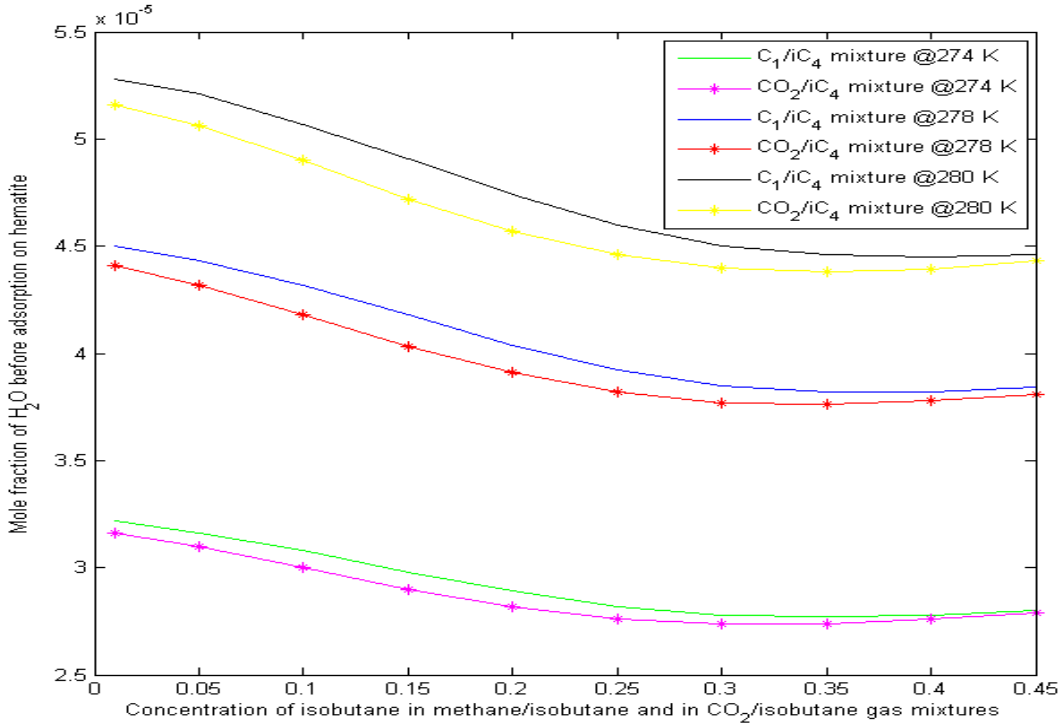

Figure 11.24: Maximum concentration of water that can be permitted in methane/isobutane and CO_2/isobutane gas binary mixtures before water is adsorbed on hematite at 9000 kPa

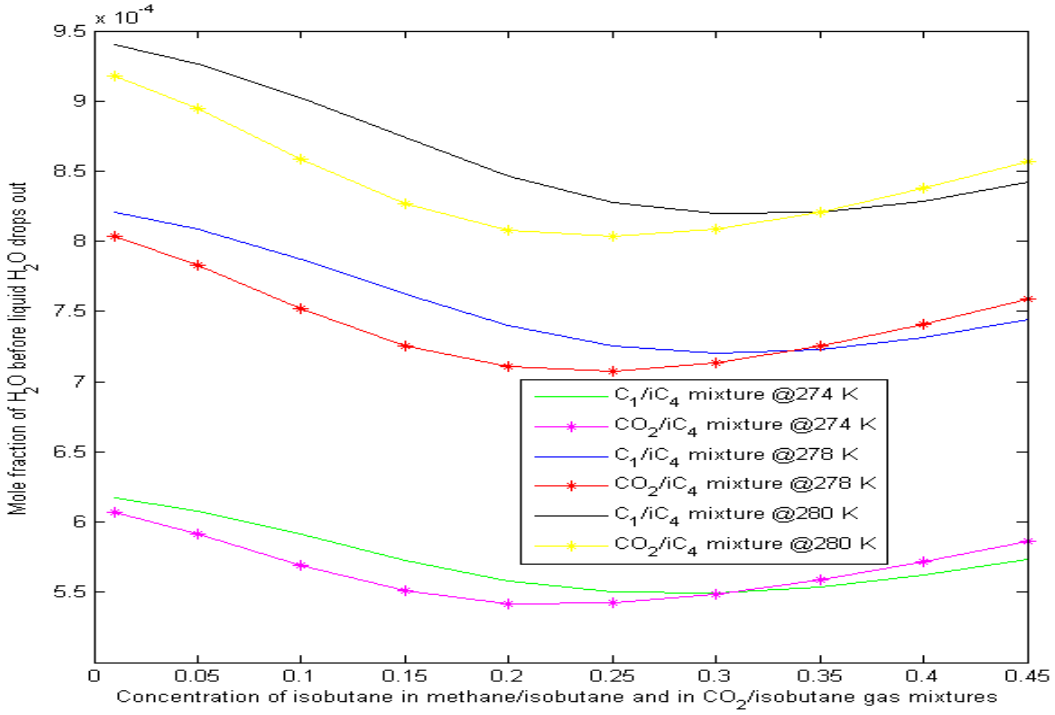

Figure 11.25: Maximum concentration of water that can be permitted in methane/isobutane and CO_2/isobutane gas binary mixtures before liquid water drops out at 13000 kPa

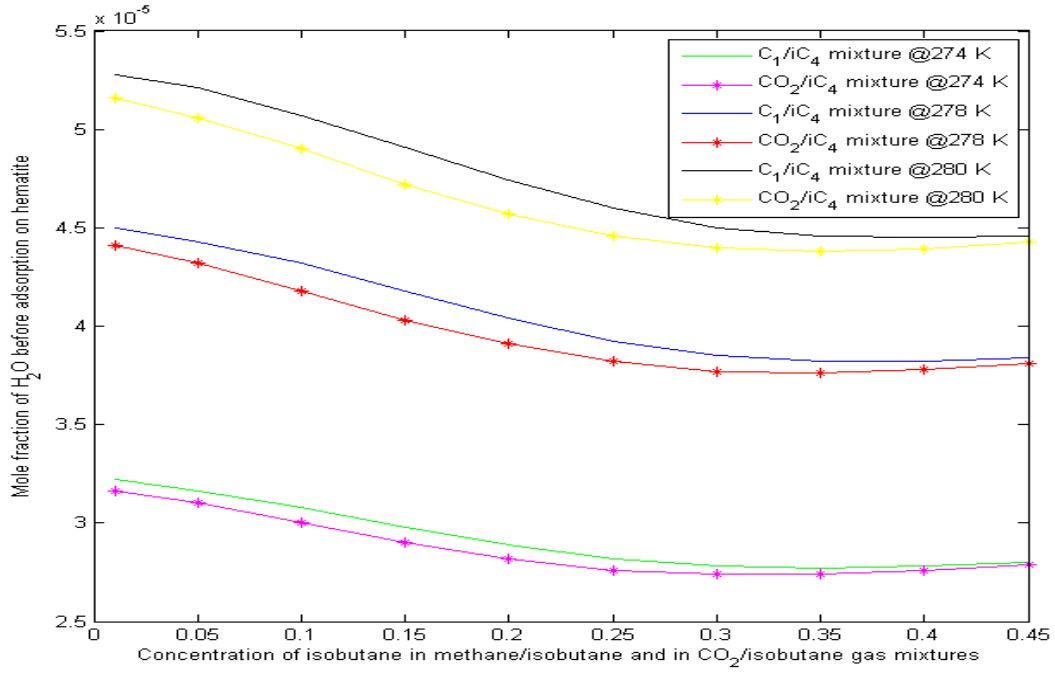

Figure 11.26: Maximum concentration of water that can be permitted in methane/isobutane and CO_2/isobutane gas binary mixtures before water is adsorbed on hematite at 13000 kPa

11.4 Comparison of the impacts of propane and isobutane on the two binary mixtures.

Figures 11.27 to 11.30 show the relative impacts of propane at the varying concentration in the binary gas mixtures to that of isobutane. The impact of propane is higher at 5000 kPa for both mixtures from 0.01 to 0.45 mole fractions. At higher pressures of 9000 kPa, even though higher impact is observed for propane, this impact begins to reduce at 0.20 and 0.25 mole fractions of propane in the binary mixtures with CO_2 and methane respectively for the classical dew-point approach at 274 K and 280 K. The trends observed for the route of water adsorbed on hematite at 9000 kPa are the same for both binary gas mixtures and they show an increase in mole fraction of maximum allowable water in both gas mixtures from propane concentration of 0.01 to 0.2 where a reduction in mole fraction of maximum allowable water in both gas mixtures commences with increase in mole fraction of propane. But at the highest pressure (13000 kPa), the impact of propane relative to isobutane is almost unity from concentration 0.01 to 0.15. The effect of isobutane dominates from concentration of 0.15.

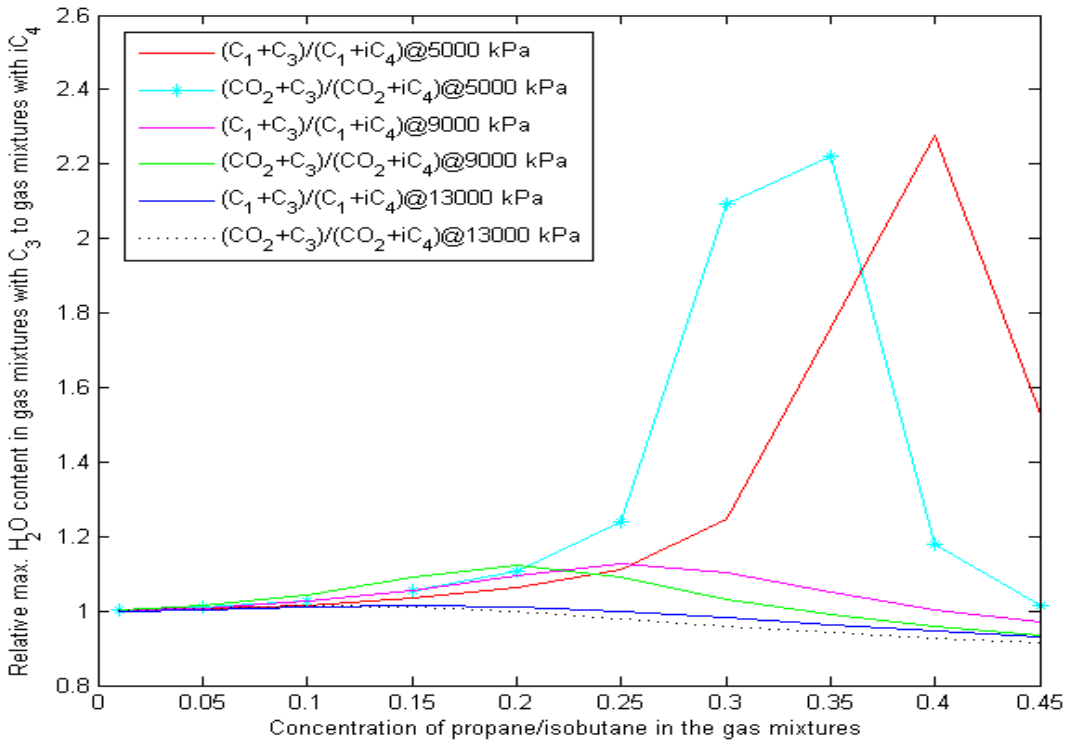

Figure11.27: The impact of propane relative to isobutane on the binary mixtures for the classical liquid water drop-out route at 274 K

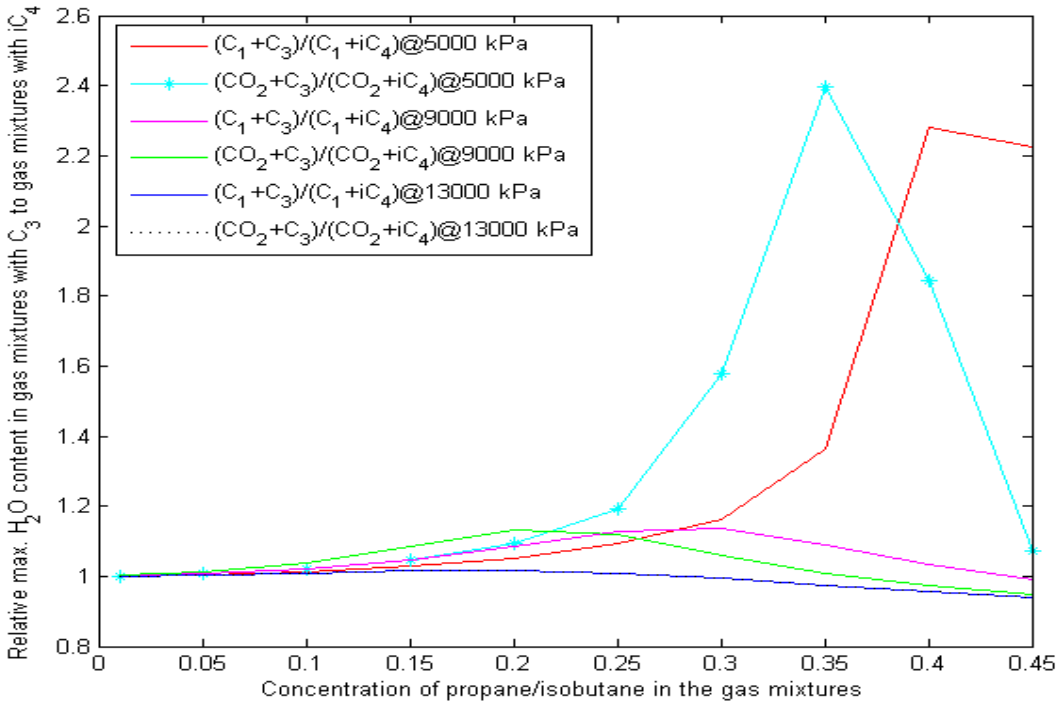

Figure11.28: The impact of propane relative to isobutane on the binary mixtures for the classical liquid water drop-out route at 280 K

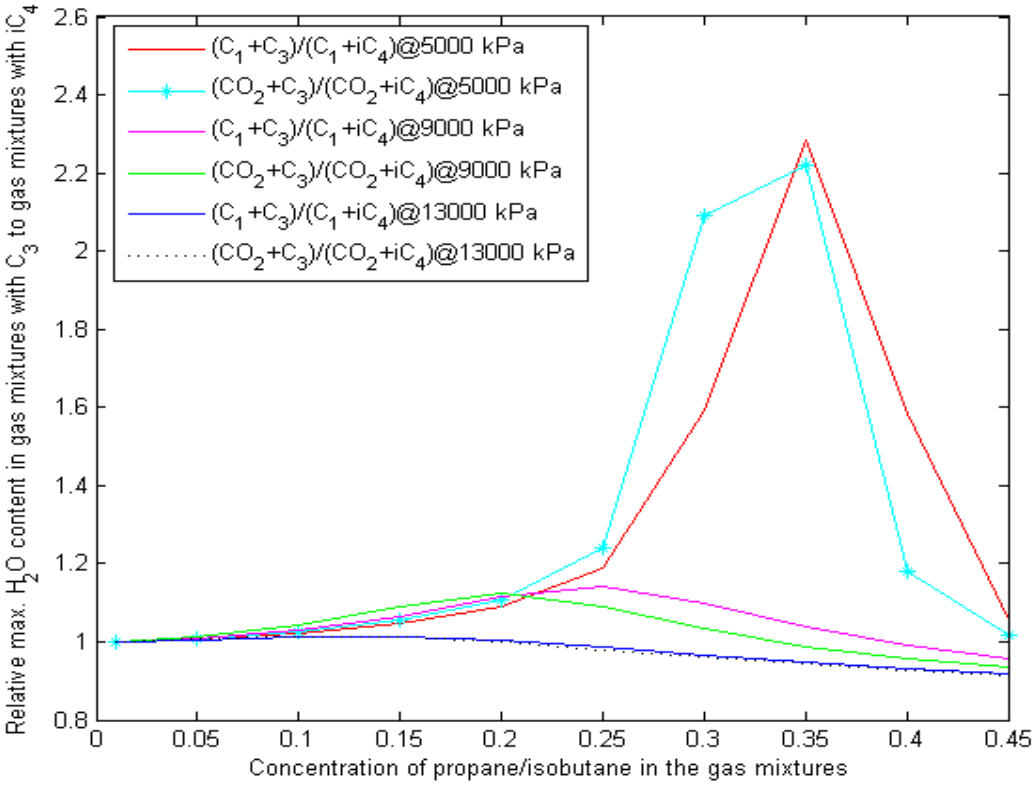

Figure11.29: The impact of propane relative to isobutane on the binary mixtures for the route of absorbed water on hematite at 274 K

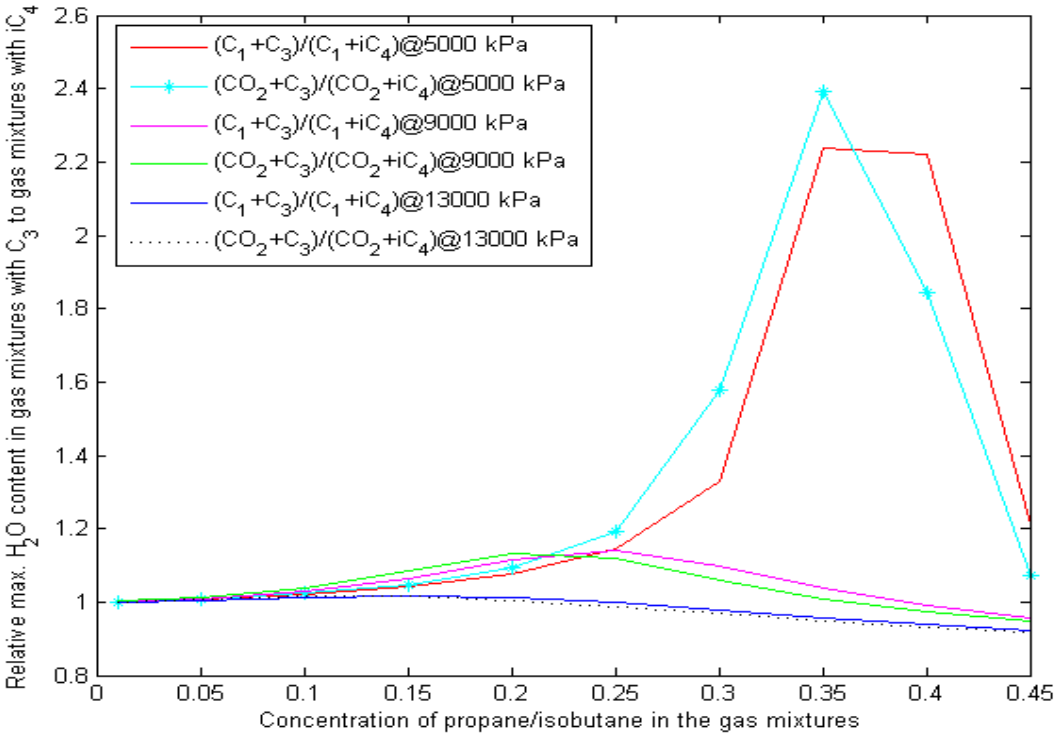

Figure11.30: The impact of propane relative to isobutane on the binary mixtures for the route of absorbed water on hematite at 280 K

12 Analysis and Discussion of Results IV: Hydrogen Sulphide (H_2S) and Carbon dioxide (CO_2) in Hydrocarbons Gas Streams

Sensitivity analysis of some impurities in hydrocarbons is done in this section. The impact of the presence of hydrogen sulphide (H_2S) and carbon dioxide (CO_2) on the maximum content of water that can be permitted in a stream of hydrocarbon gas mixtures during processing and pipeline transport has been investigated. The effects of these inorganic gases are evaluated because they are present in natural gas from some gas fields, for example, significant amount of CO_2 is present in Sleipner gas [135].

H_2S is a well-recognized vigorous hydrate former and it also gives extra stabilization to hydrates. And CO_2 is also a better hydrate former compared to methane. It is therefore pertinent to evaluate their impacts on hydrocarbon gas streams based on allowable maximum water content in the gas streams without the risk of hydrate formation. Troll gas well-head stream data [131] is the main gas stream used for this investigation.

12.1 The maximum content of water that can be permitted in Troll gas wellhead stream (without H_2S and CO_2) during processing and pipeline transport

Figure 0.1 and 0.2 present the qualitative illustration of the maximum water content tolerable in Troll gas wellhead stream to ensure prevention of hydrate formation during processing and pipeline transport. These two figures are presented here as reference cases for comparison to evaluate the effects of inclusion of both hydrogen sulphide and carbon dioxide in the subsequent subsections. The composition [131] of Troll gas wellhead fluid already presented in Table 7.1 is used for this analysis.

12.2 Impact of the presence of H_2S on the maximum content of water that can be permitted in hydrocarbon gas stream during processing and pipeline transport

The effect of the presence of hydrogen sulphide in hydrocarbon gas mixtures (natural gas) on the maximum content (safe limit) of water to prevent liquid water dropping out from the gas stream, which can eventually lead to the risk of hydrate formation has been investigated, and the results are presented in this subsection. Investigation has been conducted for both the classical dew-point approach and the new or alternative route to hydrate formation based on water adsorbing onto the rusty surfaces of the internal walls of gas processing equipment and transport pipelines. Rust here refers to hematite (Fe_2O_3) which is the most dominant and one of the most thermodynamically stable form of the ordinary rust (oxides of iron). Troll gas data is used since there is neither hydrogen sulphide nor carbon dioxide in it.

The results for introducing 1%, 5% and 10% molar concentrations of hydrogen sulphide into the Troll gas wellhead stream are presented in Figures 0.3 to 0.8 in Appendix, and in Table 12.1, and Table 0.1 to 0.3 also in Appendix. The evaluation has been performed with the temperature and pressure conditions of the North Sea floor, which are typically from 272 K to 279 K and from around 5000 kPa to about 25000 kPa respectively. However, emphasis for analysis is based on pressure range of 5000 kPa to 17000 kPa because as from or above this pressure range, change in absolute value of upper limit of water for methane dominated gas stream is negligible. This insensitivity to increase in pressures is as a result of the high density non-polar phase of especially the presence of higher hydrocarbons (C_{2+}) at the high pressures as can be observed in Figures 0.3 to 0.8 in Appendix. The curves of 17000 kPa to 25000 kPa almost overlap. Moreover, a shift from methane dominated maximum water content trend to that of higher hydrocarbons (C_{2+}) could expected as from 17000 kPa when C_{2+} is present but depending on the composition of the C_{2+} (this has been shown in Section 10 and 11).

Introducing 1% molar concentration of H_2S into the Troll gas will result in reduction of the maximum water content (in absolute values) that can be allowed in the gas stream with average of approximately 1.2% for pressure range of 5000-17000 kPa at a temperature of 274 K from the classical dew-point approach analysis. While the analysis from the method involving water adsorption onto surfaces covered with hematite shows only 0.8% reduction in upper limit of water that should be allow without the risk of hydrate formation. Though reductions are observed, they are very marginal. At 280 K, almost no change is observed

within this pressure range; precisely, only average of about 0.3% reduction in absolute value in maximum allowable concentration of water with the dew-point water dropout approach and no change with the adsorption of water on hematite approach. This may be a result of reduction in density of the gas as the temperature increases.

With 5% molar concentration of H_2S at a temperature of 274 K and for pressure range of 5000-1700 kPa, the reduction in upper limit of mole-fraction of water in absolute value reduced further to average of 2.3% with the dew-point water dropout calculations and 2.2% with evaluations based on the alternative route to hydrate formation involving adsorption of water onto rusty surfaces. Calculations from both approaches for the same pressure range at 280 K show reduction of average of 1.3% each in absolute value of the safe-limit of water in the gas stream.

A further increase of H_2S in the gas stream to 10% at a temperature of 274 K for pressure range of 5000-17000 kPa will cause the maximum water content that can be permitted in the gas stream to reduce in absolute value of average of 4.0% and 4.5% from dew-point analysis and from the evaluations from the approach of adsorption of water on rust respectively. And at 280 K for the same pressure range, the reduction in safe-limit of water in absolute values becomes average of 2.9% and 3.3% for both dew-point water dropout method and the water dropout through adsorption on hematite (rust) respectively. At this molar concentration (10%) of H_2S, the hematite approach has a higher impact compared to the cases of 1% and 5% molar concentrations.

It is important to state here that the alternative route to hydrate formation via adsorption on hematite also absolutely dominates in examining the risk of water dropping out from mixture of hydrocarbon gases with hydrogen sulphide to form a separate water phase and eventually leading to hydrate formation. From the analysis presented in Figures 0.3 to 0.8 in Appendix, and Tables 0.1 to 0.3 also in Appendix, they show that the alternative to hydrate formation based on adsorption on hematite is 19 times more risky at a lower temperature of 274 K and 18 times more risky at 280 K within the pressure range of 5000-25000 kPa. This can be explained based on the fact that the average chemical potential of the water adsorbed on hematite (rusty surfaces) is approximately 3.4 kJ/mol [8, 78] more negative than the chemical potential of liquid water. And thermodynamic processes move towards minimum energy.

12.3 Impact of the presence of CO_2 on the maximum content of water that can be permitted in hydrocarbon gas stream during processing and pipeline transport

In this section, similar analysis to that in Subsection 11.2 is performed but with carbon dioxide as the impurity introduced into the Troll gas. Molar concentration of 1%, 5% and 10% of carbon dioxide is introduced and the upper limit of water content in the gas stream evaluated to investigate the impact of the impurity using both the classical dew-point water dropout analysis employed by the industry and the new alternative approach for examining hydrate formation based on adsorption on hematite. Qualitative illustrations of the results are presented in Figures 0.9 to 0.14 in Appendix, and in Tables 0.1 to 0.3 also in Appendix.

With 1% molar concentration of CO_2 introduced into the Troll gas, for the same pressure range of 5000-17000 kPa at a temperature of 274 K, the maximum allowable water content in the gas stream will only reduce 0.9% and 0.5% in absolute value with the dew-point technique and the approach of adsorption onto hematite (rusty surface) respectively. And with the same pressure range at 280 kPa, no reduction is observed from the calculations with both alternative routes to hydrate formation. Increase of the molar concentration of CO_2 introduced into the gas stream to 5% and 10% at 274 K and 280 K for the same pressure range of 5000-17000 kPa give the same results obtained with 1% molar concentration of CO_2 above.

In this investigation also, the alternative path to hydrate formation through adsorption on hematite also completely dominates in examining the risk of liquid water dropping out from mixture of hydrocarbon gases with carbon dioxide and subsequently resulting in hydrate formation. The alternative path to hydrate formation that involves adsorption on hematite is also 19 times more risky at a lower temperature of 274 K and 18 times more risky at 280 K within the pressure range of 5000-25000 kPa investigated.

12.4 Comparison of the impacts of H_2S and CO_2 on the maximum content of water that can be permitted in hydrocarbon gas stream during processing and pipeline transport

The impacts of H_2S and CO_2 as impurities in natural gas (hydrocarbon gas mixtures) on the upper limit of water that can be tolerated in the gas during processing and pipeline transport are compared in Tables 0.1, 0.2 and 0.3 in Appendix. A summary of these results are tabulated in Table 12.1.

The comparison is done for molar concentrations of 1%, 5% and 10% of H_2S and CO_2 as done in Subsection 12.2 and Subsection 12.3 above. The result show that CO_2 permits slightly higher water content compared to H_2S. At temperature of 274 K, and for pressure range of 5000 kPa to 17000 kPa, with 1% molar concentration of both H_2S and CO_2, gas mixtures with CO_2 allows only average of 0.3% more water than gas mixtures with H_2S with both hydrate risk examination approaches in this work. But at 280 K with the same pressure range, it is average of 0.2% with the dew-point method and average of 0.3% with the approach of adsorption of water on hematite.

Increasing the molar concentrations of H_2S and CO_2 to 5% each resulted in widening the difference in the upper limit of water that can be permitted in the gas stream to prevent the risk of hydrate formation. At temperature of 274 K, and for pressure range of 5000-17000 kPa, hydrocarbon gas mixture with CO_2 tolerates average of 1.5% and 2% more water than H_2S according to the dew-point technique and adsorption mechanism approach respectively. But at 280 K for the same pressure range, it is 1.3% and 1.6% with the dew-point method and the calculation with perspective of adsorption of water onto rusty surfaces respectively.

And with molar concentrations of 10% each for both H_2S and CO_2, mixture with CO_2 records average 3.3% and 4.2% more water tolerance than that with H_2S with dew-point calculations and the approach of adsorption onto rusty surfaces respectively at 274 K and for pressure range of 5000 kPa to 17000 kPa. However, gas mixture with CO_2 water tolerance is average of 2.9% and 3.7% more than that of gas with H_2S from dew-point approach analysis and from adsorption mechanism approach calculations at 280 K and for pressure range of 5000-17000 kPa.

Comparing the impacts of introducing CO_2 with the same molar concentrations of 0.01, 0.05 and 0.10 into the Troll gas with the original gas stream shows no significant reduction in upper limit of water tolerable in the gas stream. The maximum reduction of the safe-limit of water that can be permitted in the gas stream at 10% molar concentration of CO_2 has effect of

less than 1%. And almost no reduction is recorded at temperatures of 274 K and 280 K with the classical dew-point technique and the adsorption of water on Hematite approach respectively for all the concentrations investigated in subsection.

On other hand, introduction of H_2S results in a considerable decline in the upper-limit of water especially at molar concentrations of 0.05 and 0.10. Reductions in maximum allowable water content up to 4.1 and 4.5% are estimated at 274 K from the conventional dew-point approach and the new concept of water dropping out through adsorption on Hematite respectively. Refer to Table 12.1 for details.

Table 12.1 : Summary of the impact of H_2S and CO_2 on the average maximum water content permitted in hydrocarbons during processing and pipeline transport for a pressure range of 5000-17000 kPa

Systems	How many times higher is Dew-point over Hematite?		Reduction in maximum water content compared with Troll gas as reference case (absolute values)			
			Dew-point		Hematite	
			[%]			
	274 K	280 K	274 K	280 K	274 K	280 K
Kvamme & Sapate (2016)	18		n/a	n/a	n/a	n/a
Reference case: Troll gas	19	18	-	-	-	-
Sleipner gas	19	18	2.6	2.4	2.6	2.3
0.01 H_2S on Troll gas	19	18	1.1	0.2	0.4	0.4
0.05 H_2S on Troll gas	19	18	2.3	1.3	2.7	1.5
0.10 H_2S on Troll gas	19	18	4.1	2.9	4.5	3.5
0.01 CO_2 on Troll gas	19	18	0.8	no reduction	no reduction	0.4
0.05 CO_2 on Troll gas	19	18	0.8	no reduction	no reduction	0.4
0.10 CO_2 on Troll gas	19	18	0.9	0.01	no reduction	0.4

n/a: Not available

12.5 Maximum tolerance of water to prevent the risk of hydrate formation for 0.5 mole of hydrocarbon and 0.5 mole of inorganic gases (H_2S and CO_2).

The impacts of H_2S and CO_2 on methane (structure I hydrate former) and on propane (structure II hydrate former) have been investigated in this subsection. Binary mixtures of hydrocarbon and inorganic gases, each having 0.5 mole-fraction in each mixture, are evaluated at 274K and 280K and within the pressure range of 5000 to 25000 kPa for the safe-limit of water to prevent hydrate formation. Both approaches for examining the risk of hydrate formation, that is the dew-point technique and the approach of adsorption of water on rusty surfaces have been applied in this study. Then, the effects of H_2S and CO_2 in the mixture at these high concentrations are compared and also compared with pure propane, Troll gas and Sleipner gas qualitatively as illustrated in Figures 0.15 to 0.18 in Appendix.

For mixtures involving hydrocarbon structure I hydrate former (methane), the binary mixture of 0.5 mole-fraction each of methane and hydrogen sulphide shows less tolerance for water compared to that of methane-carbon dioxide (also with 0.5 mole-fraction each) mixture, to ensure prevention of the risk of hydrate formation. And in the case of mixtures with structure II hydrate former (propane), both binary mixtures, that is 0.5 H_2S and 0.5 C_3H_8 and that of 0.5 CO_2 and 0.5 C_3H_8 record lower maximum mole-fraction of water that can be allowed to avoid the risk of hydrate nucleation and growth compared to pure propane (100% C_3H_8). And the binary mixture with H_2S also has less tolerance in terms of maximum water content that can be permitted in the gas mixture compared to that with CO_2. This indicates that hydrogen sulphide as a hydrate guest molecule, besides being a very vigorous hydrate former and giving extra stabilization to hydrates (due to some coulombic interactions as has been discussed in Subsection 2.3), it also has effect on the tolerance for maximum water content that can be allow in hydrocarbon gas(es). Even though methane (structure I hydrate guest molecule) and propane (structure II hydrate former) exhibits opposite trends in maximum water content (findings from Sections 9 and 10) that should be allowed in bulk gas, the safe-limit of water is lowered by the presence of H_2S in both methane and propane and the amount depends on its concentration in the mixture. Nevertheless, at this higher concentration of the inorganic gases, CO_2 also reduces the maximum water content that can be permitted in propane gas.

Analysing the results for both Troll gas and Sleipner gas, both from the North Sea, Sleipner gas permits less water to avoid the risk of hydrate nucleation and growth during

processing and pipeline transport. It can also be said that the lesser the methane in the gas mixture, the lesser the maximum water content that can be allowed to operate safe from occurrence of hydrate formation in the system.

The estimated maximum water content that can be allowed in binary mixture of 0.5 mole fraction of H_2S and 0.5 mole fraction of CH_4 by the classical dew-point method is about 20 to 21 times more than the estimates with the approach of water adsorption on hematite for pressures of 5000 kPa, 9000 kPa and 13000 kPa at temperature of 274 K. While it is 19 times higher for all other mixtures investigated in this subsection at the same temperature and for pressures of 5000 kPa to 25000 kPa. Estimates at temperature of 280 K for pressures of 5000 kPa to 25000 kPa shows the from classical dew-point approach having water tolerance of about 18 to 19 times higher than estimates with the new concept of adsorption of water on hematite approach currently employed by the industry. Therefore, the new approach for examining the risk of hydrate formation based on adsorption on hematite as a means of water dropping out from these gas mixtures also unquestionably dominates in these binary mixtures evaluated. This is because the average chemical potential of the water adsorbed on hematite is around 3.4 kJ/mol [8, 78] less than the chemical potential of liquid water. And thermodynamics moves in the direction of minimum energy.

The effects of H_2S and CO_2 on the upper limit of water content in methane (structure I hydrate guest molecule) and propane (structure II hydrate guest molecule) gases at higher molar concentration of 0.5 each in the binary mixtures have also been investigated. Dew-point estimations show about 18% reduction, while about 20% reduction is calculated with the new approach of adsorption of water on Hematite for the system of 0.5 H_2S and 0.5 CH_4. And for the gas system of 0.5 H_2S and 0.5 C_3H_8, 20% reduction in maximum content of water is calculated with both approaches. While the system of 0.5 CO_2 and 0.5 CH_4 shows less than 1% reduction in maximum amount of water tolerable in the binary mixture, and about 16% reduction at 274 K and around 14% reduction at 280 K for 0.5 CO_2 and 0.5 C_3H_8 with both methods.

Table 12.2: Summary of the impact of 0.5 H_2S and 0.5 CO_2 on the average maximum water content permitted in hydrocarbons during processing and pipeline transport

Systems	How many times higher is Dewpoint over Hematite?		Average maximum water content reduction compared with reference cases (absolute values)			
			Dew-point		Hematite	
	274 K	280 K	274 K	280 K	274 K	280 K
			[%]			
Kvamme & Sapate (2016)	18		n/a	n/a	n/a	n/a
Reference case: 1.0 CH_4	19	18	-	-	-	-
Troll gas	19	18	0.07	0.04	0.04	0.08
Sleipner gas	19	18	3.40	3.08	3.42	3.05
0.5 H_2S and 0.5 CH_4	19-21	18-20	18.00	18.09	19.81	20.44
0.5 CO_2 and 0.5 CH_4	19	18	0.28	0.37	0.33	0.41
Reference case: Pure C_3H_8	19	18	-	-	-	-
0.5 H_2S and 0.5 C_3H_8	19	18	19.69	19.78	19.67	19.75
0.5 CO_2 and 0.5 C_3H_8	19	18	15.68	14.00	15.69	14.00

n/a: not available

*****The maximum allowable water content with dew-point technique over the hematite approach in this system is highest between 5000-13000 kPa, but it is same with other systems between 17000-25000 kPa.

13 Discussion, Conclusion and Further Works

In this section, the main findings from Sections 10, 11, and 12 are brought together and discussed in Subsection 13.1 titled “General Discussion”. The section also contains the conclusions from this project and proposed further works.

13.1 General discussion

A novel thermodynamic scheme [81] for examining different routes to hydrate formation, applying ideal gas as reference state for every component in all phases including hydrate phase, and also accounting for lattice movements and corresponding effects of different hydrate formers, unlike that of van der Waal and Platteuw (1959) [31] that assumed rigid lattice. Comparison of different routes to hydrate nucleation and growth is made transparent and consistent in free energy changes and associated enthalpy change [5, 78] with this thermodynamic scheme.

In this project, real hydrocarbon mixtures have been investigated for the first time using this novel thermodynamic scheme, with composition data that are openly available for the Troll gas and Sleipner gas from the North Sea of Norway. The model has been comprehensively validated in this work for pure and mixtures of hydrocarbons, CO_2, H_2S, and hydrocarbon mixtures with these inorganic gases with experimental data from 35 established literature [7, 141-165, 167-171, 173, 175, 176].

At the North Sea, gas pipelines are laid on the seafloor with temperatures that could be as low as 272.15 K in the north because of water salinity, and seldom rise above 279.15 K at the south, with operating pressures ranging from 5000 kPa to 30000 kPa. These conditions are favourable for hydrate nucleation and growth if free water is available together with favourable mass and heat transport.

Hydrate can plug hydrocarbon gas pipelines and processing equipment, thus, can halt operations, thereby resulting in economic losses and could also lead to loss of lives. About one billion dollar (USD) [2] is spent for prevention of hydrate formation yearly by the petroleum industry. Therefore, the importance of evaluating the risk of hydrate formation cannot be overemphasized. The classical concept the industry currently employ to evaluate the risk of hydrate formation is classically based on a three step evaluation. The first step involves an estimation of water dew-point for the gas in question. If any condition of temperature and pressure in the pipeline is above water dew-point so that water drops out

then a second step involves evaluation of how much water will drop out. And the third step is the hydrate formation evaluation, including maximum amount of hydrate that can be expected to form from the condensed water.

The shortcoming of the classical scheme is that it totally disregards another (a new) concept that involves water dropping out of the bulk through the mechanism of adsorption on rusty surfaces. These rusty surfaces provide water adsorption sites that can also lead to hydrate formation. Rust here refers to Hematite which is the most thermodynamically stable forms of ordinary rust. By ordinary rust we refer to different oxides of iron formed by the exposure of iron to water and oxygen. However, hydrate formation cannot occur directly on the surfaces covered by Hematite. This is because the distribution of partial charges of hydrogen and oxygen in the lattice are incompatible with the atom charges in the rusty (Hematite) surface. But the rusty surfaces work as catalyst that help to take out the water from the gas stream via the process of adsorption, and hydrate formation can follow slightly outside of the first two or three water layers of about one nanometre.

The estimates from evaluation of the risk of hydrate formation in both Troll gas and Sleipner gas in this study indicate that it is more probable for free water to be made available for hydrate to subsequently form through the alternative route involving adsorption on Hematite than the conventional dew-point route currently used by the industry. The estimates from the new concept for evaluating the risk of hydrate formation, which is based on adsorption mechanism on hematite show that the maximum water content (safe-limit) that can be permitted during processing and pipeline transport of hydrocarbon gas streams to prevent the risk of hydrate nucleation and growth should be only about five to six per cent (5-6 %) of the estimates using the classical dew-point technique. In other words, the safe limit of water (mole fraction) with the classical dew-point method is over 18 to 19 times higher (See Table 12.1) than the values estimated using the approach of adsorption onto Hematite. Similarly, Kvamme and Sapate (2016) [48] estimated an 18 times higher values with the traditional dew-point approach over the new method involving adsorption of water onto Hematite for a gas system containing methane and ethane. And Kvamme et al. (2017) [78] calculated about 20 times higher values for gas systems of methane and methane-dominated binary mixtures with ethane and propane. This explains why hydrate nucleation and growth could still occur in industrial processes if only the dew-point approach is used as a measure to operate safe from hydrate formation. Thus, the alternative route to hydrate formation through adsorption of water on surfaces covered by Hematite cannot be neglected if the risk of hydrate formation without applying inhibitions or using other expensive measures during

processing and pipeline transport of natural gas from the North Sea is to be prevented. However, it is not possible for initial hydrate nuclei to attach directly to the surface of the rusty surfaces due to the low chemical potential of adsorbed water. The hydrate formed will be bridged (as a minimum) by three to four layers of structured water on the surface of the Hematite.

The heavier hydrocarbons (C_{2+}), ethane, propane and isobutane exhibit opposite trends for maximum water tolerance (see Figures 10.5 to 10.8, and Figures 11.9 to 11.14) as also observed by [78]. This is caused by the high density non-polar phase at the high pressures which makes ethane, propane and isobutane exhibit opposite trend to that of methane, methane dominated gas streams (natural gas, e.g., Troll gas and Sleipner gas) and carbon dioxide (CO_2). The higher the pressure for the C_{2+} systems the more the maximum amount of water that can be allowed without the risk of hydrate formation (refer Figures 10.5 to 10.8, and Figures 11.9 to 11.14). This C_{2+} trend is opposite to that of methane-rich gases where the maximum concentration of water declines as pressure increases (as can be observed by comparing Figures 10.1 to 10.4, and Figures 11.1 to 11.8 with Figures 10.5 to 10.8, and Figures 11.9 to 11.14). Therefore, the presence of ethane and heavier structure II hydrate guest molecules of propane and isobutane causes the maximum content of water tolerable in Troll gas stream relatively insensitive to increase in pressure from 17000 kPa to 25000 kPa (the last three higher pressure curves almost overlap) (refer to Figures 10.1 to 10.4). But in Sleipner gas stream, the relative insensitivity to increase in pressure occurs from 13000 kPa to 25000 kPa, that is the last four higher pressure curves virtually overlap (see Figures 11.1 to 11.4). As has been explained above, this is due to the high density non-polar phase at these high pressures, with natural gas from Sleipner field having a higher molar concentration of C_{2+} (about 12% of the gas) and Troll gas having only about 4% molar concentration of C_{2+}. Furthermore, for the gas mixture containing only the C_{2+}, the higher the number of carbon in each component's molecule, the higher the allowable amount of water without the risk of hydrate formation.

Comparing the systems of pure methane and pure CO_2, both systems exhibit similar trends with only a negligible difference in absolute values of maximum water content that can be tolerated, with methane having the very slightly higher values (see Table 11.1 and Figure 11.5 to 11.8).

Sensitivity analysis of varying molar concentration of propane and isobutane components in binary mixtures with methane and with CO_2 at temperatures of 274 K, 278 K and 280 K and at pressure of 5000 kPa, 9000 kPa and 13000 kPa was performed using both

the classical dew-point technique and the new concept of adsorption on Hematite. The trends illustrate a decline in tolerable maximum mole-fraction of water with increasing concentration of propane and isobutane for both binary mixtures at all the temperatures investigated. This is because the non-polar heavy hydrocarbons (structure II hydrate formers) will act to draw down the maximum concentration of water that can be permitted in the gas mixture to a point when they completely dominate or dictate the trends. This explains why the upper limit of water tolerable in Sleipner gas is 2.3-2.6 % lower than that of Troll gas that contains lesser amount of C_{2+} (refer to Table 7.1, Table 7.2 and Table 12.1).

Sensitivity analysis of introducing hydrogen sulphide (H_2S) and carbon dioxide (CO_2) into the Troll gas was also conducted at temperatures of 274 K and 280 K and for pressure range of 5000-17000 kPa with molar concentrations of 0.01, 0.05 and 0.10 of the inorganic gases. CO_2 had very insignificant impact on the gas mixture in respect of upper limit of water. In fact no reduction was calculated with hematite method for the three concentrations at 274 K (See Table 12.1, Table 0.1 to 0.3 and Figures 0.9 to 0.14 in Appendix). On the other hand, the maximum tolerable water content for Troll gas reduces with increase in the molar concentration of H_2S (See Table 12.1, Table 0.1 to 0.3, and Figures 0.3 to 0.8 in Appendix).

The impact of both H_2S and CO_2 in binary mixture with methane (structure I hydrate guest molecule) and propane (structure II hydrate former) have also been investigated but with 0.5 molar concentration each of the inorganic gases in their different binary mixtures. The system with molar concentrations of 0.5 H_2S and 0.5 CH_4 records impacts of 18 to over 20% reduction in upper limit of water compared to the reference system of pure CH_4. And in the system with molar concentrations of 0.5 H_2S and 0.5 C_3H_8, a reduction of approximately 20% in maximum allowable water content compared to pure C_3H_8 is estimated. While a reduction of less than 1% is calculated for the system of 0.5 CO_2 and 0.5 CH_4 in comparison with that of pure CH_4. But a significant reduction is estimated for the binary mixture of CO2 and the heavier hydrocarbon (structure II hydrate former) propane gas, that is 0.5 CO_2 and 0.5 C_3H_8. About 14 % and 16% reduction in safe-limit of water is calculated at 274 K and 280 K respectively with both the classical dew-point approach and the new concept based on adsorption on Hematite.

The systems with H_2S have the lowest absolute tolerance for water. The system with molar concentrations of 0.5 H_2S and 0.5 CH_4 records the highest ratio of estimates of absolute values of upper limit of water tolerance with dew-point technique to the new concept of water adsorption on Hematite. Estimates with dew-point approach are 19-21 times higher than those with adsorption of water on Hematite at 274 K, and 18-20 times higher at 280 K as

against the 19 and 18 times higher at 274 K and 280 K respectively for all other systems investigated in this project.

From this study, the alternative route to hydrate formation through adsorption of water on hematite absolutely dominates in evaluating the risk of water dropping out from the gas mixtures (and pure components investigated) to form a separate water phase and eventually lead to hydrate formation. This can be understood from the fact that the average chemical potential of the water adsorbed on Hematite could be about 3.4 kJ/mol [8, 78] more negative than the chemical potential of liquid water. And thermodynamics favours minimum free energy. Therefore, the petroleum industry may need to review their best practice to adopt the concept of adsorption of water on Hematite (rust) to be able to carry out natural gas pipeline transport and gas processing operations without the risk of hydrate nucleation and growth, since pipes are usually already covered with some rust before mounting them together to form network of gas transport pipelines.

13.2 Conclusion

The main conclusion from this project is that estimates of maximum mole-fraction of water tolerable in hydrocarbon gas systems containing structure I and structure II guest molecules during processing and pipeline transport with the classical dew-point technique is in order of 18-21 times higher than the estimates with the new concept of evaluating the risk of hydrate formation based on water dropping out by the process of adsorption on Hematite (rusty pipelines and processing equipment). In other words, the alternative route to hydrate formation through adsorption of water on hematite totally dominates in evaluating the risk of water dropping out from the gas mixtures (and pure components investigated) to form a separate water phase and eventually lead to hydrate formation. This is due to the fact that the average chemical potential of the water adsorbed on Hematite is approximately 3.4 kJ/mol less than the chemical potential of liquid water. And thermodynamics favours minimum free energy. Some other conclusions include:

- The typical trend exhibited by methane, methane-dominated gas mixtures like Troll gas and Sleipner gas, and carbon dioxide is decline in the upper limit of water with increasing pressure.
- The heavier hydrocarbon (ethane, propane, and isobutane) gases exhibits opposite trend to that of CH_4 and CH_4-dominated gas mixtures where the permitted maximum water content increases with increase in pressure. However, this manifestation can be explained as a result of the high density non-polar phase at the high pressures of the C_{2+}.
- The non-polar heavier hydrocarbons (especially of structure II hydrate formers) will act to draw down the maximum concentration of water that can be permitted in the gas

mixture to a point where they completely dominate or dictate the trends. This is why the safe-limit of water tolerable in Sleipner gas is lower than that of Troll gas which contains lesser amount of C_{2+}

- The safe-limit of water to prevent the risk of hydrate formation during processing and pipeline transport of CO_2 is only very slightly less than that CH_4.
- Higher concentrations of H_2S up to 5% and above would have a significant reduction effect on the maximum concentration of water that can be permitted in hydrocarbon gas mixtures during processing and pipeline transport operations, usually at elevated pressures and low temperatures.
- The petroleum industry may need to review their best practice to adopt the concept of adsorption of water on Hematite (rust) to be able to carry out natural gas pipeline transport and gas processing operations without the risk of hydrate nucleation and growth, since pipes are usually already covered with some rust before mounting them together to form network of gas transport pipelines.

13.3 Further works

Subsection 13.3.1 to 13.2.4 present future works needed to be done based on the work done in this thesis.

13.3.1 Application of this theory to more solid surfaces

In this thesis the alternative route to hydrate formation via adsorption of water on hematite completely dominates in examining the risk of water dropping out from the gas mixtures (and pure components investigated) to form a separate water phase and eventually lead to hydrate formation. There may be a need to investigate other absorbed surfaces like plastic, iron carbonates etc. and qualitatively determine the surface which is most risky in respect of hydrate formation during transport and processing of hydrocarbons. Iron carbonates are some of the foremost corrosion products in the carbon dioxide lead corrosion process. Carbon dioxide can be present in water as a dissolved gas in petroleum reservoirs underground. It can be converted to carbonic acid (H_2CO_3) which can cause corrosion of gas pipeline through the formation of solid ferrous carbonate ($FeCO_3$) on the surface of steel if the product of ferrous ion concentration and carbonate ion concentration is over a given solubility product [177, 178].

13.3.2 Impacts of the presence of other gases that cannot form hydrate but can affect hydrate formation

In this thesis, only guest molecules that can directly form hydrates by themselves (methane, ethane, propane, isobutane, carbon dioxide and hydrogen sulphide) are considered. However, in hydrate formation process, other gases like nitrogen and normal-butane usually have dilution impact on the main hydrate formers mentioned above. There is need to investigate the impacts of the presence of these gases on the upper limit of water before liquid water can drop out of the bulk.

13.3.3 More experimental works involving carbon dioxide and structure II hydrate formers

During this project, hydrate equilibrium experimental data for mixtures of carbon dioxide and propane or isobutane were found to be very limited. In fact there is a lack of data sets with much temperature-pressure data points for any given composition. This has been confirmed long ago by Adisasmito and Sloan (1992) [165] as at 1992. Thus, it will be worthwhile to carryout experiments to produce such data since probutane and isobutane could be present in significant amount in natural gas from some fields.

Moreover, the system of propane and carbon dioxide as studied by Adisimoto and Sloan [165] (Figure 9.15) appear to be more complex in terms of phase transitions. In this study this system has been studied using different equations of state and in-house software as well as commercial software. In all of these studies this systems undergo phase transitions for some of the higher temperatures. Therefore, it would also be worthwhile to experimentally re-examine this system.

13.3.4 Kinetic modelling

A theoretical method with the capability of evaluation of the competing phase transitions under the constraints of both mass transport and heat transport has been illustrated in this thesis. The findings in this work represent simple kinetic theories of the classical theory with couplings to heat exchange dynamics via the relationships between free energy changes and enthalpy changes as given by the combined 1st and 2nd laws of thermodynamics. This needs an additional formulation of heat transport kinetics by conduction and convection [178]. One alternative method as stated in Section 6 is the Density Function Theory (DFT). This is based

on the theory which states that the kinetics of phase transition is proportional to the changes in the molecular structure [178]. Phase Field Theory (PFT) can be regarded as a simple reformulation of DFT as molecular structure is proportional to free energy according to the canonical ensemble in statistical mechanics [108, 178].

Nomenclature

ΔG or dG	Free energy change	[J]
$\Delta \underline{G}^{Total}$	Total free energy change	[J]
$\Delta G^{Phase\ transition}$	Free energy change per unit volume	[J/m^3]
γ	The interface free energy per unit area	[J/m^2]
R^H	Hydrate critical core	[m]
ρ_N^H	Molar or molecular density of the hydrate core	[mole/m^3]
μ	Chemical potential	[J/mole]
v_i	Fraction of cavity type *i* per water molecule	[-]
n_{guest}	Number of guest molecules in the system	[-]
τ	Degrees of freedom	[-]
π	Number of actively coexisting phases	[-]
n	Number of active components in terms of hydrate phase transitions	[-]
J	Classical nucleation rate due to mass transport	[mole/(m^2.s)]
$\Delta \underline{H}^{Total}$	Total enthalpy change	[J]
$\vec{N}$	Vector of mole numbers in the system	[-]
T	Temperature	[K]
T_c	Critical temperature of the guest molecule in consideration	[K]
P	Pressure	[Pa or bar]
$P_{H_2O}^{SAT}$	Saturation pressure of water at temperature T	[[Pa]
R	The universal gas constant	[J/mole·K]
γ	Activity coefficient, used with superscript (phase) and subscript (component)	[-]
x or X	Liquid mole-fraction used with superscript (phase) and subscript (component)	[-]
y	Vapour mole-fraction used with superscript (phase) and subscript (component)	[-]
$\emptyset$	Fugacity coefficient	[-]
f	Fugacity	[-]
∞	Infinite dilution	[-]
$\underline{U}$	Internal energy	[J]
μ	Chemical energy	[J/mole]
$\underline{V}$	Volume	[m^3]
$\underline{S}$	Entropy	[J/K]
N_j	Number of particles of a component	[-]
θ_{ij}	Filling fraction of component *j* in cavity type *i*	[-]
x_{ij}^H	Mole fraction of component *j* in cavity type *i*	[-]
Δg_{ij}^{inc}	Energy of inclusion parameters	[J/mol]
Δg^H	Free energy changes associated with a hydrate phase transition	[-]
k	Ratio of mole-fraction gas versus mole-fraction liquid of the same component (gas/liquid *k*-values)	[-]

References

[1] E. Hammerschmidt, "Formation of gas hydrates in natural gas transmission lines," *Industrial & Engineering Chemistry*, vol. 26, pp. 851-855, 1934.

[2] Y. F. Makogon, "Natural gas hydrates–A promising source of energy," *Journal of Natural Gas Science and Engineering*, vol. 2, pp. 49-59, 2010.

[3] E. D. Sloan Jr and C. Koh, *Clathrate hydrates of natural gases*, 3rd ed. Boca Raton, Florida CRC press, 2007.

[4] Chartsbin. (Accessed: 16.01.2017). *Total Length of Pipelines for Transportation by Country*. Available: http://chartsbin.com/view/1322

[5] B. Kvamme, T. Kuznetsova, J. M. Bauman, S. Sjöblom, and A. Avinash Kulkarni, "Hydrate Formation during Transport of Natural Gas Containing Water and Impurities," *Journal of Chemical & Engineering Data*, vol. 61, pp. 936-949, 2016/02/11 2016.

[6] F. Woehler, "Krystallisirtes Schwefelwasserstoff-Hydrat," *Justus Liebigs Annalen der Chemie*, vol. 33, pp. 125-126 Cross referenced from Hammerschmidt (1934), 1840.

[7] P. Englezos and Y. T. Ngan, "Incipient equilibrium data for propane hydrate formation in aqueous solutions of sodium chloride, potassium chloride and calcium chloride," *Journal of Chemical and Engineering Data*, vol. 38, pp. 250-253, 1993.

[8] B. Kvamme, "Fundamentals of Natural Gas Hydrates and Practical Implications, Unpublished Work: PTEK 232, Course Material, Spring Semester 2017, Department of Physics and Technology, University of Bergen, Norway," ed, 2017.

[9] S. Kumar, *Gas Production Engineering*: Gulf Publishing Company, Book Division, 1987.

[10] V. John and G. Holder, "Hydrates of methane+ butane below the ice point," *Journal of Chemical and Engineering Data*, vol. 27, pp. 18-21, 1982.

[11] H.-J. Ng and D. B. Robinson, "Equilibrium-phase properties of the toluene-carbon dioxide system," *Journal of Chemical and Engineering data*, vol. 23, pp. 325-327, 1978.

[12] J. M. Campbell, *Gas Conditioning and Processing, Volume 1. Basic Principles. Pp 157-200*, 2003.

[13] W. Schroeder, "In Ahren's Sammlung Chemischer und Chemisch-Technik Vortrage, pp.21-71, Cross referenced from Hammerschmidt (1934)," 1926-28.

[14] M. T. Vafaei, "Reactive transport modelling of hydrate phase transition dynamics in porous media," PhD Dissertation for PhD, University of Bergen, Norway, 2015.

[15] M. Faraday and H. Davy, "On Fluid Chlorine," *Philosophical Transactions Royal Society London*, vol. 113, pp. 160-165, 1823

[16] S. Wroblewski, "On the laws of solubility of carbonic acid in water at high pressures (in French)," *Acad. Sci. Paris, ibid.,* pp. 1355–1357, 1882c.

[17] S. Wroblewski, "On the composition of the hydrate of carbonic acid (in French)." *Acad. Sci. Paris, ibid,* pp. 954–958, 1882b.

[18] S. Wroblewski, "On the combination of carbonic acid and water (in French) " *Acad. Sci. Paris, Comptes rendus,* vol. 94, pp. 212–213, 1882a.

[19] A. Ditte, "Crystallisation of Chlorine Hydrate " *Compt. rend.,* vol. 95, pp. 1283-1284, 1882.

[20] E. Maumene, *Chem. N,* vol. 47, 1883.

[21] H. W. B. Roozeboom, "Sur l'hydrate de l'acide sulfureux" *Rec. Trav. Chim. Pays-Bas.,* vol. 3 pp. 29-58. Cross referenced from:Ripmeester, J. A.; Alavia, S. (2016), https://doi.org/10.1016/j.cossms.2016.03.005, 1884.

[22] L. P. Cailletet and R. Bordet, "Sur divers hydrates qui se forment par la pression et la détente," *Compt. Rend. ,* vol. 95, pp. 58–61, 1882.

[23] P. Villard, "Sur quelques nouveaux hydrates de gaz," *Compt. rend,* vol. 106, pp. 1602-1603, 1888.

[24] J. A. Ripmeester and S. Alavi, "Some current challenges in clathrate hydrate science: Nucleation, decomposition and the memory effect," *Current Opinion in Solid State and Materials Science,* vol. 20, pp. 344-351, 2016/12/01/ 2016.

[25] W. F. Claussen, "Suggested structures of water in inert gas hydrates," *The Journal of Chemical Physics,* vol. 19, pp. 259-260, 1951.

[26] W. F. Claussen, " Erratum: Suggested Structures of Water in Inert Gas Hydrates. ," *The Journal of Chemical Physics,* vol. 19, pp. 662-662, 1951.

[27] W. Claussen, "A second water structure for inert gas hydrates," *The Journal of Chemical Physics,* vol. 19, pp. 1425-1426, 1951.

[28] M. v. Stackelberg and H. R. Muller, "On the structure gas hydrate," *J. Chem. Phys.,* vol. 19, 1951.

[29] H. R. Muller and M. v. Stackelberg, "Zur Struktur de Gashydrate " *Naturwissensch,* vol. 39, 1952.

[30] L. Pauling and R. E. Marsh, "The structure of chlorine hydrate," *Proceedings of the National Academy of Sciences,* vol. 38, pp. 112-118, 1952.

[31] J. H. Van der Waals and J. C. Platteeuw, "Clathrate solutions," *Advances in Chemical Physics,* vol. 2, pp. 1-57, 1959.

[32] R. M. Barrer and W. I. Stuart, "Non-stoicheiometric clathrate compounds of water," in *Proceedings of the Royal Society of London A: Mathematical, Physical and Engineering Sciences,* 1957, pp. 172-189.

[33] J. A. Ripmeester, S. T. John, C. I. Ratcliffe, and B. M. Powell, "A new clathrate hydrate structure," *Nature*, vol. 325, pp. 135-136, 1987.

[34] L. Amundsen and M. Landrø. (2012, Accessed: 03.06.2017). *Gas Hydrates - Part I: Burning Ice*. Available: http://www.geoexpro.com/articles/2012/12/gas-hydrates-part-i-burning-ice

[35] Y. Makogon, "A gas hydrate formation in the gas saturated layers under low temperature," *Gas Industry*, vol. 5, pp. 14-15, 1965.

[36] Y. Makogon, "Les hydrates de gaz: de l'énergie congelée," *La Recherche*, vol. 18, pp. 1192-1200, 1987.

[37] G. D. Ginsburg and V. A. Soloviev, "Submarine gas hydrate estimation: theoretical and empirical approaches," in *InProc. 27th Annual Offshore Technology Conference*, Houston, Texas, 1995.

[38] A. A. Trofimuk, N. V. Cherskii, Y. F. Makogon, and V. P. Tsarev, presented at the 11th ASA Conference on Conventional and Unconventional World Natural Gas Resources, 1980.

[39] T. S. Collett, "Detection and Evaluation of Natural Gas Hydrates from Wall Logs, Prudhoe Bay, Alaska," M. S. Thesis, UniversityTAlaska, Fairbanks, Alaska, 1983.

[40] C. Bily and J. W. L. Dick, *Bull. Can. Petr. Geol.*, vol. 22, 1974.

[41] J. Weaver and J. Stewart, "In situ hydrates under the Beaufort Sea shelf," in *Proceedings, Fourth Canadian Permafrost Conference, March*, 1982, pp. 2-6.

[42] L. Franklin, *In Natural Gas Hydrates: Properties, Occurence and Recovery* vol. 115. Butterworth, Boston, MA 1983.

[43] A. S. Judge, "Natural gas hydrates in Canada," in *Proceedings of the 4th Canadian Permafrost Conference*, 1982, pp. 320-328.

[44] T. S. Collett, "National Assessment of United States Oil and Gas Resources on CD-ROM," USGS Digital Data Series 30, Washington DC 2327-638X, 1995.

[45] G. A. Jeffrey, "Inclusion Compounds, (Atwood, J.L., Davies, J.E.D., MacNichol, D.D., eds.)," vol. 1, ed. London: Academic Press, 1984, p. 135.

[46] J. Brooks, M. Kennicutt, R. Fay, T. McDonald, and R. Sassen, "Thermogenic gas hydrates in the Gulf of Mexico," *Science*, vol. 225, pp. 409-411, 1984.

[47] D. Davidson, S. Garg, S. Gough, Y. Handa, C. Ratcliffe, J. Ripmeester, *et al.*, "Laboratory analysis of a naturally occurring gas hydrate from sediment of the Gulf of Mexico," *Geochimica et Cosmochimica Acta*, vol. 50, pp. 619-623, 1986.

[48] B. Kvamme and A. Sapate, "Hydrate Risk Evaluation during Transport and Processing of Natural Gas Mixtures containing Ethane and Methane," *Research & Reviews: Journal of Chemistry*, vol. 5, 2016.

[49] R. Sassen and I. R. MacDonald, "Evidence of structure H hydrate, Gulf of Mexico continental slope," *Organic Geochemistry*, vol. 22, pp. 1029-1032, 1994.

[50] A. P. Mehta and E. D. Sloan Jr, "Structure H hydrate phase equilibria of methane+ liquid hydrocarbon mixtures," *Journal of Chemical and Engineering Data*, vol. 38, pp. 580-582, 1993.

[51] J. A. Ripmeester and C. I. Ratcliffe, "Inclusion Compounds (Atwood, J. L., Davies, J.E.D., McNichol, D. D., eds.)," ed: Oxford University Press, Oxford, UK, 5, 1991.

[52] M. Maslin, M. Owen, R. Betts, S. Day, T. D. Jones, and A. Ridgwell, "Gas hydrates: past and future geohazard?," *Philosophical Transactions of the Royal Society of London A: Mathematical, Physical and Engineering Sciences*, vol. 368, pp. 2369-2393, 2010.

[53] B. Tohidi. (Accessed: 04.09.2017). *What are Gas Hydrates?* Available: http://www.pet.hw.ac.uk/research/hydrate/hydrates_what.cfm?hy=what

[54] E. D. Sloan, "Fundamental principles and applications of natural gas hydrates," *Nature*, vol. 426, pp. 353-363, 2003.

[55] B. Kvamme and O. K. Førrisdahl, "Polar guest-molecules in natural gas hydrates. Effects of polarity and guest-guest-interactions on the Langmuir-constants," *Fluid phase equilibria*, vol. 83, pp. 427-435, 1993.

[56] B. Kvamme and A. Lund, "The influence of gas-gas interactions on the Langmuir constants for some natural gas hydrates," *Fluid phase equilibria*, vol. 90, pp. 15-44, 1993.

[57] J. M. Bauman, "Kinetic Modelling of Hydrate Formation, Dissociation, and Reformation " Dissertation for the Degree of Philosophiae Doctor (PhD), University of Bergen, Norway, 2015.

[58] B. Kvamme, E. Iden, J. Tveit, V. Veland, M. Zarifi, and K. Qorbani, "Effect of H2S Content on Thermodynamic Stability of Hydrate Formed from CO2/N2 Mixtures," *Journal of Chemical & Engineering Data*, vol. 62, pp. 1645-1658, 2017.

[59] J.-M. Herri, A. Bouchemoua, M. Kwaterski, A. Fezoua, Y. Ouabbas, A. Cameirao, *et al.*, "Gas hydrate equilibria for CO 2-N 2 and CO 2-CH 2 gas mixtures, experiments and modelling," in *7th International Conference on Gas Hydrates (ICGH 2011)*, 2011, p. 435.

[60] E. Sloan Jr, "Hydrate nucleation from ice," in *69th Annual Gas Proceedings Conference, Phoenix, Ariz*, 1990b.

[61] M. Volmer and A. Weber, "Keimbildung in übersättigten Gebilden. Z. Phys. Chem.," vol. 119, 1925.

[62] D. Becker and W. Döring, " The kinetic treatment of nuclear formation in supersaturated vapors. ," *Annalen der Physik.*, vol. 24, pp. 719-52, 1935.

[63] J. A. Frenkel, "A general theory of heterophase fluctuations and pretransition phenomena," *The Journal of Chemical Physics*, vol. 7, pp. 538-547, 1939.

[64] J. B. Zeldovich, "Acta Physicochimica USSR 18, 1 " 1943.

[65] J. W. Mullen, *Crystallization*, 3rd Edition ed. Oxford, U.K.: Butterworth-Heinmann, 1993.

[66] D. Kashchiev and A. Firoozabadi, "Nucleation of gas hydrates," *Journal of crystal growth,* vol. 243, pp. 476-489, 2002.

[67] B. Kvamme, "Kinetics of hydrate formation from nucleation theory," *International Journal of Offshore and Polar Engineering,* vol. 12, 2002.

[68] B. Kvamme, *Initiation and growth of hydrate from nucleation theory* vol. 12, 2002.

[69] B. Kvamme, "Droplets of dry ice and cold liquid CO2 for self-transport of CO2 to large depths," *International Journal of Offshore and Polar Engineering,* vol. 13, 2003.

[70] K. Qorbani, B. Kvamme, and T. Kuznetsova, "Utilizing Non-Equilibrium Thermodynamics and Reactive Transport to Model CH4 Production from the Nankai Trough Gas Hydrate Reservoir," *Energies,* vol. 10, p. 1064, 2017.

[71] K. Qorbani, B. Kvamme, and T. Kuznetsova, "Using a Reactive Transport Simulator to Simulate CH4 Production from Bear Island Basin in the Barents Sea Utilizing the Depressurization Method," *Energies,* vol. 10, p. 187, 2017.

[72] B. Kvamme, T. Kuznetsova, P.-H. Kivelæ, and J. Bauman, "Can hydrate form in carbon dioxide from dissolved water?," *Physical Chemistry Chemical Physics,* vol. 15, pp. 2063-2074, 2013.

[73] Z.-M. Xia, X.-S. Li, Z.-Y. Chen, Q.-N. Lv, C.-G. Xu, and C. Chen, "Hydrate-based Capture CO2 and Purification CH4 from Simulated Landfill Gas with Synergic Additives Based on Gas Solvent," *Energy Procedia,* vol. 61, pp. 450-454, 2014.

[74] V. Belandria, "Hydrate Phase Equilibria Study of CO2 Containing Gases in Thermodynamic Promoter Aqueous Mixtures," Ecole Nationale Supérieure des Mines de Paris, 2012.

[75] H. Dashti, L. Z. Yew, and X. Lou, "Recent advances in gas hydrate-based CO 2 capture," *Journal of Natural Gas Science and Engineering,* vol. 23, pp. 195-207, 2015.

[76] C.-G. Xu and X.-S. Li, "Research progress of hydrate-based CO 2 separation and capture from gas mixtures," *RSC Advances,* vol. 4, pp. 18301-18316, 2014.

[77] T. Buanes, "Mean-field approaches applied to hydrate phase transition kinetics," PhD thesis, University of Bergen, Norway, 2008.

[78] B. Kvamme, M. Austrheim, A. Knarvik, and M. Zarifi, "Hydrate Formation During Transport of Natural Gas Containing Water And Impurities," *International Journal of Engineering Research and Development,* vol. 13, pp. .01-16, 2017.

[79] J. P. Long, "Gas hydrate formation mechanism and kinetic inhibition," PhD Thesis, Colerado School of Mines, 1994.

[80] B. Kvamme, "A New Theory for the Kinetics of Hydrate Formation," in *Proc. 2nd Int Conf Natural Gas Hydrates,* Toulouse, France, 1996, pp. 131–146.

[81] B. Kvamme and H. Tanaka, "Thermodynamic stability of hydrates for ethane, ethylene, and carbon dioxide," *The Journal of Physical Chemistry,* vol. 99, pp. 7114-7119, 1995.

[82] B. Kvamme, "Kinetics of Hydrate Formation on Unstirred Water Surfaces from Classical Nucleation Theory,," presented at the 13th Int. Symp. Thermophy Properties, Boulder, Colorado, USA., 1997.

[83] G. Song and R. Kobayashi, "NMR studies of hydrate formation," presented at the Submitted for presentation on the sixth International Offshore and Polar Engineering Conference, Honolulu, Hawaii, 1996.

[84] R. Kobayashi, "Rice University, Houston, US, private communication with Prof. Bjørn Kvamme of University of Bergen," ed, 1997.

[85] Y. F. Makogon, *Hydrates of Hydrocarbons*: PennWell Books, 1997.

[86] E. Sloan and F. Fleyfel, "A molecular mechanism for gas hydrate nucleation from ice," *AIChE Journal*, vol. 37, pp. 1281-1292, 1991.

[87] S. Davies. (Accessed: 20.03.2017). Nucleation Theory: A Literature Review and Applications to Nucleation Rates of Natural Gas Hydrates. Available: http://inside.mines.edu/~dwu/classes/chen610/projects/Davies%20Summary%20Report.pdf

[88] C. Koh, R. Westacott, W. Zhang, K. Hirachand, J. Creek, and A. Soper, "Mechanisms of gas hydrate formation and inhibition," *Fluid Phase Equilibria*, vol. 194, pp. 143-151, 2002.

[89] R. Radhakrishnan and B. L. Trout, "A new approach for studying nucleation phenomena using molecular simulations: application to CO 2 hydrate clathrates," *The Journal of chemical physics*, vol. 117, pp. 1786-1796, 2002.

[90] R. L. Christiansen and E. D. Sloan, "Mechanisms and kinetics of hydrate formation," *Annals of the New York Academy of Sciences*, vol. 715, pp. 283-305, 1994.

[91] P. Skovborg, "Gas Hydrate Kinetics," PhD Dissertation, Inst. for Chem Eng, Danmarks Tekniske Højskole, Lyngby, Denmark, 1993.

[92] V. Natarajan, "Thermodynamics and nucleation of gas hydrates,," PhD, University of Calgary, Alberta, 1993.

[93] M. Yousif, "The kinetics of hydrate formation," in *SPE Annual Technical Conference and Exhibition*, 1994.

[94] P. Englezos, N. Kalogerakis, P. Dholabhai, and P. Bishnoi, "Kinetics of gas hydrate formation from mixtures of methane and ethane," *Chemical Engineering Science*, vol. 42, pp. 2659-2666, 1987.

[95] P. Englezos and P. Bishnoi, "Gibbs free energy analysis for the supersaturation limits of methane in liquid water and the hydrate-gas-liquid water phase behavior," *Fluid Phase Equilibria*, vol. 42, pp. 129-140, 1988.

[96] P. Skovborg and P. Rasmussen, "A mass transport limited model for the growth of methane and ethane gas hydrates," *Chemical Engineering Science*, vol. 49, pp. 1131-1143, 1994.

[97] B. Kvamme, "Kinetics of Hydrate Formation," in *Proc. 5th Asian Thermophys. Properties Conf.*, Seoul, 1998, p. 95.

[98] B. Kvamme, "Initiation and Growth of Hydrate," presented at the 3rd Int. Conf. Natural Gas Hydrates, Park City, Utah, USA, 2000a.

[99] W. L. Jorgensen, J. Chandrasekhar, J. D. Madura, R. W. Impey, and M. L. Klein, "Comparison of simple potential functions for simulating liquid water," *The Journal of chemical physics*, vol. 79, pp. 926-935, 1983.

[100] J. Tse, B. Powell, V. Sears, and Y. Handa, "The lattice dynamics of clathrate hydrates. An incoherent inelastic neutron scattering study," *Chemical physics letters*, vol. 215, pp. 383-387, 1993.

[101] A. Svandal, "Modeling hydrate phase transitions using mean-field approaches," Degree philosophiae doctor (PhD), University of Bergen, 2006.

[102] A. Haymet and T. Barlow, "Nucleation of Supercooled Liquids," *Annals of the New York Academy of Sciences*, vol. 715, pp. 549-551. Cross referenced from Almenningen, S. (2015). An Experimental Study of Methane Hydrates in Sandstone Cores, MSc Thesis, University of Bergen., 2006.

[103] E. D. Sloan, *Clathrate Hydrates of Natural Gases*, 2nd ed.: New York: Marcel Dekker, Inc., 1998.

[104] B. Kvamme, "Feasibility of simultaneous CO2 storage and CH4 production from natural gas hydrate using mixtures of CO2 and N2," *Canadian Journal of Chemistry*, vol. 93, pp. 897-905, 2015.

[105] B. Kvamme, "Thermodynamic limitations of the CO2/N2 mixture injected into CH4 hydrate in the Ignik Sikumi field trial," *Journal of Chemical & Engineering Data*, vol. 61, pp. 1280-1295, 2016.

[106] J. W. Gibbs, "On the Equilibrium of Heterogeneous Substances," *Scientific Papers, Dover, New York*, 1961.

[107] J. Gibbs, "The Collected Works of J. Willard Gibbs, Thermodynamics, vol. 1, 55–349," ed: Longmans, Green and Co., New York, 1928.

[108] B. Kvamme, T. Kuznetsova, B. Jensen, S. Stensholt, J. Bauman, S. Sjøblom, *et al.*, "Consequences of CO2 solubility for hydrate formation from carbon dioxide containing water and other impurities," *Physical Chemistry Chemical Physics*, vol. 16, pp. 8623-8638, 2014.

[109] B. Kvamme, "Oil and Gas Processing, Unpublished Work: PTEK 231, Course Material, Autumn Semester 2016, Department of Physics and Technology, University of Bergen, Norway," ed, 2016.

[110] A. Vysniauskas and P. Bishnoi, "A kinetic study of methane hydrate formation," *Chemical Engineering Science*, vol. 38, pp. 1061-1072, 1983.

[111] V. Natarajan, P. Bishnoi, and N. Kalogerakis, "Induction phenomena in gas hydrate nucleation," *Chemical Engineering Science*, vol. 49, pp. 2075-2087, 1994.

[112] R. L. Christiansen and E. D. Sloan Jr, "A compact model for hydrate formation," San Antonio, TX (United States), 1995.

[113] D. Kashchiev and A. Firoozabadi, "Driving force for crystallization of gas hydrates," *Journal of crystal growth*, vol. 241, pp. 220-230, 2002.

[114] M. R. Anklam and A. Firoozabadi, "Driving force and composition for multicomponent gas hydrate nucleation from supersaturated aqueous solutions," *J. Chem. Phys.* , vol. 121, 2004.

[115] M. Arjmandi, B. Tohidi, A. Danesh, and A. C. Todd, "Is subcooling the right driving force for testing low-dosage hydrate inhibitors?," *Chemical engineering science*, vol. 60, pp. 1313-1321, 2005a.

[116] K. Jemai, B. Kvamme, and M. T. Vafaei, "Theoretical studies of CO2 hydrates formation and dissociation in cold aquifers using RetrasoCodeBright simulator," *Reactive transport modelling of hydrate phase transition dynamics in porous media*, 2014.

[117] A. Rojey, C. Jaffret, S. Cornot-Gandolphe, B. Durand, S. Jullian, and M. Valais, "Natural Gas Production," *Processing, Transport, Editions Technip, Paris, France*, 1997.

[118] R. N. Maddox, *Gas Conditioning and Processing; V. 4: Gas and Liquid Sweetening*: Campbell Petroleum Series, 1982.

[119] M. Chabrelie, -F., "European Natural Gas Trading by pipelines," ed. Rueil-Malmaison, FRA, June 186p.: Centre International d'Informationsur le Gaz Naturel et tous les Hydrocabures Gazeux (Cedigaz), 1993.

[120] S. Cornot-Gandolphe and M. chabrelie, -F., "European Natural Gas Trading by pipelines," ed. Rueil-Malmaison, FRA, June 140p.: Center International d'Informationsur le Gaz Naturel et tous les Hydrocabures Gazeux (Cedigaz), 1995.

[121] B. Kvamme, T. Kuznetsova, and P.-H. Kivelæ, "Adsorption of water and carbon dioxide on hematite and consequences for possible hydrate formation," *Physical Chemistry Chemical Physics*, vol. 14, pp. 4410-4424, 2012.

[122] N. H. de Leeuw and T. G. Cooper, "Surface simulation studies of the hydration of white rust Fe (OH) 2, goethite α-FeO (OH) and hematite α-Fe 2 O 3," *Geochimica et Cosmochimica Acta*, vol. 71, pp. 1655-1673, 2007.

[123] S. Tsuzuki, T. Uchimaru, K. Tanabe, S. Kuwajima, N. Tajima, and T. Hirano, "Refinement of nonbonding interaction parameters for carbon dioxide on the basis of the pair potentials obtained by MP2/6-311+ G (2df)-level ab initio molecular orbital calculations," *The Journal of Physical Chemistry*, vol. 100, pp. 4400-4407, 1996.

[124] B. Kvamme, T. Kuznetsova, B. Jensen, and S. Sjoblom, "Routes to hydrate formation during transport of carbon dioxide containing water and impurities," in *In Proceedings of the 8th International Conference on Gas Hydrates (ICGH8-2104)*, Beijing, China, 2014.

[125] B. Kvamme, T. Kuznetsova, and K. Aasoldsen, "Molecular dynamics simulations for selection of kinetic hydrate inhibitors," *Journal of Molecular Graphics and Modelling*, vol. 23, pp. 524-536, 2005.

[126] O. K. Forrisdahl, "Methane clathrate hydrates: melting, supercooling and phase separation from molecular dynamics computer simulations," *Molecular Physics*, vol. 89, pp. 819-834, 1996.

[127] J. S. Tse, M. L. Klein, and I. R. McDonald, "Molecular dynamics studies of ice Ic and the structure I clathrate hydrate of methane," *The Journal of Physical Chemistry*, vol. 87, pp. 4198-4203, 1983.

[128] B. Kvamme, A. Graue, E. Aspenes, T. Kuznetsova, L. Gránásy, G. Tóth, *et al.*, "Kinetics of solid hydrate formation by carbon dioxide: Phase field theory of hydrate nucleation and magnetic resonance imaging," *Physical chemistry chemical physics*, vol. 6, pp. 2327-2334, 2004.

[129] G. Tegze, T. Pusztai, G. Tóth, L. Gránásy, A. Svandal, T. Buanes, *et al.*, "Multiscale approach to CO 2 hydrate formation in aqueous solution: Phase field theory and molecular dynamics. Nucleation and growth," *The Journal of chemical physics*, vol. 124, p. 234710, 2006.

[130] Statoil. (Accessed: 20.12.2016). Available: https://www.statoil.com

[131] H. K. Ebbrell, "The composition of Statoil (Norway) gas well," 1984.

[132] N. Petroleum. (Accessed: 04.05.2017). *Sleipner Vest*. Available: http://www.norskpetroleum.no/en/facts/field/sleipner-vest/

[133] Statoil. (Accessed: 07.05.2017). *Sleipner area*. Available: https://www.statoil.com/en/what-we-do/norwegian-continental-shelf-platforms/sleipner.html

[134] N. G. Infrastructure. (12.05.2017). *Gassled*. Available: http://njordgasinfra.no/gassled/

[135] J. S. Gudmundsson, "Title," unpublished|.

[136] Wikipedia. (Accessed: 04.06.2017). *Gibbs free energy*. Available: https://en.wikipedia.org/wiki/Gibbs_free_energy

[137] J. W. Gibbs, "A Method of Geometrical Representation of the Thermodynamic Properties of Substances by Means of Surfaces," *Transactions of the Connecticut Academy of Arts and Sciences* vol. 2, pp. 382-404, 1873.

[138] G. Soave, "Equilibrium constants from a modified Redlich-Kwong equation of state," *Chem. Eng. Sci.* , vol. 27, p. 1197−1203, 1972.

[139] B. Kvamme, M. Qasim, K. Baig, P.-H. Kivelä, and J. Bauman, "Hydrate phase transition kinetics from Phase Field Theory with implicit hydrodynamics and heat transport," *International Journal of Greenhouse Gas Control*, vol. 29, pp. 263-278, 2014.

[140] B. Chazallon, A. Klapproth, and F. Pauer, "Filling-isotherms in clathrate-hydrates," *The Review of High Pressure Science and Technology,* vol. 7, pp. 1147-1149, 1998.

[141] S. Adisasmito, R. J. Frank III, and E. D. Sloan Jr, "Hydrates of carbon dioxide and methane mixtures," *Journal of Chemical and Engineering Data,* vol. 36, pp. 68-71, 1991.

[142] T. Maekawa, "Equilibrium conditions for gas hydrates of methane and ethane mixtures in pure water and sodium chloride solution," *GEOCHEMICAL JOURNAL,* vol. 35, pp. 59-66, 2001.

[143] E. A. Smelik and H. King, "Crystal-growth studies of natural gas clathrate hydrates using a pressurized optical cell," *American Mineralogist,* vol. 82, pp. 88-98, 1997.

[144] W. Deaton and E. Frost Jr, "Gas hydrates and their relation to the operation of natural-gas pipe lines," Bureau of Mines, Amarillo, TX (USA). Helium Research Center1946.

[145] T. Svartas and F. Fadnes, "Methane hydrate equilibrium data for the methane-water-methanol system up to 500 bara," in *The Second International Offshore and Polar Engineering Conference*, 1992.

[146] V. K. Verma, *Gas hydrates from liquid hydrocarbon-water systems*, 1974.

[147] J. L. Thakore and G. D. Holder, "Solid vapor azeotropes in hydrate-forming systems," *Industrial & Engineering Chemistry Research,* vol. 26, pp. 462-469, 1987.

[148] T. Nakamura, T. Makino, T. Sugahara, and K. Ohgaki, "Stability boundaries of gas hydrates helped by methane—structure-H hydrates of methylcyclohexane and cis-1, 2-dimethylcyclohexane," *Chemical engineering science,* vol. 58, pp. 269-273, 2003.

[149] J. Jhaveri and D. B. Robinson, "Hydrates in the methane-nitrogen system," *The Canadian Journal of Chemical Engineering,* vol. 43, pp. 75-78, 1965.

[150] G. Holder and G. Grigoriou, "Hydrate dissociation pressures of (methane+ ethane+ water) existence of a locus of minimum pressures," *The Journal of Chemical Thermodynamics,* vol. 12, pp. 1093-1104, 1980.

[151] G. Holder and J. Hand, "Multiple-phase equilibria in hydrates from methane, ethane, propane and water mixtures," *AIChE Journal,* vol. 28, pp. 440-447, 1982.

[152] P. Englezos and P. Bishnoi, "Experimental study on the equilibrium ethane hydrate formation conditions in aqueous electrolyte solutions," *Industrial & Engineering Chemistry Research,* vol. 30, pp. 1655-1659, 1991.

[153] O. L. Roberts, E. R. Brownscombe, and L. S. Howe, *Oil Gas Journal,* vol. 39, 1940.

[154] D. Avlonitis, "Multiphase equilibria in oil-water hydrate forming systems M. Sc," Thesis, 1988: Heriot-Watt University, Edinburgh, 1988.

[155] H. Reamer, F. Selleck, and B. Sage, "Some properties of mixed paraffinic and olefinic hydrates," *Journal of Petroleum Technology*, vol. 4, pp. 197-202, 1952.

[156] D. Robinson and B. Metha, "Hydrates in the propanecarbon dioxide-water system," *Journal of Canadian Petroleum Technology,* vol. 10, 1971.

[157] H. Kubota, K. Shimizu, Y. Tanaka, and T. MakIta, "Thermodynamic properties of R13 (CCIF3), R23 (CHF3), R152a (C2H4F2), and propane hydrates for desalination of sea water," *Journal of chemical engineering of Japan,* vol. 17, pp. 423-429, 1984.

[158] B. Miller and E. Strong, "Hydrate storage of natural gas," *American Gas Association Monthly,* vol. 28, pp. 63-67, 1946.

[159] G. R. Schneider and J. Farrar, "OSW R and D Progress Report No. 292, Rocketdyne," 1968.

[160] O. S. Rouher and A. J. Barduhn, "Hydrates of iso-and normal butane and their mixtures," *Desalination,* vol. 6, pp. 57-73, 1969.

[161] B.-J. Wu, D. B. Robinson, and H.-J. Ng, "Three- and four-phase hydrate forming conditions in methane + isobutane + water," *The Journal of Chemical Thermodynamics,* vol. 8, pp. 461-469, 1976/05/01/ 1976.

[162] V. Verma, J. Hand, and D. Katz, "Gas hydrates from liquid hydrocarbons (methane-propane-water system)," in *GVC/AIChE Joint Meeting,* 1975.

[163] V. John, K. Papadopoulos, and G. Holder, "A generalized model for predicting equilibrium conditions for gas hydrates," *AIChE Journal,* vol. 31, pp. 252-259, 1985.

[164] P. Dharmawardhana, W. Parrish, and E. Sloan, "Experimental thermodynamic parameters for the prediction of natural gas hydrate dissociation conditions," *Industrial & Engineering Chemistry Fundamentals,* vol. 19, pp. 410-414, 1980.

[165] S. Adisasmito and E. D. Sloan Jr, "Hydrates of hydrocarbon gases containing carbon dioxide," *Journal of Chemical and Engineering Data,* vol. 37, pp. 343-349, 1992.

[166] C. H. Unruh and D. L. Katz, "Gas hydrates of carbon dioxide-methane mixtures," *Journal of Petroleum Technology,* vol. 1, pp. 83-86, 1949.

[167] K. Ohgaki, Y. Makihara, and K. Takano, "Formation of CO2 Hydrate in Pure and Sea Waters," *Journal of Chemical Engineering of Japan,* vol. 26, pp. 558-564, 1993.

[168] S. D. Larson, *Phase Studies of the Two-component Carbon Dioxide-water System: Involving the Carbon Dioxide Hydrate*: University of Illinois, 1955.

[169] J. Vlahakis, H. Chen, M. Suwandi, and A. Barduhn, "The growth rate of ice crystals: Properties of carbon dioxide hydrate, a review of properties of 51 gas hydrates, Syracuse U," *Research and Development Report,* vol. 830, 1972.

[170] C. H. Unruh and D. L. Katz, "Gas hydrates of carbon dioxide-methane mixtures," *Journal of Petroleum Technology,* vol. 1, pp. 83-86, 1949.

[171] F. Selleck, L. Carmichael, and B. Sage, "Phase behavior in the hydrogen sulfide-water system," *Industrial & Engineering Chemistry,* vol. 44, pp. 2219-2226, 1952.

[172] D. C. Bond and N. B. Russell, "Effect of Antifreeze Agents on the Formation of Hydrogen Sulphide Hydrate," 1949/12/1/.

[173] A. H. Mohammadi and D. Richon, "Phase equilibria of semi-clathrate hydrates of tetra-n-butylammonium bromide+ hydrogen sulfide and tetra-n-butylammonium bromide+ methane," *Journal of Chemical & Engineering Data*, vol. 55, pp. 982-984, 2009.

[174] Z. T. Ward, C. E. Deering, R. A. Marriott, A. K. Sum, E. D. Sloan, and C. A. Koh, "Phase Equilibrium Data and Model Comparisons for H2S Hydrates," *Journal of Chemical & Engineering Data*, vol. 60, pp. 403-408, 2015/02/12 2015.

[175] J. Schroeter, R. Kobayashi, and M. Hildebrand, "Hydrate decomposition conditions in the system hydrogen sulfide-methane-propane," *Industrial & engineering chemistry fundamentals*, vol. 22, pp. 361-364, 1983.

[176] Z. T. Ward, R. A. Marriott, A. K. Sum, E. D. Sloan, and C. A. Koh, "Equilibrium Data of Gas Hydrates containing Methane, Propane, and Hydrogen Sulfide," *Journal of Chemical & Engineering Data*, vol. 60, pp. 424-428, 2015/02/12 2015.

[177] O. A. Nafdy and S. Nesic, "Iron Carbonate Scale Formation and CO_2 Corrosion in The Presence of Acetic Acid," *Corrosion* 2005.

[178] A. A. Kulkarni, "New hydrate risk evaluation for processing and transport of natural gas containing water and impurities," Master of Science Thesis, Department of Physics and Technology, The University of Bergen, Bergen, 2014.

Appendix

A1. Maximum content of water that can be permitted in Troll gas wellhead stream (without H_2S and CO_2) during processing and pipeline transport

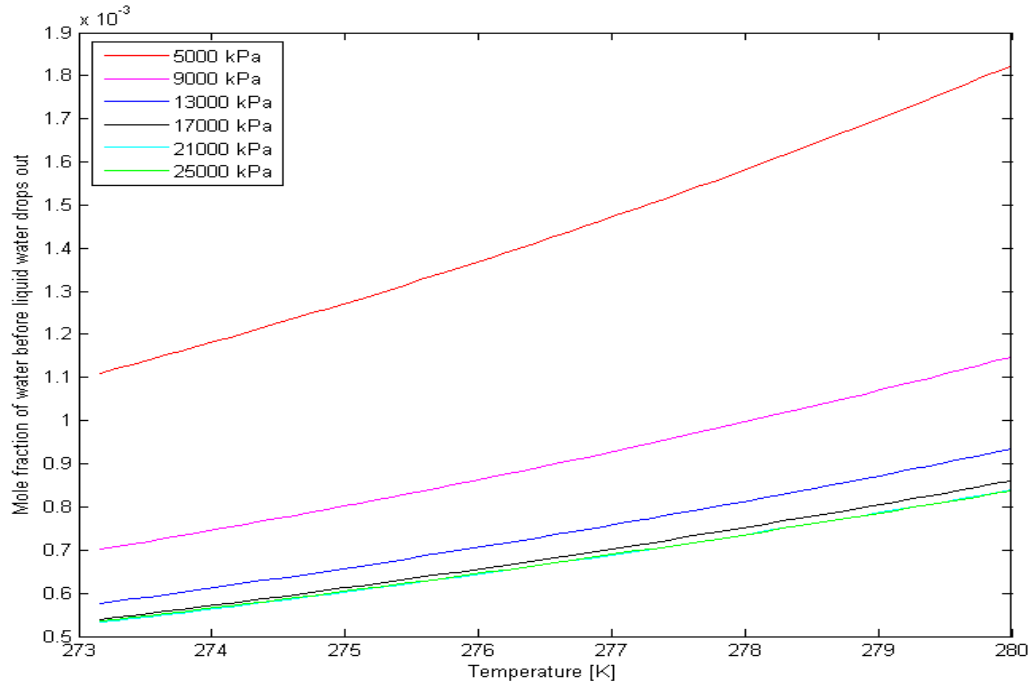

Figure 0.1: Maximum water content that can be permitted in Troll gas before liquid water drops out (without H_2S and CO_2).

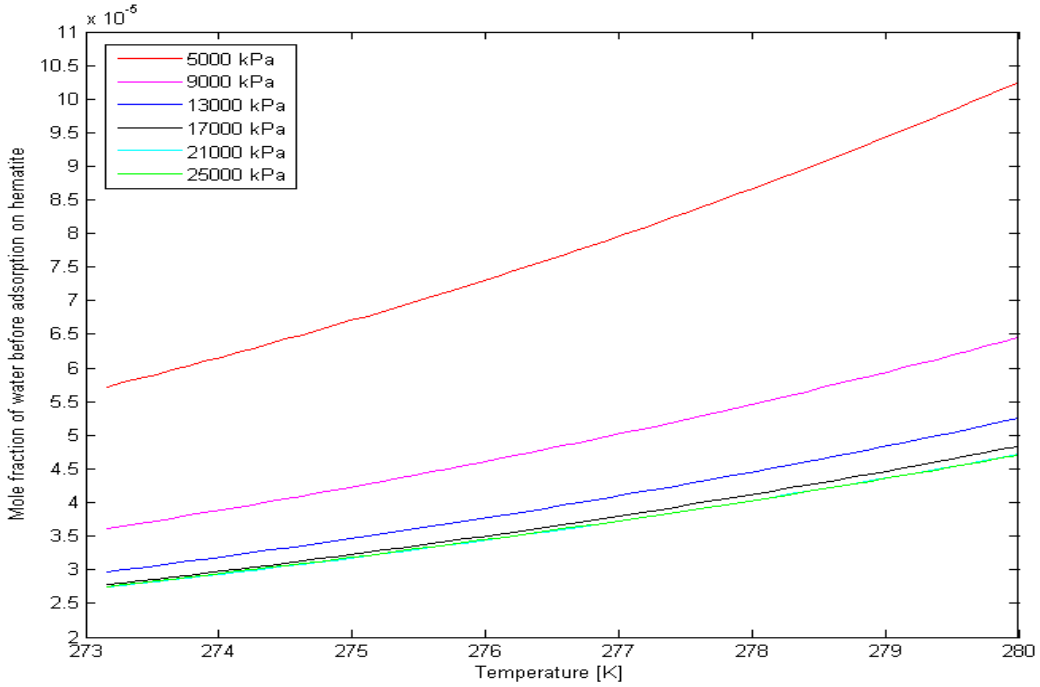

Figure 0.2: Maximum content of water that can be permitted in Troll gas before water can be absorbed on hematite (without H_2S and CO_2).

A2. Impact of the presence of H_2S on the maximum content of water that can be permitted in hydrocarbon gas stream during processing and pipeline transport

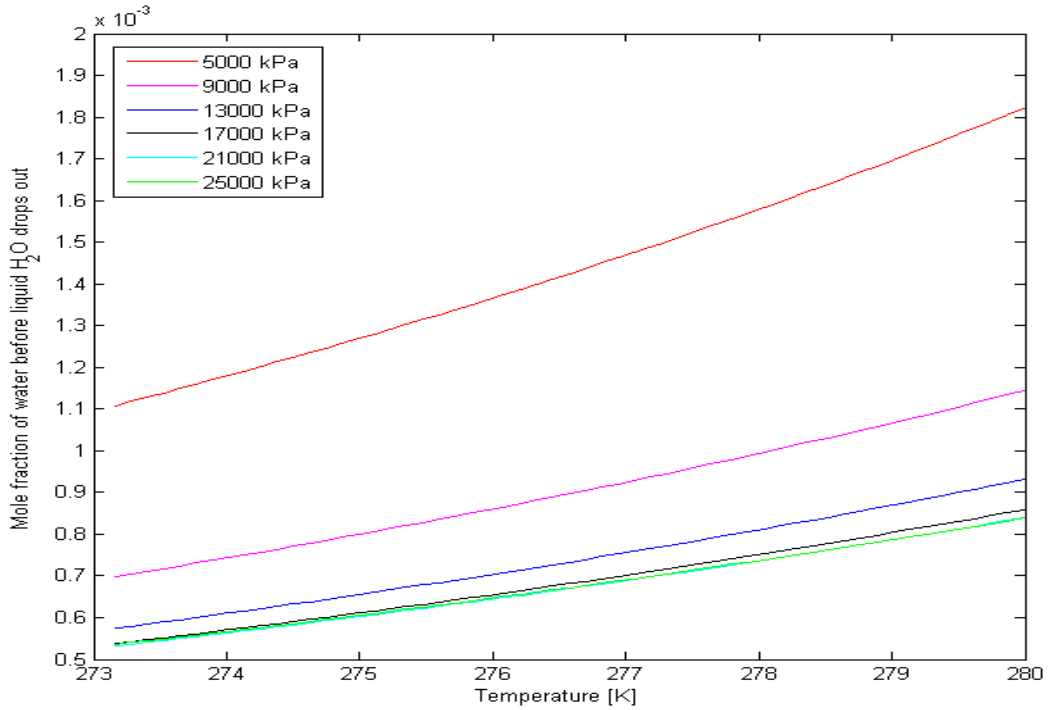

Figure 0.3*: Maximum water content that can be permitted in Troll gas before liquid water drops out if 0.01 H_2S is present*

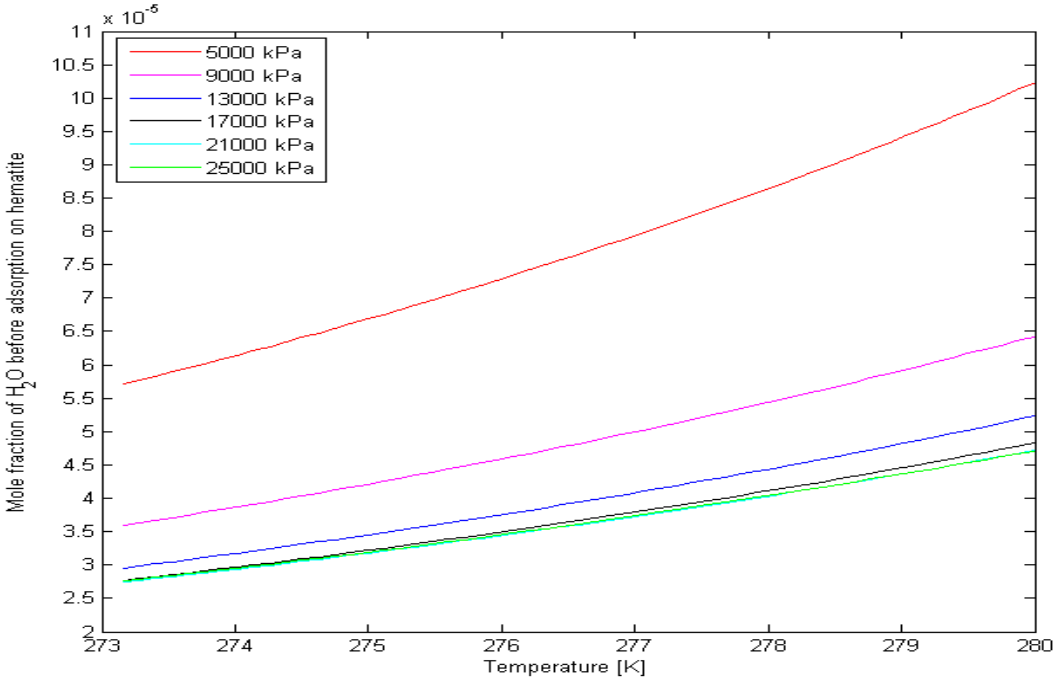

Figure 0.4: Maximum content of water that can be permitted in Troll gas before water can be absorbed on hematite if 0.01 H_2S is present

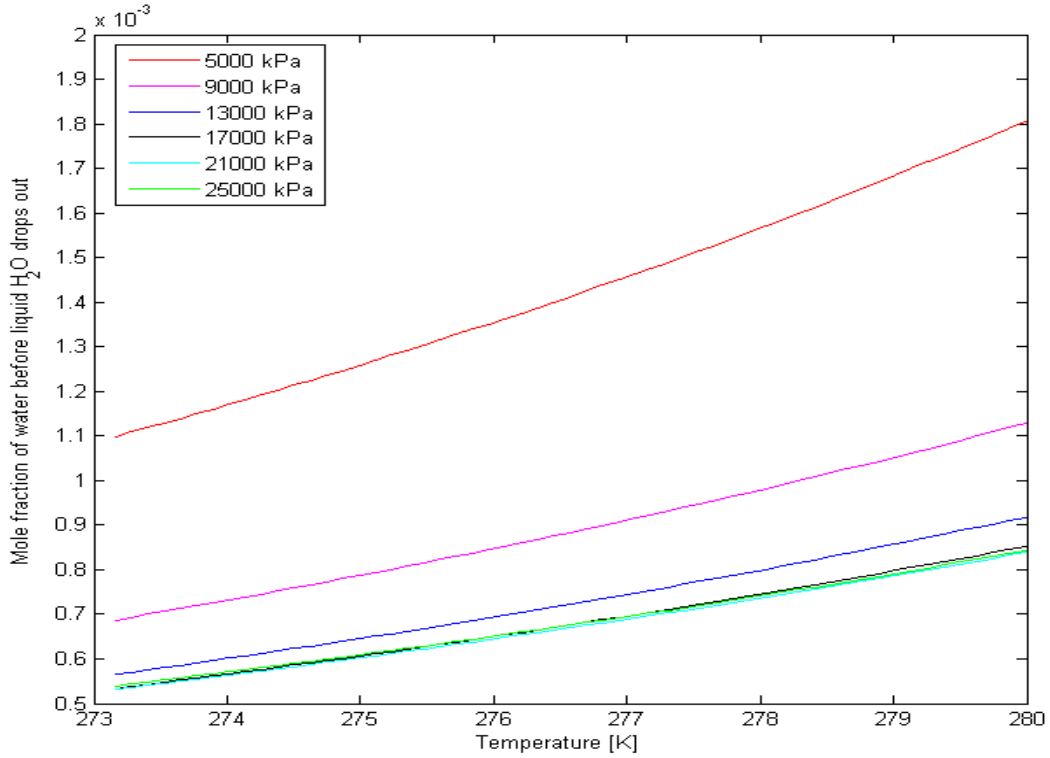

Figure 0.5: Maximum water content that can be permitted in Troll gas before liquid water drops out if 0.05 H_2S is present

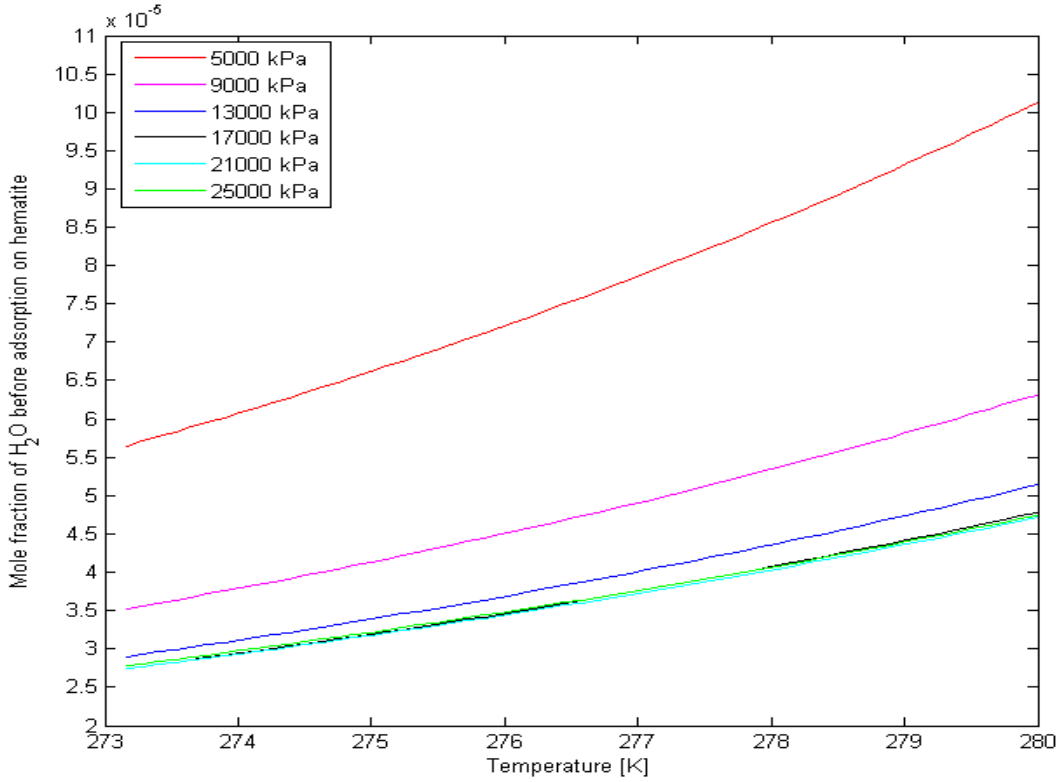

Figure 0.6*: Maximum content of water that can be permitted in Troll gas before water can be absorbed on hematite if 0.05 H_2S is present*

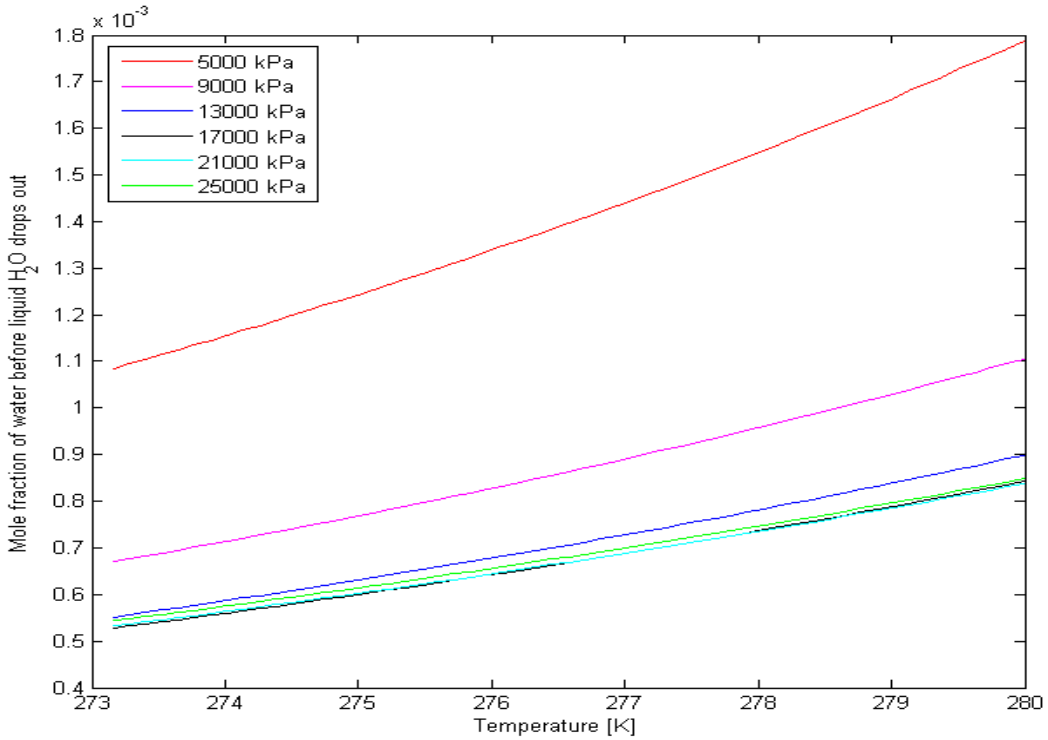

Figure 0.7: Maximum water content that can be permitted in Troll gas before liquid water drops out if 0.1 H_2S is present

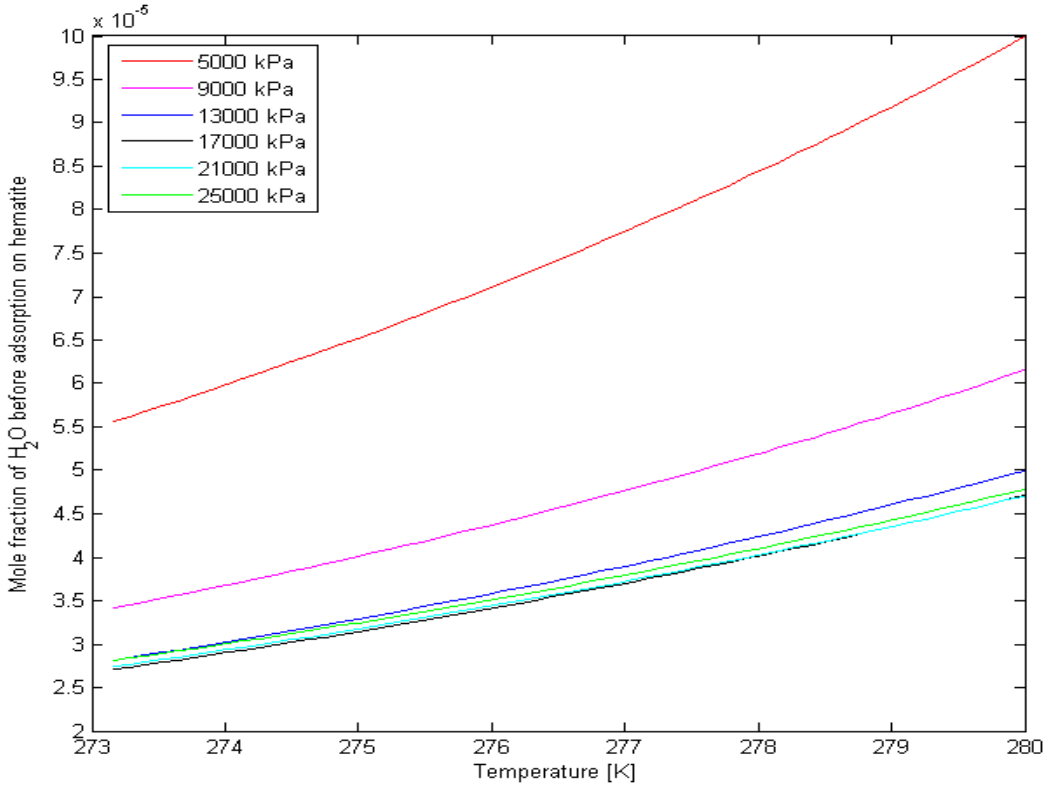

Figure 0.8: Maximum content of water that can be permitted in Troll gas before water can be absorbed on hematite if 0. 1 H_2S is present

A3. Impact of the presence of CO_2 on the maximum content of water that can be permitted in hydrocarbon gas stream during processing and pipeline transport

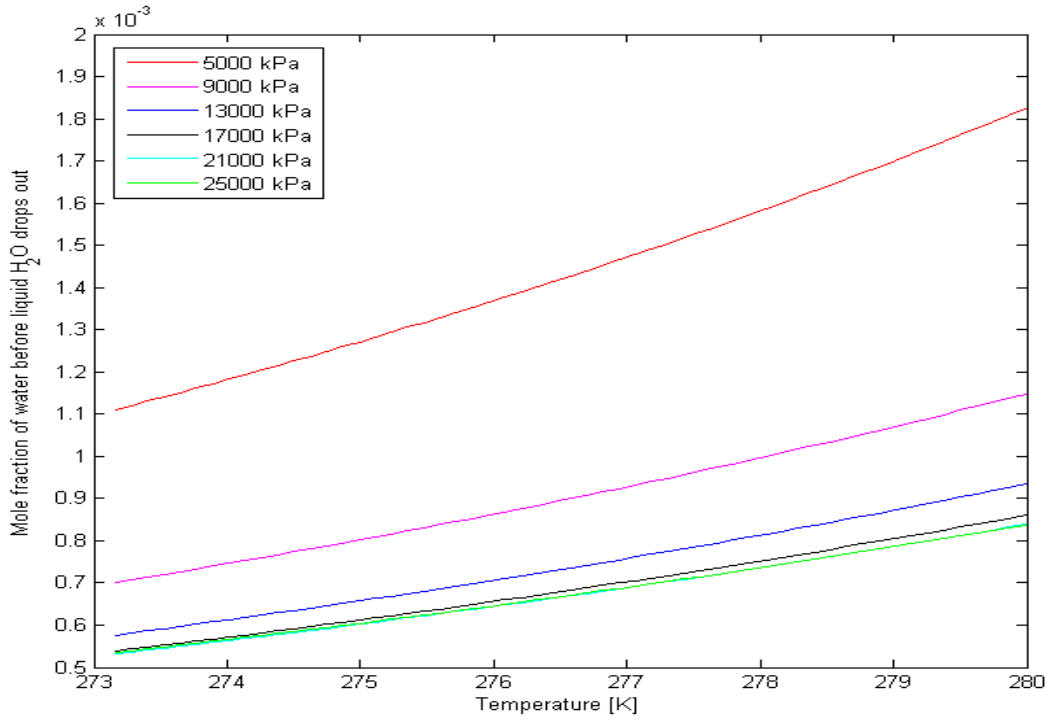

Figure 0.9: Maximum water content that can be permitted in Troll gas before liquid water drops out if 0.01 CO_2 is present

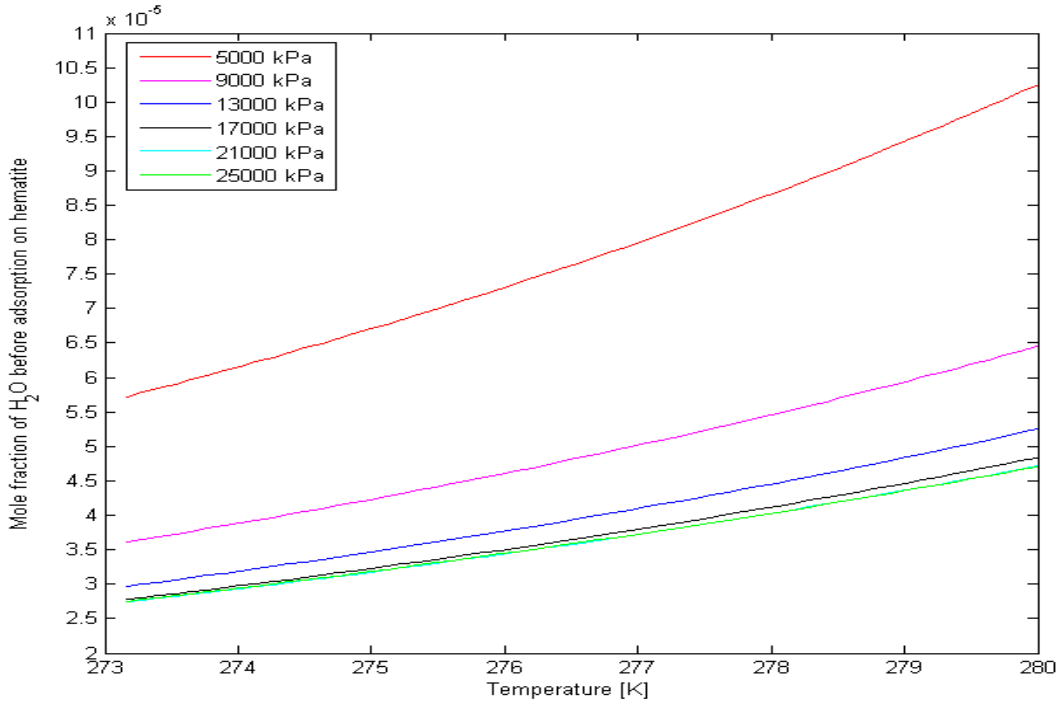

Figure 0.10: Maximum content of water that can be permitted in Troll gas before water can be absorbed on hematite if 0.01 CO_2 is present

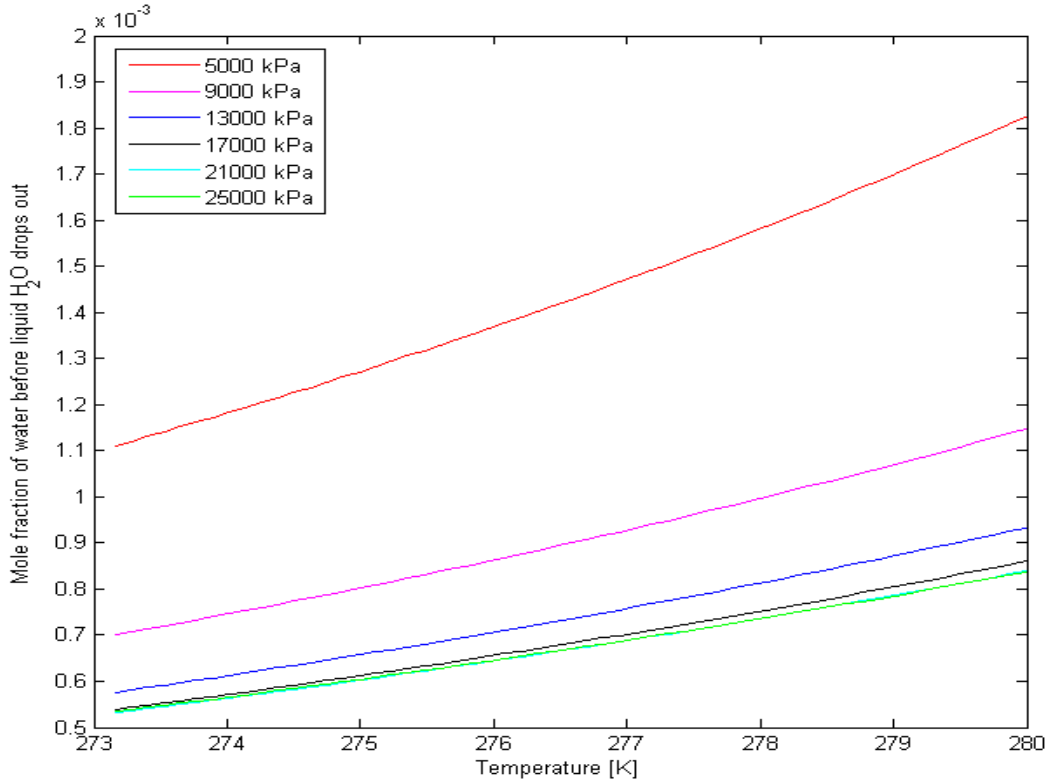

Figure 0.11: Maximum water content that can be permitted in Troll gas before liquid water drops out if 0.05 CO_2 is present

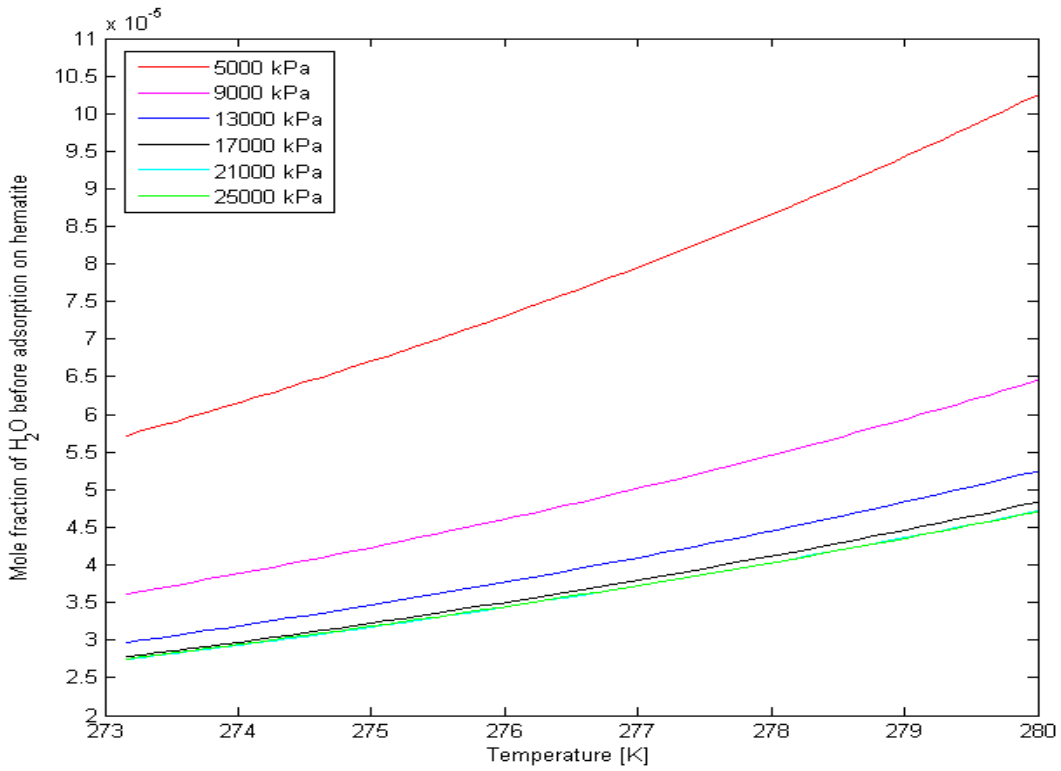

Figure 0.12: Maximum content of water that can be permitted in Troll gas before water can be absorbed on hematite if 0.05 CO_2 is present

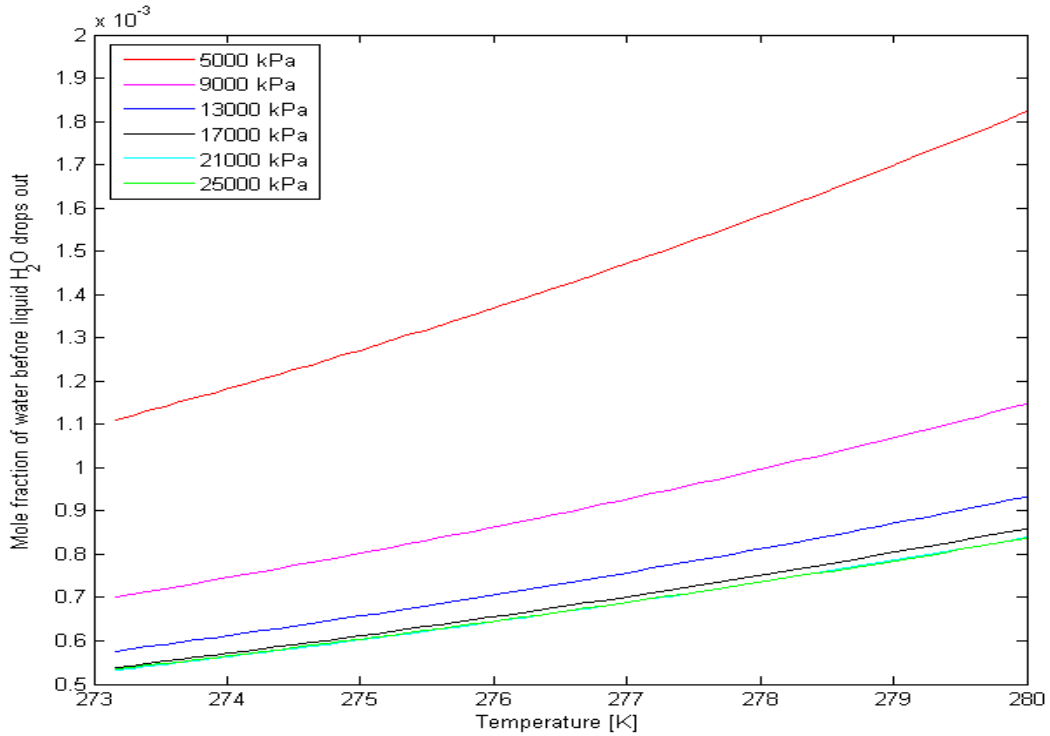

Figure 0.13*: Maximum water content that can be permitted in Troll gas before liquid water drops out if 0.1 CO_2 is present*

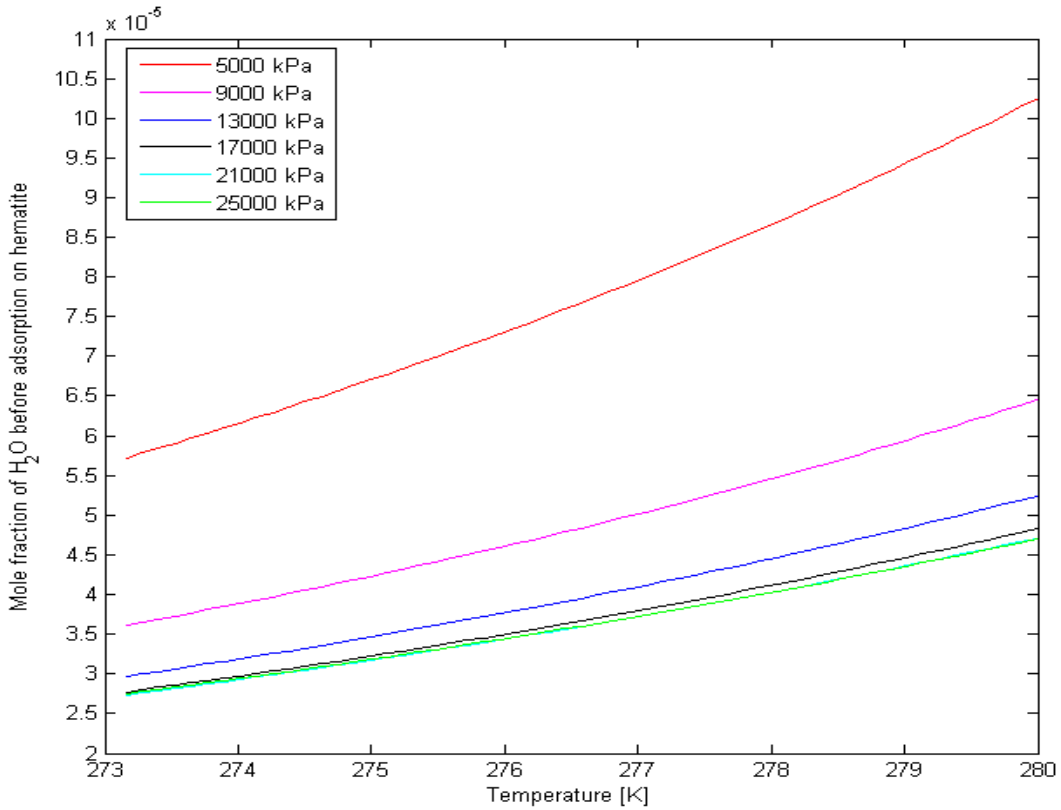

Figure 0.14: Maximum content of water that can be permitted in Troll gas before water can be absorbed on hematite if 0.1 CO_2 is present

A4. Comparison of the impacts of H_2S and CO_2 on the maximum content of water that can be permitted in hydrocarbon gas stream during processing and pipeline transport

Table 0.1: Maximum content of water that can be permitted in Troll gas before water to avoid the risk of hydrate formation if 0.01 H_2S or 0.01 CO_2 are present

Temperature [K]	Pressure [kPa]	Troll gas		Troll gas with 0.01 H_2S		Troll gas with 0.01 CO_2	
		Dew-point	Hematite	Dew-point	Hematite	Dew-point	Hematite
274	5000	0.001194	0.000062	0.001181	0.000061	0.001183	0.000062
	9000	0.000753	0.000039	0.000744	0.000039	0.000747	0.000039
	13000	0.000618	0.000032	0.000611	0.000032	0.000613	0.000032
	17000	0.000577	0.000030	0.000571	0.000030	0.000572	0.000030
	21000	0.000568	0.000030	0.000564	0.000029	0.000564	0.000029
	25000	0.000571	0.000030	0.000567	0.000030	0.000566	0.000029
280	5000	0.001822	0.000102	0.001819	0.000102	0.001822	0.000102
	9000	0.001148	0.000065	0.001144	0.000064	0.001148	0.000064
	13000	0.000934	0.000052	0.000931	0.000052	0.000934	0.000052
	17000	0.000860	0.000048	0.000859	0.000048	0.000860	0.000048
	21000	0.000839	0.000047	0.000839	0.000047	0.000839	0.000047
	25000	0.000837	0.000047	0.000838	0.000047	0.000837	0.000047

Table 0.2: Maximum content of water that can be permitted in Troll gas before water to avoid the risk of hydrate formation if 0.05 H_2S and 0.05 CO_2 are present

Temperature [K]	Pressure [kPa]	Troll gas		Troll gas with 0.05 H_2S		Troll gas with 0.05 CO_2	
		Dew-point	Hematite	Dew-point	Hematite	Dew-point	Hematite
274	5000	0.001194	0.000062	0.001171	0.000061	0.001183	0.000062
	9000	0.000753	0.000039	0.000732	0.000038	0.000747	0.000039
	13000	0.000618	0.000032	0.000601	0.000031	0.000613	0.000032
	17000	0.000577	0.000030	0.000567	0.000029	0.000572	0.000030
	21000	0.000568	0.000030	0.000564	0.000029	0.000563	0.000029
	25000	0.000571	0.000030	0.000571	0.000030	0.000566	0.000029
280	5000	0.001822	0.000102	0.001806	0.000101	0.001822	0.000102
	9000	0.001148	0.000065	0.001128	0.000063	0.001147	0.000064
	13000	0.000934	0.000052	0.000918	0.000051	0.000933	0.000052
	17000	0.000860	0.000048	0.000852	0.000048	0.000860	0.000048
	21000	0.000839	0.000047	0.000839	0.000047	0.000839	0.000047
	25000	0.000837	0.000047	0.000843	0.000047	0.000837	0.000047

Table 0.3: Maximum content of water that can be permitted in Troll gas before water to avoid the risk of hydrate formation if 0.1 H_2S and 0.1 CO_2 are present

Temperature [K]	Pressure [kPa]	Troll gas		Troll gas with 0.1 H_2S		Troll gas with 0.1 CO_2	
		Dew-point	Hematite	Dew-point	Hematite	Dew-point	Hematite
274	5000	0.001194	0.000062	0.001156	0.000060	0.001183	0.000062
	9000	0.000753	0.000039	0.000714	0.000037	0.000747	0.000039
	13000	0.000618	0.000032	0.000587	0.000030	0.000613	0.000032
	17000	0.000577	0.000030	0.000560	0.000029	0.000571	0.000030
	21000	0.000568	0.000030	0.000564	0.000029	0.000563	0.000029
	25000	0.000571	0.000030	0.000575	0.000030	0.000566	0.000029
280	5000	0.001822	0.000102	0.001787	0.000100	0.001822	0.000102
	9000	0.001148	0.000065	0.001105	0.000061	0.001147	0.000064
	13000	0.000934	0.000052	0.000899	0.000050	0.000933	0.000052
	17000	0.000860	0.000048	0.000842	0.000047	0.000859	0.000048
	21000	0.000839	0.000047	0.000838	0.000047	0.000838	0.000047
	25000	0.000837	0.000047	0.000848	0.000048	0.000836	0.000047

A5. Maximum tolerance of water to prevent the risk of hydrate formation for 0.5 mole of hydrocarbon and 0.5 mole of inorganic gases (H_2S and CO_2).

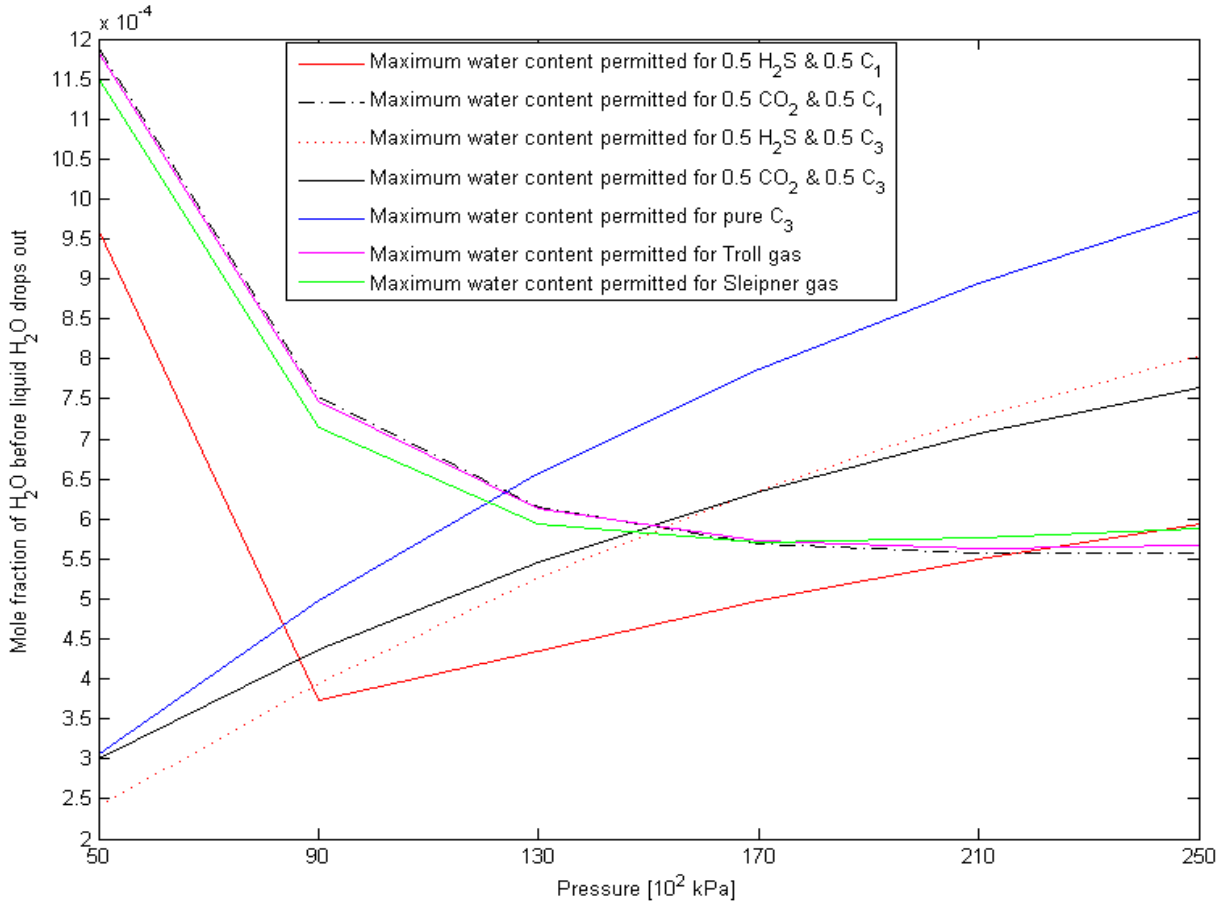

Figure 0.15: Maximum tolerance of water in gas mixtures to avoid liquid water drop out at 274 K

Table 0.4: Maximum tolerance of water in gas mixtures to avoid liquid water drop out at 274 K

Temperature [K]	274					
Pressure [kPa]	5000	9000	13000	17000	21000	25000
Gas mixture	Maximum concentration of water [ ]					
1.0 CH_4 (*Reference*)	0.0011944	0.0007575	0.0006192	0.0005715	0.0005576	0.000556
Troll Gas	0.0011832	0.0007467	0.000613	0.0005718	0.0005636	0.000566
Sleipner Gas	0.0011514	0.0007138	0.0005937	0.0005709	0.0005762	0.000588
0.5 H_2S and 0.5 CH_4	0.0009614	0.0003728	0.0004354	0.0004973	0.0005498	0.000594
0.5 CO_2 and 0.5 CH_4	0.0011899	0.0007526	0.0006152	0.0005695	0.0005577	0.000558
Pure C_3H_8 (*Reference*)	0.0003056	0.000498	0.000656	0.0007866	0.0008947	0.000984
0.5 H_2S and 0.5 C_3H_8	0.0002399	0.0003954	0.0005257	0.0006353	0.0007274	0.000805
0.5 CO_2 and 0.5 C_3H_8	0.0002992	0.0004362	0.000546	0.0006344	0.000706	0.000764

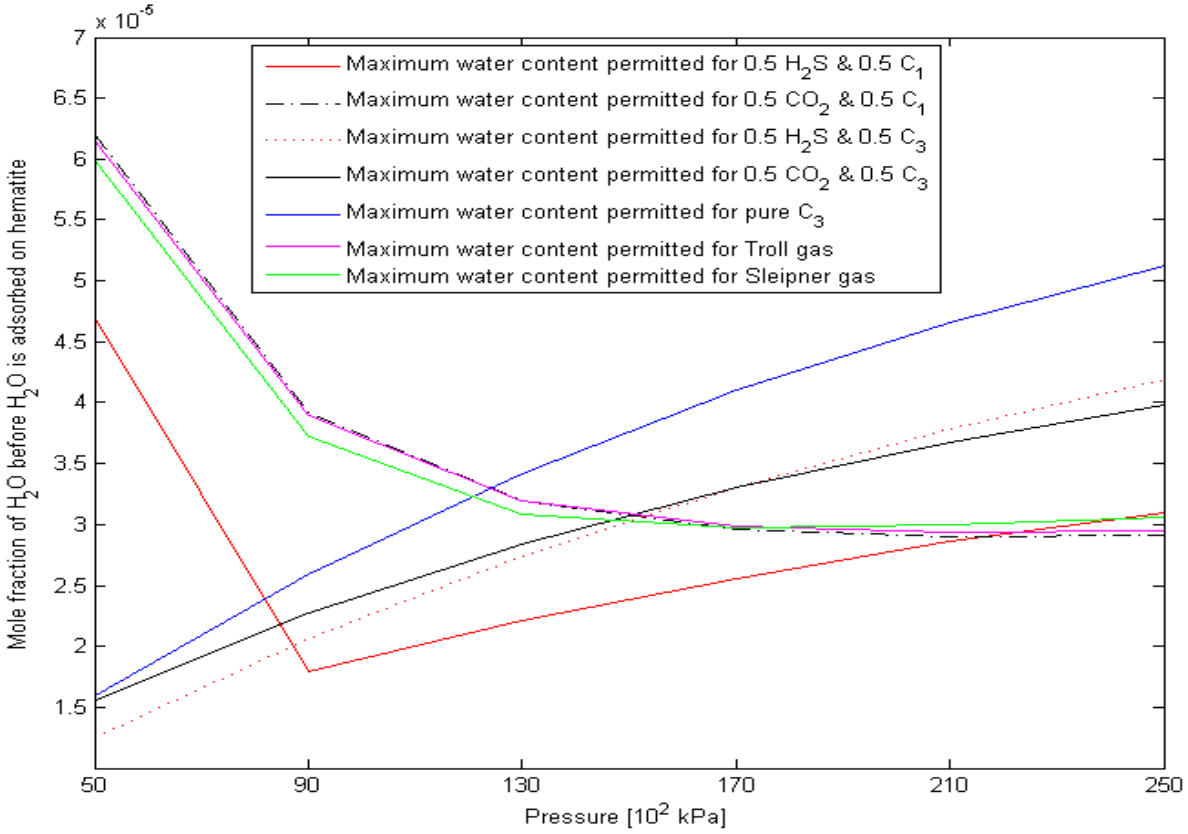

Figure 0.16: Maximum tolerance of water in gas mixtures to avoid adsorption of water on hematite at 274 K

Table 0.5: Maximum tolerance of water in gas mixtures to avoid adsorption of water on hematite at 274 K

Temperature [K]	274					
Pressure [kPa]	5000	9000	13000	17000	21000	25000
Gas mixture	Maximum concentration of water [ ]					
1.0 CH_4 (*Reference*)	0.000062	0.000039	0.000032	0.000030	0.000029	0.000029
Troll Gas	0.000062	0.000039	0.000032	0.000030	0.000029	0.000030
Sleipner Gas	0.000060	0.000037	0.000031	0.000030	0.000030	0.000031
0.5 H_2S and 0.5 CH_4	0.000047	0.000018	0.000022	0.000026	0.000029	0.000031
0.5 CO_2 and 0.5 CH_4	0.000062	0.000039	0.000032	0.000030	0.000029	0.000029
Pure C_3H_8 (*Reference*)	0.000016	0.000026	0.000034	0.000041	0.000047	0.000051
0.5 H_2S and 0.5 C_3H_8	0.000013	0.000021	0.000027	0.000033	0.000038	0.000042
0.5 CO_2 and 0.5 C_3H_8	0.000016	0.000023	0.000028	0.000033	0.000037	0.000040

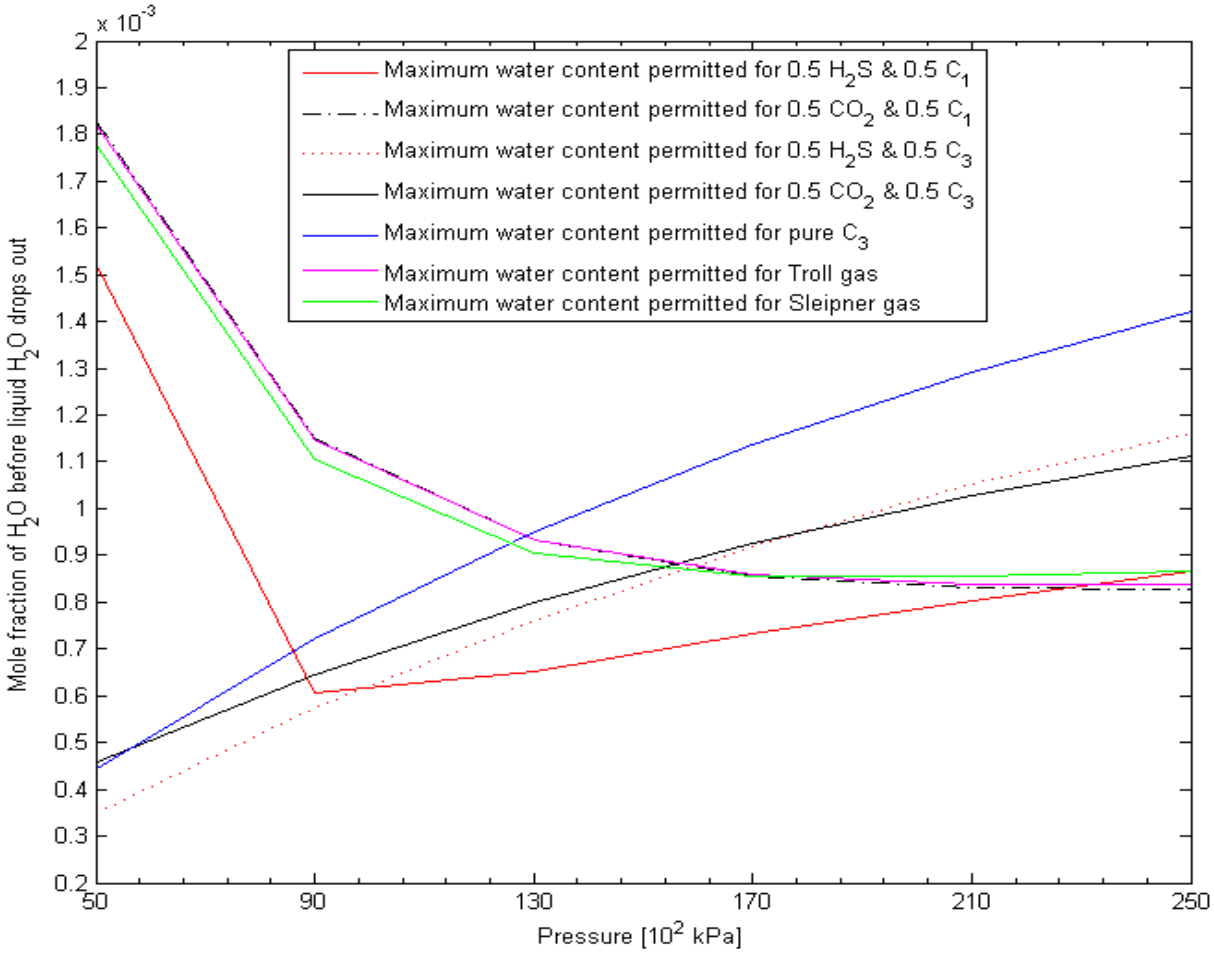

Figure 0.17: Maximum tolerance of water in gas mixtures to avoid liquid water drop out at 280 K

Table 0.6: Maximum tolerance of water in gas mixtures to avoid liquid water drop out at 280 K

Temperature [K]	280 K					
Pressure [kPa]	5000	9000	13000	17000	21000	25000
Gas mixture	Maximum concentration of water [ ]					
1.0 CH_4 (*Reference*)	0.001838	0.001162	0.000942	0.000860	0.000831	0.000823
Troll Gas	0.001823	0.001148	0.000934	0.000860	0.000839	0.000837
Sleipner Gas	0.001779	0.001104	0.000907	0.000857	0.000855	0.000867
0.5 H_2S and 0.5 CH_4	0.001525	0.000606	0.000652	0.000733	0.000805	0.000865
0.5 CO_2 and 0.5 CH_4	0.001829	0.001152	0.0009341	0.0008559	0.0008311	0.0008266
Pure C_3H_8 (*Reference*)	0.000445	0.0007225	0.00095	0.0011377	0.001293	0.0014214
0.5 H_2S and 0.5 C_3H_8	0.000349	0.0005732	0.0007609	0.0009185	0.001051	0.0011623
0.5 CO_2 and 0.5 C_3H_8	0.000459	0.0006455	0.0008008	0.0009266	0.0010286	0.0011114

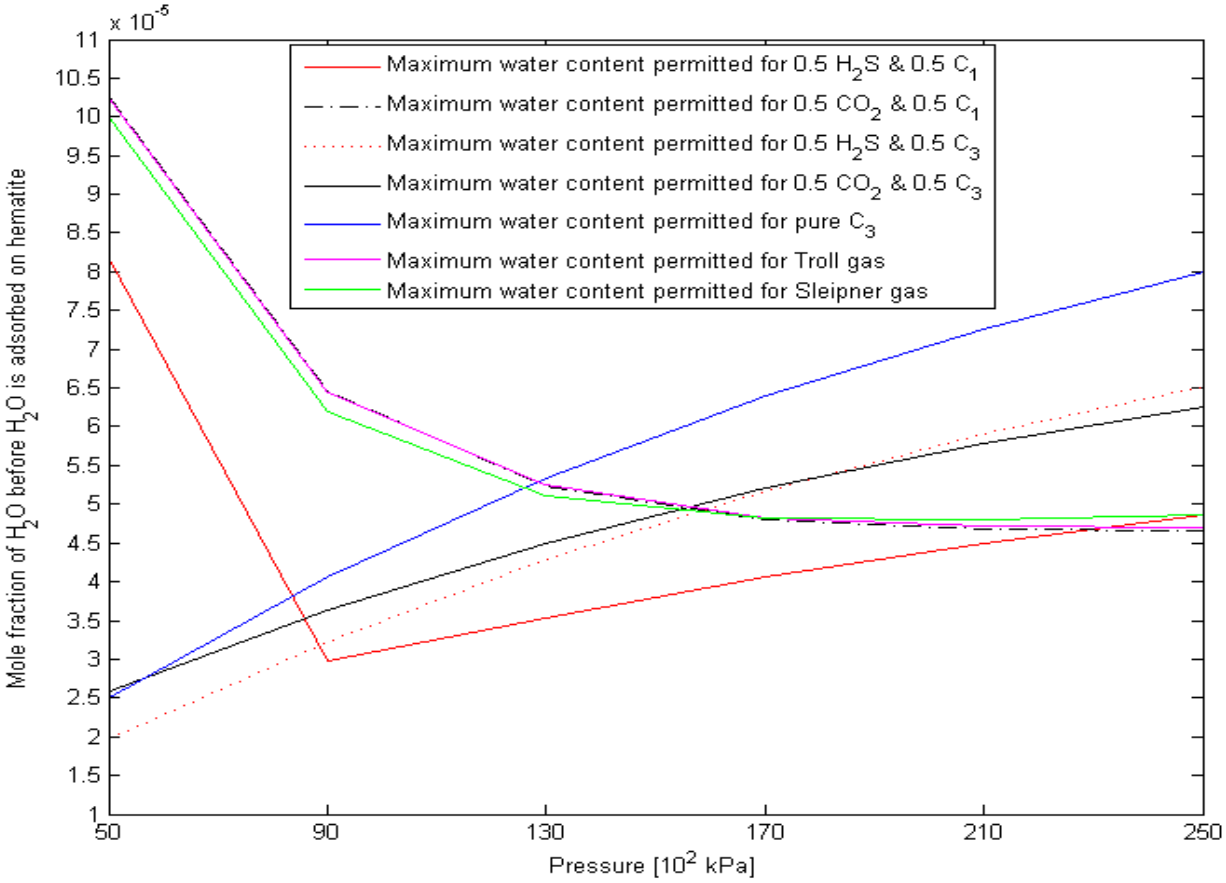

Figure 0.18: Maximum tolerance of water in gas mixtures to avoid adsorption of water on hematite at 280 K

Table 0.7: Maximum tolerance of water in gas mixtures to avoid adsorption of water on hematite at 280 K

Temperature [K]	280					
Pressure [kPa]	5000	9000	13000	17000	21000	25000
Gas mixture	Maximum concentration of water [ ]					
1.0 CH_4 (*Reference*)	0.000103	0.000065	0.000053	0.000048	0.000047	0.000046
Troll Gas	0.000102	0.000065	0.000053	0.000048	0.000047	0.000047
Sleipner Gas	0.000100	0.000062	0.000051	0.000048	0.000048	0.000049
0.5 H_2S and 0.5 CH_4	0.000082	0.000030	0.000035	0.000041	0.000045	0.000049
0.5 CO_2 and 0.5 CH_4	0.000103	0.000065	0.000052	0.000048	0.000047	0.000047
Pure C_3H_8 (*Reference*)	0.000025	0.000041	0.000053	0.000064	0.000073	0.000080
0.5 H_2S and 0.5 C_3H_8	0.000020	0.000032	0.000043	0.000052	0.000059	0.000065
0.5 CO_2 and 0.5 C_3H_8	0.000026	0.000036	0.000045	0.000052	0.000058	0.000063